UNIVERSITY OF SALFORD

DEPARTMENT OF CIVIL ENGINEERING

POLYPROPYLENE FIBRE REINFORCEMENT OF HARDENED CEMENT PASTE

BY

DINESH GANDHI

A THESIS SUBMITTED FOR

THE DEGREE OF

DOCTOR OF PHILOSOPHY

1982

Dedicated to my Parents

DECLARATION

No part of this work has been previously submitted in support of an application for any degree or qualification from this or any other university or institution of learning.

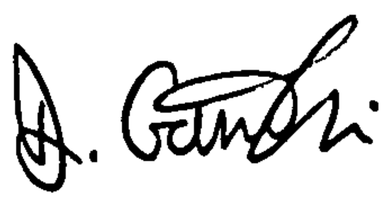

D. GANDHI

1982

ACKNOWLEDGEMENTS

The work presented in this thesis has been carried out under the supervision of Dr. R. Baggott who guided both the progress of the experimental work and the preparation of this thesis. It has been a pleasure to work with him.

Invaluable assistance has been given by Messrs. N. Beaver and P. Burton with the experimental work. The author is particularly indebted to Mr. Beaver, who not only helped with the testing of specimens and showed a genuine interest in the work, but made himself readily available at all times.

Special thanks are extended to the Science Research Council and Plasticisers Limited for the award of a CASE Research Studentship, during the tenure of which this work has been undertaken.

Finally, the author is indebted to his parents for their constant encouragement.

ABSTRACT

This thesis considers the tensile deformation characteristics of polypropylene fibre reinforced hardened cement paste having heterogeneous fibre geometries and a range of volume concentrations.

Polypropylene fibres were prepared under various manufacturing conditions using a laboratory extruder, to ascertain the effect of these conditions on fibre characteristics.

The relevant properties of cement paste likely to influence the polypropylene fibres and the eventual composite were investigated.

An investigation of continuous aligned fibre composites in tension, containing various volume concentrations of fibres, showed that multiple cracking occurred despite the elastic modulus of the fibre being considerably lower than that of the hardened cement paste. Factors which enabled fibre/matrix contact to be maintained during the multiple cracking process, despite the unfavourable Poisson's ratio of polypropylene, were considered.

Discontinuous aligned fibre composites were tested in tension, to ascertain the effect of volume concentration and length of fibres on the shear stress transfer between fibre and matrix and on multiple cracking.

Composites containing parallel fibres, with fibre directions at varying angles to the direction of applied tensile stress, allowed an assessment to be made of the role of inclination. Crack distributions, pull-out behaviour of fibres and the ultimate stress

of composites were investigated.

Finally, random fibre reinforced composites were evaluated to provide a comparison with the Continuous, Discontinuous and Inclined fibre reinforced systems.

In addition to determining the mechanical deformation of the various composites, the acoustic emission associated with internal deformation mechanisms was studied. This was undertaken with equipment capable of monitoring a range of acoustic pulse parameters.

CONTENTS

CONTENTS

NOTATION

A_c	Cross-section area of composite
C	Fibre/matrix cohesion
d	Fibre diameter
d_c	Critical diameter
E_c	Elastic modulus of the composite
E_f	Elastic modulus of the fibre
E_m	Elastic modulus of the matrix
F	Force
K	Constant
ℓ	Fibre length
ℓ_c	Critical fibre length
N	Number of fibres
Q	Relative displacement of fibre and matrix
r	Fibre radius
S	Spacing between the centroids of the fibres
V_f	Volume fraction of the fibre
V_m	Volume fraction of the matrix
x'	Transfer length for stress for long fibres
x_d	Transfer length for stress for short fibres
ε_c	Composite strain
ε_{ft}	Longitudinal strain in the fibre bridging the crack
ε_{fu}	Fibre ultimate strain
ε_{mu}	Matrix ultimate strain
μ	Coefficient of friction
ν_c	Poisson's ratio of the composite
ν_f	Poisson's ratio of the fibre
ν_m	Poisson's ratio of the matrix

σ_c	Stress in the composite
σ_m	Stress in the matrix
σ_n	Normal compressive force at fibre/matrix interface
σ'_f	Fibre stress at onset of cracking
σ_{fu}	Fibre ultimate stress
σ_{mu}	Matrix ultimate stress
τ	Fibre/matrix shear stress
τ_o	Initial frictional stress
τ_q	Local value of frictional stress

LIST OF TABLES

LIST OF FIGURES

LIST OF PLATES

7.3 Acoustic emission preamplifiers

7.4 Transducers secured on to the test specimen with insulating tape and preamplifiers are located near the transducers

7.5 Shows entire test set-up, which includes Losenhausen testing machine, Dunegan/Endevco 3000 series acoustic emission equipment with various X-Y recorders

7.6 Hewlett-Packard X-Y recorder plotting load v acoustic energy

7.7 Typical example of events in amplitude mode of continuous aligned fibre reinforced cement paste containing 5.5% V_f

7.8 Typical example of events in sum amplitude mode of continuous aligned fibre reinforced cement paste containing 5.5% V_f (summation of Plate 7.7 data from right to left)

7.9 Typical example of events in counts mode of continous aligned fibre reinforced cement paste containing 5.5% V_f

7.10 Typical example of events in sum counts mode of continuous aligned fibre reinforced cement paste containing 5.5% V_f (summation of Plate 7.9 data from right to left)

7.11 Typical example of events in pulse width mode of continuous aligned fibre reinforced cement paste containing 5.5% V_f

7.12 Typical example of events in sum pulse width mode of continuous aligned fibre reinforced cement paste containing 5.5% V_f (summation of Plate 7.11 data from right to left)

INTRODUCTION

CHAPTER ONE

INTRODUCTION

1.1 GENERAL

Today's construction industry requires the development of new types of materials having combinations of various valuable properties, such as durability and stiffness. Construction materials for most applications must of necessity have a long service life of at least 50 years. This long life tends to obscure the fact that individual materials or products have also a life cycle of successful use which can range from periods of many centuries in the case of bricks, to periods of only a few years in the case of materials such as paints, mastics and sealants, with rapidly developing technologies.

There are many reasons for the death of a material or product, for instance a cheaper or a technically superior alternative becomes available, or a long term disadvantage is recognised. Exhaustion of raw material is another reason.

One material which is currently under threat is asbestos cement, which results when cement paste and asbestos fibres are combined. A considerable part of the world's asbestos production is used in the manufacture of fibre-reinforced materials, e.g. flat sheet and corrugated roofing materials, side panels, asbestos cement pipes, fire-proof and insulation materials of various types. In 1950, the world asbestos consumption was about one million tons, in 1958, two million tons and in 1970 four million tons, and it is predicted[1]* that the world's deposit of asbestos may

---

*The references are listed on page 120.

well be exhausted before the turn of the century. Furthermore, it has been realised in recent years that there is a considerable health risk for persons working with asbestos and the public health authorities in several countries have already banned the use of asbestos altogether for the manufacture of certain of the above-mentioned products. Yet another parameter in the asbestos equation is the fact that the success of asbestos cement stems back to 1900[2]. Since then a very wide range of applications has been established, this has stimulated the development of competitive materials because of the large turnover of the material involved. These materials range from steel sheeting, plastic sheeting to cementitious board reinforced with alternative fibres to asbestos.

The attraction of the latter alternative is that it retains the desirable characteristics of the cement paste. Cement paste is about six times stiffer and one hundred times cheaper than many resins and is durable under most environmental conditions encountered in building applications. However, it has the over-riding disadvantage of a very low failure strain. It was to overcome this main disadvantage that asbestos fibres were incorporated in the first instance. It follows that if an alternative fibre such as cellulose, glass, polypropylene etc. can be incorporated in the cement paste to achieve similar property improvements, then an alternative to asbestos cement will result.

However, only two types of non-asbestos fibre reinforced cement products are at present in commercial production, namely cellulose and glass fibre reinforced cement. The concept of using polypropylene fibres to reinforce cement paste is considered valid but poses some interesting problems. From the viewpoint of mechanical properties, the fibres have the advantage of high tensile strength and toughness. Moreover,

polypropylene is particularly of interest for cement reinforcement on account of its relatively low cost, see Table 1.1[3], good chemical resistance, low specific gravity and moisture resistance. It has the disadvantages of low elastic modulus and poor bonding surface. Polypropylene was discovered in 1954 and used in large scale production since 1962; therefore in terms of a time scale it is a fairly new material. Its potential as a reinforcing fibre for cement paste has not been fully evaluated. Furthermore, the basic principles associated with mechanical properties established for composites with high modular ratio (Fibre Modulus/Matrix Modulus), have not been shown to be necessarily applicable to the low modular ratio system. It is against this background that polypropylene reinforced cement paste composite was chosen for study.

1.2 OBJECTIVES

The overall objectives of this study were to identify and explain some of the major physical principles which determine the mechanical properties of polypropylene reinforced cement paste composite, with a view to providing a foundation for understanding composite behaviour.

Specific objectives were related to basic questions concerning polypropylene fibre and its role in cement paste. The most important of these questions are summarised in this chapter to give an overall perspective of the investigation, e.g.

(A) Does the variation of fibre manufacturing conditions improve the elastic modulus of fibre?

TABLE 1.1 - RELATIVE COSTS OF VARIOUS FIBRES AND MATRICES

(AFTER REFERENCE (3))

Material	Cost Per Unit of Volume
Fibres:	£/m^3
Polypropylene	
Fibrillated Tape	900-990
Filament	990-1620
Asbestos	945-1212
Glass	
E	2470-2990
Alkali-Resistant	4420-5200
Steel	3120-3900
Carbon Fibre	95000-152000
Matrix:	
Cement Paste	57
Concrete	24

(B) Does multiple cracking occur in continuous aligned polypropylene reinforced cement paste composite, and if so, do the same relationships apply as those derived for high modulus fibre composites?

(C) What type of shear stress transfer mechanism occurs between fibre and matrix in

(i) Continuous aligned fibre composite

(ii) Discontinuous aligned fibre composites

(iii) Inclined fibre composite and

(iv) Random fibre composite systems?

(D) Can acoustic emission analysis be employed to identify internal mechanisms during composite deformation?

1.3 STRUCTURE

A literature survey was carried out on fibre reinforced cementitious composites generally and polypropylene reinforced cementitious composites in particular, to determine the current state-of-the-art and to identify research objectives.

Since the final composite material was to contain polypropylene fibres in hardened cement paste, it was thought appropriate to investigate the modulus of elasticity and tensile strength of each phase separately. In view of the disadvantageously low modulus of elasticity of polypropylene fibre, an assessment was made of the effects of manufacturing conditions on polypropylene fibre modulus, by means of a laboratory extruder. This part of the investigation is detailed in chapter 3.

The logic of the subsequent investigation, was to examine the behaviour of progressively more complicated fibrous composites, under uniaxial

tensile loading. Starting with the simplest system from a theoretical point of view, i.e. continuous fibre aligned parallel to the direction of applied tensile stress. Considered in chapter 4.

The next stage was to ascertain the effect of fibre length in the aligned arrangement. This was achieved by incorporating discontinuous aligned fibres of various lengths. Studies of these investigations are reported in chapter 5.

In order to approach further towards a 'practical' composite, the effect of inclination of fibre was studied by incorporating fibres at angles ranging from 15^{o} to 75^{o} to the tensile axis. In addition, two dimensional random fibre composites incorporating fibre length of 26 and 60 mm were also investigated. This latter type of fibre composite approaches most closely to existing commercial fibre reinforced materials, see chapter 6.

Throughout the investigation, acoustic emission data was recorded during the deformation of most specimens tested. An overall assessment of which is made in chapter 7.

1.4 DEFINITION OF A COMPOSITE

Since this thesis is primarily concerned with fibre composite material, it was thought appropriate to define such a material at this stage.
A general definition of a composite material is:

> Two or more materials in which the combined material formed has improved structural properties not exhibited by any of the materials separately[4].

However, a more specific definition set down by Broutman and Krock

for a modern composite material[5] is:

(A) The composite must be man-made

(B) The composite must be a combination of at least two chemically distinct materials, with a distinct interface separating the components

(C) The separate materials forming the composite must be combined three dimensionally

(D) The composite material should be created to obtain properties which would not be achieved by any of the components acting alone.

Hence, the definition of a fibre reinforced composite would incorporate the above terms together with the additional limitation that at least one of the chemically distinct materials should be of fibrous shape. A generally accepted definition of a fibrous shape is not available, accordingly an arbitrary definition is suggested as one having an aspect ratio, i.e. (Fibre Length/Maximum Cross-Sectional Dimension) > ~ 3, where in this instance a maximum cross-sectional dimension of fibre of size less than 0.5 mm is considered adequate.

LITERATURE REVIEW

CHAPTER TWO

LITERATURE REVIEW

2.1 FIBRE COMPOSITES

2.1.1 Historical Developments

The concept of fibre reinforced materials is far from being an idea of the twentieth century. Straw[6] has been employed to reinforce sun-dried mud bricks and horse hair or sisal to reinforce gypsum plaster for many centuries. Asbestos was probably the first inorganic fibre used in composite materials. It has been established that fine anthophyllite asbestos fibres were used in Finland as early as 2500 B.C. to strengthen the sides of lightly fired pottery.

Although the significant advancement of non-asbestos fibre reinforced cement and concrete has only taken place over the last two decades, many patents on the use of miscellaneous reinforcing elements in cement matrices exist, one of the earliest being that of Berard in the year 1874[6].

During the late 19th century[2], the inclusion of asbestos fibres in cement matrices enabled a whole new range of products to be manufactured for the construction industry, this basic material i.e. asbestos cement, was probably the greatest isolated development to effect the entire field of composites.

The concept of concrete strengthened by the inclusion of short pieces of steel was demonstrated as early as 1910 by Porter[7].

Much of the pioneering work on the use of glass fibre reinforcement in cementitious matrices was carried out by Biryukovich et al[8], who

conducted investigations into E-glass fibre reinforcement and reported significant improvements in the mechanical properties. Krenchel[9], also worked with E-glass fibres incorporated in Portland cement and he investigated both theoretically and practically the strengths of such composites. Thus by 1960, the practical benefits that could be derived by incorporating fibres in cementitious matrices were well established, but there were not available detailed explanation of their mechanisms.

Since then a considerable amount of experimental work has taken place into the investigation of non-asbestos fibre reinforcement (see later sections for details). In parallel with this, theoretical models have been developed. However, progress towards understanding the mechanics of fibre reinforcement did not take place until the investigations of Romualdi and Batson [10], [11] in 1963, who proposed a crack arrest mechanism to account for the improvement in the mechanical properties of concrete incorporating steel fibres.

The next major development was in 1971, when a theory was published by Aveston, Cooper and Kelly[12], in which a new approach was adopted to explain the behaviour of fibre reinforced cements and mortar, based on the formation of fine multiple cracks. Both the Romualdi and Batson's[10,(11)] and Aveston, Cooper and Kelly's[12] work, will be discussed further in the next section.

2.1.2 Fibre Composite Theories - Cementitious Systems

2.1.2.1 The mechanics of crack arrest in cementitious matrices - Romualdi and Batson's theory

In 1963 Romualdi and Batson published two papers[10],[11], in which they gave theoretical explanations for the improvement of tensile

strength of steel fibre reinforced mortar. A detailed treatment of this theory is given in references 10 and 11.

Their analysis was based on the application of linear elastic fracture mechanics to concrete. They showed that the crack extension stress is inversely proportional to the flaw or crack diameter and argued that the inherent cracks and flaws, in the mass of the concrete, could be prevented from enlarging and propagating by the use of closely spaced fibre reinforcement. Assuming that the maximum flaw in a fibre reinforced concrete mass would have a diameter equal to the fibre spacing, they also concluded that the smaller the spacing, the smaller the flaw size and hence the higher the concrete tensile strength. Thus, for a constant volume fraction of fibres, a higher cracking stress could be expected for a decreasing fibre diameter because of decreasing fibre spacing, since the spacing is directly proportional to the fibre diameter. The average fibre spacing was shown as[13]

$$S = \frac{13.8d}{\sqrt{V_f}} \qquad .. \quad .. \quad .. \quad (2.1)$$

where S is the spacing between the centroids of the fibres,

d is the fibre diameter and

V_f is the volume fraction of the fibres.

It was further shown that the tensile strength and the first crack flexural strength should be inversely proportional to the square root of the fibre spacing. This theoretical concept was for steel wire reinforced mortar in indirect tension and the results appeared to substantiate the theory.

However, Broms and Shah[14] noted that Romualdi et al, had not consistently used the same diameter of wires for their investigation

and on recalculating the ultimate resisting moments, concluded that the effects of fibres on the ultimate strength were slight. The work of Shah and Rangan[15], suggested that fibre spacing alone had little effect on the tensile strength of the composite, but that decreasing the fibre spacing did increase the toughness of fibre reinforced concrete. Apart from the main objections to the Romualdi and Batson's[10],[11] theory made by Shah et al[15], other workers voiced their reservations regarding the experimental verifications to theory and ability of bending tests and indirect tensile tests used by Romualdi et al[10],[11] to provide true estimates of the tensile strength. Hannant[16] reviewed the different tests used to determine the tensile strength of concrete, which included direct tension, flexure at third point and centre point loading and the indirect tensile tests. /Concluding that for third point loading, the tensile strength calculated as the modulus of rupture, using the elastic beam theory and assuming full elasticity up to failure is not correct and gives an over-estimation of the true tensile stress at the extreme fibres of the beam. It was also shown by Wright[17], that the modulus of rupture is dependent on the beam size, the longer beams giving a lower measured modulus of rupture. He also showed that the modulus of rupture calculated from centre point loading, gave values which were 25% higher than those from third point loading, because the probability of a weak element being subjected to a critical stress is considerably greater under third point loading than when a central load acts, since the maximum stress in the latter case is limited to a very small region immediately underneath the load point.

These disagreements, however, were based on experimental results and no theories were suggested to fully explain the strength and fracture

behaviour of fibre reinforced cement based materials.

2.1.2.2 Single and multiple fracture - Aveston, Cooper and Kelly's theory

In 1971 Aveston, Cooper and Kelly[12], introduced a number of ideas which improved the understanding of the type of cracking found in reinforced brittle matrices. Their theory includes the consideration of matrices of small failure strain, which contain fibres having a much larger failure strain. Only the pertinent points of the theory are outlined here, a detailed account of which is given in reference 12.

Considering continuous aligned fibres bonded to the matrix, the initial modulus, for all practical purposes, is given by the rule of mixtures

$$E_c = E_m V_m + E_f V_f \qquad .. .. .. \qquad (2.2)$$

where E_c is the elastic modulus of the composite

E_m is the elastic modulus of the matrix

E_f is the elastic modulus of the fibre

V_m is the volume fraction of the matrix and

V_f is the volume fraction of the fibre.

If the fibre diameter is not too small, the more brittle matrix phase will fail at its normal failure strain and the subsequent behaviour will depend on whether the less brittle fibre phase can withstand the additional load thrown upon it[18], i.e. whether

$$\sigma_{fu} V_f > E_c \varepsilon_{mu} \quad (\varepsilon_{fu} > \varepsilon_{mu}) \qquad .. .. .. \qquad (2.3)$$

$$\sigma_{mu} V_m > E_c \varepsilon_{fu} \quad (\varepsilon_{fu} < \varepsilon_{mu}) \qquad .. .. .. \qquad (2.4)$$

where σ_{fu} is the fibre ultimate stress

σ_{mu} is the matrix ultimate stress

ε_{fu} is the fibre ultimate strain and

ε_{mu} is the matrix ultimate strain.

If the fibres cannot support this load, then they will also fracture and the composite will fail with a single crack. However, if the fibres can support the additional load then the matrix will be broken down into a series of blocks of lengths between x' and 2x'. Aveston, Cooper and Kelly[12], have shown that

$$x' = \frac{V_m \sigma_{mu} r}{V_f 2\tau} \qquad \ldots\ \ldots\ \ldots \qquad (2.5)$$

where x' is the transfer length for stress for long fibres

r is the fibre radius and

τ is the fibre/matrix shear stress.

The additional load on the fibres due to the cracking of the matrix varies between $\sigma_{mu} V_m/V_f$ at the crack and zero, at a distance between x' and 2x' from the crack surface, so that the average additional strain in the fibres is given by

$$\Delta\varepsilon_f = \frac{\varepsilon_{mu} E_m V_m}{2E_f V_f} = \frac{\alpha\varepsilon_{mu}}{2} \qquad \ldots\ \ldots\ \ldots \qquad (2.6)$$

where $\alpha = \frac{E_m V_m}{E_f V_f}$

On completion of the cracking, the blocks of matrix will all be less than the length 2x' required to transfer their breaking load $\sigma_{mu} V_m$ and so a further increase in the load on the composite results in the fibres sliding relative to the matrix.

Thus in a low strain to failure matrix, the merit, if any, of fibre inclusion must lie in the load carrying ability of the fibres after matrix cracking has occurred. If fine multiple cracking ensues, then the composite will possess greater apparent ductility and also

show rising stress/strain curve characteristics. In addition the cracks need to be invisible to the naked eye if the composite is to be acceptable as a practical material.

2.1.3 Properties of Fibre Composites

2.1.3.1 Tensile strength

Cement pastes[19] are not used on their own as a material for construction, as they crack easily due to dimensional instability which may be caused by environmental conditions. Portland cements expand slightly if allowed to set and harden in water. On drying they undergo a shrinkage which is only in part reversible if the cement paste is subsequently re-wetted. The inclusion of aggregates reduces this effect and also makes the material more economically viable, but the resulting products, mortar and concrete, are still weak in tension and fail in a brittle fashion. Fibre reinforcement is used to overcome these deficiencies. It has been shown that it can also reduce shrinkage, for example Briggs et al[20] have reported marked reductions in both the expansion and shrinkage of cements brought about by the incorporation of 5.6% volume of high modulus graphite fibres.

A very wide range of fibre types are available for use as reinforcement to cement based matrices[21]. A range of mechanical, physical and chemical properties are given in Table 2.1. These are compared with typical values for Ordinary Portland cement, high alumina cement and plaster.

Before considering the tensile strength of the composite, it is worth noting that the actual tensile strength of the reinforcing individual

TABLE 2.1 - PROPERTIES OF INDIVIDUAL FIBRES AND BINDER MATERIALS (AFTER REFERENCE (21))

	Material	Typical Diameter (μm)	Maximum fibre length (mm)	Specific Gravity	Bond with cement paste (N/mm^2)	Tensile strength (N/mm^2)	Elongation at break (%)	Elastic modulus (kN/mm^2)	Temperature at which all strength is lost (°C)	Environmental durability	
										Resistance to acids	Res. to alkalis
FIBRES	1. Crystalline silicates										
	Chrysolite('white')asbestos	0.02-20	100	2.55	0.83	3150	>3	168	fusion 1450	Fair	Fair
	Crocidolite('blue')asbestos	0.1-20	100	3.37	3.17	3500	2-3	196	fusion 1100	Good	Good
	2. Glasses										
	'E' glass	9-15	C*	2.56	6.4-10	2100-3500	2-3.5	77	800	Good	Poor
	Cem-FIL	10-20		2.71	-	2100-2800	2-3	70-84	-	-	Good
	3. Ceramics										
	Alumino-silicate (Kaowool, Fibrefrax)	2.75	254	2.73		-	-	-	mp 1750	Fair	Probably Poor
	Carbon-type 1 (Modmor)	7.5	C	1.99	-	1400-2100	0.4	385-455	400-1500	Good	Good
	Carbon-type 2 (Modmor)	7.5	C	1.74		2450-3150	1.0	245-315		Good	Good
	4. Metals										
	High tensile steel (high carbon)	5-500	C	7.84	5-11	3150	3	196-210	mp 1400	Poor	Good
	(low carbon)					1050	4	210	mp 1500	Poor	Good
	Stainless steel					2100	3	154-168	mp 1450	Good(to some acids)	Good
	5. Natural vegetables										
	Cotton	10-20	63	1.35		280-839	5-10	5.6-11.2		Poor	Fair
	Sisal	7.5-47.5	1200	1.48	-	839	2.9	-	150	Poor	-
	Hemp	15-50	1800 50	1.48		385	1.8	-		Poor	-
	6. Polymers										
	Polypropylene (filament)	>4		0.91	physical poor	650	18	4.9	120	Good	Good
	(fibrillated)	>4		0.91	mechanical good	399	8	7.7	120 mp 160	Good	Good
	Nylon (type 242)	>4	C	1.14	(fibrillated polypropylene)	868	13.5	4.2	mp 250	Fair(affected by some)	Good
	Polyester (type C Terylene)	>4		1.38		1030	10.5	11.2	mp 260	Good	Fair to poor
BINDERS	Ordinary Portland cement			2.5		2.8-14.0	0.04-0.06	7-28		Poor	Good
	High alumina cement	-	-	2.5	-	2.8-14.0	0.04-0.06	21-42	-	Poor,but slightly better than o.p.c.	Good(not caustic alkalis)
	Plaster	-	-	2.4	-	2.7-7.0	0.03-0.06	10.5-21	-	Poor	-

*C = continuous; mp = melting point

or bundles of fibres are subject to considerable variation.

Riley and Reddaway[22] considered defects either in the fibres or on the surface of the fibres which affected their strength properties. The effects varied with the length and diameter of the fibres. The mean strength of a number of fibres in a bundle was found to decrease with an increase in the length of the fibres. Defects resulted in variations in strength between individual fibres, so that when a bundle of fibres was tested, some fibres broke before others, and the strength of the bundle was thus less than the mean strength of the fibres in the bundle. It is generally known that fibres become stronger with decreasing diameter. This effect is attributed to the fact that as fibres become smaller in diameter, there are fewer surface flaws on brittle fibres and shorter internal cracks. Thus the number and magnitude of stress concentration effect is reduced. Higgins et al[23] state that in general the measured tensile strength of a fibre is one or two orders of magnitude below its theoretical value.

Irregularities on the fibre surface, however, can be an advantage, as found by Briggs[24] when he tested carbon fibre reinforced cement in tension and also studied the fibre surface under a scanning electron microscope, he found that irregularities on the carbon fibre were able to key mechanically in a matrix material like cement gel, which can conform to the microscopic surface features by micro crystalline growth during hydration of the cement. Because of the rough surface texture of the fibre, an exceptionally good frictional bond is produced. Sarkar and Bailey[25] also carried out tensile tests on carbon fibre reinforced cement specimens and reported substantial gains in the strength over unreinforced matrices.

Allen[26] investigated the tensile strength of high alumina cement paste containing 6.7% by volume of chopped strand mat of glass fibre. The composite yielded ultimate tensile strengths of 16 N/mm^2, a typical stress-strain diagram consisted of a steep nearly linear initial region followed by a shallow irregular region, this latter region corresponded to the development of multiple cracks, which were invisible. One of the major drawbacks in using commercially available low-alkali borosilicate glass fibres (e.g. E-glass) in Ordinary Portland cement as opposed to high alumina cement is that the fibre is not stable in the alkaline environment of hydrating Ordinary Portland cement. A research programme to investigate the feasibility of developing a composite material based on inorganic cements and special glass fibres, was undertaken at the Building Research Station[27], which resulted in the development of an alkali-resistant glass fibre. This was subsequently produced on a commercial scale by Pilkington Brothers and is now marketed under the trade mark of Cem-FIL. Ali et al[28] carried out tensile tests on alkali-resistant glass fibre reinforced cements, to determine the effect of fibre content. They found that although it was possible to incorporate 10% by volume of fibre in cement matrices by the spray suction method, the maximum tensile strength of the resulting composites were attained at 6% by volume of fibre addition. An ultimate tensile strength value of 18 N/mm^2 was obtained for a composite containing 40 mm length fibre.

Edgington et al[29] found that for a constant volume of steel, the measured tensile strength only marginally increased with decreasing fibre spacing, when compared with the large increases that were predicted theoretically. Thus in reality, the fibre spacing concept does not predict the cracking strength of fibre reinforced concrete. Aveston, Mercer and Sillwood[30] tested both continuous steel fibre

and carbon fibre reinforced cement. They determined the initial modulus of elasticity and the ultimate strength. Both were in agreement with the composite law of mixtures and both showed a linear increase in tensile strength with increasing fibre volume fraction. Hannant et al[31] demonstrated that a much more efficient fibre reinforcement of mortar can be achieved when fibres are aligned in the direction of the tensile stress. To achieve this, they used a device consisting of a series of closely spaced parallel plates held within the mould. By means of this technique the mortar beams produced carried a load four times the amount of the load sustained by the matrix alone, compared with about twice the matrix load for normally compacted beams of similar volume concentrations of Duoform fibres.

A comparison with the tensile strengths obtained in the commercial grades of asbestos cement can be obtained by reference to Allen's[32] work. He studied semi-compressed and fully compressed asbestos cement sheet in tension, both parallel and at right angles to the direction of preferential fibre alignment. Typical values quoted for the ultimate tensile strength of semi-compressed asbestos cement sheet were 16.1 N/mm^2 parallel to the direction of preferential fibre alignment and 9.5 N/mm^2 at right angles to this direction. For fully compressed sheets, corresponding values of 27.1 N/mm^2 and 17.2 N/mm^2 were obtained. The ultimate tensile strengths of a fully compressed material being considerably higher than the semi-compressed sheet, due to the reduction in the void content.

From this brief review of tensile strength investigations, it can be seen that technically the most effective fibre for cement paste reinforcement is carbon. However, the use of carbon fibre cannot be justified except for very specialised applications, where it may become

cost competitive with other fibres.

2.1.3.2 Flexural strength

While the tensile strength of a material is a more fundamental property[17] than the flexural strength, there are considerable experimental difficulties in carrying out uniaxial tensile tests on a brittle material without introducing bending moments or having premature failure at the grips[33]. Accordingly the flexural test is frequently used, because it is relatively easier to carry out and it also simulates in use load conditions more closely than a direct tensile test.

In tests for flexural strength, the results depend to some extent on the method of loading and on the dimensions of the test specimens, as has already been discussed. It has been observed that the modulus of rupture of a beam loaded at one third points of its span tends to be lower than if it were loaded at its centre. The reason for this is that, under third point loading, the whole of the central third portion of the beam is under maximum stress, so that there is more opportunity for the weak points to show themselves than under central loading, in which only the immediate vicinity of the centre is loaded to a maximum.

In addition to the strength differences observed in flexure compared with tension, differences occur in the elastic moduli, the flexural modulus being also dependent upon span and specimen dimensions. However, the greatest differences between the results of the two types of test arise in the non-elastic region.

Hannant[34] has explained theoretically the relationship between tensile and flexural characteristics during non-linear or pseudo plastic deformation. His analysis is based on a simplifying assumption regarding the shape of the stress block in the tensile zone after cracking, ignoring the detailed effects of fibre type, fibre volume, fibre length, water/cement ratio, age, curing conditions and crack width. Using the principle of moments of resistance, a relationship is obtained between the force carried by the fibres and the tensile cracking strength of the composite. The relationship obtained implies that provided the post-cracking strength in direct tension exceeds 0.41 of the first crack strength, then post-crack flexural strengthening can occur. This analysis is useful in determining the minimum fibre volume necessary for strengthening in flexure and this can be much lower than that required in tension.

Swamy et al[35] have presented a theory to explain the fracture behaviour of fibrous concrete reinforced with short discontinuous steel fibres randomly oriented and uniformly dispersed in concrete. Their approach has been to modify the conventional law of mixtures equation, to take into account the effect of random fibre distribution and the load transfer mechanism from matrix to fibre, giving:

$$\sigma_c = \sigma_m V_m + 2\tau\left(\frac{\ell}{d}\right) 0.41 V_f \qquad .. \quad .. \quad .. \qquad (2.7)$$

where $0.41V_f$ is the effective volume of fibres in the direction of stress and $2\tau\left(\frac{\ell}{d}\right)$ represents the stress supported by the fibres.

σ_c is the stress in the composite

σ_m is the stress in the matrix

ℓ is the fibre length

Equation (2.7) can be used to predict the first crack tensile strength and ultimate tensile strength of concrete reinforced with randomly oriented short discontinuous fibres. It can equally be applied to fibre reinforced mortar and paste without loss of generality.

Lankard[36] also investigated steel fibre reinforced concrete and found a 1.5 to 3.0 fold improvement in the flexural strength.

Marsh et al[37] have studied the effects of alkali-resistant glass fibres on the physical properties of concrete. Fibre length, fibre quantity, cement content, water/cement ratio and varying coarse/fine aggregate ratios were used. Their first crack flexural strengths increased up to 3 times, and their ultimate flexural strengths increased by 4.9 times the strength of the non-reinforced concrete. In general, the rate of the strength increase tended to decrease as the volume percentage of the fibres was increased. This was believed to be due to the greater difficulty in achieving a completely uniform fibre distribution and a wetting of the fibre surface area as the fibre content was increased.

Ali et al[38] made specimens using 30g of cement and 0.25g of carbon fibre distributed near one face only. These specimens were tested for bending strength, with the fibre reinforced surface in tension. They concluded that even small additions of carbon fibres improved the strength and stiffness of the cement in a significant way, i.e. modulus of rupture, with values of 51.1 N/mm^2 being obtained for specimens cured in water for 7 days.

Flexural strengths[39] of cement mortars using up to 7% by volume of sisal fibres, showed significant increases in strength, by factors exceeding three.

Typical values of moduli of rupture[40] for fully compressed asbestos cement sheets, quoted by the manufacturers, lie in the range 43-59 N/mm^2 in the direction of preferential fibre alignment.

Most workers agreed on an improved flexural strength with increasing fibre volume fraction. Important differences compared to the uniaxial tensile behaviour are the effects of specimen size and shape, which can cause significant variations in property values. The measured flexural moduli of rupture of fibre reinforced cementitious matrices do not correlate very well with uniaxial tensile strengths.

It can be concluded that significant improvements in flexural strength can be achieved with a range of fibre types, with carbon fibre probably the most technically effective. It appears that less are required to achieve post-crack strengthening in flexure than in tension. Other important differences between flexure and tension are the effects of specimen size and shape, and test configuration, which can cause significant variations in property values measured in flexure.

2.1.3.3 Impact strength

One of the important parameters that has to be considered in designing fibre reinforced composite structures, is the rate of loading. Since many applications of such structures involve very rapid rates of loading, i.e. impact loading.

The effects of specimen shape and size are even more important in impact tests than in flexure, as the actual test arrangement can influence significantly the results, as has been pointed out by Bader[41], who suggested that they were the major factors in

explaining the many discrepancies that exist in impact testing.

A review of impact literature is outside the scope of the present study, but the general point regarding the sometimes conflicting requirements of tensile or flexural static strength and impact resistance should be noted for fibre composites. In order to have good impact resistance, which is often synonymous with fracture toughness, it is necessary to have internal mechanisms for dissipating the energy, thus sliding within the fibre bundles, pull-out of the fibres and frictional movement between the fibre and matrix can provide such dissipative mechanisms and so improve impact resistance. Nak-Hosung et al[42] have shown that fracture toughness of a fibre reinforced composite can be improved by applying a viscous coating at the fibre/matrix interface. However, such phenomenon should reduce the static properties of the composite.

Ali and Singh[43] carried out tests on glass fibre reinforced gypsum and found that higher volume percentages of fibre content increased the porosity of the specimens. The role of increased porosity in lowering the fibre/matrix interfacial bond provided a mechanism of fibre debonding and pull-out under impact and hence increased the impact strength. A maximum impact strength value of 58 kJ/m^2 was obtained for a composite consisting of 8% by volume of 43 mm long fibres.

The extremely low impact resistance of asbestos cement[44] is probably due to well bonded short fibres providing little energy absorption by fibre pull-out during fracture. Fracture energies under impact, of 2 kJ/m^2 have been quoted for fully compressed asbestos cement sheet, which is close to that of the matrix alone.

The major problem in impact testing is separating the amount of energy expended on the test specimens at failure and the energy absorbed by the instrument during test, and hence identifying the internal deformation mechanisms. However, generally it has been found that fibre pull-out plays a dominant role in absorbing impact energy.

2.1.3.4 Bond strength

Two of the more important energy absorbing mechanisms in the failure of fibre composites are[45] fibre pull-out and multiple cracking of the matrix. The former can lead to a substantial increase in the work of fracture and also contributes significantly to the work of fracture. In both processes the bond strength between fibre and matrix is an important parameter. To ascertain the magnitude of bond strength, several investigators have used pull-out tests.

de Vekey et al[46] developed a pull-out technique suitable for determining the interfacial bond strengths for various combinations of fibres and matrix. Pinchin and Tabor[47] studied the factors affecting bond strength between steel wires and cement matrices, with smooth electro-polished and roughened steel fibres being used. Their pull-out tests indicated a major difference between the two types; the roughened fibre had a single pull-out maximum load whilst the smooth fibre exhibited a markedly different behaviour. The force required to continue the pull-out of the fibre decreased sharply after the first failure and then began to increase again, there being a distinct stick-slip movement until a final load, higher than the first failure, was reached.

Naaman and Shah[48] investigated the effects of fibre orientation and the number of fibres being pulled out simultaneously on the interfacial bond strength, between steel fibres and mortar matrices. The fibres

used were smooth, high strength steel wires 25.4 mm long and 0.40 mm in diameter. The embedded length in the pull-out tests was 12.5 mm. Three series of experiments were performed. The first series included pull-out tests on two fibres, which were symmetrically oriented with respect to the loading direction. The angle of orientation, θ, was varied from 0^{o} to 75^{o} in increments of 15^{o}. The second series consisted of pull-out tests on fibres parallel to the loading direction, with the main variable being the number of fibres, from 1 to 36, which were uniformly distributed in the available area. The third series was similar to that of the second one, except that the fibres were symmetrically oriented at an angle of 60^{o}. The authors concluded from the results obtained that:

(A) Pull-out tests on a single fibre indicated that:

(i) Inclined fibres with an angle of orientation of up to 75^{o} show a peak load of the same order as parallel fibres ($\theta = 0^{o}$)

(ii) The pull-out work of inclined fibres is higher than that of parallel fibres and seems to reach a maximum for $\theta = 45^{o}$

(iii) The pull-out distance, for the same embedded length, decreases with θ when $\theta > 45^{o}$, due to the disruption of the concrete wedge at the root of the fibre

(iv) The fail load observed just before complete pull-out for $\theta > 0^{o}$, depends on the value of θ.

(B) Pull-out load tests on increasing numbers of parallel fibres ($\theta = 0^{o}$) showed that for a number of fibres between 1 and 36, there was no substantial decrease in the peak load and pull-out work per fibre compared with the measurement on one single fibre.

(C) Pull-out load tests on an increasing number of fibres inclined at 60^{o}, have shown that for the peak load, the pull-out work and the pull-out distance per fibre decreased significantly when the

number of fibres pulling out of the same area increases.

Opoczky and Pentek[49] give some indication on how the bond between fibre and cement can be effected by natural weathering. They have examined asbestos cement sheets at the ages of 2, 16 and 58 years and found that asbestos fibres do suffer a certain amount of corrosion, which is compensated for in terms of composite strength by an increase in bond between the fibre and cement. The corrosion of the fibre is promoted by the presence of airborne carbon dioxide which causes surface carbonation of the fibre. Also certain reaction products may be formed.

In conclusion, it is generally agreed that the efficiency of discontinuous fibre reinforcement for strengthening can be increased by increasing the bond strength at the fibre/matrix interface and/or by aligning the fibres with the loading direction.

2.1.4 Polypropylene Fibre Reinforced Cementitious Matrices - State-of-the-Art

2.1.4.1 Introduction

Polypropylene fibres[50] have a low elastic modulus, high Poisson's ratio and poor physico-chemical bonding with cement pastes. They have, therefore, rarely been considered as promising fibres for the reinforcement of cement and mortars, as they are unlikely to induce closely spaced multiple cracking.

In practice, if fibres[51] are not uniformly distributed throughout the matrix, the end product may have a lower strength value than if it were left unreinforced, due to zones of less reinforcement creating notch effects. Some type of bond, whether mechanical or

chemical, is thought to be important, because it has been suggested that aligned round polypropylene monofilaments could debond in an unstable fashion at a crack due to the high Poisson contraction and hence eliminate the possibility of multiple cracking.

2.1.4.2 Tensile strength

Hannant et al[50] have used an open polypropylene network of continuous fibrillated film incorporated with a cement mortar, to produce a composite with high tensile strength, combined with fine multiple cracking. A typical load-extension curve exhibited a linear region followed by a substantial non-linear portion. This results in a cement based material with high pseudo ductility. Such a material allows the production of economic thin sheet products suitable for replacing asbestos cement in some applications.

2.1.4.3 Flexural strength

Mackintosh[52] gives an account of the effect of short monofilament polypropylene fibres on various concrete mixes. Optimum fibre lengths and diameters are identified. The ultimate flexural strength was influenced by the fibre spacing, with spacings of 5 mm giving an increase of 50% over the plain concrete. It was also found that a water/cement ratio of 0.55 gave optimum results. Hughes and Fattuhi[53] also tested polypropylene reinforced concrete beams in bending and found that increasing the coarse aggregate content generally resulted in decreasing the strength of the composite, which was possibly due to inadequate compaction of the matrix and non-uniform distribution of the fibres. Nanda[54] has reported that polypropylene fibres gave an increase in flexural strength of 1.07 times that of an

unreinforced concrete specimen. He also showed that polypropylene fibres did not affect the shrinkage properties of the concrete. It was shown by Hannant et al[50] that the inclusion of continuous opened polypropylene fibrillated films in cement mortars can more than double the load capacity of such beams and can produce closely spaced multiple cracking.

2.1.4.4 Impact strength

Goldfein[55] in his work stated that nylon, polypropylene, polyethylene and saran, gave the greatest impact strength to cement matrices in the order listed. Raouf et al[56] also carried out impact tests using small explosive charges in contact with their specimens. Ordinary Portland cement of water/cement ratio 0.3 was used as the matrix material, with polypropylene fibres as the reinforcement. The fibre orientation was random and the specimens were cured for 28 days inside sealed plastic bags. Specimens with 1.71% by volume of polypropylene exhibited hairline cracks and no spalling occurred. Fairweather[57] carried out full scale testing on concrete piles containing fibrillated polypropylene fibre and found good resistance to very high impact loading.

The most likely explanation for the high impact resistance of cement composites reinforced with polypropylene fibres is partly due to the large amount of energy absorbed in debonding, stretching and pulling out of the fibres which occurs after the matrix has cracked.

2.1.4.5 Bond strength

Walton and Majumdar[58] carried out simple pull-out tests on polypropylene monofilament fibres embedded in matrices of cement paste. Fibre embedment lengths of 10 mm and 20 mm were selected and cement pastes of water/cement ratios of 0.3, 0.35 and 0.4 were used. The strength of the cement pastes mainly depended on the water/cement ratio. In their pull-out tests, a 0.4 water/cement ratio and a 10 mm embedded fibre gave the lowest load. The maximum bond strength measured was 1 N/mm^2 for polypropylene monofilaments. The low value obtained almost certainly means that the bond is entirely frictional in character.

Ritchie et al[59] found that the bond strength of fibres was inversely proportional to the water/cement ratio. Also that the fibre should be straight and not curled when carrying out pull-out tests, so that applied loads would not have to overcome curling.

2.1.4.6 Conclusions

Monofilament polypropylene fibre when incorporated in a cementitious matrix, does not significantly improve its tensile or flexural strength, but considerable improvement is made to its resistance to impact. In the case of fibrillated polypropylene networks in cement paste, very significant improvements to the flexural and tensile strengths are achieved.

Overall, it appears that achieving good bond between fibre and matrix is the most important factor in improving tensile and flexural strength. In the case of impact strength, a good bond may be undesirable, as it reduces the energy absorbing capability of the material by minimising fibre pull-out.

POLYPROPYLENE FIBRE AND MATRIX

CHAPTER THREE

POLYPROPYLENE FIBRE AND MATRIX

3.1 PREAMBLE

The mechanical properties of fibre reinforced composites are dependent upon the mechanical properties of each component and their physico-chemical interactions.

This chapter is divided into two parts, A and B, which give details of polypropylene fibre and matrix respectively.

Part A is concerned with identifying the relevant properties of polypropylene fibre and the extent to which they can be modified by manufacturing procedure.

In order to gain experience of fibre manufacture and to understand its limitations, a laboratory extruder was used to produce 15 denier (49 μm diameter) fibre under various conditions, keeping as far as possible two of the following three major parameters constant, i.e. extrusion temperature, haul off speed ratio and roller temperature.

Probably the most important basic polypropylene fibre property is its elastic modulus, since its tensile strength is considerably greater than that of hardened cement paste. In particular the modulus of elasticity at very low strains and high strain rates is thought to be very relevant to fibre composite fracture behaviour.

The majority of the work in part A is therefore concerned with relating modulus of elasticity with fibre manufacturing parameters.

Part B considers the tensile strength and the elastic modulus of hardened cement paste, as these properties contribute directly to the strength and stiffness of the eventual composite.

A. POLYPROPYLENE FIBRE

3.2 MATERIAL

3.2.1 Polypropylene

The general properties of polypropylene include many desirable characteristics which can be utilised for fibre reinforcement of cementitious matrices. Compared with cement[40], polypropylene has a very high chemical resistance, such that the cementitious matrix will always be the first to deteriorate should there be any contact with aggressive chemicals. The hydrophobic surface, not being wet by a cement paste, helps to minimise the chopped fibres from balling up during mixing. Polypropylene has a fairly high melting point for a polymeric material (165^{o}C) and the ability to be used at temperatures over 100^{o}C for short periods. Molecular orientation during manufacture leaves polypropylene films weak in the lateral direction, which facilitates fibrillation. Fibrillation is achieved by generating longitudinal splits into films and can be controlled by the use of carefully designed pin systems on rollers over which the stretched films are led. The cement matrix can therefore penetrate into the mesh structure between the individual fibrils and create a mechanical bond between fibre and matrix. Polypropylene also has a low specific gravity and can be easily handled. Its major weaknesses include combustibility, ultra-violet degradation

and low modulus of elasticity. Since polypropylene is an organic material, it will always be combustible and thus have unsatisfactory fire resistance. Protection from ultra-violet radiation will, of course, be given by the matrix, although ultra-violet stabilisers are also available. The low modulus of elasticity, below that of the matrix, means that the inclusion of fibres will reduce the composite modulus.

3.2.2 Fibres

All the polypropylene fibres used throughout this investigation, whether standard products or specially prepared, were manufactured at Plasticisers Limited, from polypropylene granular stock material supplied by Imperial Chemical Industries.

Brief descriptions of the types of fibre and tape used during the investigation are given below:

(A) Continuous monofilament fibres, having a mean diameter of 340 μm and a tangent modulus of elasticity at 1% extension of 4.92 kN/mm^2. These fibres will be referred to subsequently as fibre type A. See Plate 3.1.

(B) Continuous monofilament fibres, having a mean diameter of 340 μm and a tangent modulus of elasticity of 2.23 kN/mm^2. These fibres were specially prepared on a laboratory extruder and will be subsequently referred to as fibre type B.

(C) Continuous monofilament fibres, having a mean diameter of 49 μm, with a range of values of tangent modulus of elasticity. These

PLATE 3.1 - CONTINUOUS MONOFILAMENT FIBRE WOUND ON MANDREL (TOP)
AND CHOPPED POLYPROPYLENE FIBRE (BOTTOM)

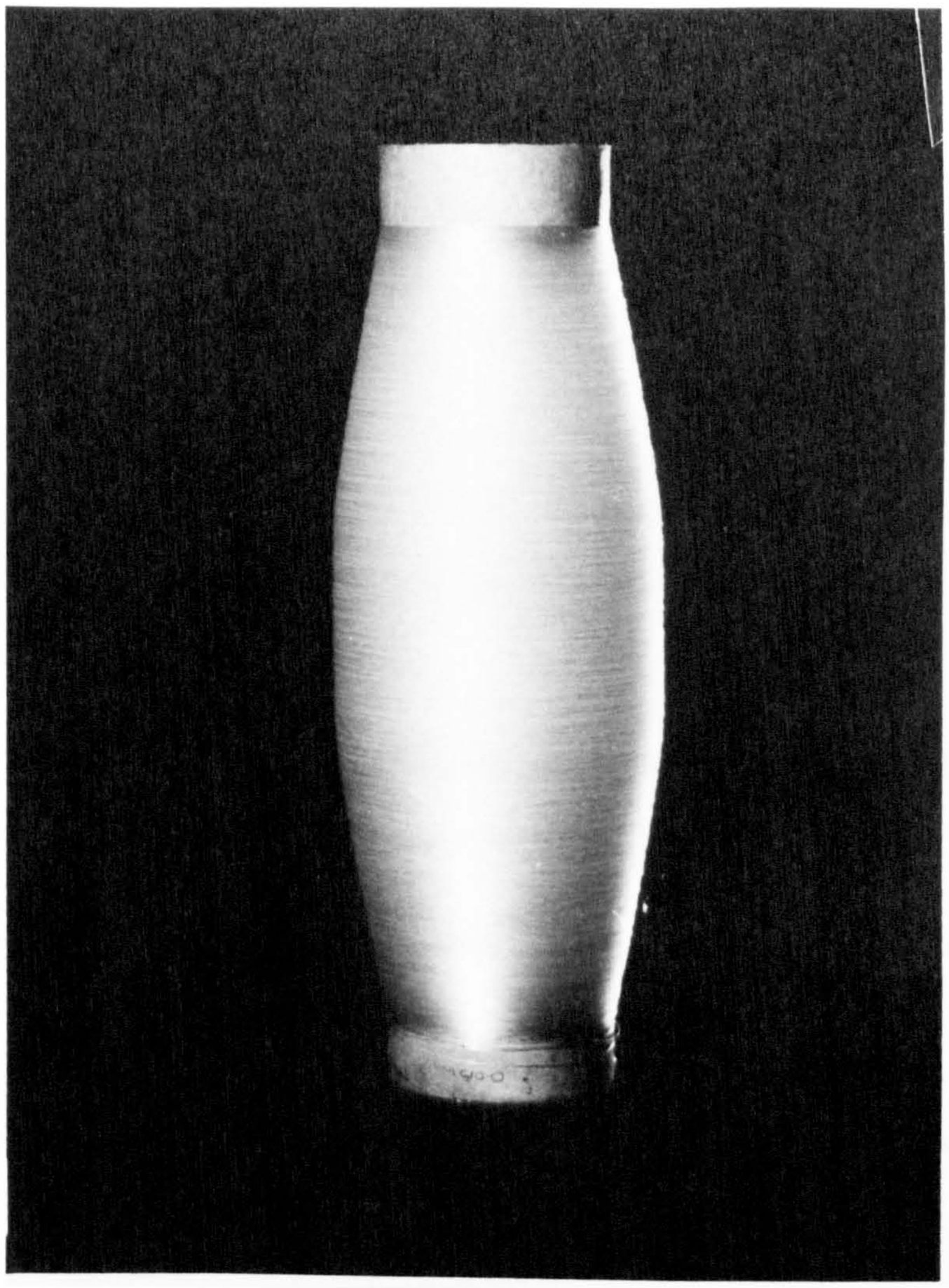

fibres were also prepared on a laboratory extruder and are the subject of investigation under the present chapter.

(D) Continuous tape of 1178 μm wide by 46.7 μm thick, having a modulus of elasticity value of 10.0 kN/mm^2, subsequently referred to as tape type A.

(E) Continuous tape of 1746 μm wide by 42.6 μm thick, having a modulus of elasticity value of 4.4 kN/mm^2, subsequently referred to as tape type B.

(F) Straight brush filament of 340 μm diameter and having modulus of elasticity value of 3.8 kN/mm^2.

(G) Chopped fibres of lengths 10, 26 and 60 mm obtained from brush filament mentioned in (F) above. See Plate 3.1.

The monofilaments and brush filaments were obtained by a straightforward extrusion process, see section 3.3.

The tape was obtained by slitting an extruded film. It is interesting to note that although the manufacturing processes of continuous monofilaments and brush filaments were the same, the continuous monofilament tended to have a spiral shape in its equilibrium state. The reason for this was that the fibres were wound warm on to a circular mandrel at the end of the production process, thus taking the shape of the mandrel upon cooling, whilst the brush filaments were cooled first before being wound on to a large square drum, the fibres being subsequently cut at the corners of the drum.

3.3 FABRICATION STUDY

3.3.1 Laboratory Extruder

Details of the laboratory extruder are shown in Plate 3.2 and a description of the prominent features of the extrusion equipment is given below:

(A) Extruder:

The extruder must be capable of delivering a homogeneous melt at high temperature and at high output rates. The high temperature ensures the minimum amount of surface irregularity in the extruded melt. For polypropylene extrusion, the optimum melt temperature is around 220^{o}C.

(B) Adaptor:

The adaptor connecting the extruder to the die is designed to ensure a non-turbulent flow of the melt, such that there are no dead spots where the melt can remain stagnant and oxidise. The adaptor is heated uniformly and fitted with a thermocouple, which protrudes into the melt stream to indicate the true temperature of the material.

(C) Die:

The die must be maintained at a standard temperature across its full width. A die plate consisting of 180 holes, with each hole of 0.4 mm diameter being used to obtain a 15 denier (49 μm diameter) fibre. The calculation of denier size was carried out by using the following formulae.

$$\text{Denier per filament} = \frac{\text{Weight of (25 metres) fibres in grammes} \times 9000}{25\,(\text{metres of fibre}) \times \text{no. of filaments (i.e. no. of holes in plate)}}$$

PLATE 3.2 - LABORATORY EXTRUDER

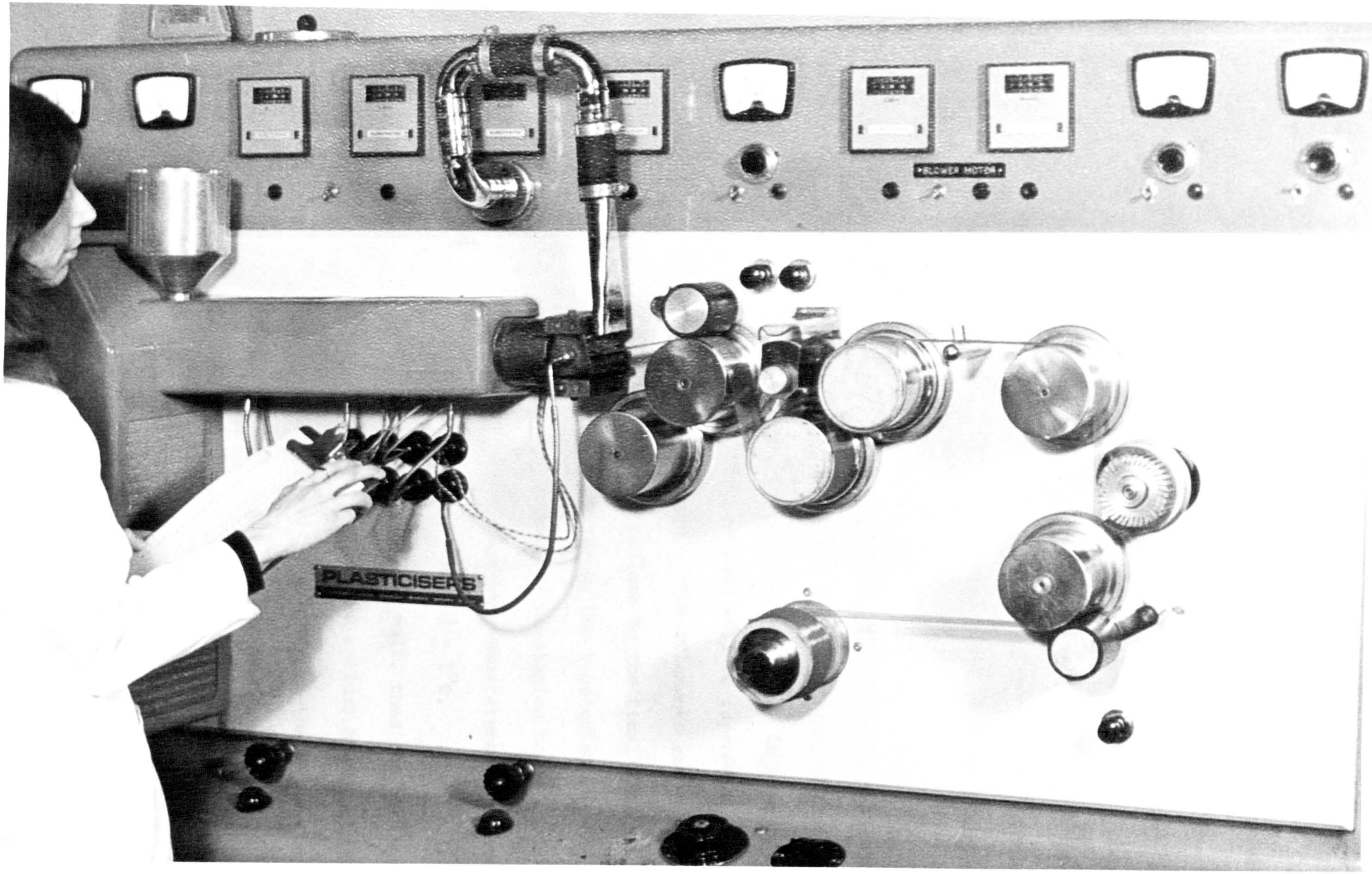
BLOWER MOTOR
PLASTICISERS

(D) Air Knife:

This is a device in which air is pumped into a tube, the longitudinal axis of which is parallel to the chill roll. The air emerges from the tube through an accurately controllable slot so that a fine jet of air impinges on the surface of the extruding melt at its point of contact with the chill roll. The use of the air knife increases the cooling rate. Excessive air pressure can produce air turbulence in the region of the extruding melt, causing the melt to vibrate.

(E) Chill Roll:

After passing under the air knife the melt is cast on to a highly polished water cooled steel drum. The surface of the chill roll is normally chrome-plated and highly polished. Any imperfections such as surface scratches or indentations will be reproduced on the filaments being made on the unit. The filaments are then passed via an idler and tensioning rollers to the final wind up station. The speed of the chill roll to the tensioning rollers can be varied. This allows the filament tensioning to be controlled. It is very important that the temperature gradient across the chill roll face should not exceed $\pm$ 1^{o}C. If a temperature gradient does exist across the roll, then the cooling of the filaments will not be uniform and the optical homogeneity of the film will be affected. The temperature of the filaments when it reaches the final wind up station should be as close as possible to the ambient room temperature. If this is not the case, then cooling continues after winding and shrinkage on the reel will result. In turn, such shrinkage will produce variations in the filament thickness.

(F) ..Haul-off Unit:

The remainder of the production line after the chill roll consists of a series of tensioning rollers (the temperature of which can be varied), with the final tensioning roll (which is set at the ambient room temperature) for tensioning purposes. The final wind up station possesses a wide range of tensioning control, which is self-compensating as the roll diameter increases. The mandrel, on to which the filaments are finally wound, is light, strong and readily detachable.

This equipment was used to study the factors which may influence the modulus of elasticity of polypropylene fibre. The parameters which were studied and thought at the time likely to influence the modulus of the fibre were:

(A) Extrusion temperature

(B) Haul-off speed ratio

(C) Hot roller temperature.

The intention was to study each parameter separately, with the other two parameters kept constant as far as possible.

3.4 TEST PROCEDURE

3.4.1 Tensile Modulus of Elasticity

An Instron model 1026 tensile test machine was used to determine the tensile properties of the 15 denier fibres. This instrument will measure tensile loads from 0-50 g to 0-500 kg full scale, at test speeds in the range 50-500 mm per minute. The load weighing accuracy of the 1026 is $\pm$ 0.5% of the scale in use, and a strip chart recorder has a pen response of approximately 0.5 seconds full scale. A 50 g load

cell was found to be adequate to carry out the tests. The fibres were gripped between the gripping faces pneumatically, with an air pressure of 0.5 N/mm^2.

The extension of fibre was measured directly from the cross-head movement using a standard 200 mm length of fibre between the grips.

The fibre diameter was checked by looping the fibre and measuring the diameters with an electronic micrometer at the apex of the loop parallel and perpendicular to the plane of the loop. This identifies the maximum and minimum diameters. It was found that the fibre was slightly eliptical in cross-section.

3.4.2 Determination of Elastic Modulus at Low Strain Using a Contraves Extensometer

To determine the elastic modulus of a fibre at low strain level, it is essential to have a straight fibre, without waves as far as possible, so that measurements can be made accurately. To satisfy this condition, a straight polypropylene brush filament of 340 μm diameter was used.

A Contraves extensometer (Plate 3.3) was used in conjunction with a Losenhausen test machine's strain socket, so that the signal output from the Contraves extensometer could be read on the Losenhausen panel in a digital form.

The Contraves extensometer consisted of an accurately pivoted probe, friction free as far as possible at the pivot and balanced by light weights at the other end, the free end being capable of moving either upwards or downwards.

PLATE 3.3 - CONTRAVES EXTENSOMETER USED TO DETERMINE ELASTIC MODULUS OF 340 μm DIAMETER FIBRE AT LOW STRAIN

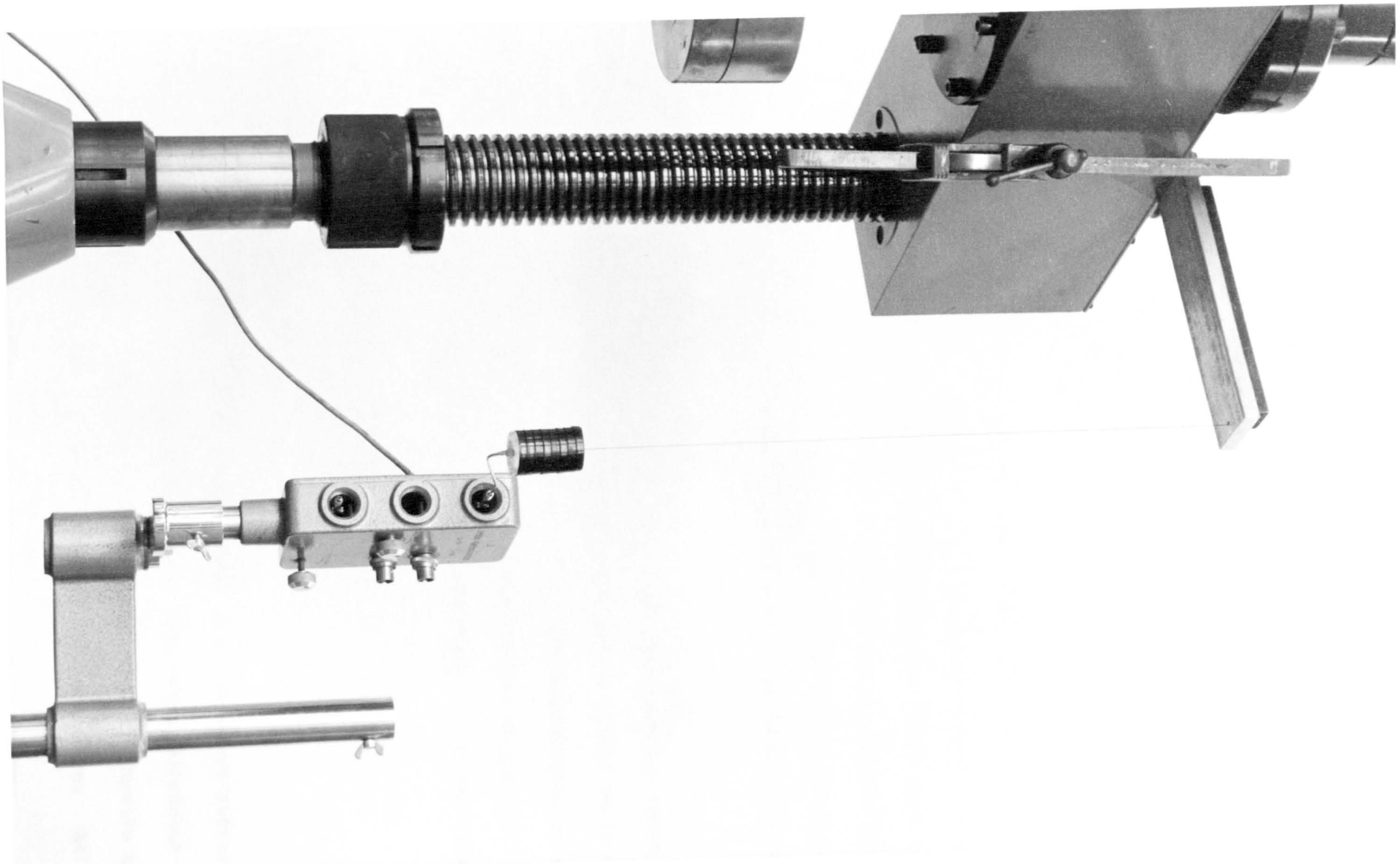

Calibration of the Contraves extensometer was carried out by using a micrometer screw, which was used in conjunction with the probe, a set movement of the probe being calibrated to the digital output of the Losenhausen. This was carried out several times to ascertain the average readings for a millimetre set movement of the micrometer screw.

A fibre of length 530 mm (a long length taken to minimise errors) and weighing 0.0516 g was used. One end of the fibre was fixed to the metal bar containing a small hole to receive the fibre, whilst the other end of the fibre was fixed to a light circular perspex tablet with a small hole at the centre. The tablet acted as a base to receive the dead weights placed upon it and a datum point for the Contraves probe. The fibre ends, perspex tablet and the probe were fixed by means of an araldite adhesive.

The fibre was loaded in increments of 4.54 g and with each increment the digital output was recorded; this procedure was continued until a fibre strain of 0.58% was reached, subsequently the dead weights were then removed at 4.54 g decrements and again the digital output was recorded, this was carried out to check for permanent set in the fibre.

3.5 ANALYSIS AND DISCUSSION OF RESULTS

3.5.1 Laboratory Extruder

15 denier (49 μm diameter) fibre was produced on a laboratory extruder by varying only a single parameter at a time, i.e. either extrusion temperature, haul-off speed ratio or roller temperature. Tensile tests were carried out at a constant cross-head speed of 500 mm/min. At

least ten specimens were tested for each given condition. Details of the various production conditions are given in Fig. 3.1 to Fig. 3.4.

Tensile tests on the fibres were also carried out at different cross-head speeds, i.e. 10, 100, 200 and 500 mm/min. for fibres produced with extrusion temperature of 220°C, roller temperature of 100°C and with haul-off speed ratios of 1:1, 1:2, 1:3, 1:4 and 1:4½. This was done to ascertain the effect of rate of test on the modulus of the fibres, see Figs. 3.5 and 3.6.

Two methods were adopted for the calculation of the modulus of elasticity of the fibres. First a chord modulus was calculated; the chord was drawn between two points on the load versus extension curve, namely 2.5% and 5.0% extension. The chord modulus was calculated to avoid any ambiguity and the method was adopted for all the curves, so that a systematic comparison could be made. Secondly, a tangent modulus was calculated for all the curves, the tangent was drawn at 0.0% extension, to obtain information at very low strains, however, there is considerable uncertainty in the graph shape at this early stage. Both methods of ascertaining the modulus, however, approximate the actual non-linear curve to a straight line, therefore only an estimate of the modulus is obtained.

Graphs of the elastic modulus of fibres versus extrusion temperature show that at 190°C the chord modulus is 1.2 kN/mm^2, whereas the tangent modulus has a much higher value of 3.0 kN/mm^2. However, for both chord and tangent modulus there are no significant changes in the modulus in the temperature ranges investigated, i.e. 190°C to 220°C. Practical difficulties however start to arise if the extrusion temperature drops below 190°C, in that the polymer viscosity changes and this in turn

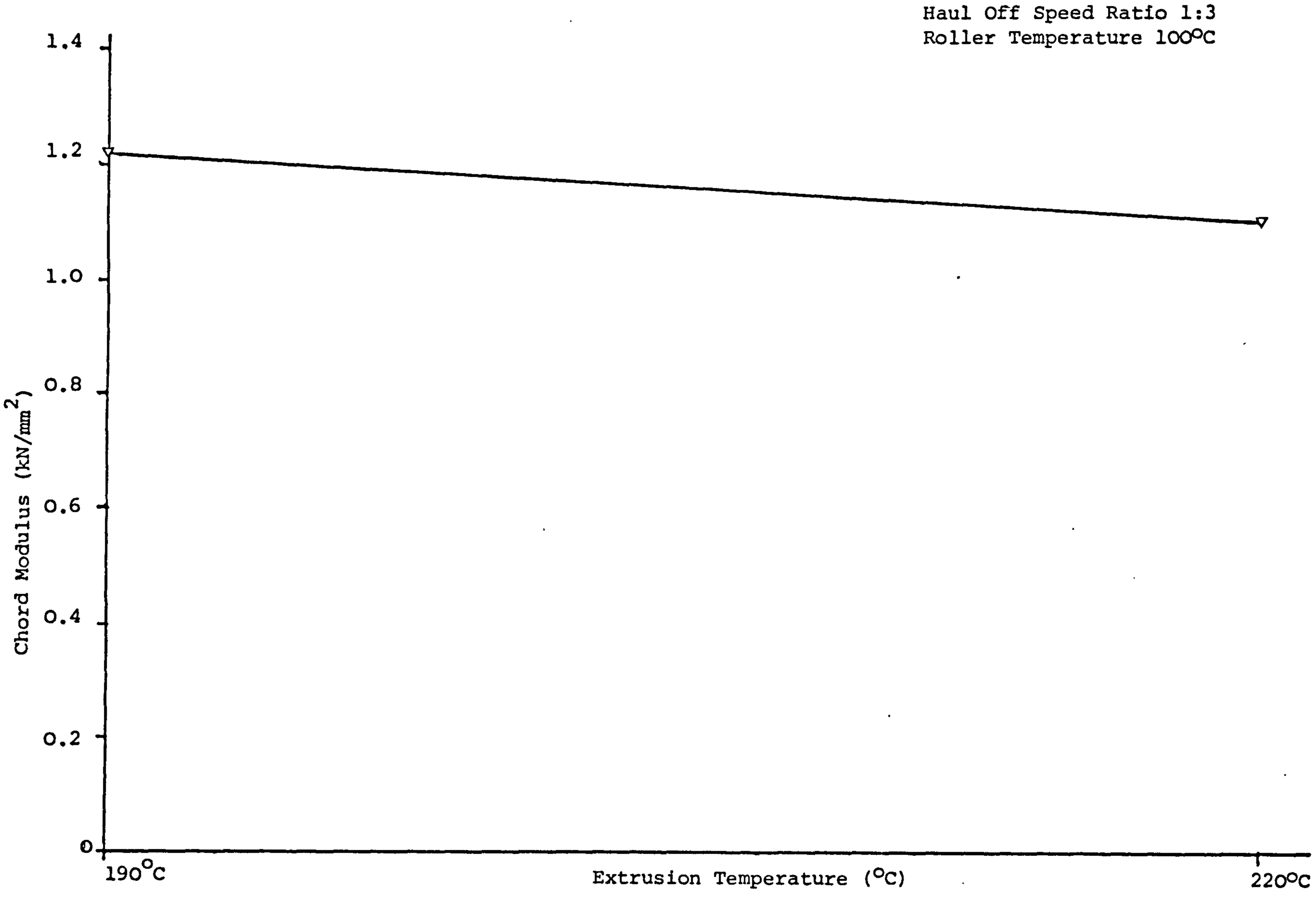

FIGURE 3.1 - CHORD MODULUS v EXTRUSION TEMPERATURE

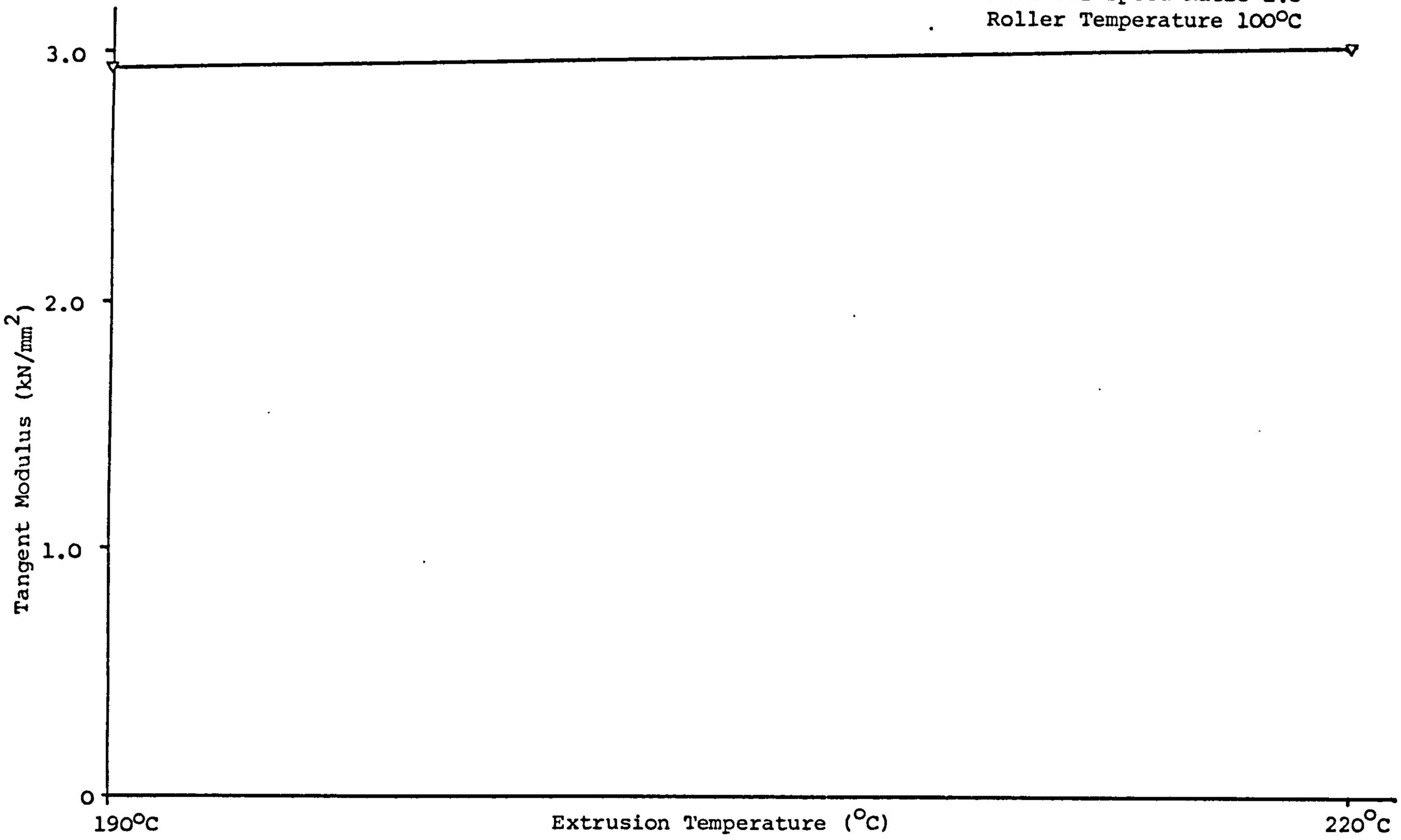

FIGURE 3.2 - TANGENT MODULUS v EXTRUSION TEMPERATURE

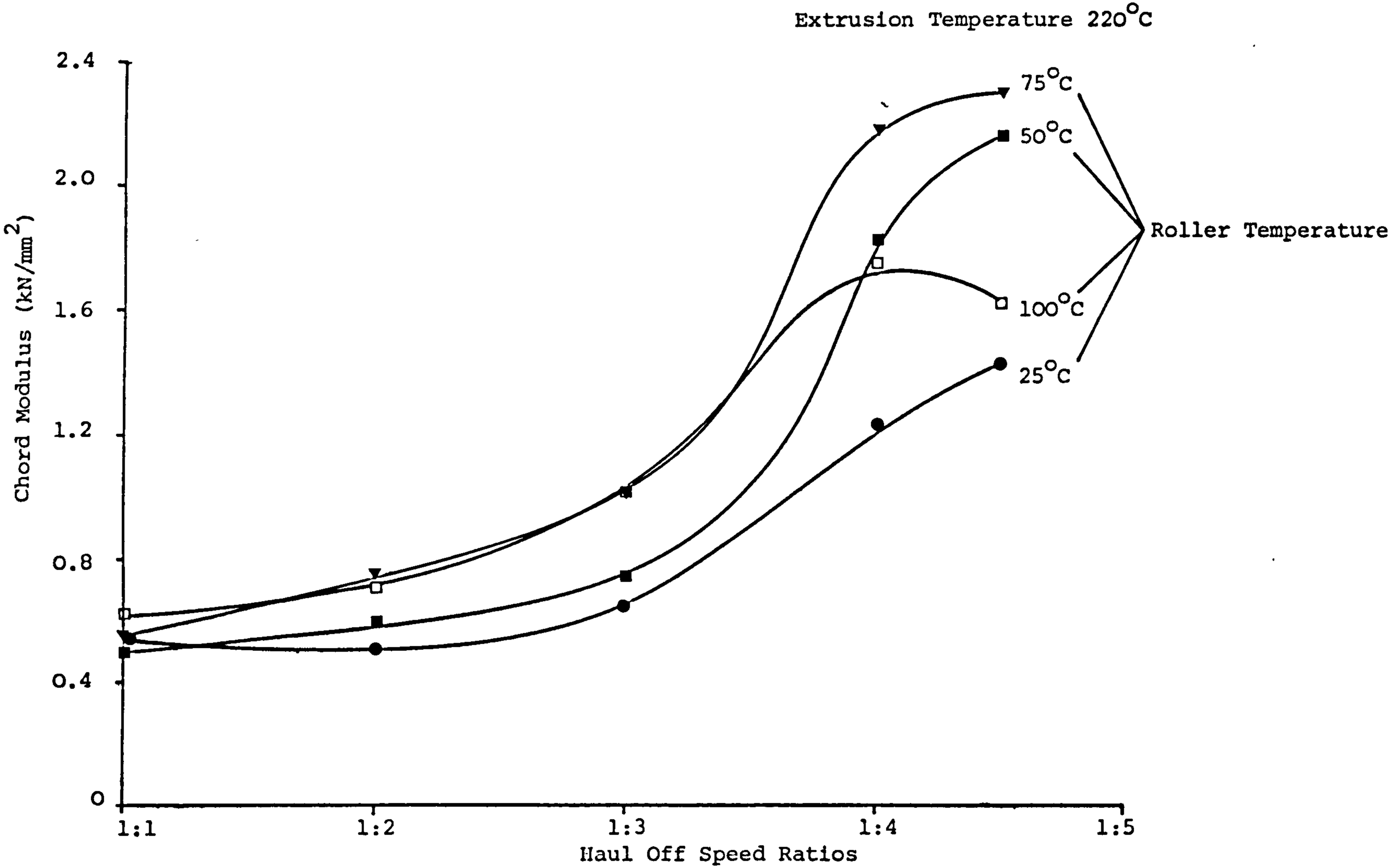

FIGURE 3.3 - CHORD MODULUS v HAUL OFF SPEED RATIOS AND ROLLER TEMPERATURE

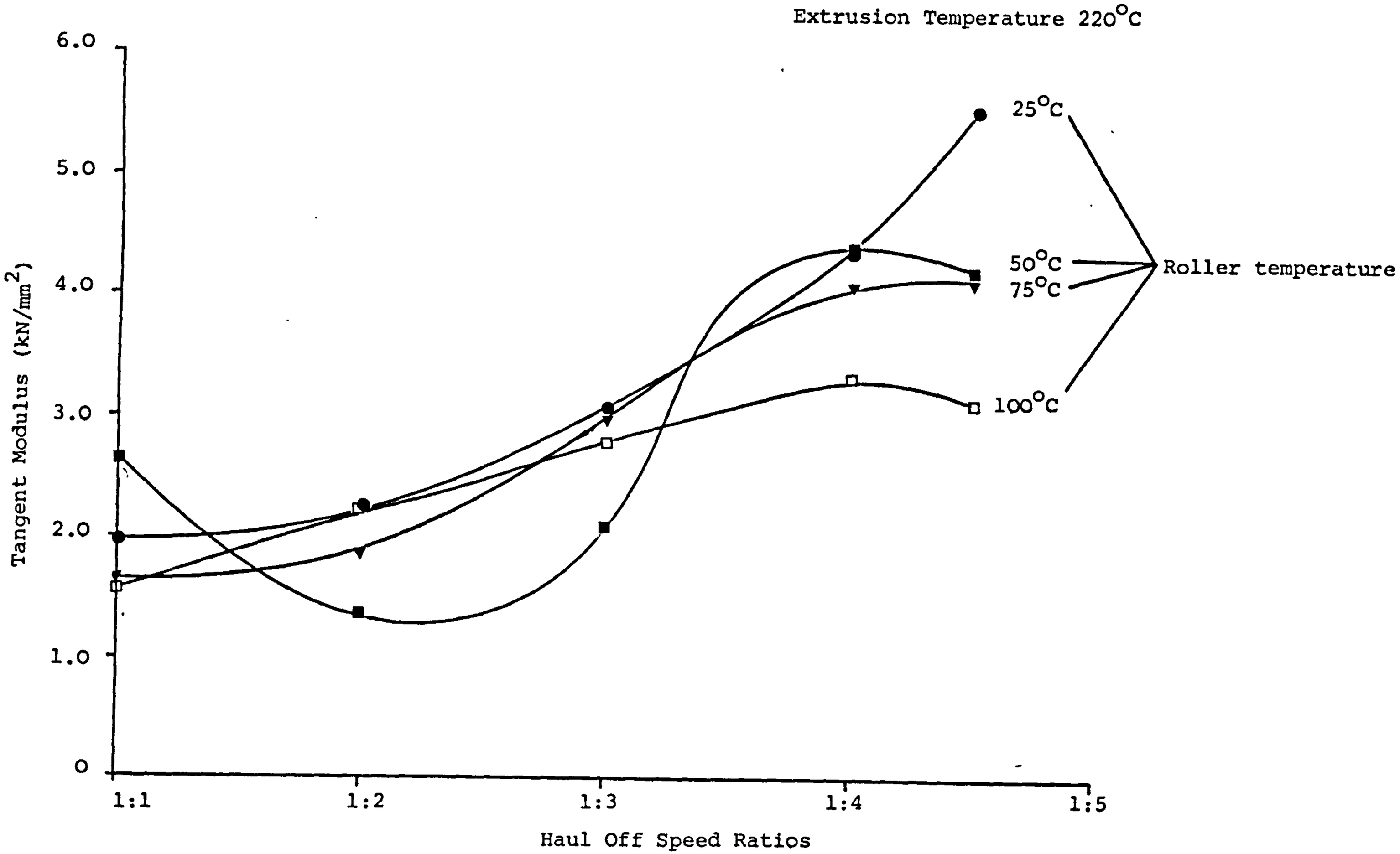

FIGURE 3.4 - TANGENT MODULUS v HAUL OFF SPEED RATIOS AND ROLLER TEMPERATURE

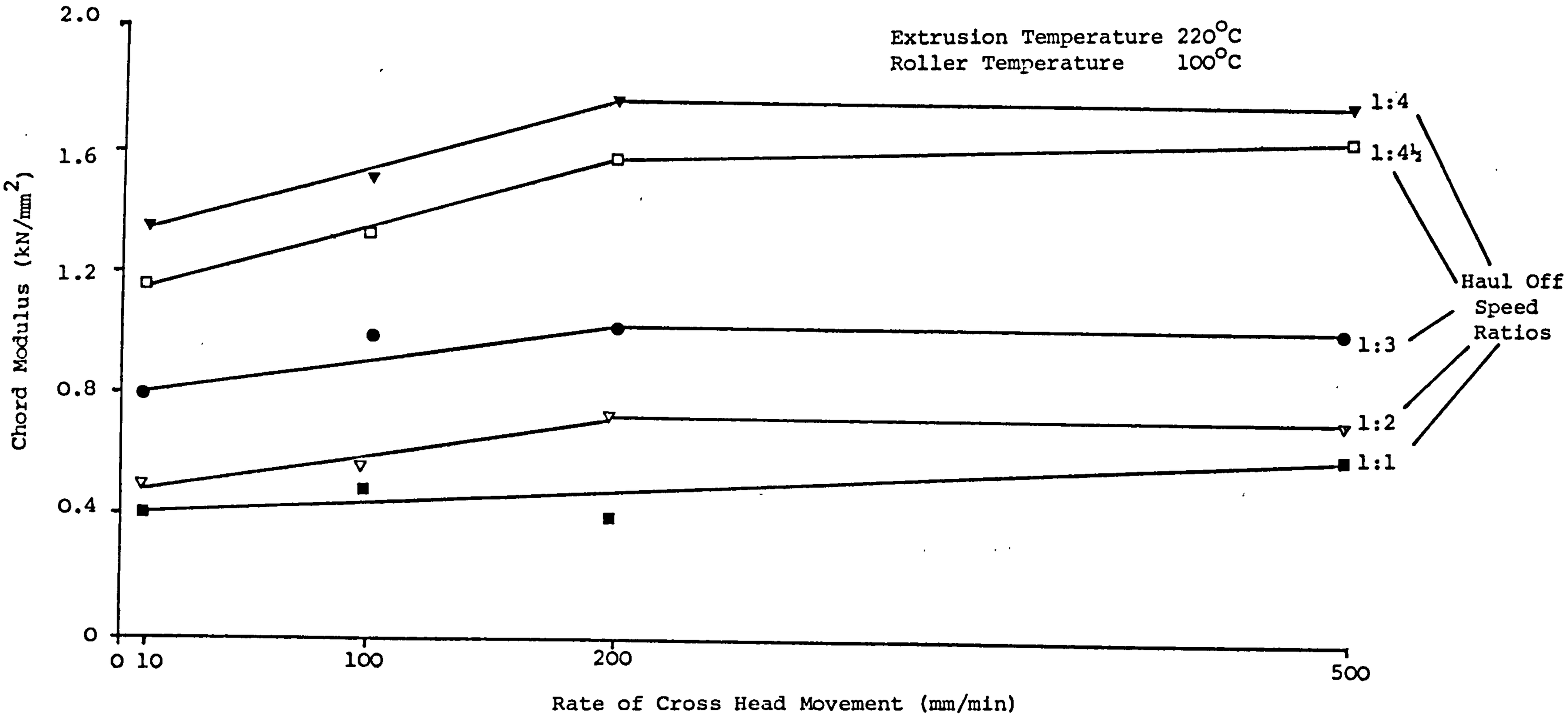

FIGURE 3.5 - CHORD MODULUS v RATE OF CROSS HEAD MOVEMENT OF INSTRON TEST MACHINE

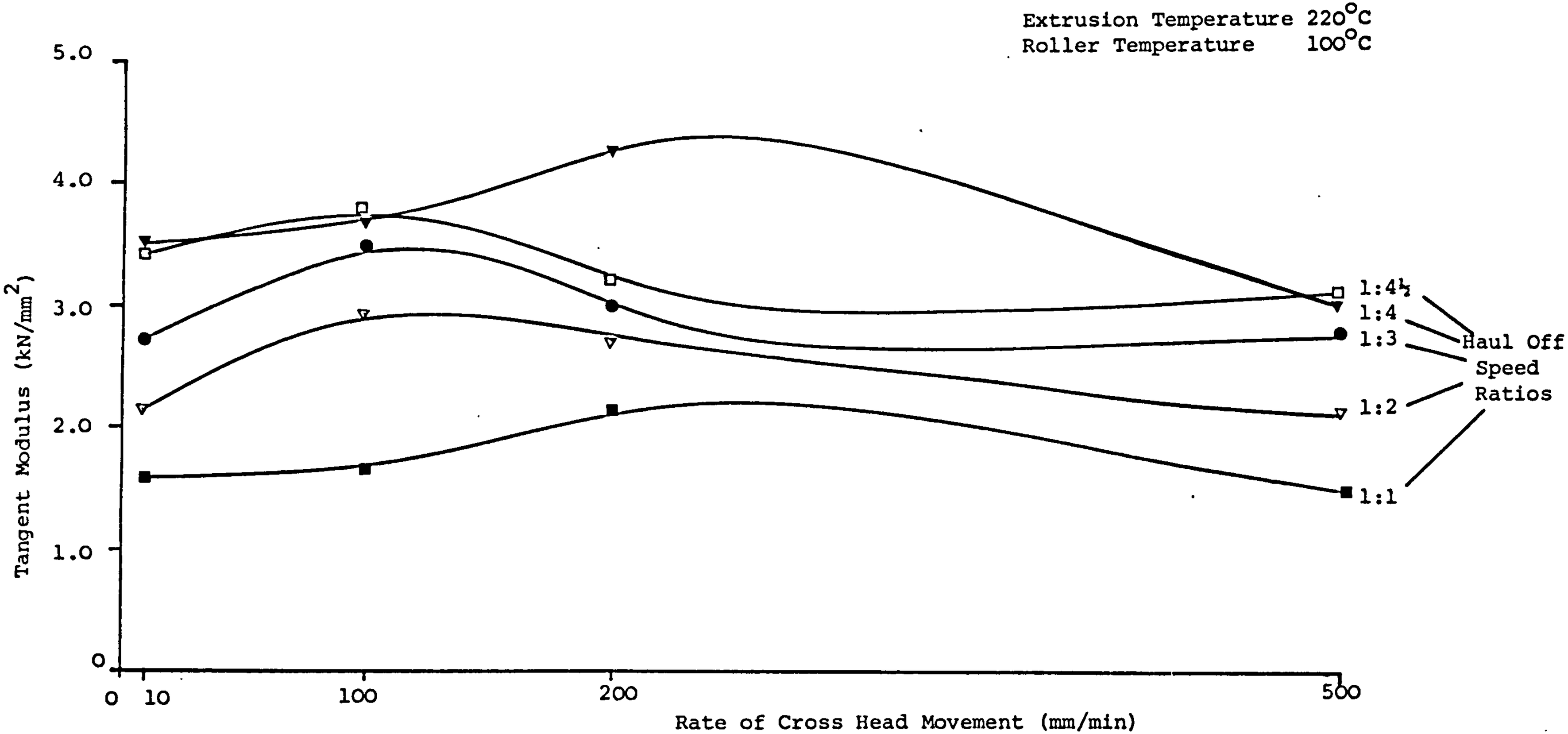

FIGURE 3.6 - TANGENT MODULUS v RATE OF CROSS HEAD MOVEMENT OF INSTRON TEST MACHINE

affects the flow characteristics of the melt. If the extrusion temperature exceeds 220°C, there is difficulty in maintaining a uniform high melt temperature.

It can be seen from Figures 3.3 and 3.4 that a haul-off speed ratio of 1:4½ gave optimum modulus values.

The optimum hot roller temperature was found to be 75°C for the chord modulus, whereas a 25°C roller temperature gave the optimum value for the tangent modulus. The reason for this is not known.

The purpose of the haul-off hot roller stage is to enable stretching of the fibres to be carried out. Over-stretching, by increasing the haul-off ratios may cause the fibre to become brittle and white. The stretching process is very important and if adequate haul-off speed ratios are used then favourable molecular orientation can take place.

The effect of rate of straining during testing is shown in Figures 3.5 and 3.6; it can be seen that it has only a small effect on both the chord and tangent moduli for the range investigated. In the case of chord modulus there is a slight linear increase (25.0% maximum) up to 200 mm/min cross-head movement with no further increase beyond this. In the case of the tangent modulus there appears to be optimum values of modulus around 200 mm/min. However, the error in identifying the value of tangent modulus is such that a more realistic interpretation is probably that there is no significant effect on tangent modulus.

It is thought that the rate of load transfer to the fibre during cracking of a composite will be very similar to impact loading. Therefore, the implications of these results for fibre composite

behaviour, is that there will be no significant difference between modulus values for impact and rapid dynamic loading.

3.5.2 Elastic Modulus at Low Strain

It is extremely difficult to measure elastic modulus of fibres at low strain, since even the weight of the fibre may influence the extension readings. It is therefore difficult to decide when a fibre has a zero strain level. With this in mind, the graph of stress versus strain was plotted (see Fig. 3.7) and the slope of the graph which was linear gave an elastic modulus value to be 3.86 kN/mm^2 for the polypropylene brush filament, which compares well with the tangent modulus value (3.8 kN/mm^2) obtained by carrying out tests on a similar fibre on an Instron 1026 test machine at a cross-head speed of 1 mm/min.

Upon unloading the fibre by removing the dead loads at a steady rate, a non-linear relationship was obtained with a permanent set of approximately 0.188% strain. This non-linearity is typical of polymeric fibres.

Unsuccessful attempts were made to carry out low strain modulus determinations at very high rates of loading.

B. MATRIX

3.6 MATERIAL

Cement

To ensure that the characteristics of the cement remained reasonably constant, one batch of blended 'Blue Circle' Ordinary Portland cement

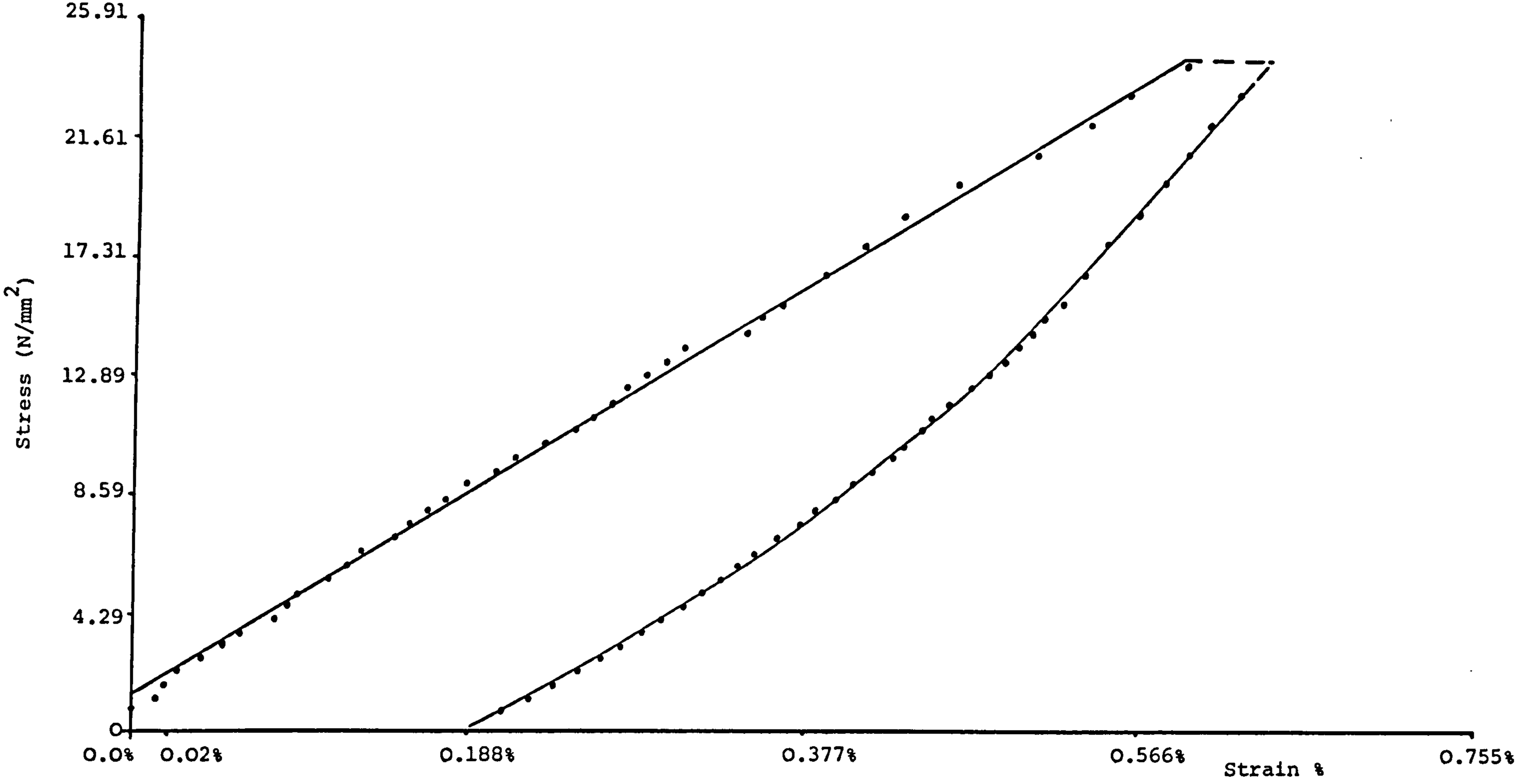

FIGURE 3.7 - ELASTIC MODULUS OF POLYPROPYLENE FIBRE AT LOW STRAIN

obtained from a single manufacturer, was used throughout the investigation. Typical oxide compositions are given in Table 3.1.

3.7 FABRICATION

3.7.1 Mix Procedure

A cement paste of water/cement ratio 0.4 was used throughout the investigation. This particular ratio was chosen to give sufficient workability for eventual fibre composite preparation. The paste was made by placing the Ordinary Portland cement powder and water into a Hobart A120 mixer and stirring for five minutes at speed two.

3.7.2 Casting and Curing

On completion of the mixing operation, the material was then transferred into vertical moulds each of size 13 mm thick, 40 mm deep and 250 mm long. Vertical casting was used in order to produce accurate parallel sided specimens. All the specimens were compacted using a laboratory vibrating table. The oil treated mould was placed unclamped on the vibrating table and filled until the paste was level with the top of the mould. The vibrating table was then switched on and additional material added continuously during compaction to avoid the possible formation of layers. In general, the period of compaction was approximately 5 minutes, until the mix appeared uniform and the material had flowed to a level surface. By this time entrapped air bubbles had apparently ceased rising to the surface of the mix. Prolonged vibration was not used, as this was found to result in segregation of the mix.

TABLE 3.1 - OXIDE COMPOSITION OF ORDINARY PORTLAND CEMENT

Oxide	Content (%)
SiO_2	20.00
Al_2O_3	6.10
Fe_2O_3	2.40
CaO	64.90
MgO	1.10
SO_3	2.80
Na_2O	0.16
K_2O	0.65
Insoluble Residue	0.70
Loss on Ignition	0.80

The top of the mix was then levelled to give a fair face. To reduce the rate of drying out during hardening, a wet cloth was placed over the top of the mould.

All the specimens were cured in water at 20°C for 6 days after an initial 24 hours in the mould.

3.7.3 Specimen Preparation for Test

The specimens were taken from the water and the excess moisture wiped off.

When testing straight sided brittle tensile cement specimens using wedge type grips (see Plate 3.4), fracture often occurred in the grip section. To eliminate this, various modifications were tried, such as the bonding of epoxy resin, neoprene tabs and canvas on to the grips themselves or attaching pads, such as aluminium tabs and emery cloths of various grades to the specimen end faces. General failure in all of these systems occurred at the glue line, whilst loading the specimen; therefore special attention was devoted to the preparation of the specimen surfaces to accept adhesives. Various adhesives were tried, such as Super glue three, Locktite, Ciba-Geigy glues, Araldite, Epoxy Resins and Polybond. The correct properties of the glue were identified as non-brittle, sufficiently flexible to give a cushioning effect and possessing high shear and bond strength values.

Finally, a stable impermeable backed hessian was chosen. The hessian was a flexible material, having minimum shrinkage or edge fraying characteristics. It was easy to handle when pasted, highly resistant to creasing and allowed the minor surface irregularities to be followed. The specimen and back of the hessian were first pasted with a thin coat of Evo-Stick adhesive, which was allowed to touch-dry for approximately

PLATE 3.4 - WEDGE TYPE GRIPS

PLATE 3.5 - SPECIMEN WITH HESSIAN ATTACHED TO THE GRIP AREA

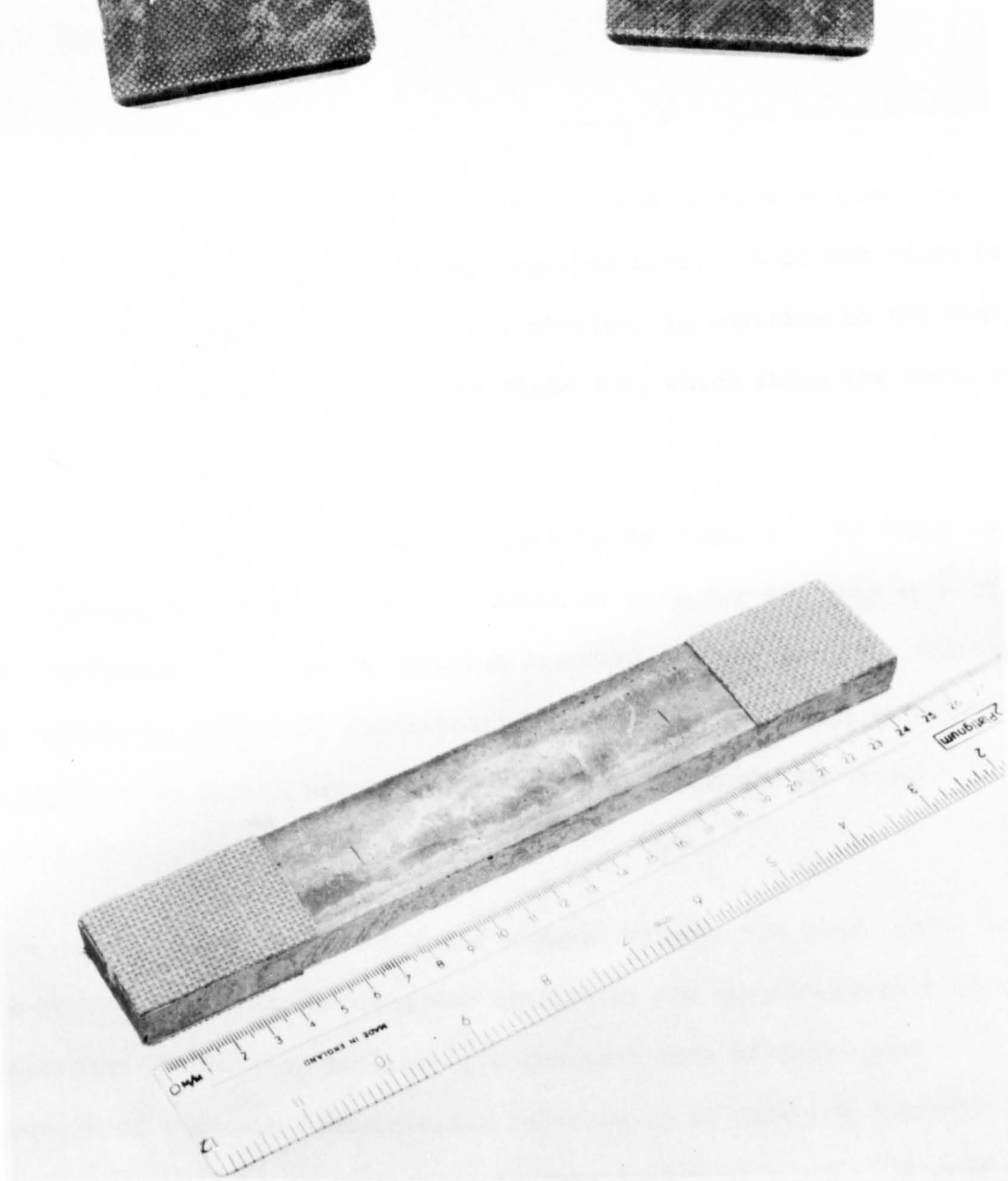
MADE IN ENGLAND

half an hour before contact was made. The occurrence of fracture in the grip section was thus considerably reduced by this method. Plate 3.5 shows a specimen with hessian attached to the grip section. This method of specimen preparation was adopted for all the specimens reported in this thesis.

3.8 TEST PROCEDURE

3.8.1 Tensile Strength

A grade A 50 kN Losenhausen Servo hydraulic UHS6 testing machine was utilised. This allowed the use of either load control or position control modes of deformation at any required rate. Load and cross-head movements were recorded, using an X-Y plotter, in addition to the digital displays on the test machine. See Plate 3.6, which shows the tensile test set up.

Wedge type grips were employed for the tensile loading. As there is no specified method of testing, or means of gripping for this type of material given in either the British Standards or the American Society for Testing and Material Specifications, conventional wedge grips were employed, with appropriately sized wedges to match the specimen dimensions (see Plate 3.4).

After the specimen was mounted and clamped between the wedge grips in the correct position, loading was applied by the upward movement of the cross-head of the test machine. A constant rate of cross-head movement of 1 mm/min (subsequently referred to as position control) was applied for all the specimens in this series of tests. A load

PLATE 3.6 - TENSILE TEST SET-UP

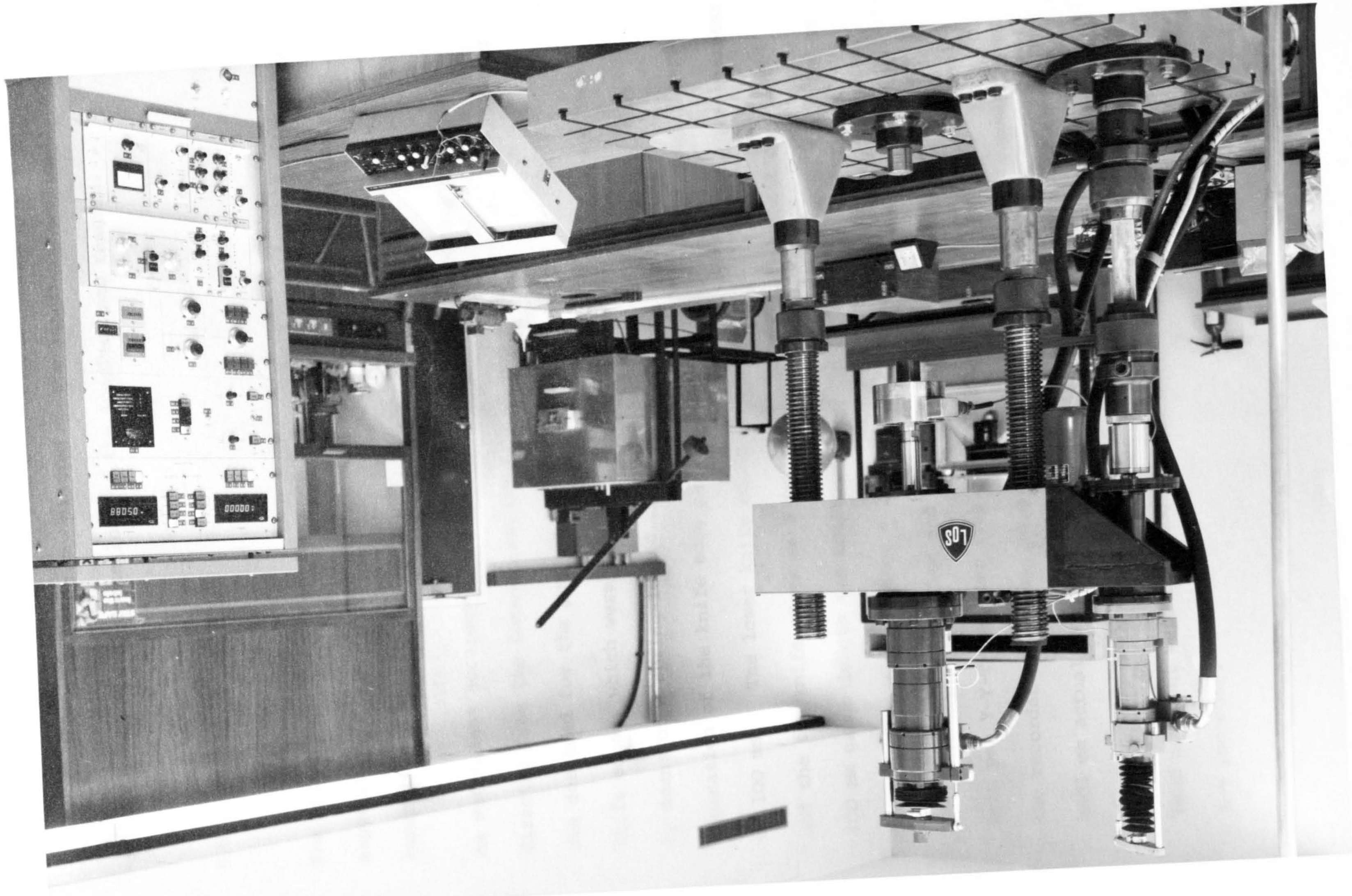

versus cross-head movement was plotted. The loading was allowed to continue until the ultimate load of the specimen was reached.

3.8.2 Strain Measurement

The strain measurement on the specimen received considerable attention, especially in the elastic deformation region, which is very small for cementitious matrices, ranging from 0.02 - 0.06% cracking strain.

As sufficient accuracy could not be achieved by measuring the strain directly from the Losenhausen cross-head movement, a clamp extensometer was designed for the purpose. The extensometer had two pairs of knife edges, which were clamped on to the flat edges of the specimen by means of a spring-loaded clamping device (see Plate 3.7). The separation of the knife edge pairs corresponded to a test gauge length of 100 mm. The lower knife edges were rigidly fixed on the extensometer and the top knife edges were free to move. This movement over the 100 mm gauge length was monitored on each side of the gauge by means of D.C. transducers of range $\pm$ 2.0 mm. Voltage signals proportional to the specimens elongation and the load applied were recorded using a twin pen Y-Y-T recorder (see Plate 3.8). The sensitivity scale on the recorder chosen was 24.0 mm full scale, representing a movement of 0.01 mm actual extension, from the plot, elastic modulus of the specimen was determined. Also as the test proceeded, load and cross-head movement were recorded via the Losenhausen test machine on to an X-Y recorder.

PLATE 3.7 - SPECIMEN CLAMPED IN THE EXTENSOMETER

PLATE 3.8 - TWIN PEN Y-Y-T RECORDER

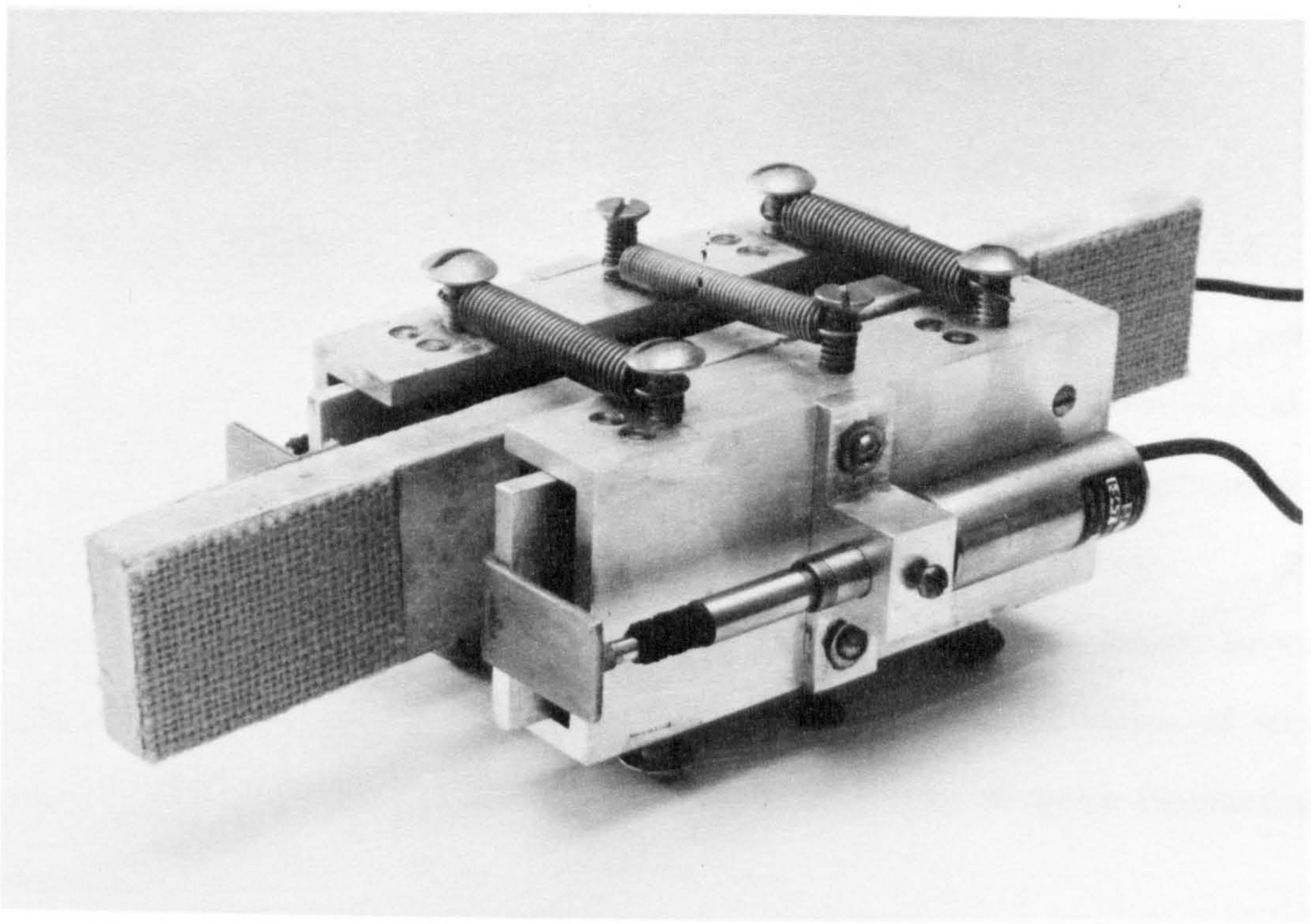

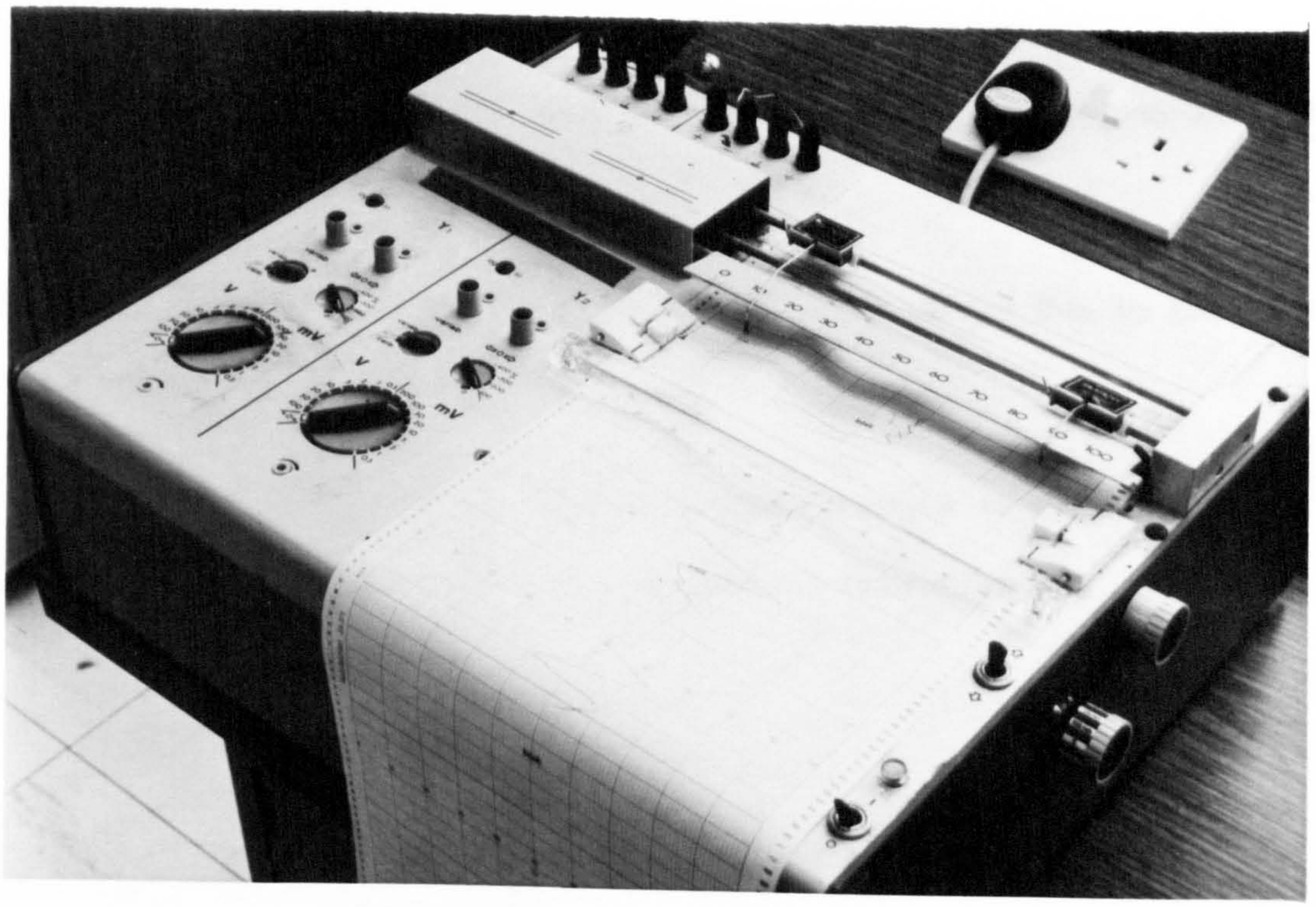

3.9 ANALYSIS AND DISCUSSION OF RESULTS

Tensile Strength

Specimens of neat cement paste of water/cement ratio 0.4 were tested to failure at intervals throughout the investigation. A mean ultimate stress of 1.74 N/mm^2 was obtained for the 20 specimens tested. However, the spread was between 1.0 - 2.5 N/mm^2. Such a large spread is typical of cementitious matrices, because of the wide range of size of pores and also because of entrapped air bubbles, despite mechanical vibration.

The elastic modulus value of the cement paste has a similar spread of values to the tensile strength, lying between 10.0 - 20.0 kN/mm^2, with a mean value of 14.76 kN/mm^2. The elastic modulus is an inherent property of the material and should not be influenced by the presence of small amounts of porosity, in the same way as the tensile strength. The reason for the large scatter in the elastic modulus values is probably the introduction of bending moments due to slight non-axiality in load application.

The low tensile strength values obtained are primarily due to the high water/cement ratio.

However, the numerical value of the matrix strength is not thought to be of particular significance in the overall investigation.

3.10 CONCLUSIONS

A. POLYPROPYLENE FIBRE

The overall conclusion is that modulus improvements of greater than

25.0% cannot be achieved by optimising production parameters.

The evidence indicates that the modulus at very low strains and at very high strain rates does not differ significantly.

Specific conclusions that can be drawn are as follows:

(1) In all cases, values of the tangent modulus were significantly higher than the chord modulus values, due to inherent non-linear load-deformation characteristics of the fibre.

(2) Extrusion temperature does not play a significant role in up-grading the modulus of the fibres.

(3) Haul-off speed ratio is the most important factor in modifying the modulus value. Generally, an increase in the ratio gives an increase in the modulus values.

(4) The rate of cross-head movement in a tensile test does not significantly influence the modulus of the fibre.

B. MATRIX

(1) A satisfactory method of gripping has been developed, which minimises grip failures.

(2) The average tensile strength of the neat cement paste was found to be 1.74 N/mm^2, which is rather low. The average elastic modulus value was found to be 14.76 kN/mm^2, which is comparable with the normally accepted range of values.

CONTINUOUS ALIGNED FIBRE REINFORCED CEMENT PASTE

CHAPTER FOUR

CONTINUOUS ALIGNED FIBRE REINFORCED CEMENT PASTE

4.1 PREAMBLE

In order to obtain an acceptable fibre reinforced cement material, it is necessary, although not sufficient, that multiple cracking of the matrix occurs.

To investigate multiple cracking systematically, the first type of composite material to be studied was one which contained continuous aligned fibres which were uniformly distributed throughout the matrix. This system not only minimised the number of parameters by eliminating fibre orientation, length and variable fibre spacing, but also provided information on the nature of fibre/matrix interaction. In addition the use of a continuous aligned system allowed the applicability of existing theories of unidirectional reinforcement to polypropylene composites to be tested.

The work in this chapter was therefore concerned with identifying the effect of fibre concentration on the deformation characteristics of aligned polypropylene fibre reinforced cement pastes.

4.2 MATERIALS

4.2.1 Cement

Standard Ordinary Portland cement was used as described in section 3.6.

4.2.2 Fibres

Continuous monofilament fibres of 340 μm diameter were used for most of the specimens; however, a limited number of tests were carried out with continuous tapes of dimensions 1178 μm wide by 46.7 μm in thickness and 1746 μm wide by 42.6 μm in thickness. See section 3.2.2 (A), (B), (D) and (E) for the detailed description of the fibres and tapes.

4.3 FABRICATION

4.3.1 Continuous Aligned Fibre System

A fabrication technique was developed to incorporate known percentages of fibres up to 8.7% by volume in a cement matrix. A perspex jig (as shown in Fig. 4.1) was constructed, with pegs protruding from the mould at either end of the mould. The procedure for fabrication was to:

(A) Place a thin shim of desired thickness on to the base of the mould, between the innermost positioning peg and end of the mould.

The purpose of the shims is to act as known spacers between the layers of the fibres required in the test specimens and to close the ends of the mould in a suitable fashion, thus avoiding excessive seepage of the cement paste via the ends of the mould.

(B) The fibre was then tied to the innermost peg and wound continuously along the length of the mould, until the last peg was reached at the opposite end of the mould; the fibre was then secured. Subsequent layers of fibre were then positioned in the same manner to give the required percentage volume of fibres.

FIGURE 4.1 - SCHEMATIC DIAGRAM OF ALIGNED FIBRE LAY-UP JIG

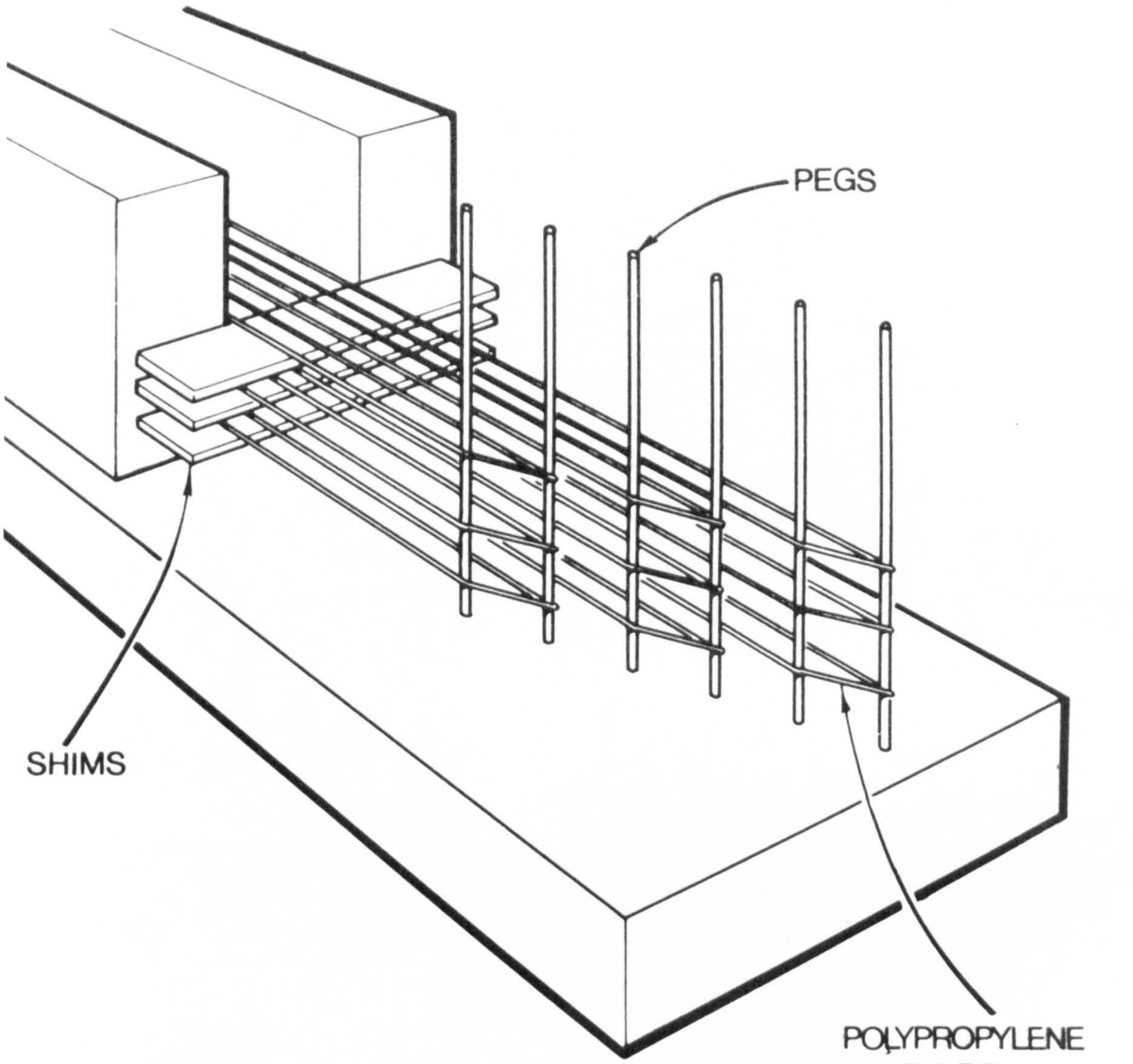
PEGS
SHIMS
POLYPROPYLENE
FIBRE

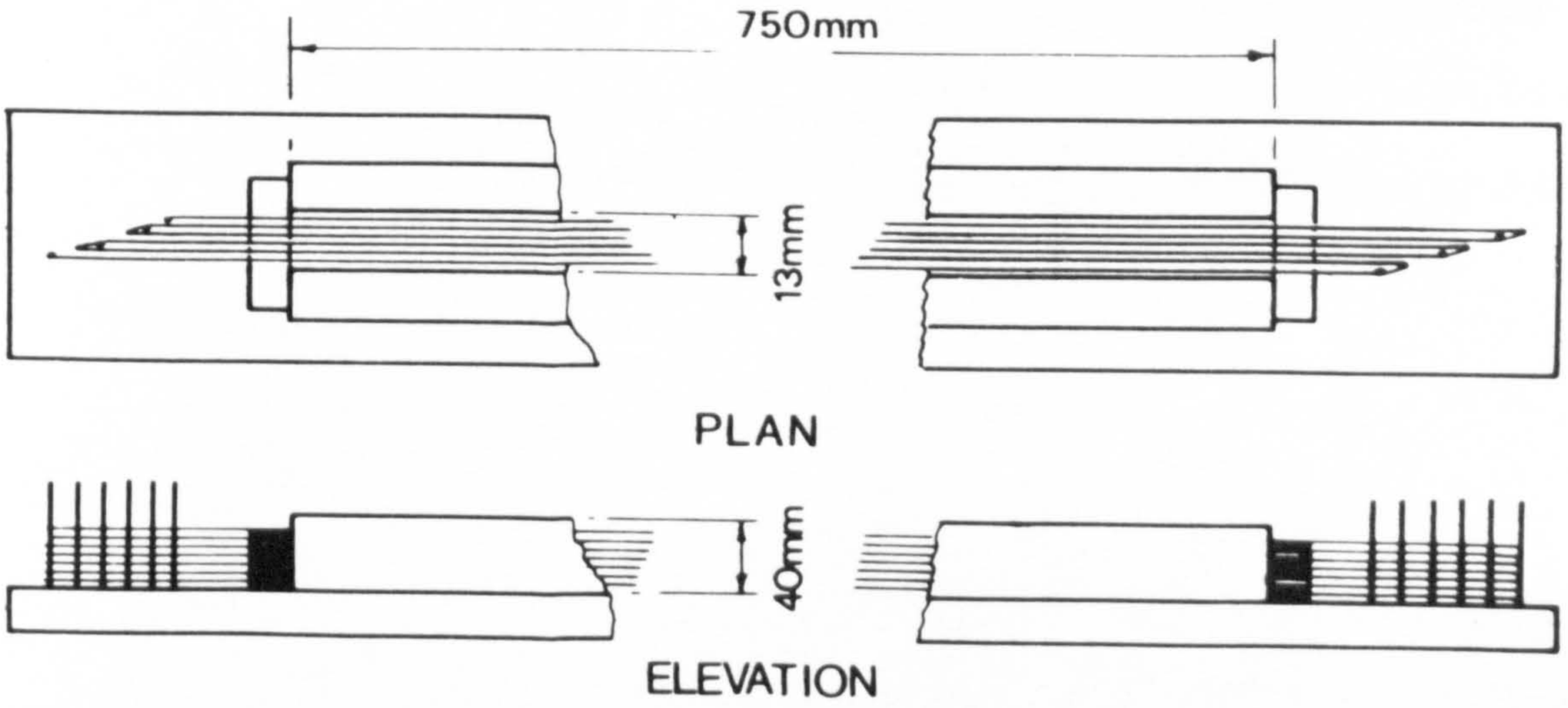
750mm
13mm
PLAN
40mm
ELEVATION

Fibres placed in this manner were thus evenly distributed throughout the mould, both in a horizontal and vertical plane, with no sag occurring on the fibres (see Plate 4.1).

The percentage by volume of fibre incorporated in the system was determined by the thickness of the shims, the number of shims between each layer of fibres and the fibre diameter used.

Throughout the investigation a mould size of 13 mm wide x 40 mm deep x 750 mm long was used, thus allowing three specimens of 250 mm length to be cut from each cast of the mould.

4.3.2 Mix Procedure

A high water/cement ratio of 0.4 was used to ensure adequate penetration of the aligned fibre lay up (see section 3.7.1).

4.3.3 Casting

The only difference to the casting procedure as described in section 3.7.2, was that with the high fibre concentrations the compacting time had to be increased in order to permit the closing of the free surface.

4.3.4 Curing

4.3.4.1 Method 1

After twenty-four hours, the specimens were removed from the mould and placed in water at 20°C for six days. The specimens were then taken from the water and left in air at room temperature for one day. This curing method was adopted in the early stages of the investigation with type A fibres, because the resin used to bond the canvas tabs

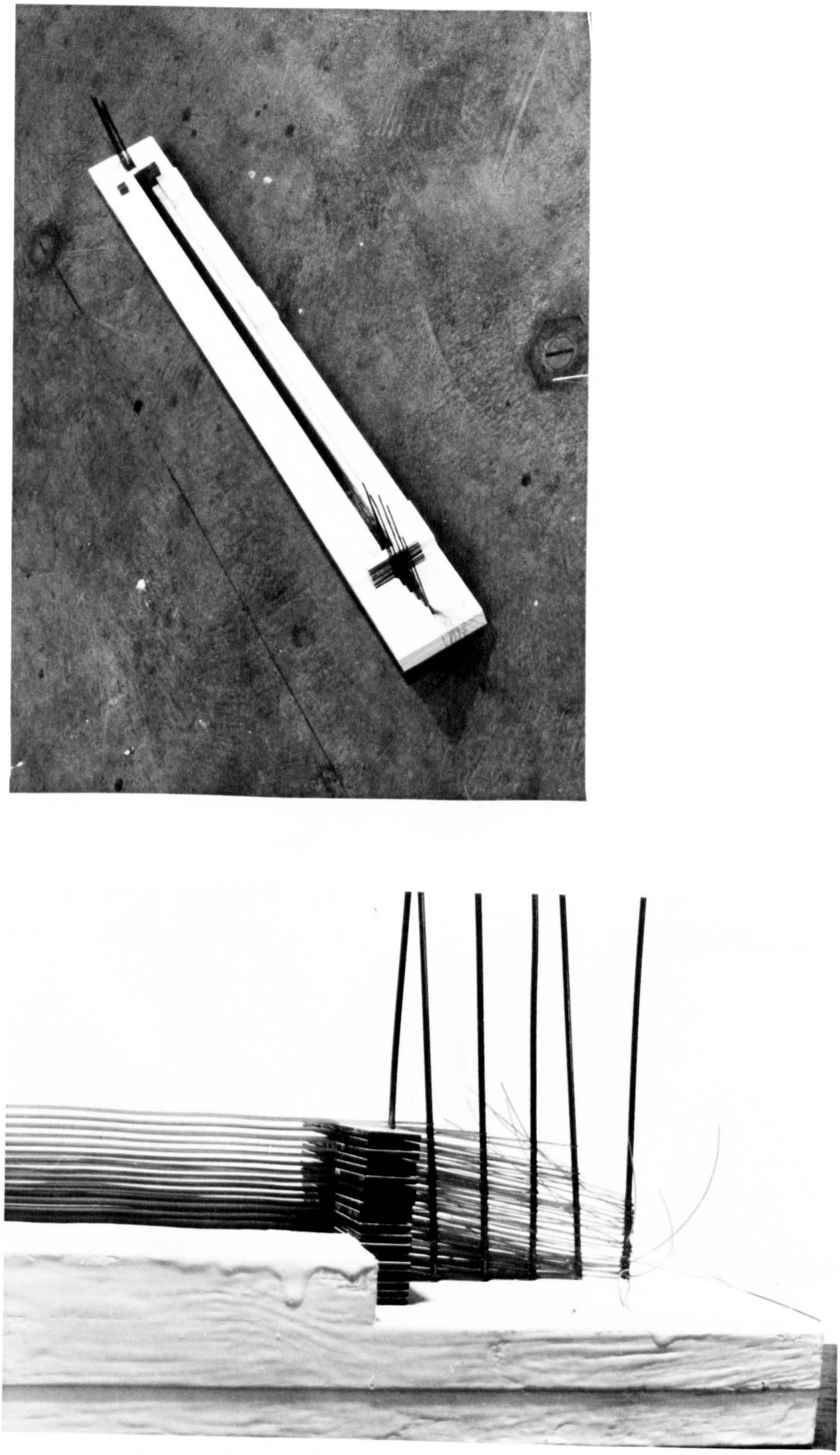

on to the specimen after removing from the curing chamber required one day air-curing.

4.3.4.2 Method 2

The specimens were cured in water at 20°C for six days, after an initial twenty-four hours in the mould. This curing method was adopted for specimens containing fibre types A and B, also tape types A and B, and was possible because of the use of Evo-Stick as an adhesive for bonding the canvas tabs to the specimens. The use of Evo-Stick, which developed strength rapidly, allowed testing to take place half an hour after the adhesive had been applied.

4.3.5 Specimen Particulars

Specimens 13 mm thick x 40 mm deep in section and 250 mm long were prepared, containing 1.4, 2.4, 4.2, 5.5 and 8.7% by volume of fibre type A, 4.2% by volume of fibre type B and 1.4 and 4.2% by volume of tapes type A and B.

4.4 TEST PROCEDURE

4.4.1 Tensile Strength

The load was applied by using the position control mode (i.e. constant rate of cross-head movement of 1 mm/min) for all the specimens, as described in section 3.8.1.

4.4.2 Strain Measurement

The initial strain up to the first crack was measured with the clamp extensometer as described in section 3.8.2, and the subsequent deformation exceeding the range of the extensometer was measured via the cross-head movement given on the Losenhausen test machine.

4.4.3 Crack Spacing Measurement

Since multiple cracking was obtained, a simple method to measure the final crack spacing was developed.

The first crack in tension occurred when the ultimate cracking strain of the matrix was reached. Loading was then continued beyond this point until the multiple cracking process in the specimen was completed. At this stage, the fine visible cracks were marked in pencil. The marking of the cracks was carried out at this stage in the test, because when the specimens were unloaded the fine cracks tended to close, thus making crack identification and hence space measurement difficult to achieve. In the event of an irregular crack path across the specimen, the average longitudinal position was used to specify the crack spacing. The measurements of the spacings were made after unloading.

4.4.4 Scanning Electron Microscopy

A limited study of the fibre surface characteristic of the as-received fibre and fibre after deformation in a composite was carried out using a Cambridge stereoscan scanning electron microscope mark 2A.

4.5 ANALYSIS AND DISCUSSION OF RESULTS

4.5.1. Cracking Stress Levels

At least three specimens containing fibre type A, cured by method 1 (see Table 4.1 for test details) and twelve specimens cured by method 2 (see Table 4.2 for test details), were tested in tension containing 1.4, 2.4, 4.2, 5.5 and 8.7% by volume. Multiple cracking occurred in all the fibre reinforced specimens. Plate 4.2 illustrates the typical crack spacings obtained with increasing volume percentage of fibre, after carrying out the tensile tests on specimens cured by method 2. Similar multiple cracking phenomena was also observed for specimens cured by method 1. It can be seen that the multiple cracks run approximately perpendicular to the tensile stress direction and generally at regular intervals along the length of the specimen.

Figures 4.2 to 4.6 show the typical load/cross-head displacement curves for each fibre concentration, for the specimens containing fibre type A cured by method 2. The curves also include the unavoidable bedding down displacement in the linear region. Similar trends were also obtained for the same fibre type, cured by method 1, except that the first crack load was lower, which was probably due to the drying shrinkage cracks induced in the specimens by leaving the specimens in the air for one day before testing. Accurate determinations of the linear deformation were made by means of the extensometer, which gave a straightforward linear load/extension relationship.

The first crack strength can be assumed to be very close to the unreinforced matrix strength, since the majority of the load will be supported by the matrix, because of the low modulus value of the

TABLE 4.1 - CONTINUOUS ALIGNED FIBRE REINFORCED CEMENT PASTE SPECIMENS CURED BY METHOD 1

(1)	(2)	(3)	(4)	(5)	(6)	(7)	(8)	(9)
Test Code	Vol.% Fibre	Average First Crack Stress (N/mm^2)	Average Final Crack Stress (N/mm^2)	Average Ultimate Stress (N/mm^2)	Average Crack Spacing (mm)	Average τ (N/mm^2) Using σ_{mu}=AV. First Crack Stress in Equation (4.1)	Average τ (N/mm^2) Using σ_{mu}=AV. Final Crack Stress in Equation (4.1)	Average τ (N/mm^2) From Columns (7) and (8) (*)
Fibre Type A	1.4	0.67	1.16	1.46	117.9	0.034	0.059	0.047 (0.01)
Fibre Type A	2.4	0.75	1.14	1.90	73.3	0.035	0.054	0.045 (0.01)
Fibre Type A	4.2	0.82	1.80	4.76	56.1	0.028	0.062	0.045 (0.02)
Fibre Type A	5.5	0.77	2.00	2.54	17.2	0.066	0.170	0.118 (0.01)
Fibre Type A	8.7	0.96	3.38	5.46	10.5	0.082	0.287	0.185 (0.01)

* Standard Deviation

TABLE 4.2 - CONTINUOUS ALIGNED FIBRE REINFORCED CEMENT PASTE SPECIMENS CURED BY METHOD 2

(1)	(2)	(3)	(4)	(5)	(6)	(7)	(8)	(9)	(10)	
Test Code	Vol.% Fibre	Average First Crack Stress (N/mm^2)	Average Final Crack Stress (N/mm^2)	Average Ultimate Stress (N/mm^2)	Average Crack Spacing (mm)	Average Elastic Modulus (kN/mm^2)	Average τ(N/mm^2), Using σ_{mu}=AV. First Crack Stress in Equation(4.1)	Average τ(N/mm^2), Using σ_{mu}=AV. Final Crack Stress in Equation(4.1)	Average τ(N/mm^2) From Columns (8) and (9)	(*)
Fibre Type A	1.4	1.59	2.01	3.41	64.7	10.31	0.148	0.186	0.167	(0.09)
Fibre Type A	2.4	2.02	2.44	4.33	77.2	11.46	0.092	0.109	0.101	(0.03)
Fibre Type A	4.2	1.21	2.35	5.27	35.6	11.51	0.066	0.128	0.097	(0.02)
Fibre Type A	5.5	1.49	3.02	6.53	38.1	8.33	0.057	0.116	0.087	(0.05)
Fibre Type A	8.7	1.70	3.54	7.18	34.3	13.13	0.044	0.091	0.068	(0.02)
Fibre Type B	4.2	2.11	3.77	5.52	55.9	14.01	0.073	0.131	0.102	(0.07)
Tape Type A	1.4	1.36	2.69	3.61	40.7	8.89	0.053	0.105	0.079	(0.01)
Tape Type A	4.2	1.53	3.28	4.40	19.3	-	0.041	0.087	0.064	(0.01)
Tape Type B	1.4	1.08	1.88	3.08	29.6	13.03	0.054	0.093	0.074	(0.02)
Tape Type B	4.2	1.62	2.82	2.68	19.2	20.90	0.040	0.070	0.055	(0.01)

* Standard Deviation

PLATE 4.2 - TYPICAL CRACK SPACING OBTAINED WITH INCREASING VOLUME % OF FIBRE AFTER CARRYING OUT TENSILE TEST.
A = 1.4% V_f; B = 2.4% V_f; C = 4.2% V_f; D = 5.5% V_f AND E = 8.7% V_f


4180
A
B
C
D
E

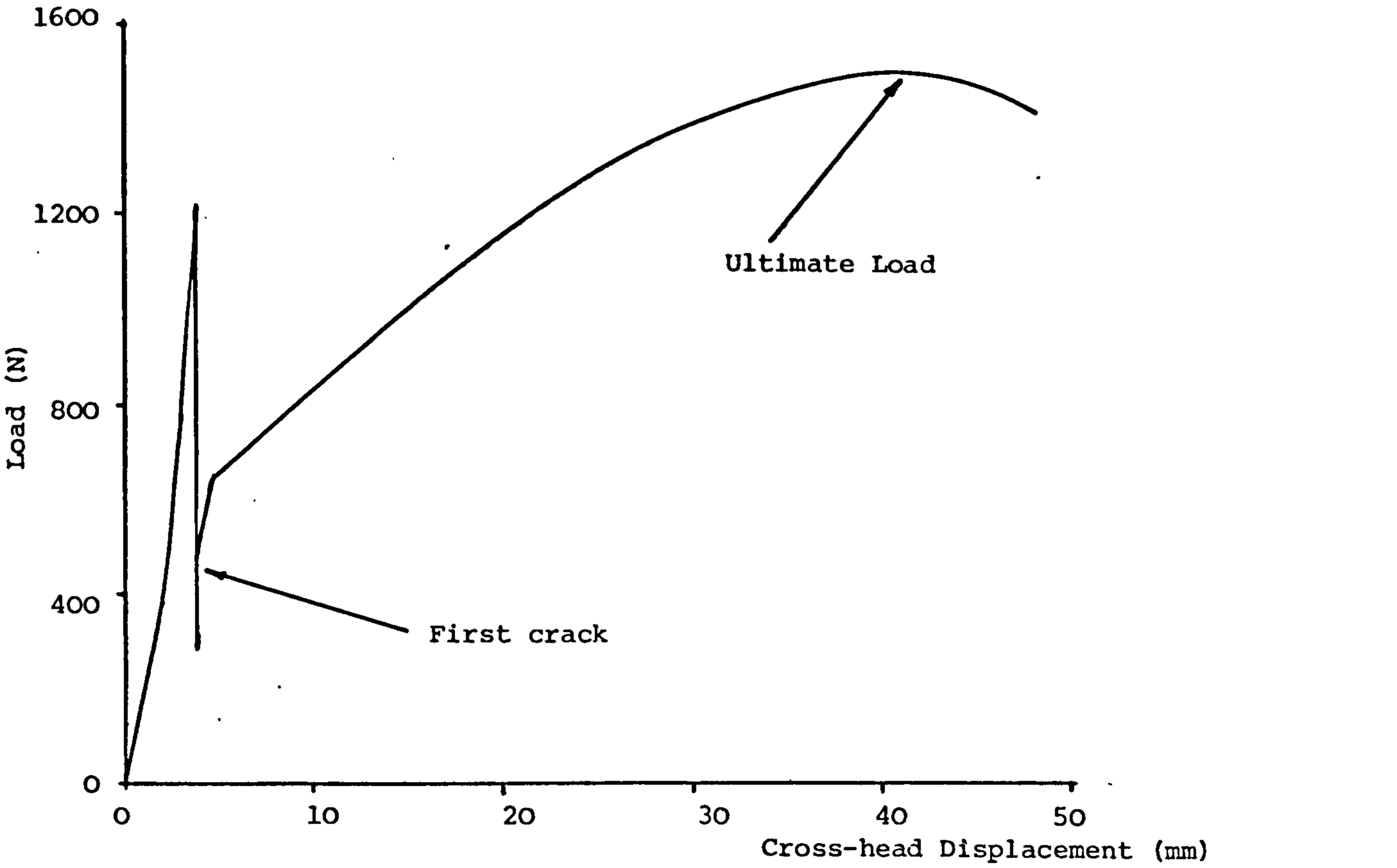

FIGURE 4.2 - TYPICAL TENSILE LOAD/CROSS-HEAD DISPLACEMENT CURVE FOR CEMENT PASTE REINFORCED WITH 1.4 VOLUME % CONCENTRATION OF 340 μm DIAMETER POLYPROPYLENE FIBRE

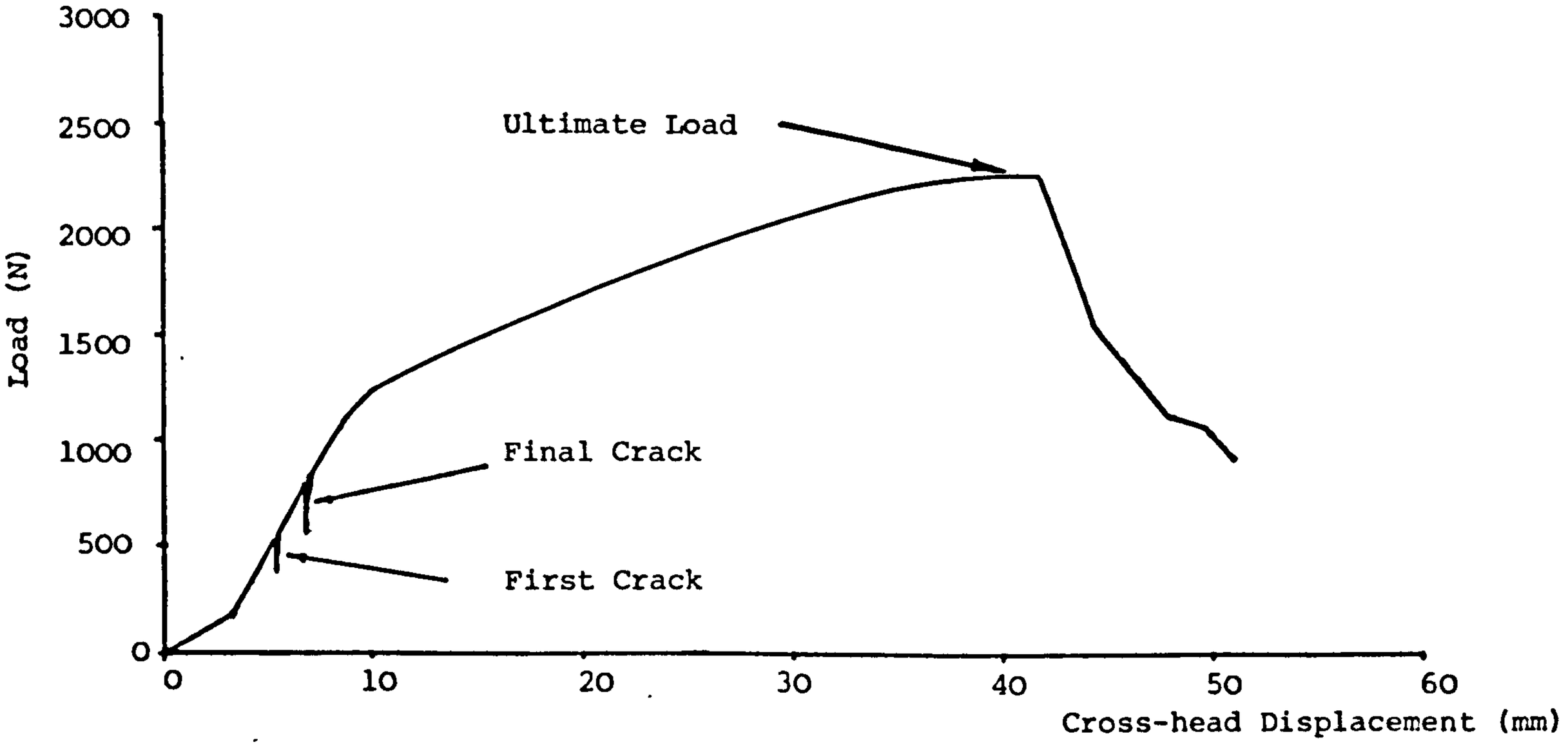

FIGURE 4.3 - TYPICAL TENSILE LOAD/CROSS-HEAD DISPLACEMENT CURVE FOR CEMENT PASTE REINFORCED WITH 2.4 VOLUME % CONCENTRATION OF 340 μm DIAMETER POLYPROPYLENE FIBRE

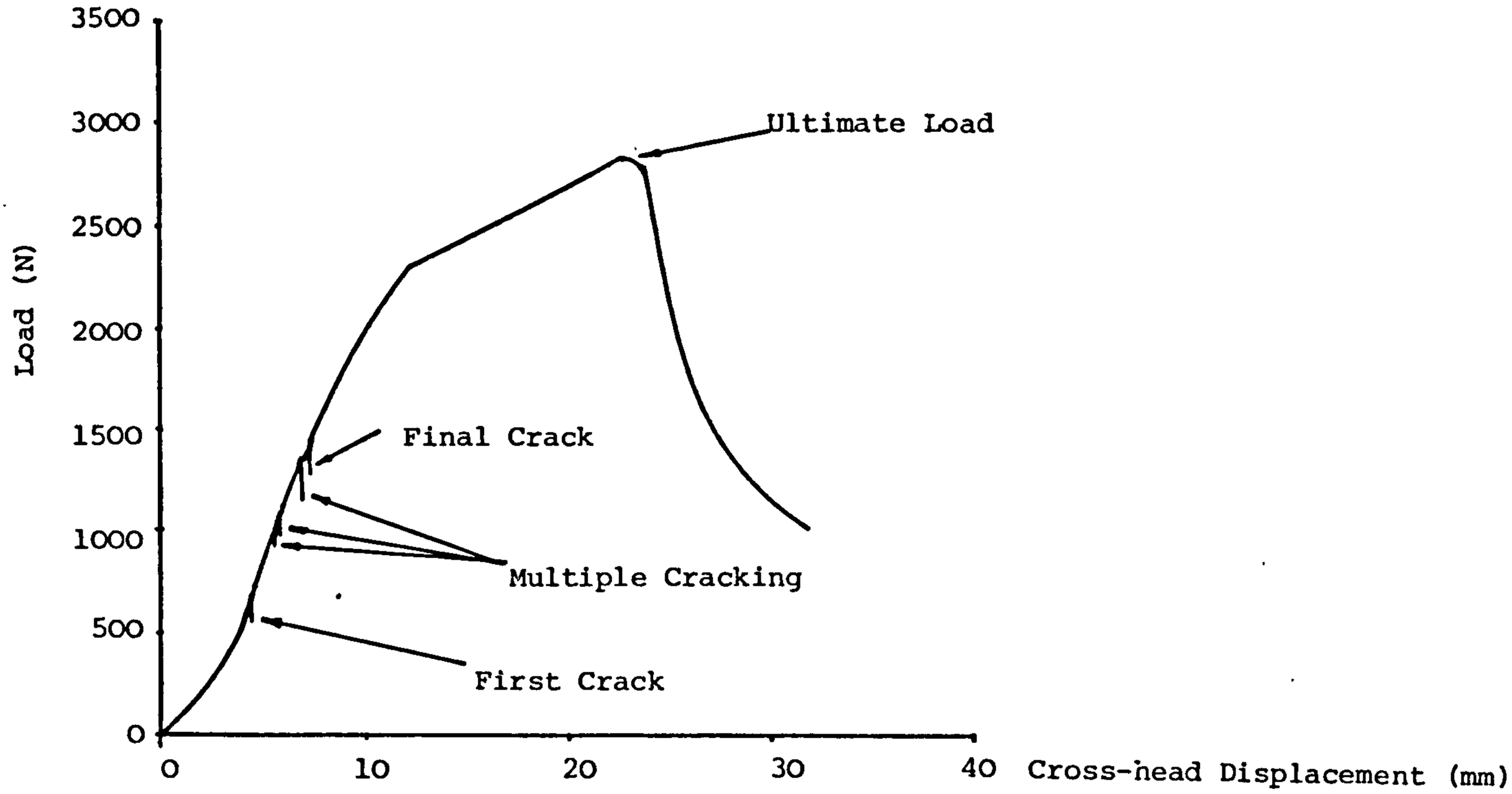

FIGURE 4.4 - TYPICAL TENSILE LOAD/CROSS-HEAD DISPLACEMENT CURVE FOR CEMENT PASTE REINFORCED WITH 4.2 VOLUME % CONCENTRATION OF 340 μm DIAMETER POLYPROPYLENE FIBRE

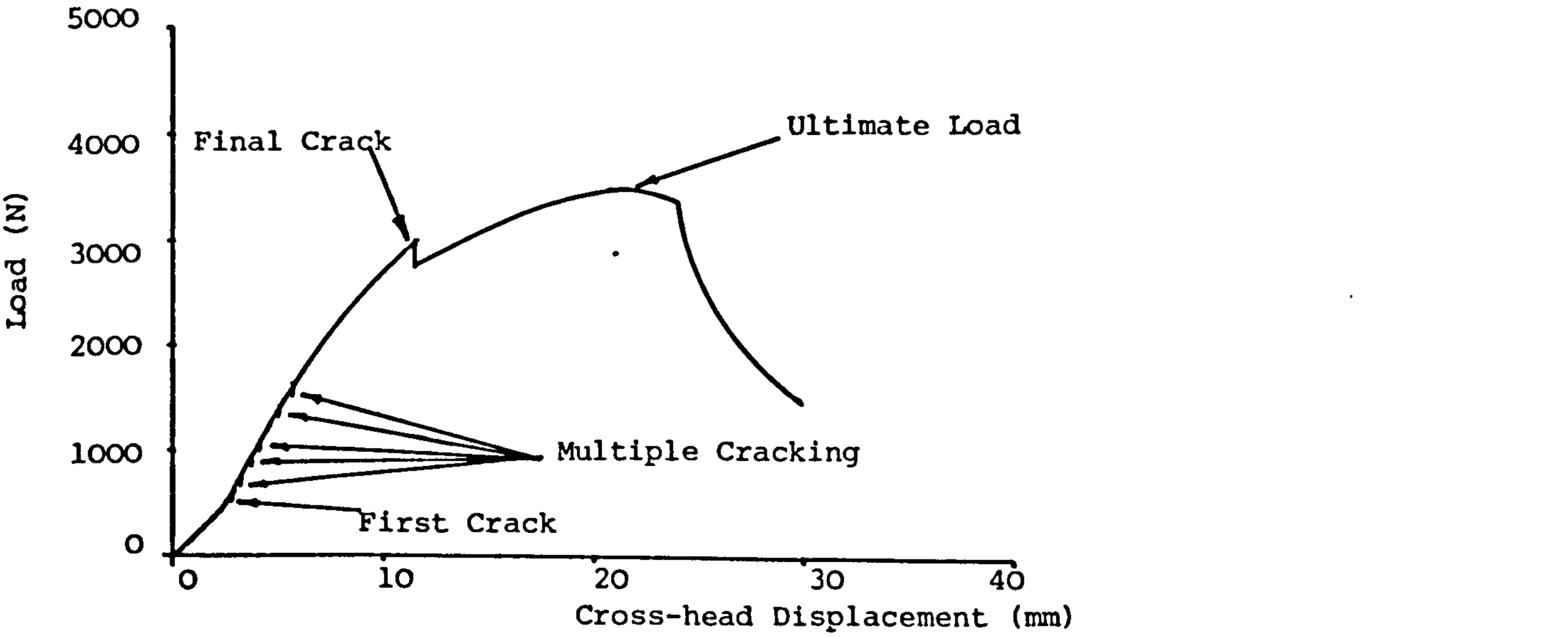

FIGURE 4.5 - TYPICAL TENSILE LOAD/CROSS-HEAD DISPLACEMENT CURVE FOR CEMENT PASTE REINFORCED WITH 5.5 VOLUME % CONCENTRATION OF 340 μm DIAMETER POLYPROPYLENE FIBRE

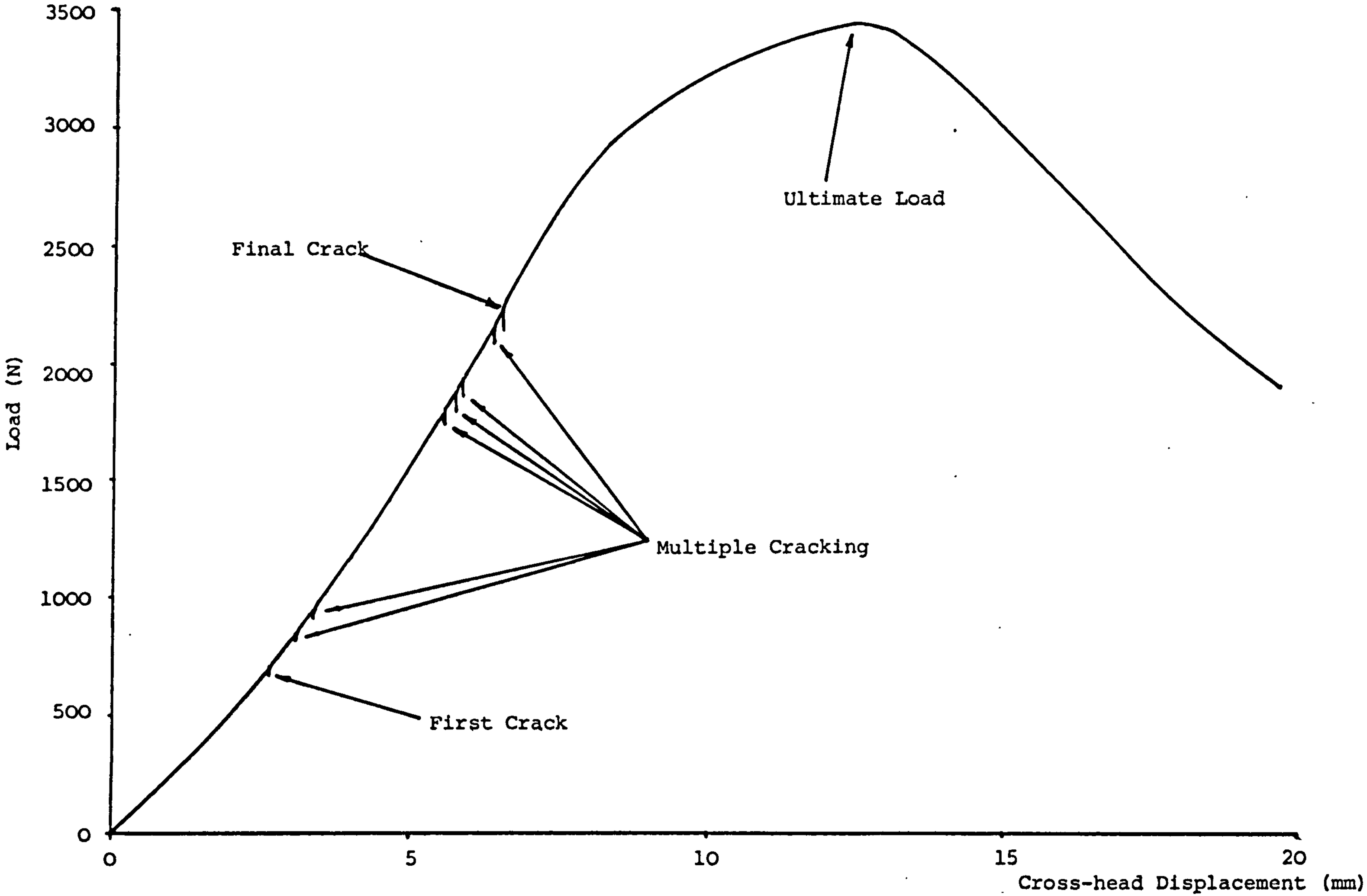

FIGURE 4.6 - TYPICAL TENSILE LOAD/CROSS-HEAD DISPLACEMENT CURVE FOR CEMENT PASTE REINFORCED WITH 8.7 VOLUME % CONCENTRATION OF 340 μm DIAMETER POLYPROPYLENE FIBRE

polypropylene fibres (as shown in Figures 4.2 to 4.6). The process of multiple cracking commences when the matrix reaches its failure strain and hence cracks, thus throwing the whole applied force on to the fibres bridging the crack. The fibres will then elongate further under the additional load, and provided that there is contact with the matrix, the load will be transferred back to the matrix by the interfacial shear stress (τ), and hence the matrix will crack again. This process is repeated until the matrix is broken into a set of blocks. It should be noted that the multiple cracking took place at successively higher stress levels, i.e. increasing stress values from the first crack to the final crack, which means that the matrix in the composite is not homogeneous and that the cracking sequence takes place as higher stresses activate progressively smaller Griffiths[60] type flaws. The above mentioned process is continued until all the multiple cracking is completed. If the matrix had been a homogeneous material, then all the cracking would have occurred at the same stress level, thus giving a horizontal plot in the cracking region rather than that of a rising curve. Any further increase of load on the composite after completion of the multiple cracking, results in the fibres being extended further until they reach their ultimate stress. The matrix, during this stage of the deformation, does not carry any load. Theoretically this region should be a straight line with a slope equal to the product of the elastic modulus and the volume fraction of the fibres. However, for most cases, the composite failed by fibre pull-out from the block of the matrix retained in the grips.

A similar composite behaviour was also observed for specimens containing fibre type B, tapes type A and B, cured by method 2.

4.5.2 Interfacial Shear Stress

One of the important mechanisms associated with fibre composite behaviour is that of interfacial stress transfer between fibre and matrix. The interfacial shear stress and its distribution along the length of a fibre provides a quantitative measure of the effect. The present data allows the average interfacial shear stress to be calculated:

(A)

(i) A systematic relationship between fibre concentration and crack spacing was observed, the greater the concentration the more cracks per unit length of specimen. The general theory derived by Aveston, Cooper and Kelly[12] for multiple cracking predicts that this relationship should be of the form

$$x' = \left(\frac{1-V_f}{V_f}\right) \frac{\sigma_{mu} r}{2\tau} \qquad .. \quad .. \quad .. \qquad (4.1)$$

where x' is the average crack spacing, i.e. transfer length for stress, V_f is the volume fraction of fibres, σ_{mu} is the matrix ultimate stress, r the fibre radius and τ the fibre/matrix shear stress. Aveston et al[12] showed that multiple cracking of a matrix would occur provided that

$$\sigma_{fu} V_f > \sigma_{mu} V_m + \sigma'_f V_f \qquad .. \quad .. \quad .. \qquad (4.2)$$

where σ_{fu} is the fibre ultimate stress, V_m is the volume fraction of the matrix and σ'_f is the fibre stress at the onset of the cracking, i.e. sufficient unbroken fibres must be present to support the load on the composite. At the end of the multiple cracking stage, the matrix will have divided into blocks of length between x' and $2x'$. The assumption made is that the shear stress, i.e.

the transferring stress from fibres to matrix has a constant limiting value and that the matrix fracture stress will be reached at a distance x' from the first crack provided that

$$2N\pi r\tau x' = \sigma_{mu} V_m \quad .. \quad .. \quad .. \quad (4.3)$$

where N is the number of fibres in the unit cross-section.

Equation (4.1) is derived from equation (4.3) since $N = V_f/\pi r^2$.

Plots of x' against $(1-V_f)/V_f$ give approximate straight lines (see Fig. 4.7 for specimens cured by method 1 and Fig. 4.8 for specimens cured by method 2). Substituting for $\sigma_{mu} = 0.794$ N/mm^2 and r = 0.17 mm, a value of $\tau = 0.04$ N/mm^2 is obtained from the gradient of Fig. 4.7 and similarly from Fig. 4.8, substituting $\sigma_{mu} = 1.60$ N/mm^2 and r = 0.17 mm a value of $\tau = 0.07$ N/mm^2 is obtained from the gradient.

In Fig. 4.8, the best straight line was drawn through the points without considering the 1.4% V_f point, as at this concentration the specimens sometimes either gave a single or double crack; thus the average value of the crack spacing is not represented at 1.4% V_f. As can be seen from the figures, the value for (τ) is approximately the same for specimens cured by both methods 1 and 2, although the specimens cured by method 2 gave higher σ_{mu} values for the first crack in equation (4.1). This was however compensated for by the different crack spacing values of these specimens.

It therefore appears that the basic theory for multiple cracking applies to low modular ratio fibre reinforced systems, and that a value of (τ) can be determined from multiple cracking data.

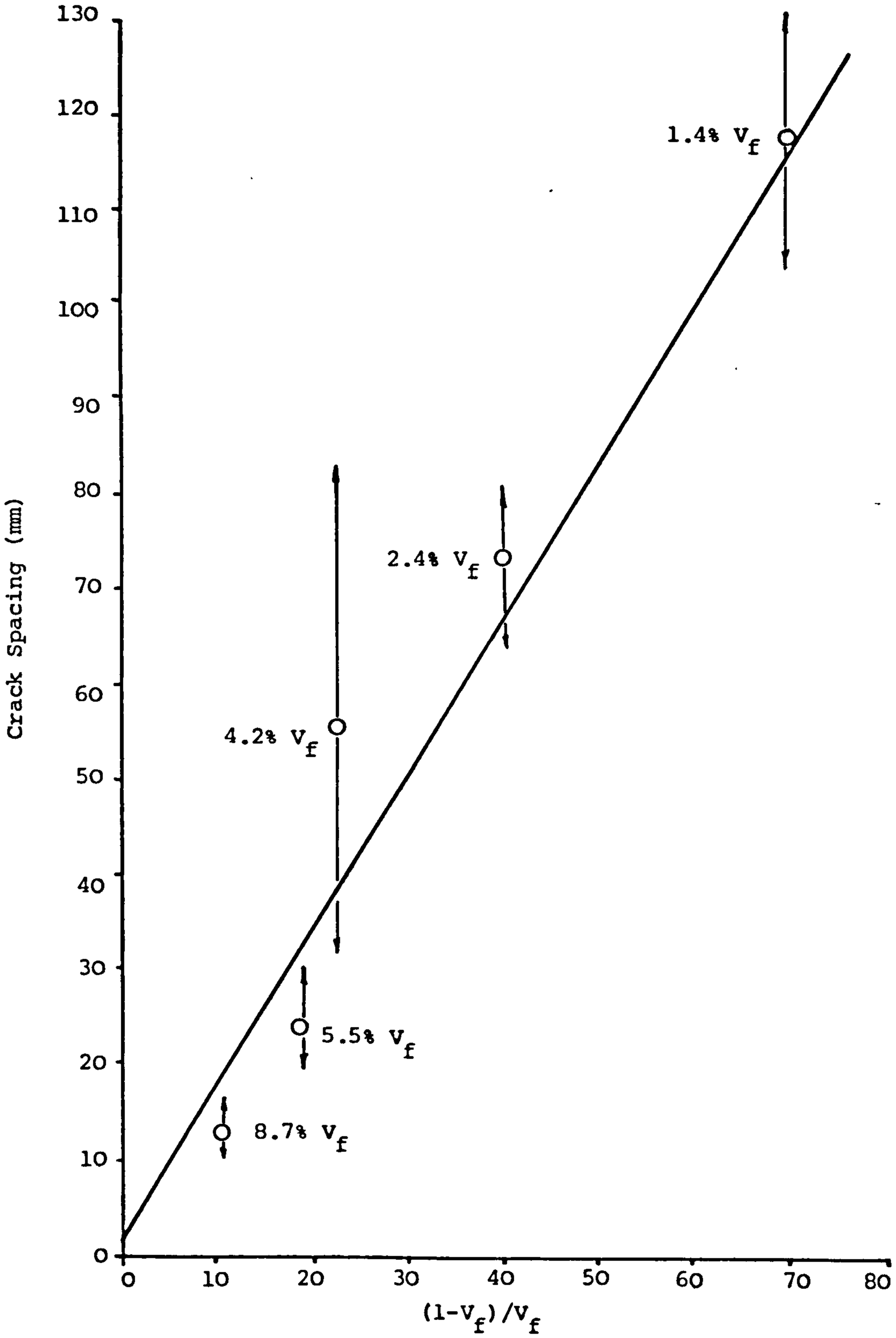

FIGURE 4.7 - CRACK SPACING v $(1-V_f)/V_f$ FOR SPECIMENS CURED BY METHOD 1

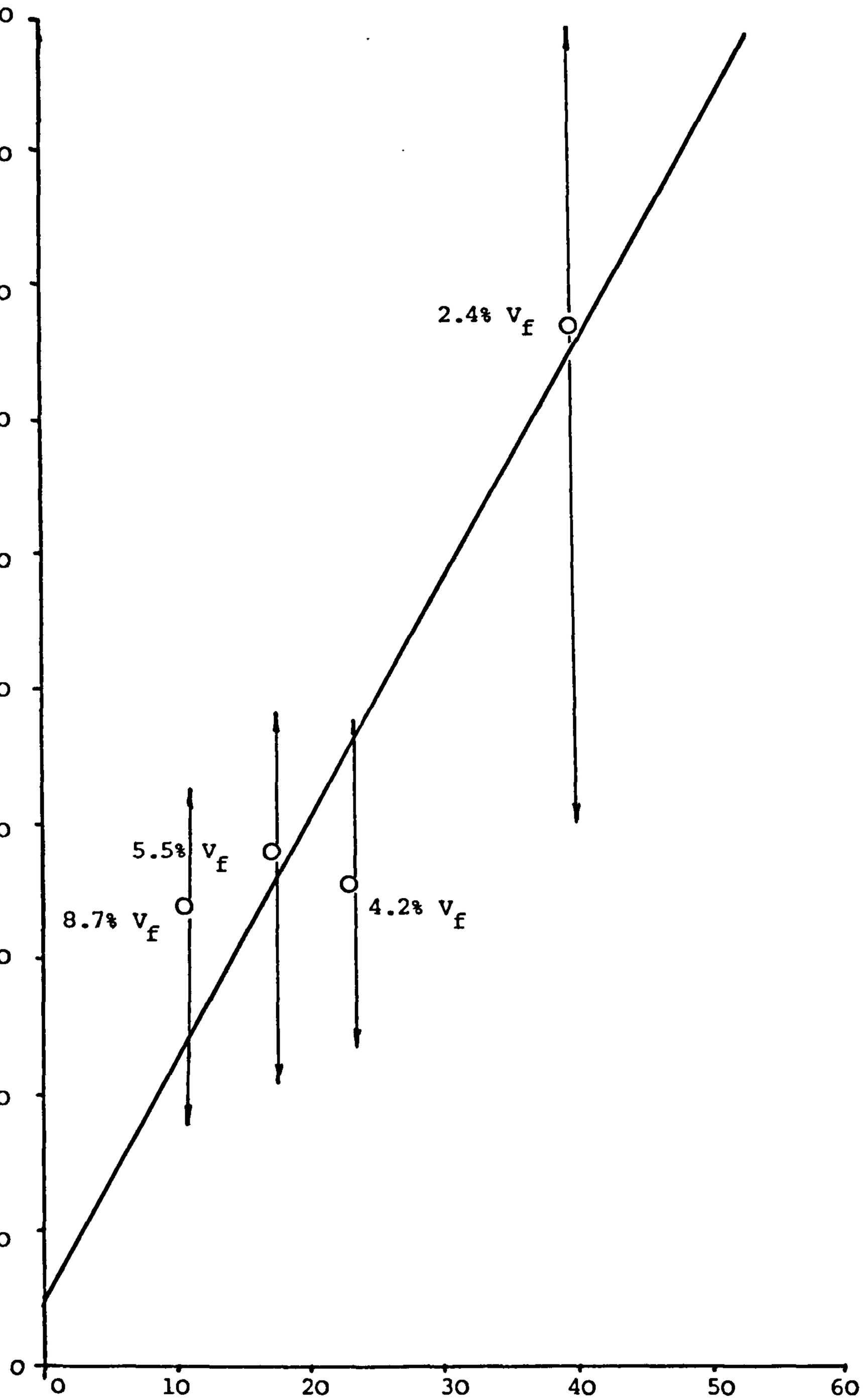

FIGURE 4.8 - CRACK SPACING v $(1-V_f)/V_f$ FOR SPECIMENS CURED BY METHOD 2

(ii) Examination of the individual load/cross-head displacement curves (Figures 4.2 to 4.6) indicates that the matrix cracks at progressively higher stress values throughout the multiple cracking region. Therefore, in view of this phenomenon, the validity of using the first crack stress (σ_{mu}) in the Aveston, Cooper and Kelly's[12] analysis becomes doubtful. The results indicate that the term σ_{mu} in equation (4.1) is not constant and hence the values of the fibre/matrix interfacial shear stress (τ) calculated from equation (4.1), substituting the first crack stress values only (σ_{mu}), will underestimate the actual value. Table 4.1, columns (7) and (8) and Table 4.2, columns (8) and (9) show respectively the values of the fibre/matrix shear stress (τ) in N/mm^2, when the first and final crack stress values are substituted in equation (4.1) for σ_{mu}. From this it can be seen that the value of the interfacial shear stress (τ) is increased, when the final crack stress σ_{mu} is substituted in equation (4.1) in every case.

No physical significance could be attached to the increasing interfacial shear stress (τ) associated with an increasing matrix strength. The most likely explanation for this was thought to be that the interfacial shear stress (τ) remained constant, whereas the crack spacing increased with increasing cracking stress. This implies that the crack spacing measured practically is the average value of the whole range of the cracking stresses, i.e. from $\sigma_{\text{first crack}}$ to $\sigma_{\text{final crack}}$. Therefore, it follows that a more realistic value of (τ) is obtained when the mean values of the sum of the first and the final crack stresses are used in combination with the crack spacing measurement. The average calculated values of interfacial shear stress (τ) are given in column (9) of Table 4.1 and column (10) of Table 4.2.

(B) To obtain further information on interfacial shear stress (τ) values, an additional method of calculating (τ) from the data can be adopted, which considers that after the completion of multiple cracking in a specimen, a multiple fibre pull-out test occurs as the fibres are pulled out from the matrix within the grips. The ultimate load taken by the composite is therefore divided by the total surface area, i.e. ultimate load/$2\pi r\ell N$ of the fibres, which should result in a crude measure of the dynamic shear stress value at the fibre/matrix interface. It should be noted that the value of ℓ in this instance will be equal to the crack distance from either ends of the specimen, i.e. ℓ_x and ℓ_y respectively (see Table 4.3), hence giving individual values for τ_x and τ_y respectively. Distinction however is made between the interfacial shear stress during pull-out ($\tau_{dynamic}$) and the interfacial shear stress (τ) calculated from the crack spacing data which may include static as well as dynamic components.

The range of $\tau_{dynamic}$ values are higher than those calculated from the crack spacing; this is possibly due to the composite stress exerted by the wedge type grips.

This type of interfacial shear stress measurement on multiple fibres perhaps gives a more realistic picture of dynamic pull-out behaviour than a single fibre pull-out test.

The pull-out method of determining interfacial shear stress is discussed further in the next chapter, when pull-out in discontinuous aligned fibre composites is considered. However, the overall average value for all the volume concentrations of $\tau_{dynamic}$ is 0.274 N/mm^2, which is significantly higher than the compared values

TABLE 4.3 - DYNAMIC INTERFACIAL SHEAR STRESS ($\tau_{dynamic}$) CALCULATED BY USING MULTIPLE FIBRE PULL-OUT DATA FOR A BATCH OF SPECIMENS CURED BY METHOD 2

Test Code	Vol.% Fibre	No.of Fibres Pulled Out(N)	ℓ_x (mm)	ℓ_y (mm)	Ultimate Load (N)	τ_x (N/mm^2)	τ_y (N/mm^2)	Average $\tau_{dynamic}$ (N/mm^2)
Fibre Type A	1.4	77	29	88	1757.6	0.737	0.243	0.356
			59	90	1820.0	0.375	0.246	
			64	94	1528.8	0.291	0.198	
			51	-	1528.8	0.364	-	
			102	46	1710.8	0.204	0.452	
			59	-	2158.0	0.445	-	
Fibre Type A	2.4	132	55	-	1913.6	0.247	-	0.293
			78	41	2776.8	0.253	0.480	
			61	40	2776.8	0.323	0.492	
			172	45	1128.4	0.047	0.178	
			126	32	1580.8	0.089	0.350	
			44	45	2392.0	0.386	0.377	
Fibre Type A	4.2	220	39	46	2017.6	0.220	0.187	0.250
			65	38	2423.2	0.159	0.271	
			49	35	2392.0	0.208	0.291	
			42	35	2620.8	0.266	0.319	
			45	44	2631.2	0.249	0.254	
			43	46	3021.2	0.299	0.279	
Fibre Type A	5.5	286	27	50	3198.0	0.388	0.209	0.270
			48	53	2620.8	0.179	0.162	
			15	55	3536.0	0.772	0.210	
			46	58	2579.2	0.184	0.146	
			58	50	3421.6	0.193	0.224	
			42	40	3562.0	0.278	0.291	
Fibre Type A	8.7	440	36	38	4300.4	0.254	0.241	0.199
			66	39	4456.4	0.144	0.243	
			49	30	4617.6	0.201	0.328	
			57	59	4290.0	0.160	0.155	
			61	46	4035.2	0.141	0.187	
			53	56	4201.6	0.169	0.160	

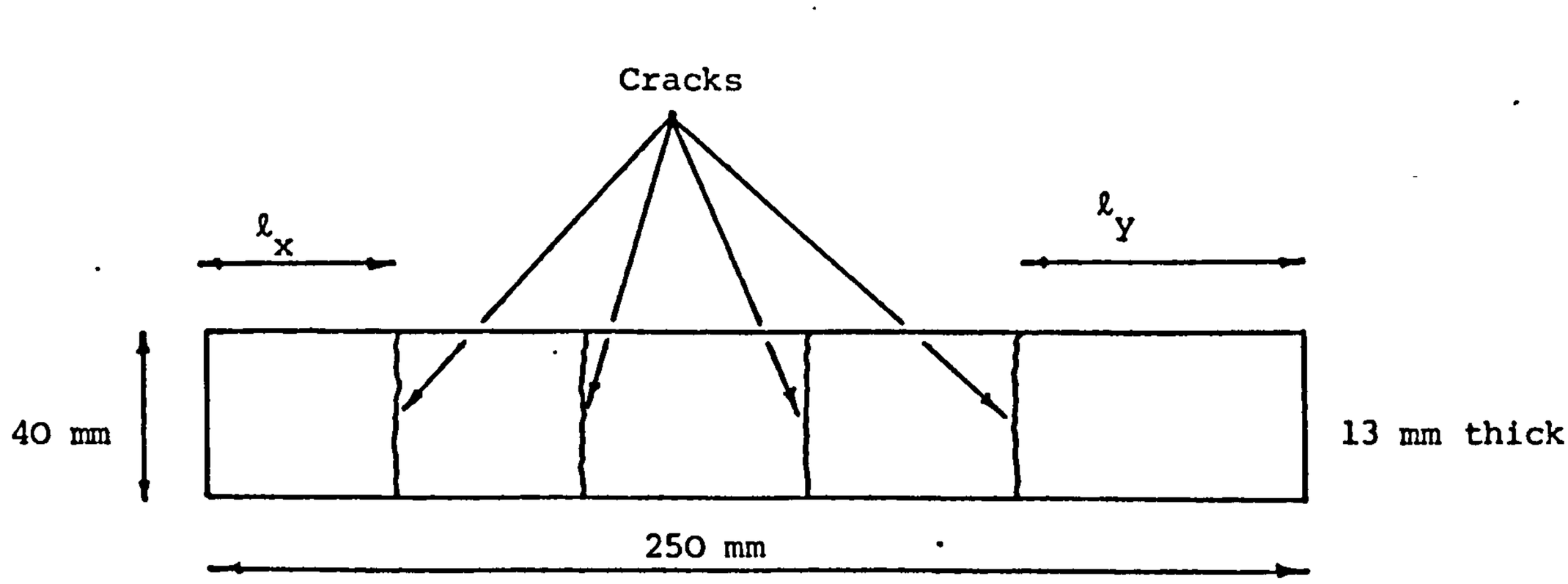

CONTINUOUS ALIGNED FIBRE REINFORCED CEMENT PASTE SPECIMEN

for (τ) measured by means of the crack spacing method, i.e. 0.104 N/mm^2.

4.5.3 Cracking Phenomena

The experimental results demonstrate that the basic phenomenon of multiple cracking in a cementitious matrix reinforced by fibres having a modulus of elasticity lower than that of the matrix, is essentially the same as that obtained with high modulus fibres. However, two theoretical treatments[61],[62] on multiple cracking have both predicted that it should not occur in the case of polypropylene fibre reinforced cement, unless shrinkage stresses or mechanical fibre/matrix interactions are also present. The high Poisson's ratio contraction of the polypropylene fibre compared to the cement is considered to lead to an unstable debonding of the fibre from the matrix. It is therefore necessary to consider in more detail the fibre/matrix interaction during multiple cracking in order to explain why it occurs in the case of polypropylene fibre reinforced cement.

Equation (4.2) is a necessary condition for multiple cracking to occur, but not a sufficient condition. Clearly, then, there must also be a fibre/matrix interaction and equation (4.3) assumes that a fibre/matrix shear stress of constant limiting value can develop as a result of friction. Kelly and Zweben[61] explain that if such a stress is present then there must also be a normal compressive force at the fibre surface. In some composite systems, such forces arise because of matrix shrinkage during curing or drying. However, in the absence of compressive forces, they consider that if the Poisson's ratio of the fibre (ν_f) is greater than a certain value related to the matrix Poisson's ratio (ν_m), then unstable debonding of the fibre from the

matrix will occur, and a single crack rather than multiple cracking will result. Fig. 4.9(a) illustrates their model, from which it can be seen that after cracking, a longitudinal element of the matrix adjacent to the crack surface is considered to relax laterally to its original unstrained lateral dimensions. The fibres are required to support the total load on the composite and hence suffer an increased lateral contraction. The difference between the matrix expansion and the fibre contraction may result in total loss of contact between the fibre and matrix. Table 4.4 indicates those composites which should not exhibit multiple cracking because of this effect.

Pinchin[62] in his work, considers that an assumption of complete matrix relaxation is not acceptable for actual composite behaviour. Furthermore, he points out that the previous model assumes a fibre/matrix contact with no interfacial pressure, when the composite is under strain just before cracking. This, however, will not be the case unless ν_f and ν_m have the same value. Pinchin's[62] treatment of the effect of Poisson's ratio is illustrated in Fig. 4.9(b). In this model it is considered that the longitudinal matrix element does not relax laterally after cracking, since it must be restrained by the adjacent matrix elements. The extreme case is analysed where the matrix lateral expansion is completely prevented. This analysis considers the external forces required to prevent complete lateral expansion of the outside diameter of a hypothetical tube of matrix surrounding a fibre. Such an external pressure will reduce the bore of the cylinder of matrix. The magnitude of this bore reduction is calculated for the same systems as analysed by Kelly et al[61] and compared with the fibre diametral contraction, in order to establish a loss of fibre/matrix contact criterion and hence the absence of multiple cracking. Table 4.4

FIGURE 4.9 - SCHEMATIC ILLUSTRATIONS OF (a) KELLY AND ZWEBEN MODEL, (b) PINCHIN MODEL, (c) PROPOSED MODEL. THE POISSON CONTRACTIONS HAVE BEEN GREATLY EXAGGERATED FOR CLARITY.

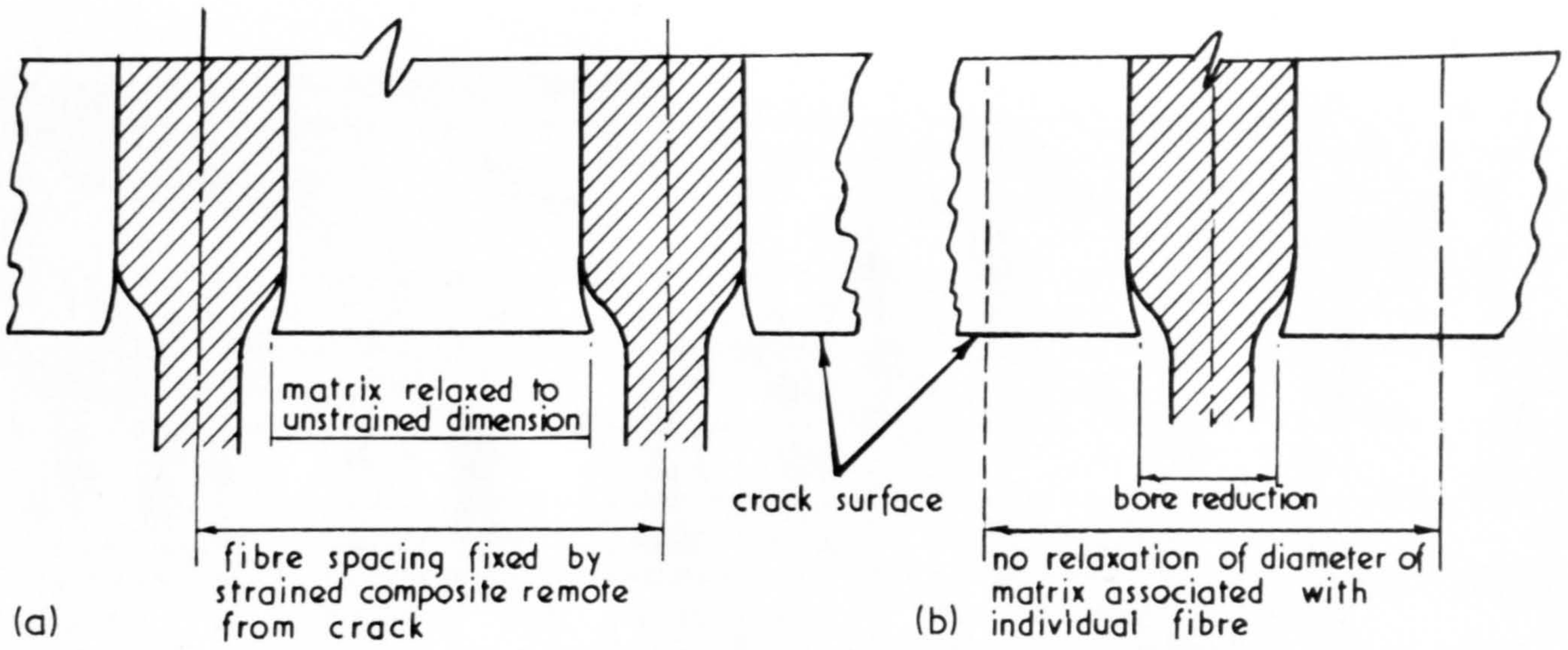
matrix relaxed to unstrained dimension
fibre spacing fixed by strained composite remote from crack
(a)
crack surface
bore reduction
no relaxation of diameter of matrix associated with individual fibre
(b)

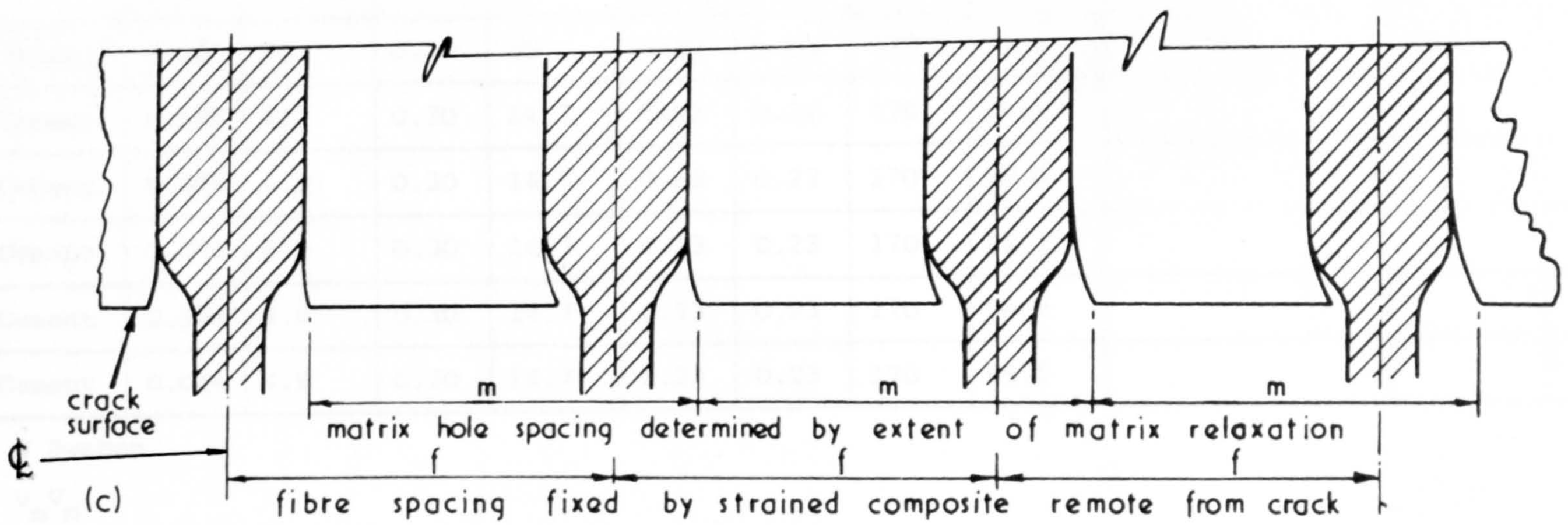
crack surface
℄
m
m
m
matrix hole spacing determined by extent of matrix relaxation
f
f
f
(c)
fibre spacing fixed by strained composite remote from crack

TABLE 4.4 - CRITERIA FOR PREDICTING MULTIPLE CRACKING

System Fibre/Matrix	V_f	E_f kN/mm^2	ν_f	E_m kN/mm^2	ν_m	ν_c*	r** (μm)	d_c (mm)	Multiple Cracking Predicted		
									Kelly & Zweben	Pinchin	d_c Criterion
Steel/Cement+	0.05	200	0.28	20	0.23	0.23	150	1.4	Yes	No	Yes
Steel/Epoxy+	0.20	200	0.28	3.5	0.30	0.30	150	0.6	Yes	Yes	Yes
Graphite/Cement+	0.02	200	0.35	20	0.23	0.23	5	0.03	No	No	Yes
Graphite/Cement+	0.05	200	0.35	20	0.23	0.24	5	0.014	Yes	No	Yes
Glass/Epoxy+	0.60	72	0.25	3.5	0.30	0.27	5	0.02	Yes	Yes	Yes
Graphite/Glass+	0.50	200	0.35	72	0.25	0.30	5	0.026	No	No	Yes
Glass/Cement+	0.05	72	0.25	20	0.23	0.23	5	0.08	No	No	Yes
Polypropylene/Cement+	0.10	10	0.30	20	0.23	0.24	170	8.4	No	No	No
Polypropylene/Cement	0.087	4.9	0.30	14.7	0.23	0.24	170	14.2			No
Polypropylene/Cement	0.055	4.9	0.30	14.7	0.23	0.23	170	23.6			No
Polypropylene/Cement	0.042	4.9	0.30	14.7	0.23	0.23	170	31.1			No
Polypropylene/Cement	0.024	4.9	0.30	14.7	0.23	0.23	170	54.9			No
Polypropylene/Cement	0.014	4.9	0.30	14.7	0.23	0.23	170	94.5			No

+ After Kelly & Zweben

* $\nu_c \simeq \nu_f V_f + \nu_m V_m$

** Nominal Values Apart from Polypropylene

compares the results of the two approaches.

It is considered that a limitation of both of these analyses is the assumption that the forces acting on a fibre are identical wherever the fibre is located. Kelly and Zweben[61] considered a single pair of fibres, from which they extrapolated for the whole array, whilst Pinchin[62] only considered a single fibre and its equivalent tube of matrix, likewise extrapolated. Furthermore, Pinchin's[62] analysis seeks to determine a criterion for the loss of fibre/matrix contact in the middle of an array of fibres, whilst relying on the fibre/matrix contact to prevent lateral expansion of the matrix.

The influence of fibre location on fibre/matrix interaction can be identified qualitatively, by considering a specimen of circular cross-section as follows. It is assumed that the composite strain remote from an initial crack is equal to the strain immediately before cracking. This assumption is also made in the two previous analyses and is also given in the general treatment by Aveston et al[12], where some matrix relaxation at the crack surface is assumed. The extent of the relaxation being dependent upon many factors including those of elastic moduli of the fibre and matrix, fibre volume fraction, fibre diameter and specimen size. Fig. 4.9(c) illustrates the implications of these assumptions. The centre line of each fibre is determined by the fully strained system. The centre line of the matrix hole at the cracked surface is determined for a given average lateral relaxation, by its distance from the centre of the whole specimen. It can be seen that the condition for fibre/matrix contact must be reached in any composite system, provided that the fibre is located sufficiently far enough from the centre line of the specimen. Thus, there is a critical diameter of the specimen which must be exceeded in order to have fibre/matrix contact and an additional thickness of material

further increasing the diameter, in order that multiple cracking should occur. The additional thickness will be dependent upon the volume fraction of the fibres and the fibre/matrix interface strength (τ). (τ) however does not have a unique value and is dependent upon several factors. A Coulomb relationship describes the general case, i.e.

$$\tau = C + \sigma_n \mu \qquad \ldots \ldots \ldots \qquad (4.4)$$

where C is the fibre/matrix cohesion = 0, in the case of a purely frictional interaction, σ_n is the normal compressive force at the fibre/matrix interface and μ is the coefficient of friction. Several investigators, however, have drawn attention to the variability of μ and σ_n during the deformation process[63],[64],[65] and the present work also indicates additional sources of σ_n variables. The greater the distance of a fibre from the centre line of a specimen beyond the critical diameter, the greater is σ_n. σ_n also varies around the circumference of an individual fibre, being at a maximum at the nearest point to the centre of the specimen. Furthermore, as the specimen diameter increases, fibre restraint will begin to restrict lateral matrix expansion.

In the absence of data regarding these various effects, it is not possible to calculate the minimum additional diameter to allow multiple cracking. However, calculation of the critical diameter, d_c, enables an assessment to be made of the likelihood of multiple cracking occurring in practical sized composites.

A cylindrical composite containing uniformly spaced longitudinally aligned fibres is considered, and it is assumed that the matrix element adjacent to the crack surface will relax laterally to its original

unstrained dimensions, provided that the diameter is less than or equal to the critical diameter d_c. The basis of the calculation is illustrated in Figure 4.10, from which it can be seen that fibre/matrix contact will occur, when the displacement of a matrix hole away from the centre of the specimen due to matrix relaxation at the crack surface (D), plus the fibre radius immediately after cracking (C) is equal to the radius of the unstrained fibre or matrix hole (r).

That is

$$r = D + C \qquad .. \quad .. \quad .. \qquad (4.5)$$

when $d = d_c$

$$\text{where } D = \left(\frac{d_c}{2} - r\right) \nu_c \varepsilon_c \qquad .. \quad .. \quad .. \qquad (4.6)$$

where d_c = critical diameter

r = radius of the fibre or matrix hole

ν_c = Poisson's ratio of a composite

ε_c = composite longitudinal strain at the onset of cracking.

Assuming that the relaxation displacement after cracking at the edge of the hole is the same as that at the centre line of the hole

$$\text{and } C = r(1 - \nu_f \varepsilon_{ft}) \qquad .. \quad .. \quad .. \qquad (4.7)$$

where ν_f = Poisson's ratio of the fibre

ε_{ft} = the longitudinal strain in the fibre bridging the crack.

Adding equations (4.6) and (4.7)

$$\therefore \quad r = \left(\frac{d_c}{2} - r\right) \nu_c \varepsilon_c + r(1 - \nu_f \varepsilon_{ft})$$

rearranging and simplifying

$$d_c = 2r\left(1 + \left(\frac{\varepsilon_{ft}}{\varepsilon_c}\right)\frac{\nu_f}{\nu_c}\right) \qquad .. \quad .. \quad .. \qquad (4.8)$$

To determine ε_{ft},

consider first stress on the composite at onset of cracking

FIGURE 4.10 - RELATIONSHIP BETWEEN FIBRE AND MATRIX DEFORMATIONS

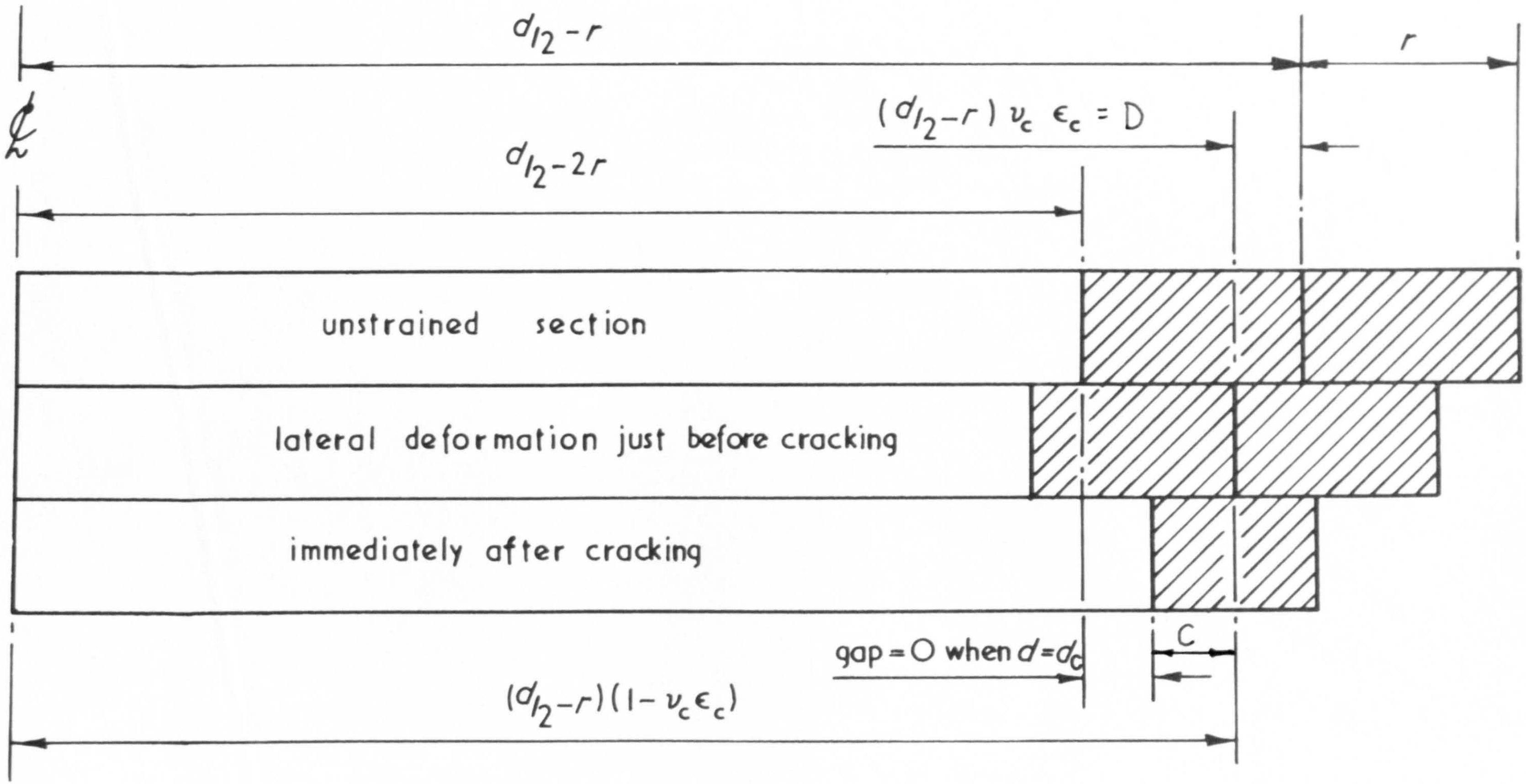
$d_{l_2} - r$
r
ℓ
$(d_{l_2} - r)\, \nu_c\, \epsilon_c = D$
$d_{l_2} - 2r$
unstrained section
lateral deformation just before cracking
immediately after cracking
gap = O when $d = d_c$
C
$(d_{l_2} - r)(1 - \nu_c \epsilon_c)$

$$\sigma_c = \sigma'_f V_f + \sigma_{mu} V_m \qquad .. \quad .. \quad .. \qquad (4.9)$$

where σ_c = stress in the composite

σ'_f = fibre stress at onset of cracking

σ_{mu} = ultimate stress on the matrix immediately before cracking

V_f = volume fraction of the fibre

V_m = volume fraction of the matrix

the load on the composite = σ_c for unit cross-section, this load is supported by the fibres, i.e.

$$\text{fibre stress} = \frac{\sigma_c}{V_f}$$

dividing equation (4.9) by V_f throughout

$$\text{fibre stress} = \frac{\sigma_c}{V_f} = \sigma'_f + \frac{\sigma_{mu} V_m}{V_f}$$

$$\text{hence fibre strain} \quad \varepsilon_{ft} = \frac{\sigma'_f + \dfrac{\sigma_{mu} V_m}{V_f}}{E_f}$$

where E_f = elastic modulus of the fibre

simplifying

$$\varepsilon_{ft} = \frac{\sigma'_f}{E_f} + \frac{\sigma_{mu} V_m}{E_f V_f} \qquad .. \quad .. \quad .. \qquad (4.10)$$

but

$$\sigma'_f = \varepsilon_c E_f \qquad .. \quad .. \quad .. \qquad (4.11)$$

$$\sigma_{mu} = \varepsilon_c E_m \qquad .. \quad .. \quad .. \qquad (4.12)$$

where E_m = elastic modulus of the matrix.

Substituting equations (4.11) and (4.12) into (4.10) and simplifying

$$\therefore \quad \varepsilon_{ft} = \varepsilon_c \left(1 + \frac{E_m V_m}{E_f V_f}\right) \qquad .. \quad .. \quad .. \qquad (4.13)$$

Substituting equation (4.13) into equation (4.8)

$$\therefore \quad d_c = 2r \left(1 + \left(\frac{\varepsilon_c (1 + \dfrac{E_m V_m}{E_f V_f})}{\varepsilon_c}\right) \frac{\nu_f}{\nu_c}\right)$$

$\therefore$ simplifying gives

$$d_c = 2r\left(1 + \left(1 + \frac{E_m V_m}{E_f V_f}\right)\frac{\nu_f}{\nu_c}\right) \quad .. \quad .. \quad .. \quad (4.14)$$

Table 4.4 lists the values of d_c for the various systems considered by Kelly and Zweben[61]. It can be seen that apart from the polypropylene reinforced cement, all the composites have a d_c less than 1.4 mm. Thus in practical sized composites, the majority of the fibres will be in contact with the matrix and multiple cracking must occur above a critical volume fraction. This will be slightly higher than that predicted by Aveston et al[12], although their general treatment of multiple cracking applies equally as well to an average fibre/matrix shear strength as to a unique value. Thus it follows that the role of the Poisson's ratio is not significant in these composites.

For polypropylene reinforced cement d_c is 94.5 mm for 1.4% and 54.9 mm for 2.4% volumes of fibre. Since these values are greater than the dimensions of the specimens in which multiple cracking occurred, other factors must therefore contribute to offset the Poisson's ratio shrinkage. In the case of 4.2%, 5.5% and 8.7% volume of fibre, d_c = 31.1 mm, 23.6 mm and 14.2 mm respectively. Therefore some fibre/matrix contact would be expected, with the larger cross-sectional dimension of the practical specimens (13 mm x 40 mm). However, it is thought that there would still be insufficient contact to develop multiple cracking according to the considered model.

It has also been suggested that matrix shrinkage or surface fibre asperities could be responsible. A certain amount of shrinkage stress in the specimens could have been induced by curing method 1.

The influence of this shrinkage can be assessed as follows. Average lateral shrinkage strains of 0.0006 were measured directly by means of transducers, during the one-day air-drying period immediately prior to testing, which resulted in an average precompression of 0.2 μm for the 340 μm diameter fibres.

The Poisson's ratio contraction of a 340 μm diameter fibre in a composite with 5.0% V_f at the onset of cracking, is calculated as follows:

Average values of matrix strain at failure (ε_m), matrix elastic modulus (E_m) and fibre elastic modulus (E_f) were determined experimentally as 0.018%. 14.7 kN/mm^2 and 4.9 kN/mm^2, respectively. The composite fails at matrix failure strain and the stress at failure on the composite $\sigma_c = E_c . \varepsilon_m$

where E_c is the composite modulus and ε_m the matrix strain. From the rule of mixtures, $E_c = E_f V_f + E_m V_m$

$$\text{i.e. } E_c = 14210 \text{ N/mm}^2$$

$$\text{since } \sigma_c = E_c . \varepsilon_m$$

$$\sigma_c = 2.56 \text{ N/mm}^2$$

Taking the unit cross-sectional area, then the load on the composite at failure = 2.56 N. The stress on the fibres bridging the crack, σ_f = load/cross-sectional area of fibre = $^{2.56}/_{0.05}$ = 51.2 N/mm^2.

$$\therefore \text{ the strain in the fibre } \varepsilon_f = \frac{\sigma_f}{E_f} = \frac{51.2}{4900} = 0.0104$$

$\therefore$ the lateral strain in the fibre = ν_f x Longitudinal Strain

where ν_f is Poisson's contraction ratio of fibre

i.e. Lateral strain = 0.3 x 0.0104 = 0.0031

$\therefore$ shrinkage in the 340 μm diameter fibre = 340 x 0.0031 = 1.060 μm,

which implies that the precompression of 0.2 μm induced by the matrix drying shrinkage, can be ignored when compared with the Poisson's ratio contraction value of 1.060 μm.

Since multiple cracking also occurred for those specimens cured by method 2, which would involve less matrix shrinkage, it can be concluded that multiple cracking in polypropylene reinforced cement paste is not dependent upon matrix shrinkage.

Pinchin[62] considers that in steel/cement systems, there is a mechanical interaction between the fibre surface asperities and the matrix, which is sufficient to develop frictional forces in the absence of direct fibre/matrix contact. Scanning electron microsopic studies of the fibre surfaces of polypropylene indicate that defects of up to 10 μm are present (see Plate 4.3). Hence a similar fibre/matrix interaction can take place in polypropylene cement systems.

A major source of fibre/matrix contact not previously discussed is thought to be the misalignment of the two surfaces of a crack after it has passed completely across a specimen. In extreme cases, the misalignment can take the form of a lateral displacement of one crack surface relative to the other. In the later stages of post-crack deformation, the misalignment can be seen with the naked eye. Several factors help to contribute to the misalignment, of which the inherent variations of the fibre/matrix shear stresses from fibre to fibre remote from the crack are possibly the most important. A slight offset between the upper and lower tensile grips, irregularities in the specimen dimensions and the response of the whole test system to the impact type load transfer from matrix to fibre at cracking, will all tend to ensure that the crack surfaces do not displace parallel to

PLATE 4.3 - ASPERITIES ON THE SURFACE OF A 340 μm DIAMETER POLYPROPYLENE FIBRE

PLATE 4.4 - SHAVINGS PRODUCED FROM 340 μm DIAMETER POLYPROYLENE FIBRE

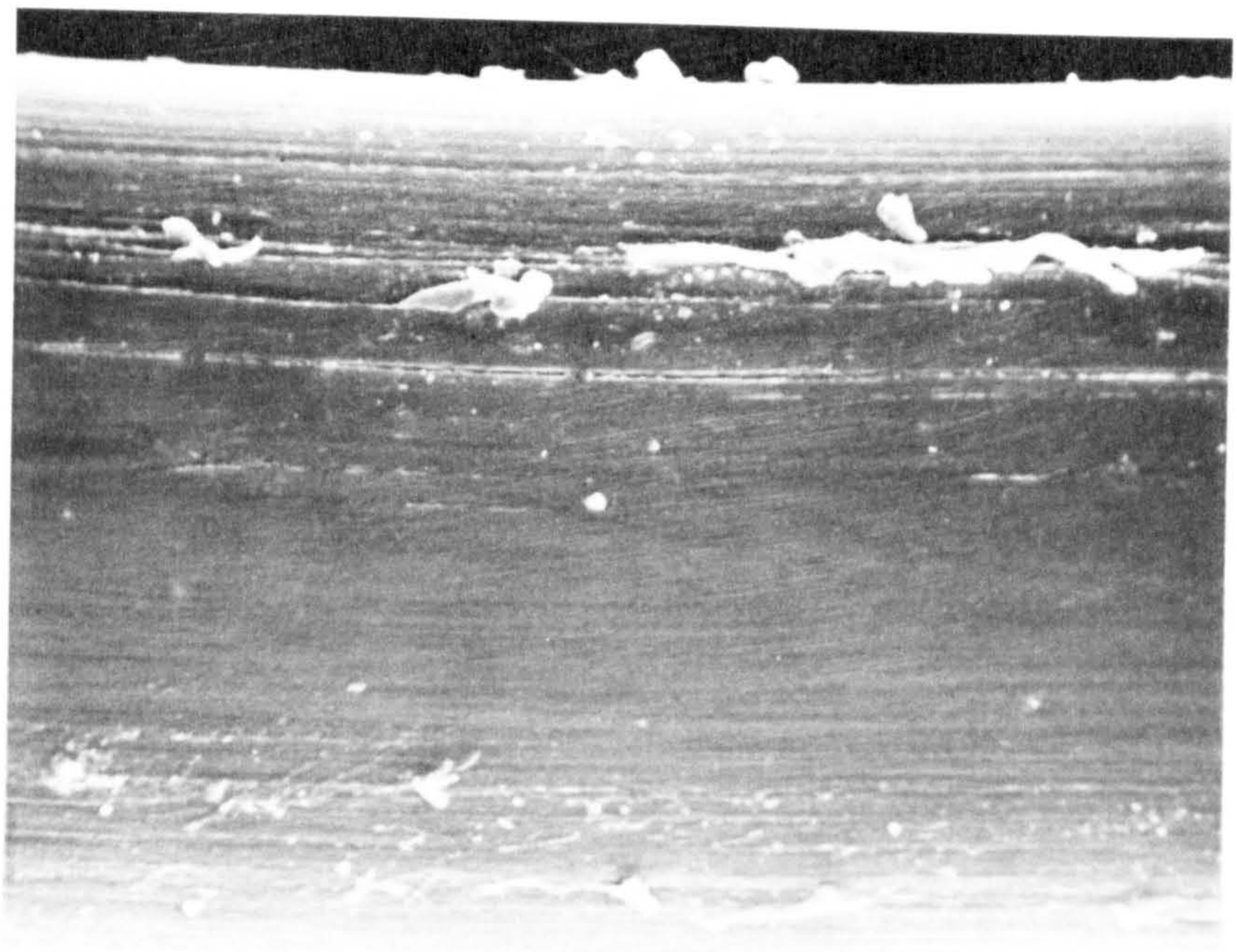

the tensile axis. These phenomena will also occur in other composites, but the very low modulus of elasticity of polypropylene gives rise to wider cracks as well as crack spacings, thus a greater opportunity for distortion. Therefore, fibre/matrix friction is possible, even at the point of intersection of the cracked surface and the fibre. Evidence of fibre/matrix interaction is considerable on both a microscopic and macroscopic scale. Polypropylene fibres being much softer than the matrix, contrary to most other reinforcing fibres, the fibres have their surfaces damaged during deformation. A common type of damage observed was the chiselling out of a long shaving of polypropylene by a matrix particle (Plate 4.4). Fibre/matrix contact will also occur if the fibres are not exactly parallel. Clearly, a slight misalignment will occur, even in the most accurate lay-up method. Also, whilst winding the fibre, a twisting of the fibre is unavoidable, which in turn creates a corkscrew effect, when the fibre is pulled out of the matrix, involving more interaction with the matrix.

Therefore, it appears that although in an ideal continuous polypropylene aligned fibre thin sheet the effect of the Poisson's contraction should be to disengage the fibre from the matrix, in a practical system several mechanisms can operate to ensure fibre/matrix contact.

4.5.4 Elastic Modulus

Increasing volume fractions of fibre type A, cured by method 2, had little effect on the modulus of elasticity of the composite. Theoretically (using the rule of mixture) a composite with 8.7%

volume fraction of fibre (E_f = 4.9 kN/mm^2) should have a value of E_c = 13.90 kN/mm^2 compared to that of E_m = 14.70 kN/mm^2. Such a difference lies within the overall scatter of the result.

Tapes type A (elastic modulus value of 10.0 kN/mm^2) exhibited narrower crack widths when compared with fibre type A (elastic modulus value of 4.92 kN/mm^2) for the same volume fraction incorporated in the specimens. This indicates that the elastic modulus value influences the crack widths, although the observations were qualitative by nature only.

4.6 CONCLUSIONS

The general conclusions that can be drawn are:

(1) Multiple cracking occurs in uniaxially aligned polypropylene fibre reinforced cement composites, despite the unfavourable fibre modulus and Poisson's ratio. The fibre/matrix contact necessary to induce this multiple cracking is thought to result from

(A) the presence of asperities on the fibre surface;

(B) the surfaces of a matrix crack displacing laterally as well as longitudinally, relative to each other and to the fibre array;

(C) the slight departure from parallelism of the reinforcing fibres.

(2) A simple theoretical model for the influence of Poisson's ratio on multiple cracking predicted that multiple cracking should occur in any fibrous composite, providing that a critical specimen diameter and a critical volume fraction of fibres is exceeded.

In the case of composites utilising fibres of higher modulus than the matrix, this diameter is less than the likely minimum dimension of the practical material, whereas in polypropylene reinforced cement it is much greater for some cases. The mechanism by which the Poisson's ratio contraction of the fibres is offset to ensure fibre/matrix contact in these systems, arises from the interaction of the relaxing matrix element at the crack surface with the non-relaxing fibre array.

(3) The average interfacial shear stress (τ) was found to be 0.104 N/mm^2, when determined by the crack spacing method and 0.274 N/mm^2 ($\tau_{dynamic}$) when determined by the multiple fibre pull-out method. However, the normal compressive stress at the surface of a fibre after matrix cracking was shown to increase with increasing distance from the centre of a specimen and to vary around the surface of a fibre. This implies that there is not a unique limiting fibre/matrix frictional shear stress.

Specific conclusions can be listed as follows:

(1) Multiple cracking takes place at successively higher stress levels rather than at a constant limiting value.

(2) Curing method effects the first crack stress of a composite, i.e. those specimens cured in air for one day prior to testing gave a slight reduction in strength than those specimens tested immediately after removal from the water.

(3) The number of cracks and the ultimate tensile stress increased as the fibre volume increased.

(4) Final failure of the specimens invariably occurred by fibre pull-out and not fibre failure.

(5) Reinforcement with fibre tapes, having a higher elastic modulus value than the fibres, exhibited qualitatively narrower crack width.

(6) The influence of the fibres on the composite modulus up to the first crack could not be established because of experimental scatter.

DISCONTINUOUS ALIGNED FIBRE REINFORCED CEMENT PASTE

CHAPTER FIVE

DISCONTINUOUS ALIGNED FIBRE REINFORCED CEMENT PASTE

5.1 PREAMBLE

In order to follow on from the objectives of chapter four, the next stage of the investigation was to introduce variables of fibre length, whilst keeping fibre alignment in the specimens as far as possible, parallel to the eventual tensile stress axis. Three levels of fibre volume concentrations were investigated, to provide a comparison with the continuous aligned fibre reinforced cement paste systems.

The fibre lengths used, i.e. 10, 26 and 60 mm, were chosen arbitrarily, in order to identify the conditions below, which interfacial shear stress transfer between fibre/matrix is not sufficient for multiple cracking to ensue. The lower limit of the fibre length was determined by the width of the mould used to achieve general alignment, since smaller fibres than the mould width would undoubtedly tend to orientate into non-preferential directions.

The major objective in this chapter was to obtain an insight into interfacial shear stress transfer mechanisms involved between fibre and matrix.

5.2 MATERIALS

5.2.1 Cement

Standard Ordinary Portland cement was used as described in section 3.6 for this series of test and Table 3.1 shows the typical oxide compositions.

5.2.2 Fibres

340 μm diameter straight polypropylene brush filament fibres, having a tangent modulus of elasticity value of 3.8 kN/mm^2 and lengths of 10, 26 and 60 mm, were used.

5.3 FABRICATION

5.3.1 Mix Procedure

A neat cement paste of water/cement ratio 0.4 was used, as described in section 3.7.1, to give a sufficient workability for fibre composite preparation.

5.3.2 Casting and Curing

The general methods described in section 3.7.2 were employed, except that the matrix and fibres were hand laid into the mould, in a layer by layer fashion. First a sufficient amount of matrix was poured into the mould (13 mm wide by 40 mm deep by 250 mm long) to coat the bottom surface, and then the fibres were placed so that they were generally aligned along the length of the mould. This cycle was repeated until the mould was full and the desired volume fractions of fibres incorporated, namely 1.4 and 4.2% by volume concentration, for 10, 26 and 60 mm fibre lengths and 8.7% by volume for 60 mm fibre length. Although great care was taken in the preparation of these specimens, it was found that not all the fibres were exactly aligned and that slight inclination of the fibres was unavoidable, together with variation in their distribution.

5.4 TEST PROCEDURE

5.4.1 Tensile Strength

The load was applied using the position control of the Losenhausen test machines cross-head, via a constant rate of cross-head movement of 1 mm/min. For details see section 3.8.1.

5.4.2 Strain Measurement

The same technique of measuring deformation of the specimens was used as for the continuous aligned fibre composite specimens, i.e. the deformation to first crack was measured with an extensometer and subsequent deformations by means of the test machine's cross-head movement.

5.4.3 Crack Spacing Measurement

Having once obtained multiple cracking in the specimens during uniaxial testing, the final crack spacing was measured as described in section 4.4.3.

5.5 ANALYSIS AND DISCUSSION OF RESULTS

5.5.1 Cracking Phenomena

Multiple cracking was observed in the specimens containing 4.2% by volume concentration of fibre with lengths of 10, 26 and 60 mm, the longer the length the greater the number of cracks. Only one fibre length, i.e. 60 mm was used at 8.7% by volume concentration and at

this concentration, the specimens exhibited the largest number of cracks. Specimens containing 1.4% by volume concentration with fibre lengths of 10, 26 and 60 mm failed with a single crack. Figures 5.1 to 5.7 show the shape of the load versus cross-head displacement plots, in particular the stress drops associated with multiple cracking, where applicable, for the various fibre concentrations and lengths.

A comparison between the continuous and discontinuous aligned systems shows that multiple cracking occurred in both types of systems at 4.2% and 8.7% by fibre volume concentration. In the case of the 1.4% by volume concentration, the continuous aligned specimens either exhibited one or two cracks, whereas the discontinuous aligned specimens invariably failed with a single crack. Specimen failure eventually occurred by means of the fibres pulling out of the matrix. In the 1.4% by volume concentration of discontinuous aligned fibre specimens, the ultimate load was higher than the pull-out load, whereas at higher volume concentrations, the pull-out load was either equal to or greater than the final crack load.

Multiple cracking took place progressively, at slightly higher stress levels for successive cracks in a similar manner to the continuous aligned fibre composite specimens. However, the difference between the ultimate stress and the first crack stress for these specimens was smaller than that of the corresponding continuous aligned fibre composite specimens. When the average ultimate stress values of the discontinuous aligned fibre composites (see Table 5.1) were compared with those of the continuous aligned fibre composites (see Table 4.2) containing the same percentage by volume of fibre, there was a marked difference between the two, whereas there was only a slight difference for the first crack stress. The significantly lower

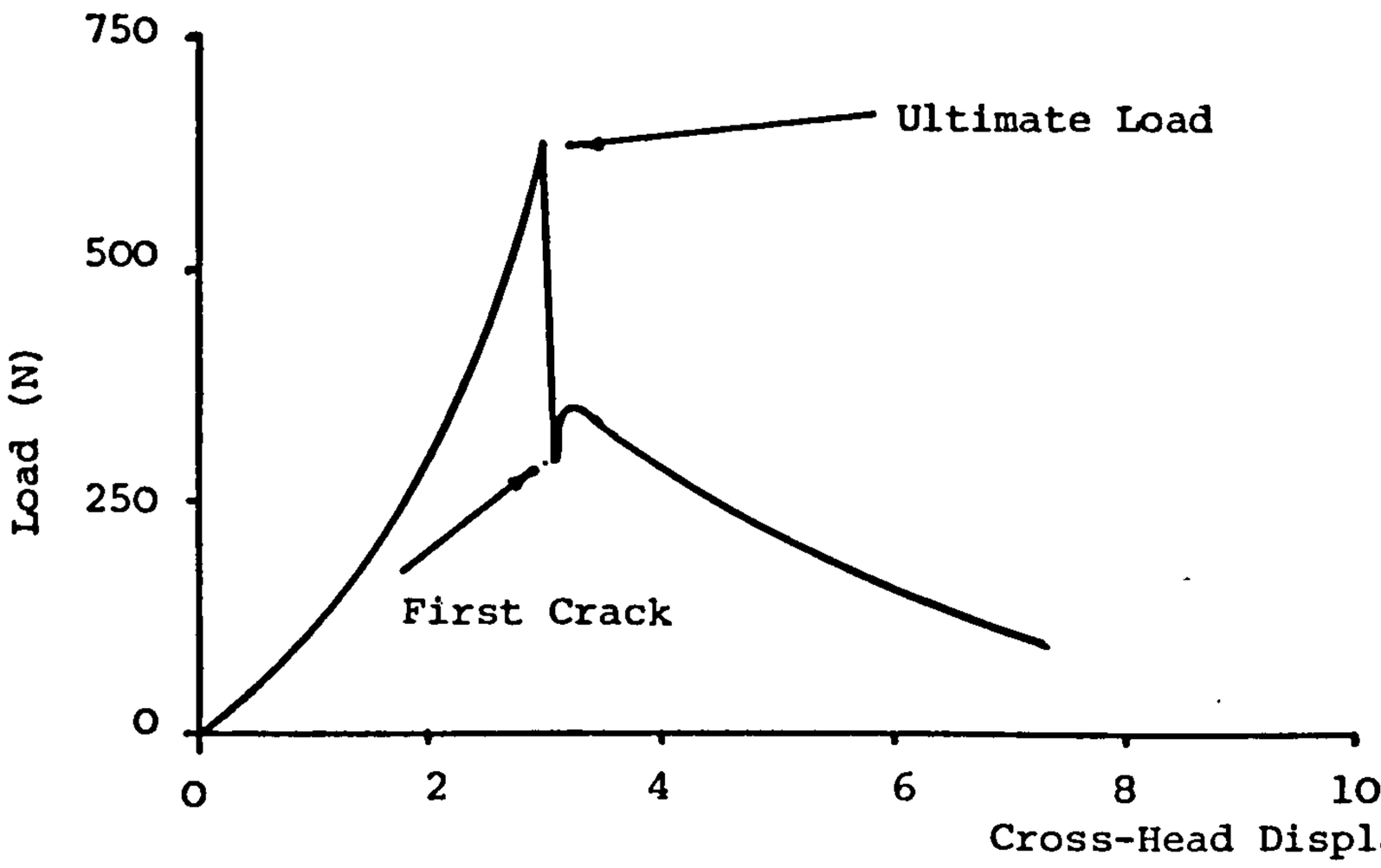

FIGURE 5.1 - TYPICAL TENSILE LOAD/CROSS-HEAD DISPLACEMENT CURVE FOR DISCONTINUOUS ALIGNED FIBRE COMPOSITE CONSISTING OF 10 mm CHOPPED FIBRE AND 1.4% VOLUME CONCENTRATION

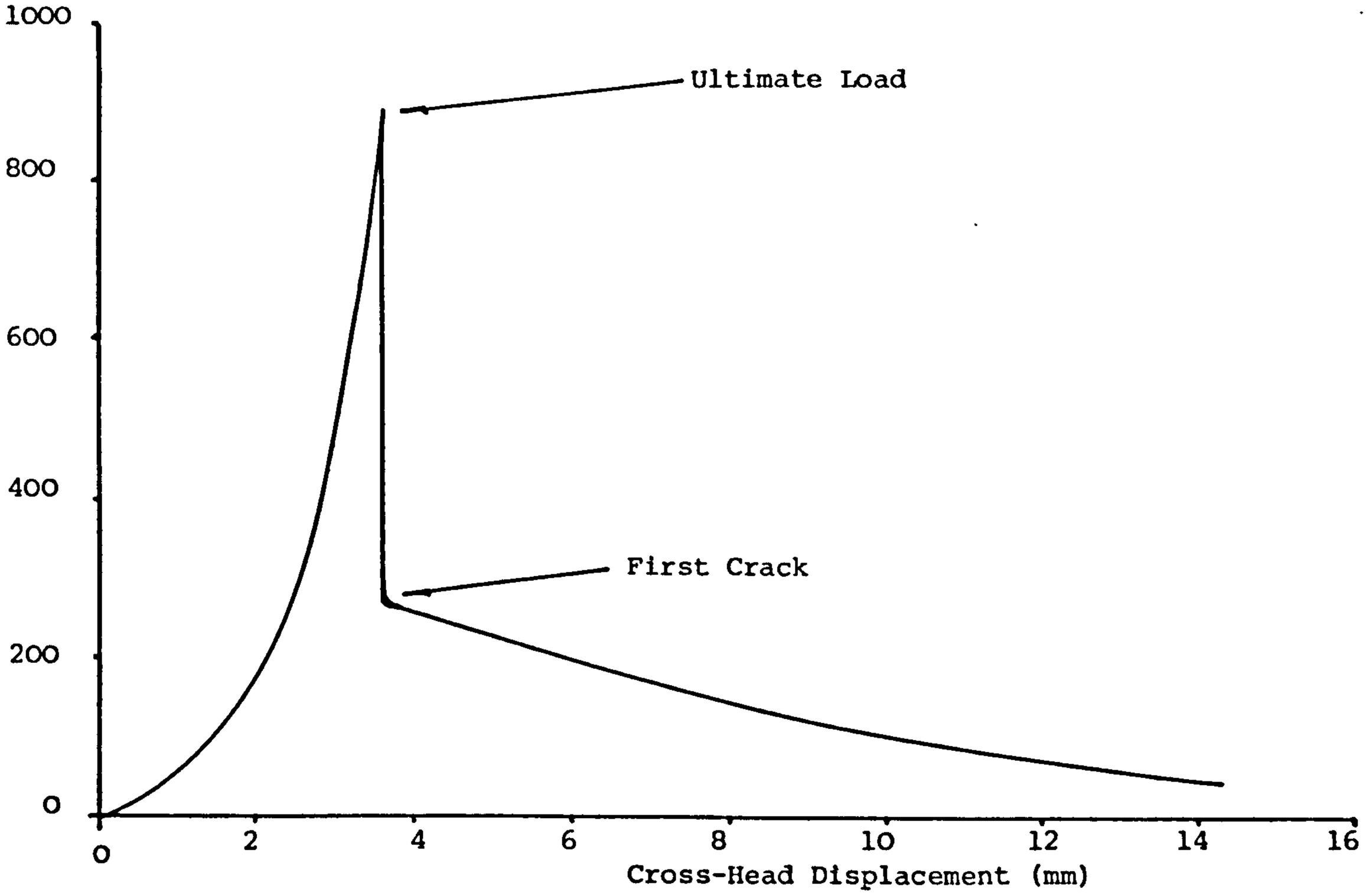

FIGURE 5.2 - TYPICAL TENSILE LOAD/CROSS-HEAD DISPLACEMENT CURVE FOR DISCONTINUOUS ALIGNED FIBRE COMPOSITE CONSISTING OF 26 mm CHOPPED FIBRE AND 1.4% VOLUME CONCENTRATION

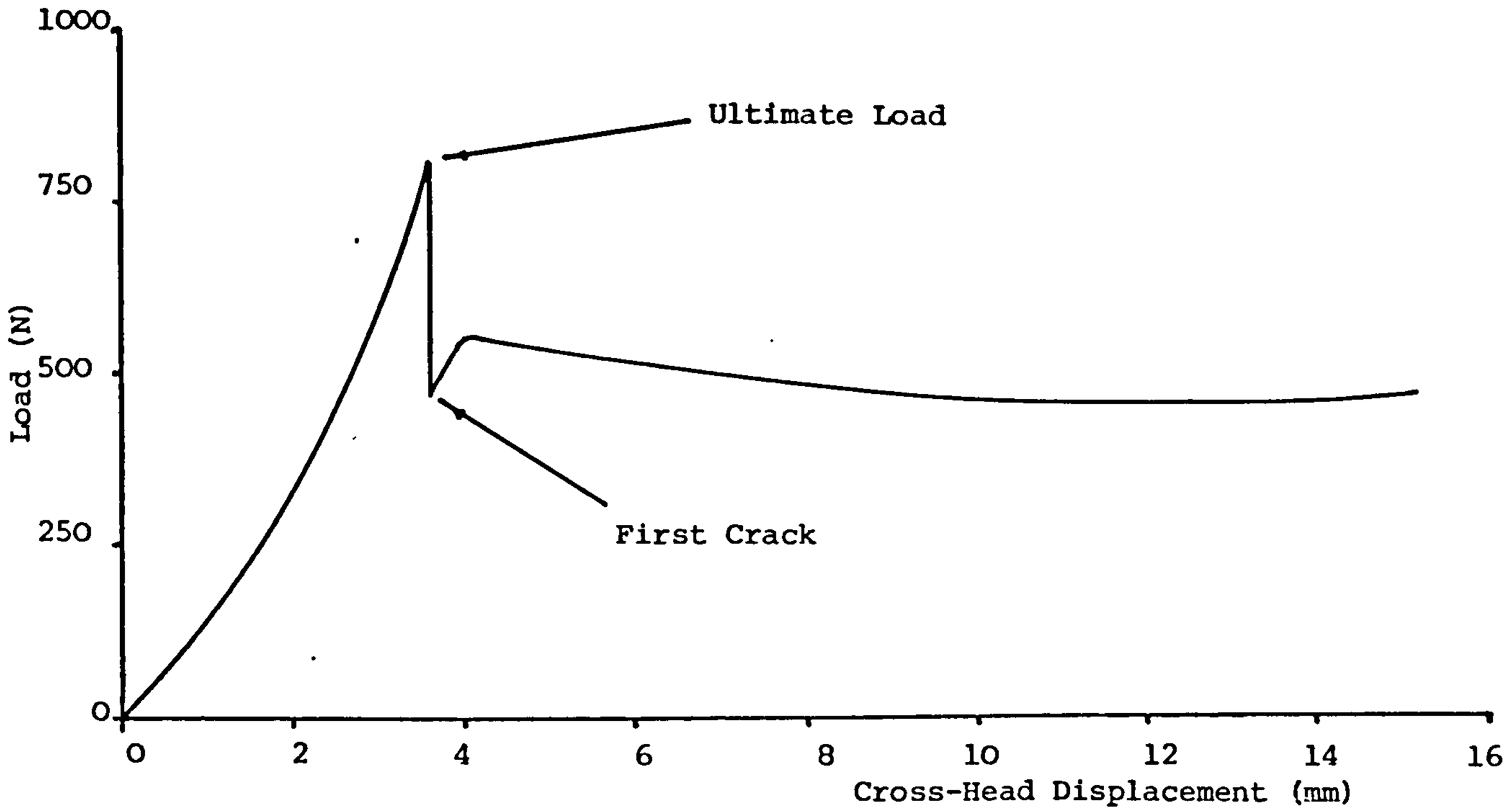

FIGURE 5.3 - TYPICAL TENSILE LOAD/CROSS-HEAD DISPLACEMENT CURVE FOR DISCONTINUOUS ALIGNED FIBRE COMPOSITE CONSISTING OF 60 mm CHOPPED FIBRE AND 1.4% VOLUME CONCENTRATION

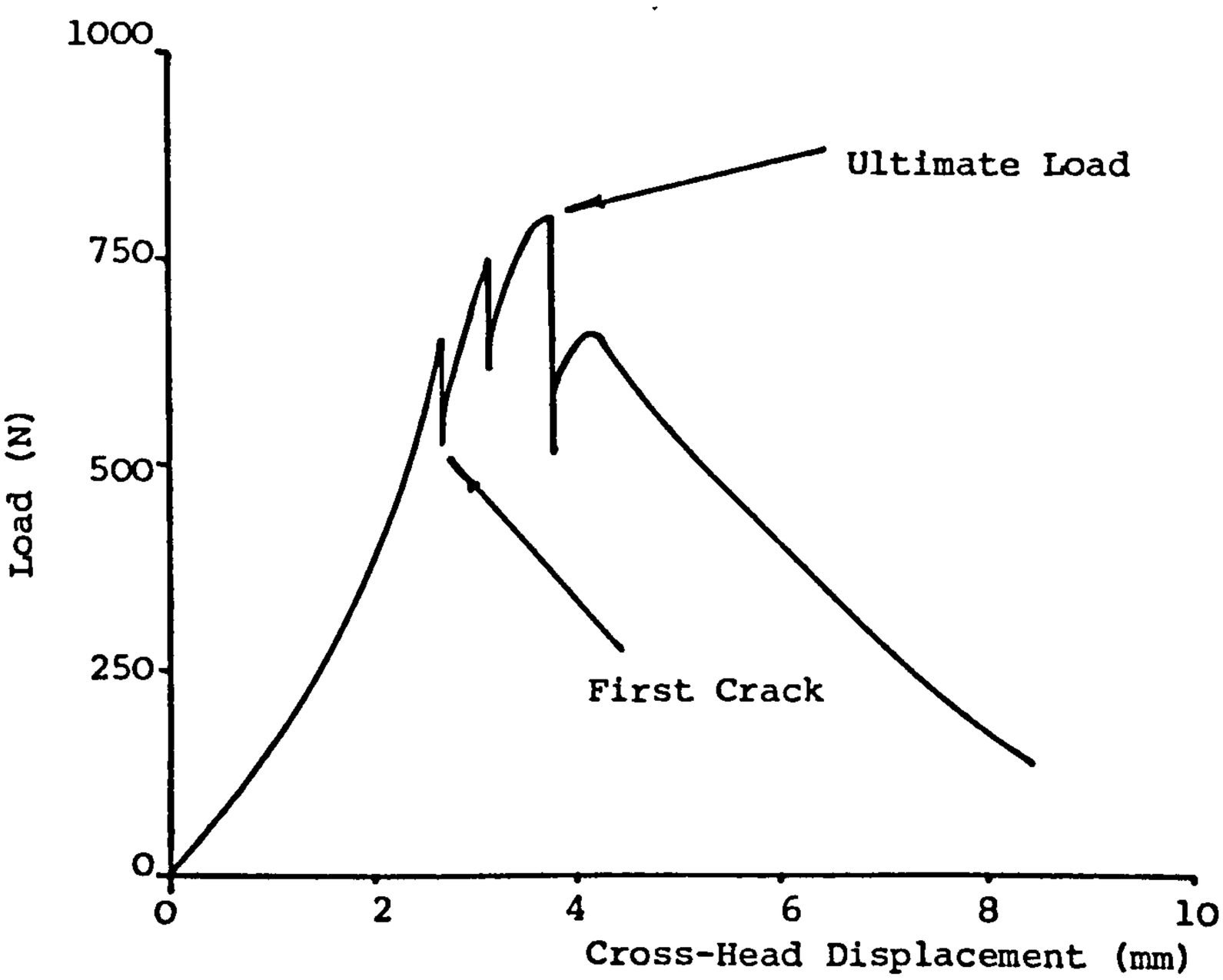

FIGURE 5.4 - TYPICAL TENSILE LOAD/CROSS-HEAD DISPLACEMENT CURVE FOR DISCONTINUOUS ALIGNED FIBRE COMPOSITE CONSISTING OF 10 mm CHOPPED FIBRE AND 4.2% VOLUME CONCENTRATION

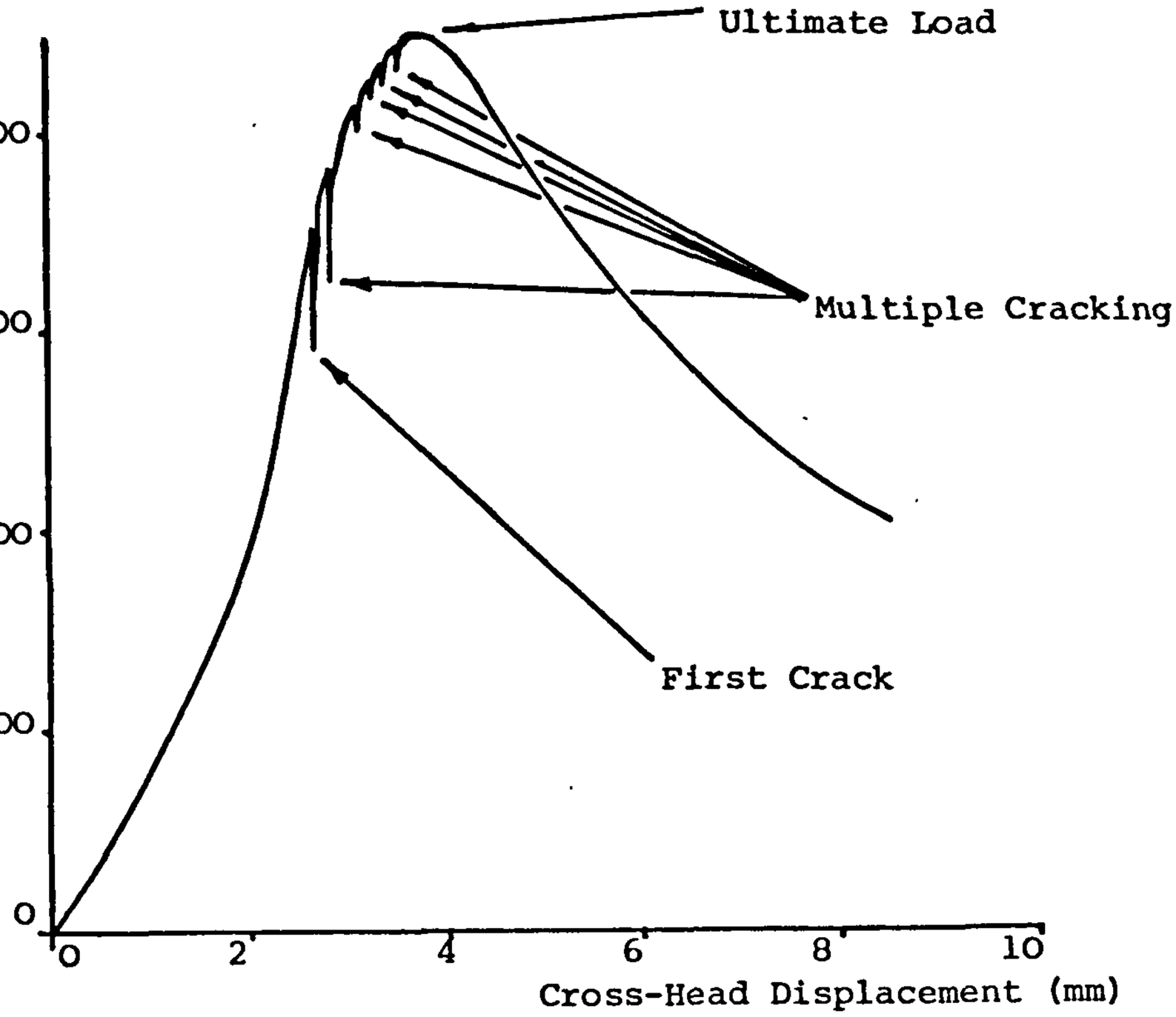

FIGURE 5.5 - TYPICAL TENSILE LOAD/CROSS-HEAD DISPLACEMENT CURVE FOR DISCONTINUOUS ALIGNED FIBRE COMPOSITE CONSISTING OF 26 mm CHOPPED FIBRE AND 4.2% VOLUME CONCENTRATION

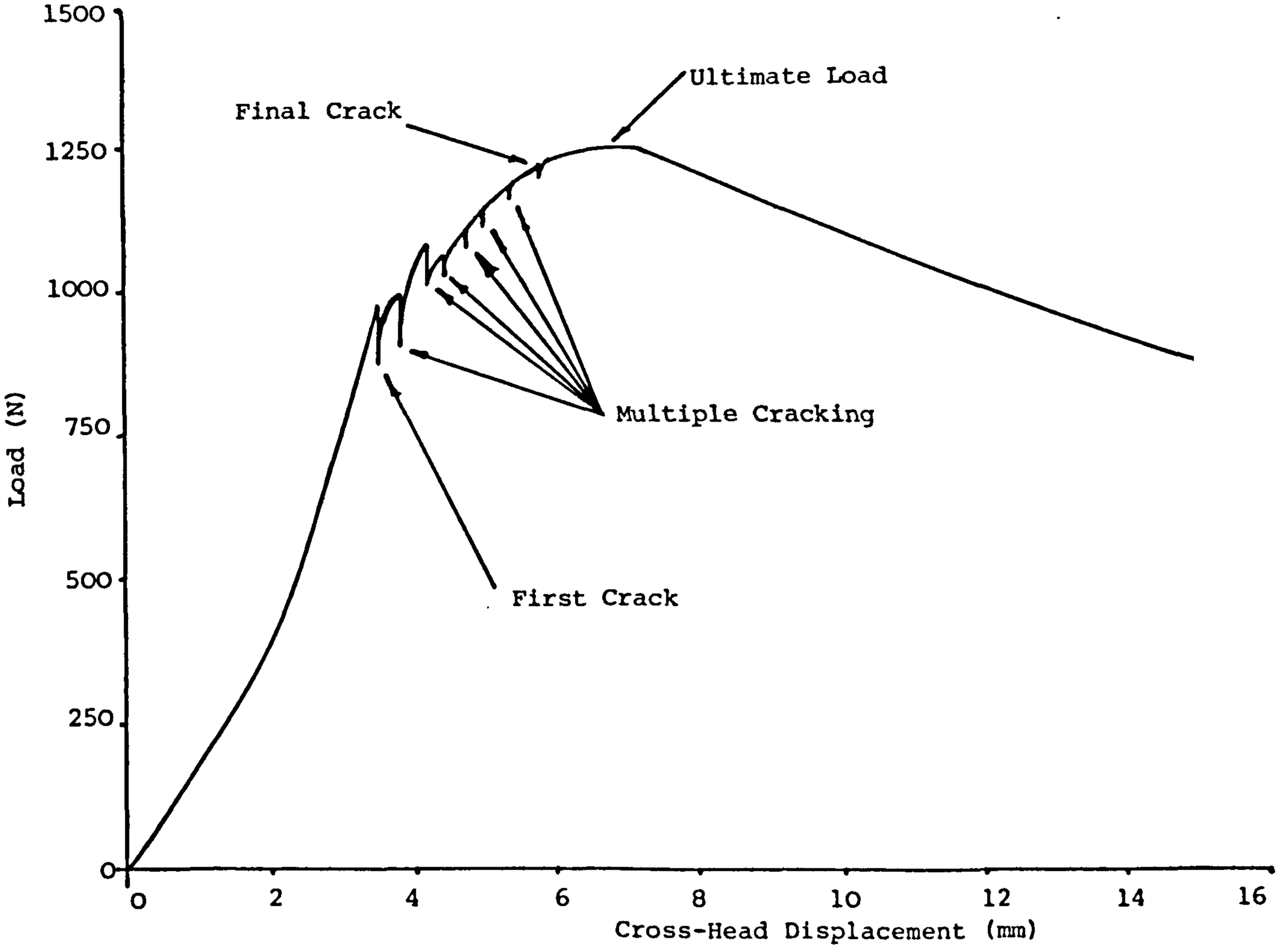

FIGURE 5.6 - TYPICAL TENSILE LOAD/CROSS-HEAD DISPLACEMENT CURVE FOR DISCONTINUOUS ALIGNED FIBRE COMPOSITE CONSISTING OF 60 mm CHOPPED FIBRE AND 4.2% VOLUME CONCENTRATION

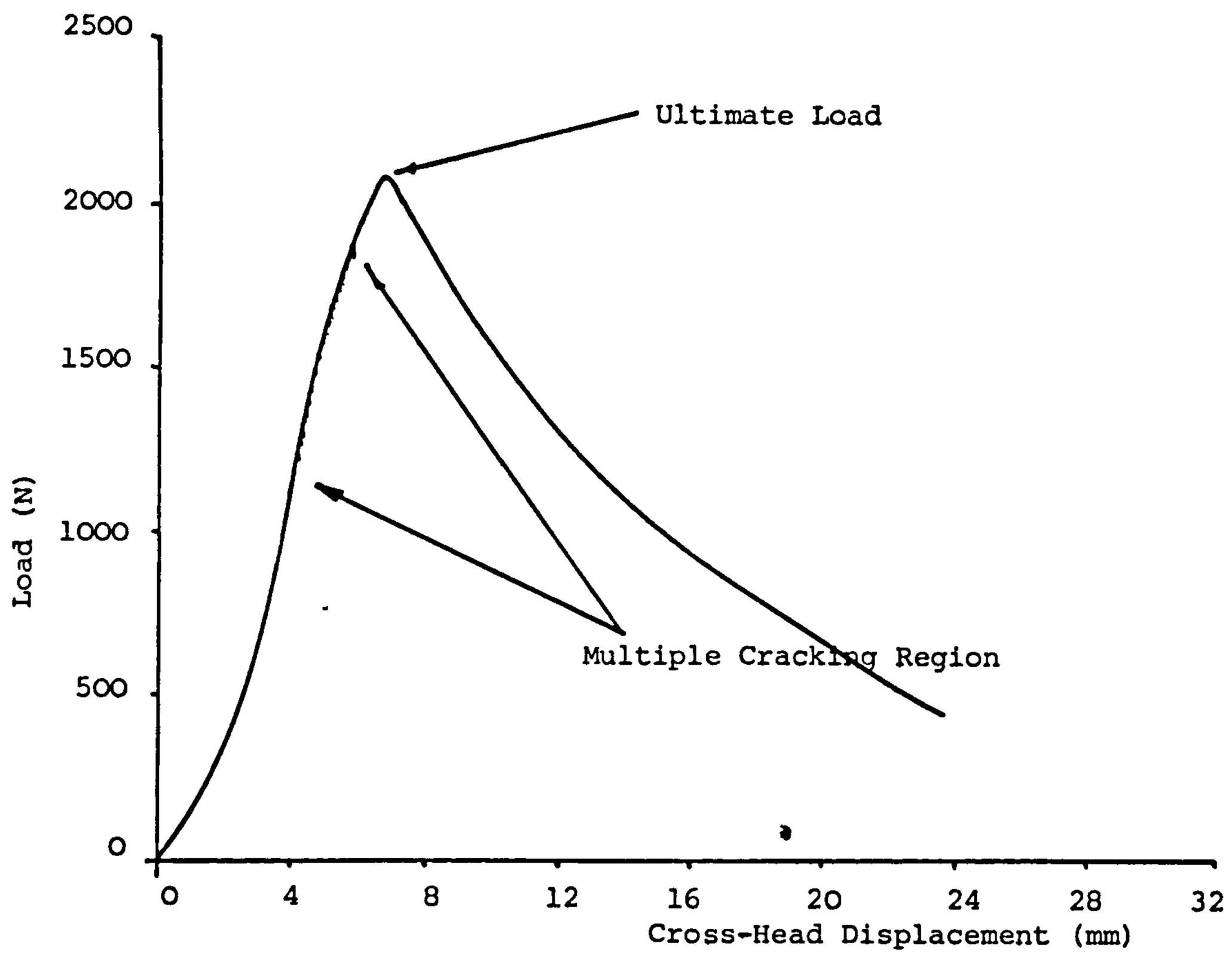

FIGURE 5.7 - TYPICAL TENSILE LOAD/CROSS-HEAD DISPLACEMENT CURVE FOR DISCONTINUOUS ALIGNED FIBRE COMPOSITE CONSISTING OF 60 mm CHOPPED FIBRE AND 8.7% VOLUME CONCENTRATION

TABLE 5.1 - DISCONTINUOUS ALIGNED FIBRE REINFORCED CEMENT PASTE SPECIMENS

Fibre Length (mm)	Vol.% Fibre	Average First Crack Stress (N/mm^2)	Average Final Crack Stress (N/mm^2)	Average Crack Spacing (mm)	Average Ultimate Stress (N/mm^2)	Average Elastic Modulus (kN/mm^2)
60	1.4	1.21	-	Single Crack	1.21	10.22
26	1.4	1.47	-	Single Crack	1.47	-
10	1.4	1.48	-	Single Crack	1.48	14.30
60	4.2	1.59	2.12	25.5	2.21	6.49
26	4.2	1.68	1.80	42.3	1.80	14.90
10	4.2	1.03	1.38	71.3	1.54	14.96
60	8.7	1.19	2.83	11.9	3.52	10.05

ultimate stress values indicate that, although the discontinuous aligned fibre composites were able to exhibit multiple cracking and hence pseudo-ductility, the reinforcing ratio, i.e. ultimate stress level/first crack stress level, was small.

Another difference between the deformation characteristics of the two types of fibre composite systems was that the discontinuous fibre composite specimens did not exhibit a rising Load/Cross-head displacement region after the final crack, whereas the continuous fibre composite specimens did.

5.5.2 Interfacial Shear Stress

The results in this chapter allow an assessment to be made of the average value of the interfacial shear stress and the quantitative nature of its distribution along the fibre length.

(A) During Multiple Cracking

A modification of the Aveston, Cooper and Kelly[12] equation (4.1) for the continuous fibre composite system was theoretically developed by Aveston, Mercer and Sillwood[66], to predict the properties of cement reinforced with discontinuous aligned fibres. An attempt was made to use their treatment to calculate the average interfacial shear stress using the crack spacing data.

In the Aveston et al[66] method the crack spacing was considered as the distance x_d (transfer length for stress) required from the first crack, for the fibres to transfer the load ($\sigma_{mu}V_m$) i.e. (the product of the matrix ultimate stress and volume fraction of the matrix per

unit area of the composite), back into the matrix in the same way as the crack spacing for the continuous aligned fibre composites, as was previously calculated (see section 2.1.2.2). The number of fibres with both ends at a distance greater than (x_d) from the crack and thus able to transfer their full share of the load is $N(1 - 2x_d/\ell)$ where $N = V_f/\pi r^2$; and N is defined as the number of fibres in the unit cross-section, V_f is the volume fraction of the fibres, r is the fibre radius and ℓ is the fibre length.

The remaining $(2x_dN)/\ell$ fibres have one end less than (x_d) from the crack and transfer load over a mean distance $(x_d)/2$. The total load transferred is equal to ($\sigma_{mu}V_m$) to give

$$2\pi r\tau x_d N(1 - \frac{x_d}{\ell}) = \sigma_{mu}V_m \qquad .. \quad .. \quad (5.1)$$

or

$$x_d = \frac{1}{(1 - \frac{x_d}{\ell})} \cdot \frac{V_m}{V_f} \cdot \frac{\sigma_{mu}r}{2\tau} = \frac{x'}{(1 - \frac{x_d}{\ell})} \qquad .. \quad .. \quad (5.2)$$

$$\text{where} \quad x' = \frac{V_m}{V_f} \cdot \frac{\sigma_{mu}r}{2\tau} \qquad .. \quad .. \quad (5.3)$$

where τ is the fibre/matrix shear stress.

Hence from equation (5.2)

$$x_d = \frac{\ell \pm(\ell^2 - 4\ell x')^{\frac{1}{2}}}{2} \qquad .. \quad .. \quad (5.4)$$

It can be seen from equation (5.4) that term $\ell^2 - 4\ell x' > 0$, i.e. the final crack spacing must be less than $\ell/4$ for equation (5.4) to apply. However, since crack spacing for discontinuous aligned polypropylene fibre composites is greater than ℓ, for 10 and 26 mm fibre lengths the theory is not applicable.

(B) <u>After Multiple Cracking</u>

After multiple cracking was completed, specimen deformation continued by fibre pull-out across the crack surfaces. The interfacial shear stress under these conditions is therefore dynamic ($\tau_{dynamic}$) in nature, and can be calculated by using the post-cracking portion of the load/cross-head displacement curves. This occurs because the monofilament polypropylene fibres were shorter than the critical length for fibre breakage to occur, i.e.

$$\ell_c = \frac{\sigma_{fu} r}{\tau}$$

where σ_{fu} is the fibre ultimate stress and ℓ_c is the critical fibre length.

Aveston et al[30] have shown that the mean fibre pull-out length is $(\ell/4)$. Hence, the average pull-out force per fibre (F) is given by

$$F = 2\pi r(\ell/4)\tau$$

Therefore, for N, fibres bridging the crack, the force in the fibres equals

$$F = 2\pi r(\ell/4)\tau N \quad .. \quad .. \quad .. \quad (5.5)$$

where $$N = \frac{\dot{V}_f}{\pi r^2} \cdot A_c \quad .. \quad .. \quad .. \quad (5.6)$$

where A_c is the cross-sectional area of the composite. Substituting N, of equation (5.6) into equation (5.5)

$$\therefore \quad F = \frac{\ell V_f A_c \tau}{2r}$$

rearranging gives,

$$\tau = \frac{2Fr}{\ell V_f A_c} \quad .. \quad .. \quad .. \quad (5.7)$$

Values for (τ), which will be referred to as ($\tau_{dynamic}$) in this section, can be calculated by substituting the maximum fibre pull-out load in equation (5.7). Table 5.2 shows the ($\tau_{dynamic}$) values for each respective volume % of fibre and fibre lengths. The effect of increasing the volume concentration of fibre is to decrease the ($\tau_{dynamic}$) shear stress.

The results indicate that the ($\tau_{dynamic}$) value increases as the fibre length decreases, for a given volume % of fibre. This is in agreement with the explanation as given by Aveston et al[30] for fibre pull-out, that the shear strength at the interface ($\tau_{dynamic}$) decreases as a result of the Poisson's contraction of the fibre as the load on the composite is increased. It can be seen that for the same volume concentration of fibre, the pull-out load increases as the fibre length increases and thus the stress in a long fibre is greater than that in a short fibre and so consequently the Poisson's contraction is greater.

Another aspect of pull-out behaviour is that the ($\tau_{dynamic}$) decreases with increasing fibre pull-out. The results for specimens containing 1.4% by volume of fibre are shown in Table 5.3. Hale[45] developed a relationship between interfacial shear stress and progressive fibre displacement relative to matrix in the form that $\tau_q = \tau_o(1 + KQ/\ell)$ ..(5.8) where τ_q is the local value of the frictional stress, τ_o is the initial frictional stress, Q is the relative displacement of the fibre and matrix, K is the constant and ℓ is the fibre length. However, although Table 5.3 indicates that there is an approximate linear decrease in interfacial shear stress with increasing fibre pull-out, a unique value for K in equation (5.8) was not apparent. The decrease in frictional resistance as fibre pull-out progresses, is thought to be

TABLE 5.2 - DYNAMIC INTERFACIAL SHEAR STRESS ($\tau_{dynamic}$) CALCULATED BY USING MULTIPLE FIBRE PULL-OUT DATA FOR DISCONTINUOUS ALIGNED FIBRE REINFORCED CEMENT PASTE SPECIMENS

Fibre Length (mm)	Vol.% Fibre	Maximum Fibre Pull-Out Load(N)*	Average Interfacial Shear Stress($\tau_{dynamic}$) = $(2Fr)/(\ell V_f A_c)$ N/mm^2
60	1.4	475.0	0.370
26	1.4	526.7	0.946
10	1.4	370.8	1.732
60	4.2	1154.2	0.300
26	4.2	926.7	0.555
10	4.2	650.0	1.012
60	8.7	1808.3	0.227

* Average for six specimens

TABLE 5.3 - DYNAMIC INTERFACIAL SHEAR STRESS ($\tau_{dynamic}$) CALCULATED USING RESPECTIVE FIBRE LENGTH WITH PROGRESSIVE FIBRE PULL-OUT LOAD, FOR DISCONTINUOUS ALIGNED FIBRE COMPOSITE

(1)	(2)	(3)	(4)	(5)	(6)
Test Code	Vol.% Fibre	Initial Fibre Length Incorporated in the Composite (mm)	Effective Fibre Length During Pull-Out (mm)	Fibre Pull-Out Load (N) At Specific Fibre Lengths	Average Interfacial Shear Stress $\tau_{dynamic}=(2Fr)/\ell V_f A_c)$ N/mm^2
A	1.4	60	14.5	475	0.382
			14.0	400	0.334
			13.5	375	0.324
			13.0	350	0.314
			12.5	325	0.304
B	1.4	60	14.5	275	0.221
			14.0	250	0.208
			13.5	225	0.195
			13.0	200	0.180
C	1.4	60	14.5	400	0.322
			14.0	375	0.313
			13.5	360	0.311
			13.0	350	0.314
D	1.4	60	14.5	525	0.423
			14.0	510	0.425
			13.5	505	0.437
E	1.4	60	14.5	325	0.262
			14.0	300	0.250
			13.5	275	0.238
			13.0	250	0.225

. . . Continued...

TABLE 5.3 (continued)

(1)	(2)	(3)	(4)	(5)	(6)
F	1.4	60	14.5	400	0.322
			14.0	375	0.313
			13.5	350	0.303
			13.0	300	0.269
A	1.4	26	6.25	360	0.673
			6.00	270	0.525
B	1.4	26	6.25	480	0.897
			6.00	360	0.701
C	1.4	26	6.25	290	0.542
			6.00	240	0.467
			5.75	200	0.406
			5.50	160	0.340
			5.25	140	0.311
			5.00	120	0.280
A	1.4	10	2.25	250	1.297
			2.00	200	1.167
			1.75	125	0.834
B	1.4	10	2.25	175	0.908
			2.00	125	0.730
			1.75	100	0.667
C	1.4	10	2.25	300	1.557
			2.00	225	1.314
			1.75	150	1.001
D	1.4	10	2.25	275	1.427
			2.00	175	1.168
			1.75	150	1.001
E	1.4	10	2.25	200	1.038
			2.00	150	0.876
			1.75	100	0.667

due to the gradual rearrangement or removal of obstructing cement paste particles.

The range of the interfacial shear stress values for the discontinuous fibre composite specimens, lie in the range of 0.227 N/mm^2 to 1.732 N/mm^2. In the case of the continuous aligned fibre composite specimens, a range 0.068 to 0.356 N/mm^2 was found. These wide ranges of interfacial shear stress values reflect the significant influences of the parameters, such as fibre length and fibre volume concentration and indicate that there is not a unique value of interfacial shear stress (τ).

5.5.3 Elastic Modulus

Table 5.1 shows the elastic moduli values for the different volume % of fibre concentrations and their respective fibre lengths. The elastic moduli values lie within the normally quoted values for neat cement paste specimens, i.e. between 10-20 kN/mm^2. The variation is due to the variation in specimen manufacture and the variation in fibre distribution.

5.6 CONCLUSIONS

(1) Multiple cracking occurs in discontinuous aligned polypropylene fibre reinforced cement paste specimens when 10, 26 and 60 mm fibre lengths are incorporated, provided that a minimum concentration of fibres is utilised.

(2) The interfacial shear stress increased with decreasing fibre length.

(3) The interfacial shear stress decreased with increasing volume concentration of fibre.

(4) The dynamic interfacial shear stress ($\tau_{dynamic}$) value decreased with increasing fibre pull-out.

(5) The ultimate stress values were very much lower than those for specimens containing the same volume fraction of fibres, but continuously aligned.

(6) The difference between the first crack stress and the ultimate stress values were small, when compared with those as observed in the continuous aligned fibre composite specimens; hence the reinforcing ratios are smaller.

(7) Elastic moduli values lie between 6.49 - 14.96 kN/mm^2.

INCLINED AND RANDOM FIBRE REINFORCED CEMENT PASTE

CHAPTER SIX

INCLINED AND RANDOM FIBRE REINFORCED CEMENT PASTE

6.1 PREAMBLE

Parallel spaced fibres, with fibre directions of varying angle to the direction of the tensile stress axis, were tested to allow an assessment to be made of the role of inclination on fibre composite materials. For the standard sized tensile specimens used, it is not possible to incorporate fibres of the same length for every angle of inclination, since greater the inclination with respect to the tensile stress axis, the shorter the fibre length.

However, it was thought that useful information regarding the possible effects of inclination could still be obtained, despite the confounding of the orientation with regard to fibre length. Therefore, a programme of tests was undertaken on prepared specimens with angles of inclination of 15^{o}, 30^{o}, 45^{o}, 60^{o}, 75^{o} and 90^{o} in order to identify their deformation characteristics.

A limited number of specimens were also prepared, in order to relate the effect of random fibre distribution to that of the other systems previously studied. For this investigation only two fibre lengths, i.e. 60 and 26 mm were used.

6.2 MATERIALS

6.2.1 Cement

Standard Ordinary Portland cement was used, as described in section 3.6.

6.2.2 Fibres

For the inclined fibre system, continuous monofilament fibre of 340 μm diameter was used as previously described in section 3.2.2(A).

For the random orientation investigation, fibre lengths of 60 and 26 mm were used, having tangent modulus of elasticity value of 3.8 kN/mm^2 (see section 3.2.2(G)).

6.3 FABRICATION

6.3.1 Inclined Fibre System

A fabrication technique was developed to incorporate known volume percentages of fibres in an inclined manner in a cement matrix. A perspex jig, as shown in Fig. 6.1, was constructed, with rows of pegs protruding from the north and south side of the perspex mould. The pegs were staggered in two rows, so that the holes which received the pegs were not too closely spaced together, which would otherwise make the fibre winding task by hand difficult. The centres of the pegs were 5 mm apart and the pegs were 1.5 mm in diameter.

A square of dimensions 250 by 250 mm was constructed between the pegs on the north and the south side of the perspex mould, by means of stacked shims. The square could be orientated at an appropriate angle relative to the pegs, and was subsequently filled with cement paste.

The purpose of the shims was to provide a suitable vertical spacing between the layers of the fibres required in the test specimens and also to act as a periphery for the plate mould, thus confining the cement paste.

FIGURE 6.1 - SCHEMATIC DIAGRAM OF INCLINED FIBRE LAY-UP JIG

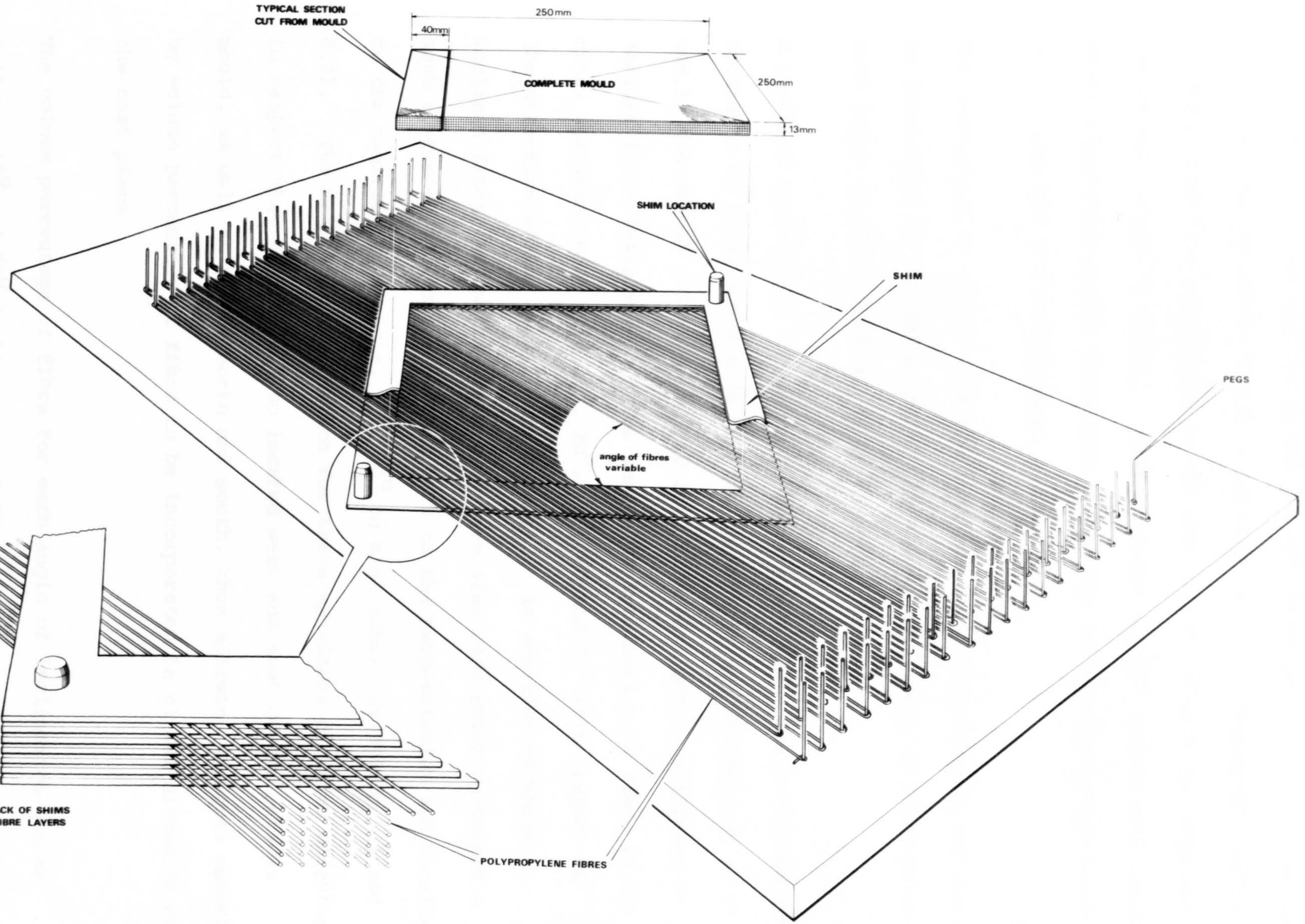
TYPICAL SECTION
CUT FROM MOULD
250mm
40mm
COMPLETE MOULD
250mm
13mm
SHIM LOCATION
SHIM
PEGS
angle of fibres
variable
STACK OF SHIMS
& FIBRE LAYERS
POLYPROPYLENE FIBRES

The fibre was first tied to an end peg and wound progressively from end to end across the mould to give a parallel array. Subsequent layers of fibre were then positioned in the same manner to give the required percentage volume of fibres. Fibres placed in this manner were evenly distributed without sag throughout the mould, at the appropriate angle of inclination in the horizontal plane.

The percentage by volume of fibre that can be incorporated in the system is determined by the thickness of the shims, the number of shims between each layer of fibres and the fibre diameter used.

A plate of size 250 by 250 mm by 13 mm deep was cast, which allowed six specimens of 13 mm thick x 40 mm wide in section and 250 mm long to be cut, by the use of a diamond tipped saw, from each plate containing a similar fibre inclination. The angles of inclination of fibre in the final specimens cast were 15^{o}, 30^{o}, 45^{o}, 60^{o} and 75^{o} with respect to the direction of the tensile stress axis. In addition to these inclined fibre composites, specimens were also cast which contained a mesh system of fibres, orientated both to the perpendicular and parallel to the tensile stress axis, i.e. 90^{o} to each other (see Plates 6.1 and 6.2). The method of preparation for these specimens differed slightly in respect that pegs were also located west and east of the perspex mould, as well as to the north and south, thus allowing an equal amount by volume percentage of fibre to be incorporated in either direction of the cast plate.

The volume percentage of fibre for each angle of inclination was as follows: 15^{o} and 75^{o} inclination - 3.5%, for 30^{o} and 60^{o} inclination - 3.65% and for 45^{o} inclination - 3.61%. For the specimens with the mesh construction a 3.86% by volume fraction was incorporated.

15° AND 75° INCLINED FIBRES OBTAINED FROM THE FABRICATION

30° AND 60° INCLINED FIBRES OBTAINED FROM THE FABRICATION

PLATE 6.1 - SHOWS SPECIMEN FABRICATION JIGS

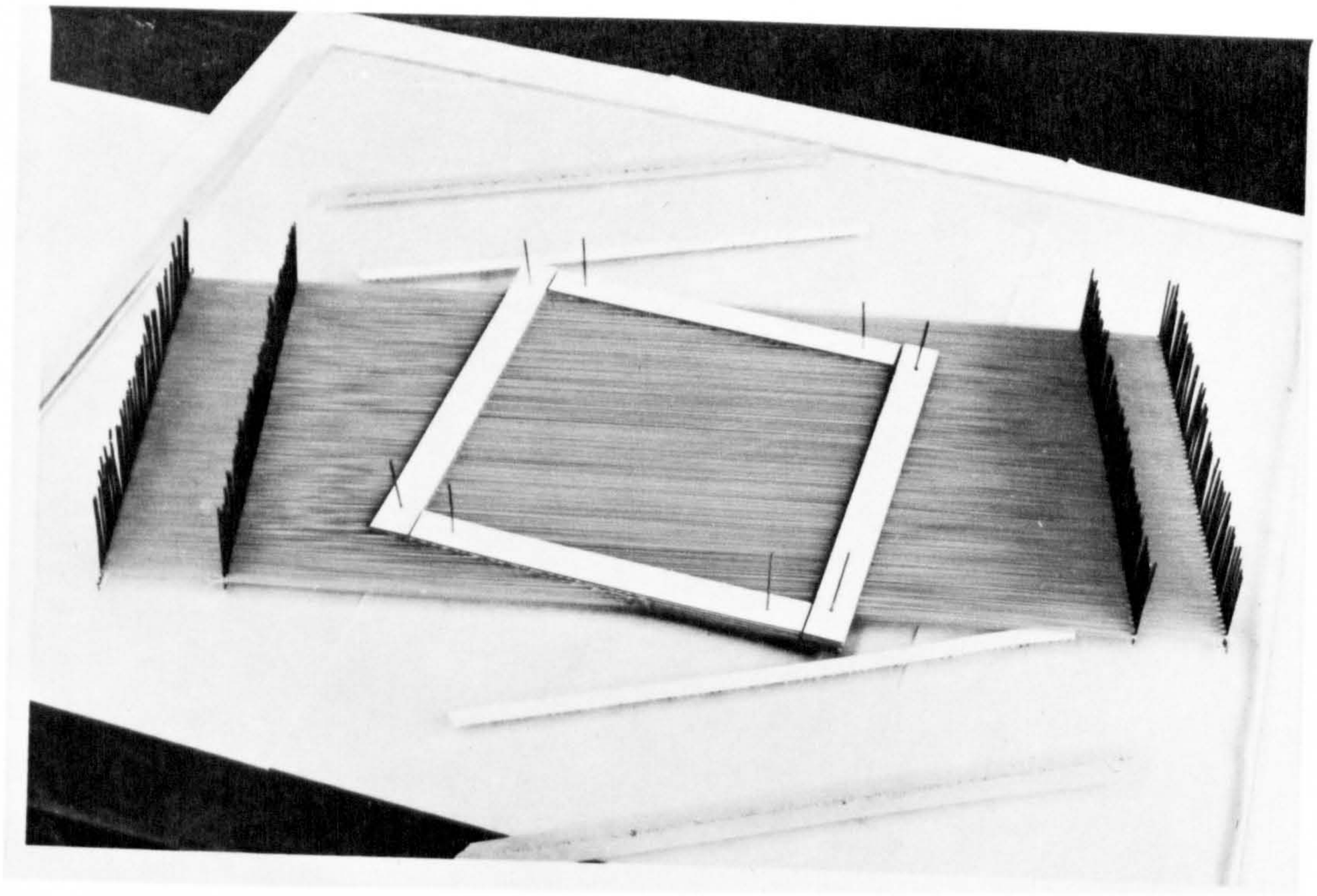

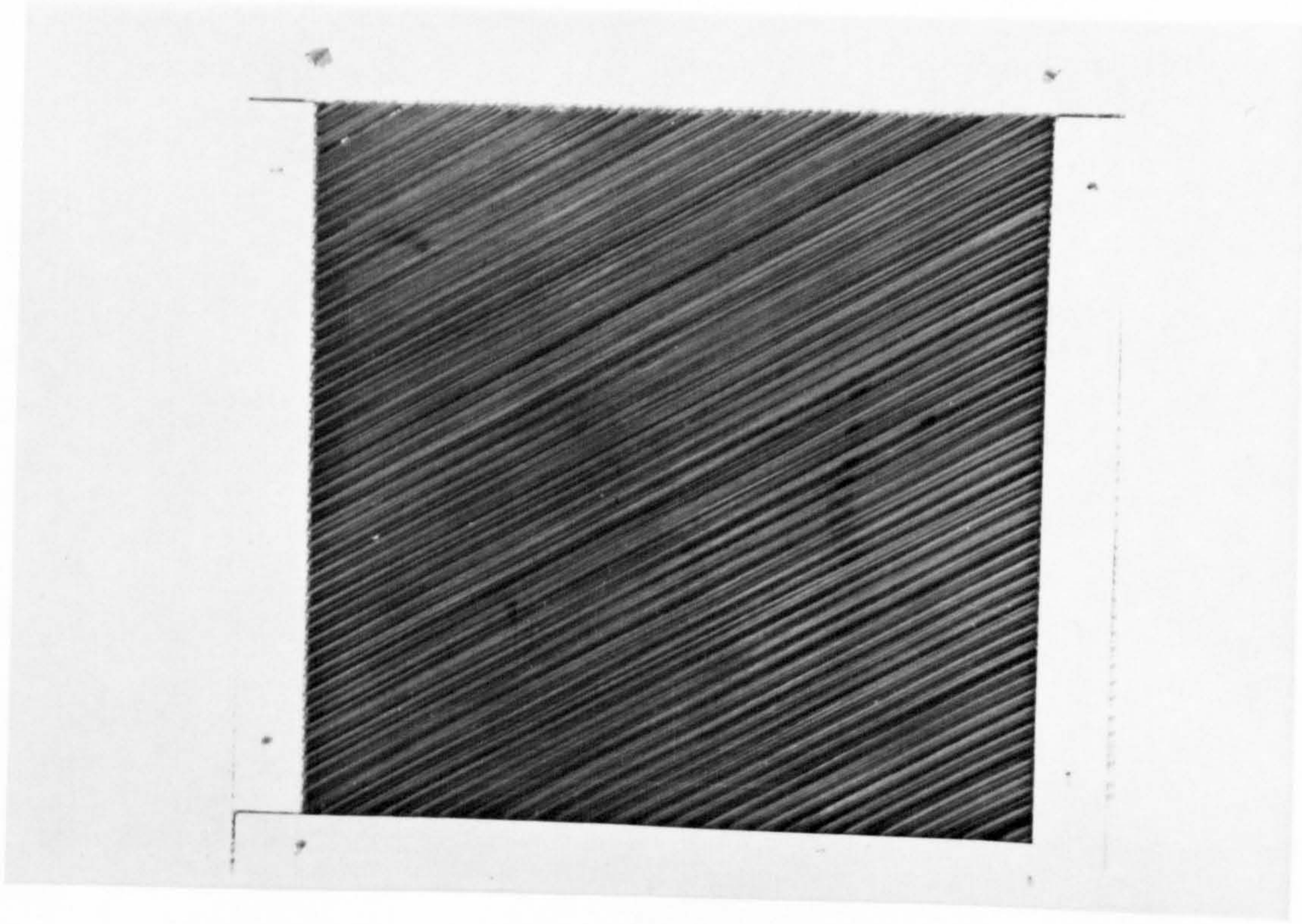

45° INCLINED FIBRES OBTAINED FROM THE FABRICATION

90°-90° MESH OBTAINED FROM THE FABRICATION

PLATE 6.2 - SHOWS SPECIMEN FABRICATION JIGS

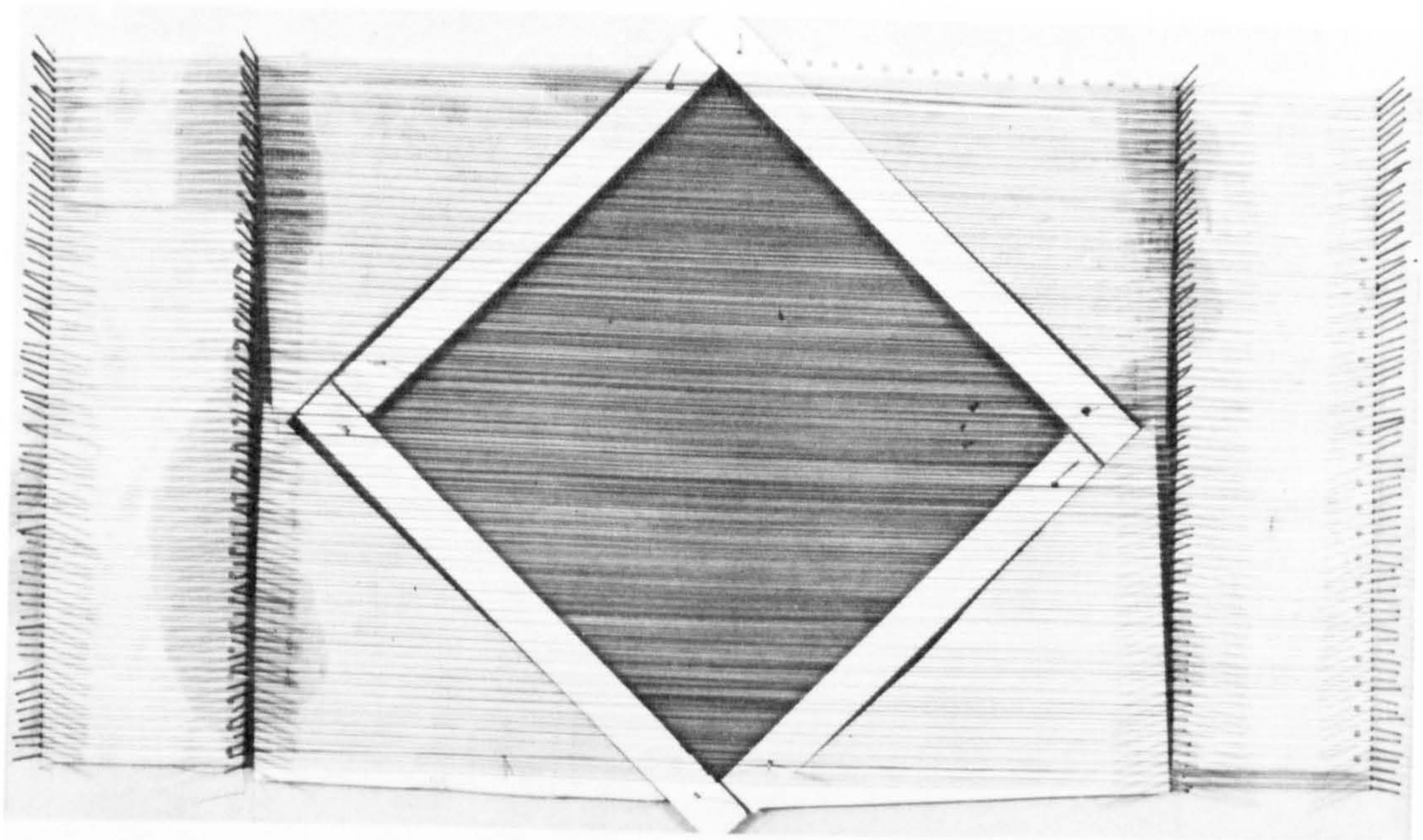

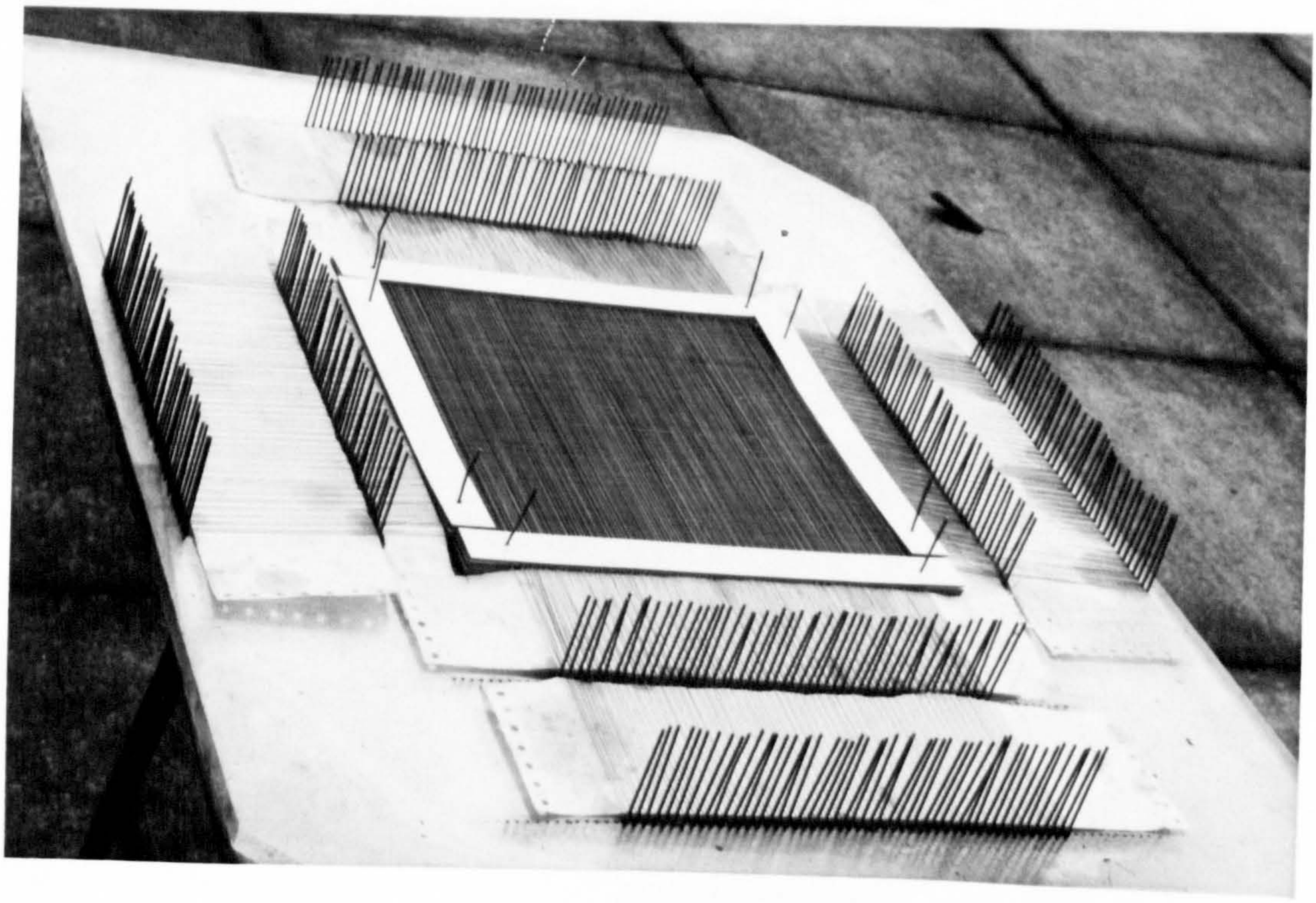

6.3.2 Random Fibre System

A plate mould of 250 by 250 mm by 13 mm deep was cast, which allowed six specimens to be cut, 13 mm thick x 40 mm wide in section x 250 mm long, by use of a diamond tipped saw.

The procedure for cast was that enough matrix was poured into the bottom of the mould to coat the surface and then measured amount of fibre was evenly sprinkled on top in a random fashion, which was gently tamped into the matrix until all the fibres were coated. Subsequent layers of fibre and matrix were likewise placed until the desired volume fractions of fibre were incorporated. The mould was then finally vibrated and the top struck smooth.

Specimens cast in this manner allowed known volume of fibre to be randomly distributed; in this investigation this comprised of 4.2% by volume fraction. Only two fibre lengths, i.e. 60 and 26 mm were used at this concentration. Some fibres tended to incline themselves at an angle to the casting plane.

6.3.3 Mix Procedure

A neat cement paste of water/cement ratio 0.4 was used for these castings, as previously described in section 3.7.1.

6.3.4 Curing

As described in section 3.7.2.

6.4 TEST PROCEDURE

6.4.1 Tensile Strength

The load was applied by using the position control mode of the Losenhausen test machine (i.e. constant rate of cross-head movement of 1 mm/min), as described in section 3.8.1.

6.5 ANALYSIS AND DISCUSSION OF RESULTS

6.5.1 Cracking Phenomena - Inclined Fibre System

At least six specimens of each fibre inclination were tested in tension and typical load versus cross-head displacement curves are shown in Figures 6.2 to 6.7. Plate 6.3 illustrates the typical crack patterns obtained for the different fibre inclinations after testing. From this it can be seen that the crack pattern is considerably more complex than that observed with those specimens containing fibres parallel to the tensile axis (see chapter four).

Figures 6.2 to 6.7 show a series of momentary stress drops, as deformation of the specimen proceeds beyond the first crack. It is thought that at least three mechanisms could cause a stress drop. The most severe type of stress drop is probably due to a major crack propagating across the width of the specimen. It is interesting to note that this type of crack propagates sufficiently slowly for it to be observed progressing from one side of the specimen to the other. In the case of the continuous aligned fibre composite specimens, the

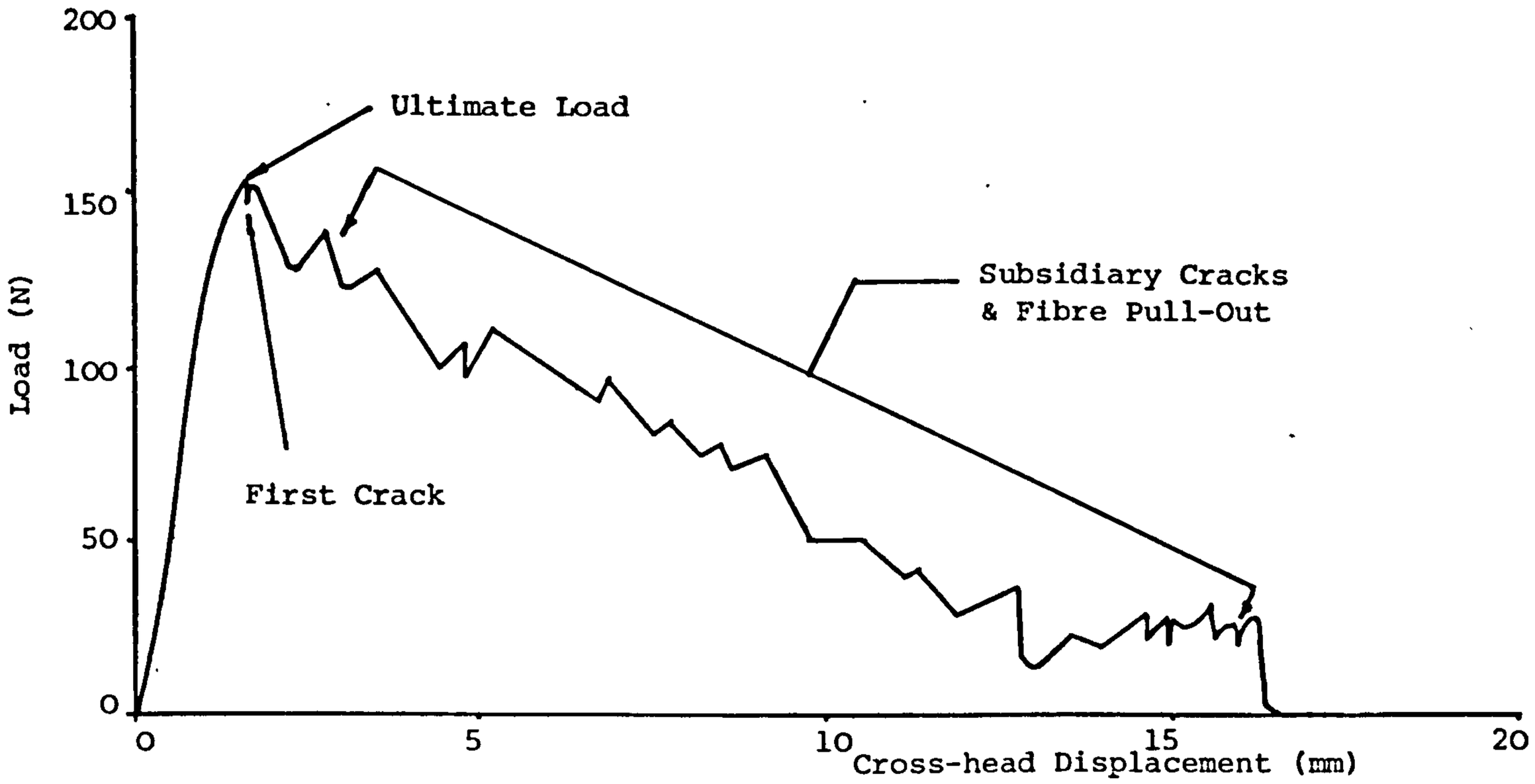

FIGURE 6.2 - TYPICAL TENSILE LOAD/CROSS-HEAD DISPLACEMENT CURVE FOR CEMENT PASTE REINFORCED WITH 3.5 VOLUME % CONCENTRATION OF 340 μm DIAMETER POLYPROPYLENE FIBRE INCLINED AT 75°

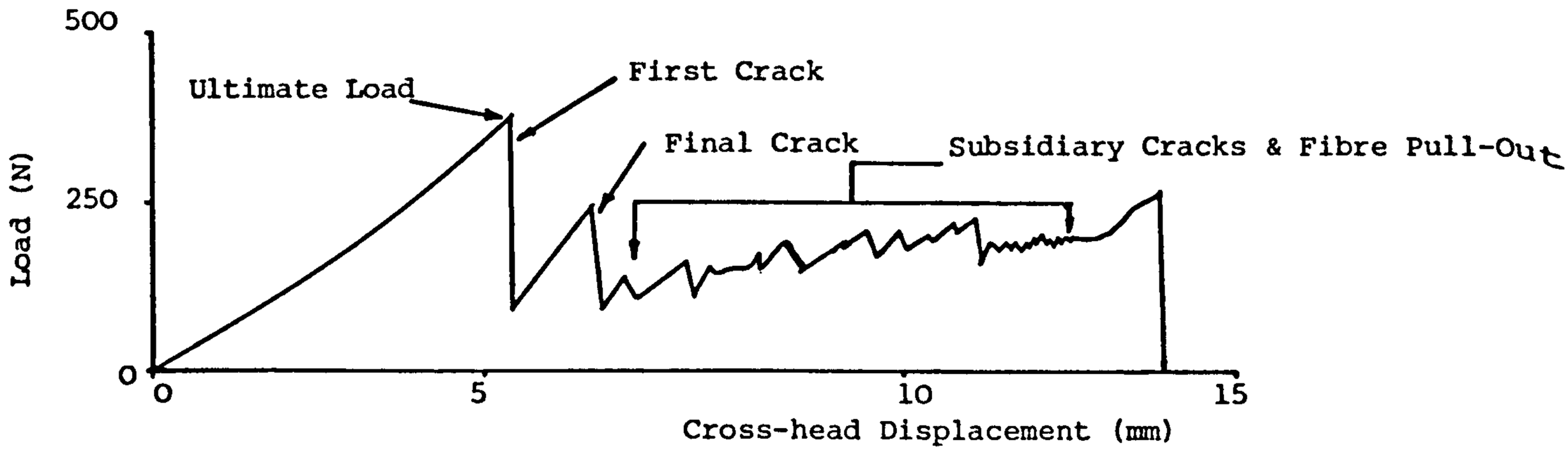

FIGURE 6.3 - TYPICAL TENSILE LOAD/CROSS-HEAD DISPLACEMENT CURVE FOR CEMENT PASTE REINFORCED WITH 3.65 VOLUME % CONCENTRATION OF 340 μm.DIAMETER POLYPROPYLENE FIBRE INCLINED AT 60°

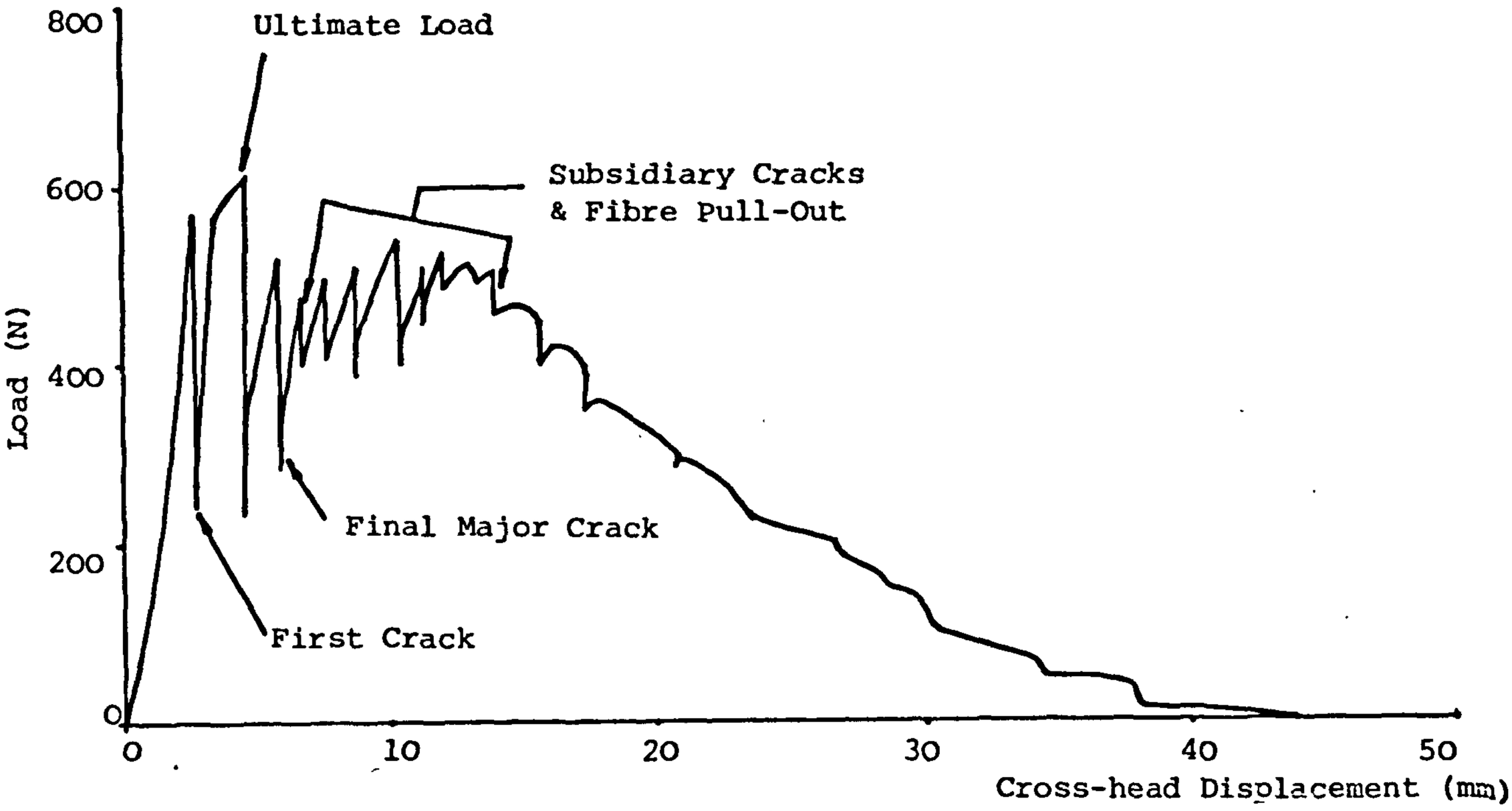

FIGURE 6.4 - TYPICAL TENSILE LOAD/CROSS-HEAD DISPLACEMENT CURVE FOR CEMENT PASTE REINFORCED WITH 3.61 VOLUME % CONCENTRATION OF 340 μm DIAMETER POLYPROPYLENE FIBRE INCLINED AT 45°

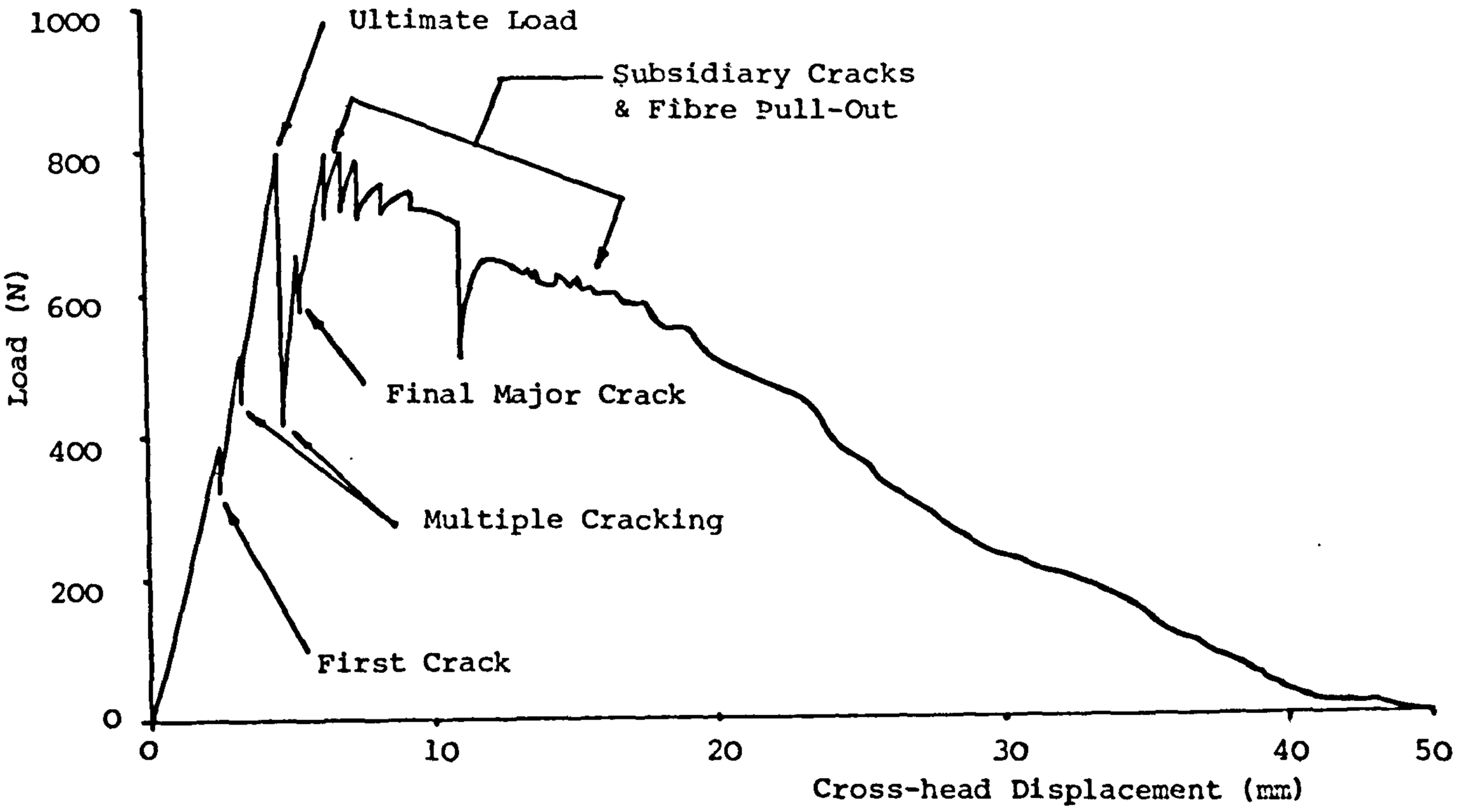

FIGURE 6.5 - TYPICAL TENSILE LOAD/CROSS-HEAD DISPLACEMENT CURVE FOR CEMENT PASTE REINFORCED WITH 3.65 VOLUME % CONCENTRATION OF 340 μm DIAMETER POLYPROPYLENE FIBRE INCLINED AT 30°

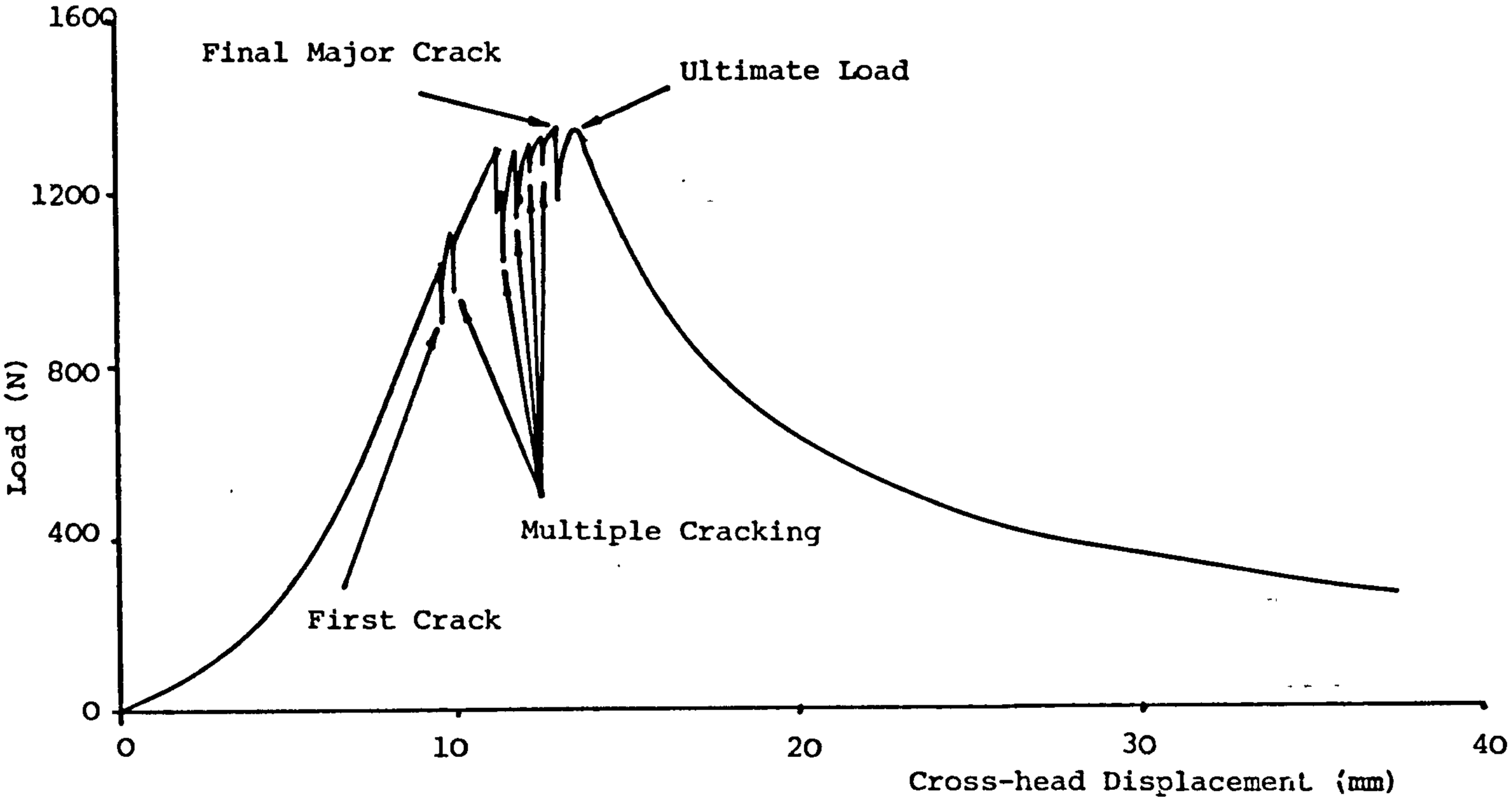

FIGURE 6.6 - TYPICAL TENSILE LOAD/CROSS-HEAD DISPLACEMENT CURVE FOR CEMENT PASTE REINFORCED WITH 3.5 VOLUME % CONCENTRATION OF 340 μm DIAMETER POLYPROPYLENE FIBRE INCLINED AT 15^{o}

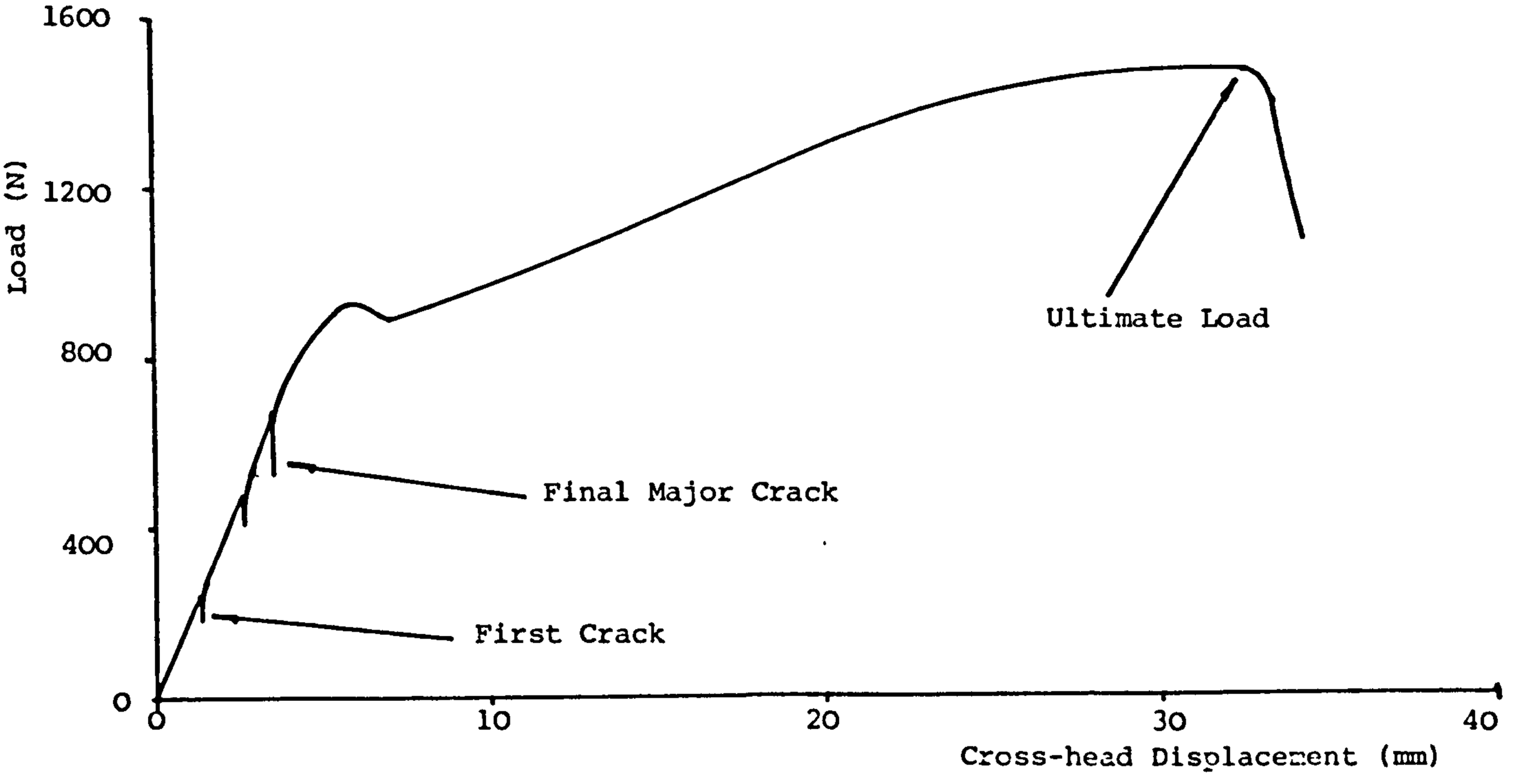

FIGURE 6.7 - TYPICAL TENSILE LOAD/CROSS-HEAD DISPLACEMENT CURVE FOR CEMENT PASTE REINFORCED WITH 3.86 VOLUME % CONCENTRATION OF 340 μm DIAMETER POLYPROPYLENE FIBRE IN A MESH FORM 90^{o}-90^{o}

PLATE 6.3 - TYPICAL CRACK PATTERNS OBTAINED FOR THE DIFFERENT FIBRE INCLINATIONS, A = 75°; B = 60°; C = 45°; D = 30°; E = 15° AND F = 90°-90° MESH.
INCLINATION ANGLE MEASURED WITH RESPECT TO TENSILE AXIS.

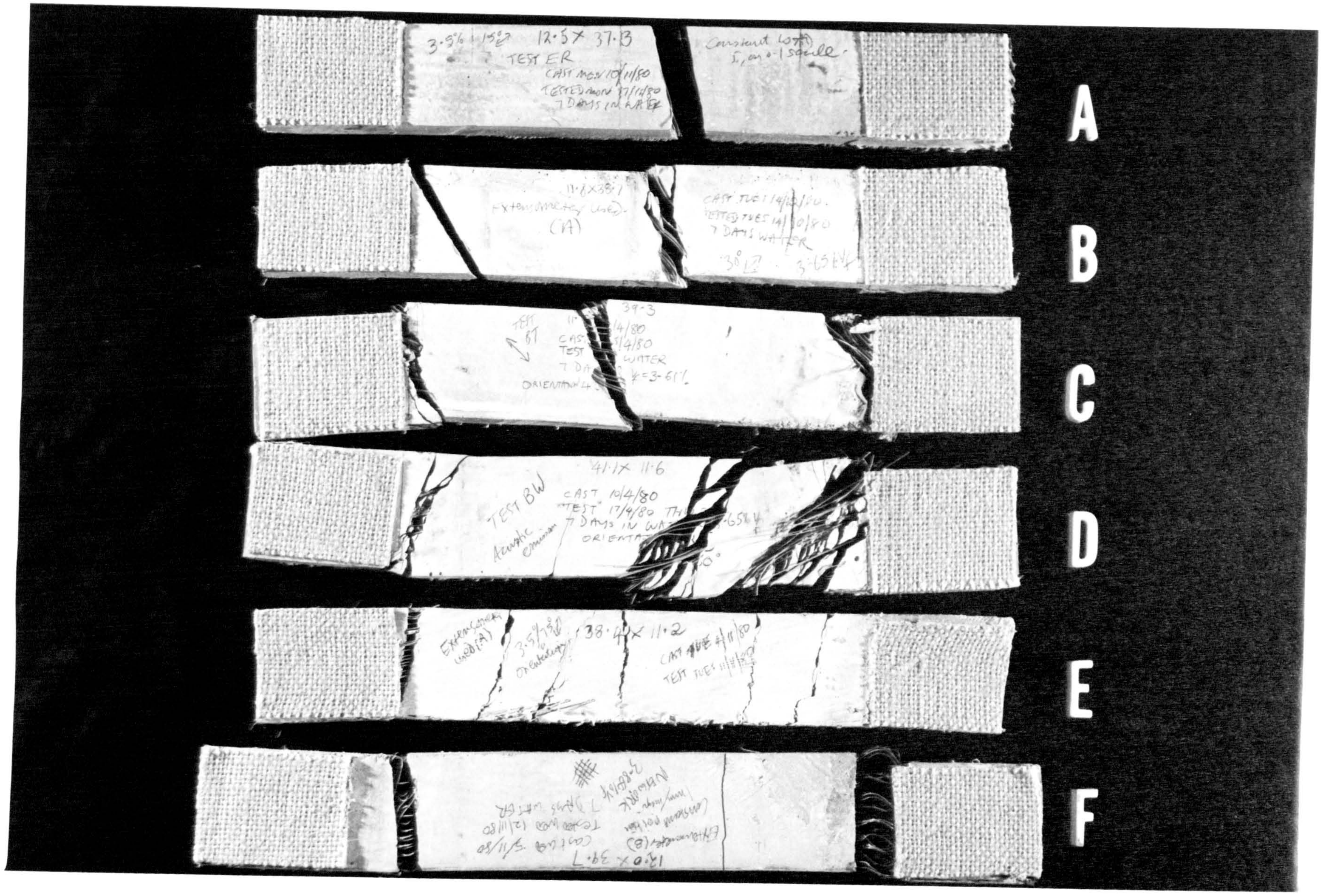
A
B
C
D
E
F

crack propagation was effectively instantaneous. A further source of the stress drop is the development of subsidiary cracks, i.e. cracks branching from the major crack. As a result of this crack branching, small portions of the matrix can be isolated from the main body adjacent to the main crack surfaces; these portions or chippings remain suspended between the fibres as further deformation occurs. In addition to the momentary stress drops, a gradual decrease in stress also takes place after a cross-head displacement of, say, 15 mm, as in the case of the 75^{o} fibre inclined specimens (Figure 6.2), which is thought to be due to fibre pull-out.

It might be expected that inclined fibres would have a greater pull-out load than fibres running parallel to the tensile axis. Present results however do not allow an assessment to be made of this aspect of fibre inclination. In addition to the problem of increasing fibre length with decreasing angle of fibre inclination, the results indicate that specimens containing large angles of fibre inclinations are significantly weaker than those with small angles of inclination. Therefore it was not possible to assess the direct effect of angle of inclination on pull-out load.

In a straightforward tensile test for a brittle material, the crack path should lie in a plane perpendicular to the tensile stress axis, i.e. plane of maximum tensile stress. This phenomenon was observed in the continuous aligned fibre composite specimens. This perpendicularly orientated plane is subsequently referred to as plane 'P' for convenience. In the inclined fibre composite specimens the major crack surface also tends to lie in a plane; the inclination of this plane (subsequently referred to as plane 'C') is perpendicular to the largest surface of

the specimen and inclined at an angle to the tensile stress axis. The angle of inclination of plane 'C' measured relative to the tensile stress axis varies with the angle of inclination of the fibres, also measured relative to the tensile stress axis (subsequently referred to as plane 'F'). It can be seen from Plate 6.3 that as the angle of fibre inclination increases, the angle between plane 'C' and plane 'F' decreases, until at a fibre inclination angle of 75^{o} the crack plane is almost parallel to the fibre inclination plane. It can also be seen that the angle of inclination between crack plane 'C' and plane 'P' increases with the increasing fibre inclination angle to a maximum of approximately 40^{o} at a fibre inclination plane of 30^{o} and then decreases with a further increase in fibre inclination.

It therefore appears that failure occurs in a tensile fracture mode for angles of inclination for fibres orientated from 0^{o} to 15^{o}. For the range of 60^{o} to 90^{o} inclination, the fracture mode is primarily intralaminar (i.e. occurring in the plane of the fibres). For the intermediate range of 30^{o} to 45^{o} inclination, a mixed mode of fracture occurs, with both intralaminar and tensile fracture combining. This mixed mode of fracture gives rise to a very complicated distribution of cracks and considerable distortion of the fibres, which results qualitatively in an increase in the work to fracture, as compared to the single modes of failure.

In addition to the relationships between the crack plane and fibre plane inclinations, there is also a relationship between the number of cracks developed in the specimen and the fibre inclination. For example, at 75^{o} fibre inclination, there is only a single crack, since at this fibre inclination the crack plane is almost parallel to the fibre and

hence there are very few fibres bridging the crack to transfer the stress. As the fibre inclination angle decreases, the number of major cracks increase.

Another aspect of the results shown in Table 6.1, is that there is a very significant decrease in the first crack stress compared with the increase in fibre inclination, which ranges from 1.26 N/mm^2 for the 15^o fibre inclination to 0.46 N/mm^2 for the 75^o fibre inclination. The most likely explanation for this phenomenon is that the fibres are tending to behave as voids in the specimen up to the first crack; thus the greater the angle of inclination of the fibre to the tensile stress axis, the greater the strength reducing effect of what is in effect a plane containing parallel elongated voids. Further evidence of this reduction in first crack strength was also obtained for the specimens fabricated with the fibres arranged in the form of a mesh, i.e. continuous fibres parallel and perpendicular to the tensile stress axis. In these specimens, multiple cracking was observed, with the number of cracks corresponding to those expected from the continuous aligned fibre reinforced specimens of approximate equivalent fibre volume concentration. However, the matrix first crack strength was reduced significantly. The magnitude of the reduction corresponds to what is expected from the inclined fibre composite data, e.g. 3.5% V_f for a 75^o inclined fibre, gives a stress reduction of 0.8 N/mm^2, compared with the 15^o inclined fibre value, and 1.93% V_f perpendicular to the tensile stress axis gives a stress reduction of 0.54 N/mm^2.

If the above observations are compared with the effects of the crack deflection associated with the inclined fibres, it appears that on balance any likely beneficial effect due to the inclined fibres giving

TABLE 6.1 - INCLINED FIBRE REINFORCED CEMENT PASTE SPECIMENS PROPERTIES

Fibre Inclination Angle	Vol.% Fibre	Average First Crack Stress (N/mm^2)	Average Ultimate Stress (N/mm^2)
15^o	3.50	1.26	4.23
30^o	3.65	1.70	1.94
45^o	3.61	1.05	1.23
60^o	3.65	0.60	1.20
75^o	3.50	0.46	0.59
Mesh 90^o-90^o	3.86	0.72	2.94

TABLE 6.2 - RANDOM FIBRE REINFORCED CEMENT PASTE SPECIMENS PROPERTIES

Fibre Length (mm)	Vol. % Fibre	Average First Crack Stress (N/mm^2)	Average Ultimate Stress (N/mm^2)
60	4.2	1.10	1.39
26	4.2	0.82	1.23

increased work to fracture, will be offset by the reduction in the matrix first crack strength.

6.5.2 Cracking Phenomena - Random Fibre System

With both fibre lengths incorporated in the system, the first cracking stress was comparable to that of the 45^{o} inclined fibre composite specimens,(see Table 6.2) with the same stress reducing mechanisms thought to apply as those occurring in the inclined fibre system, namely that the fibres at an angle greater than 45^{o} to the tensile stress direction, behave as voids up to the first crack.

The values of the ultimate stress were also comparable with those of the 45^{o} inclined fibre system. However, insufficient data is available to establish whether there is a significant correlation between the two systems other than a general indication.

For the specimens tested in this series, an average of two cracks were observed, with no clear distinction made between the 60 and 26 mm length of fibres used (see Figures 6.8 and 6.9). The direction of the matrix crack being always perpendicular to the tensile stress axis, which in this respect the observations are significantly different from the 45^{o} inclined fibre systems. However, it is thought unlikely that a crack deflection mechanism could operate with random fibres and the results in effect confirm this.

6.6 APPRAISAL

The comparison of the results given in this chapter compared with those given in chapters four and five, indicate clearly that the most

efficient reinforcement system is obtained with the continuous aligned fibres. The reason offered for this is the very low bond strength between the fibre and matrix, which results in fibre pull-out, which invariably takes place during the post-crack deformation. It also follows that the longer the fibre, the greater is the amount of frictional stress transfer between the fibre/matrix. The critical fibre length was not exceeded in any of the fibre composite systems tested. However, from what has been stated, it does not necessarily follow that other fibre composite systems will not produce useful reinforced materials.

The criteria used to identify a practical fibre reinforced cementitious composite is that the tensile stress/strain characteristics should at least include a large post-cracking strain at the matrix cracking load, with associated multiple cracking and closely spaced fine cracks. These criteria were met for all the fibre reinforced composite systems tested except for the closely spaced fine cracks. Closely spaced fine cracks could, however, be achieved if one or all of the following criteria were met:

(A) improved bond between fibre/matrix

(B) increased modular ratio of fibre to matrix

(C) increased aspect ratio of fibre above the critical fibre length (in practical terms, this means reducing the fibre diameter)

provided that there is a sufficient concentration of fibre present.

6.7 CONCLUSIONS

The general conclusion that can be drawn is that inclined and random fibre reinforcement is not as effective as the aligned fibre reinforcement

in increasing the ultimate strength of the composite. Furthermore, the presence of fibres inclined at an angle greater than 45^{o} reduces the first crack strength.

Specific conclusions that can be drawn are as follows:

(1) The number of cracks induced along the length of the specimen increases with a decreasing fibre inclination angle.

(2) The mode of fracture was found to be dependent upon the inclination angle, i.e. tensile from 0^{o} to 15^{o}, intralaminar from 60^{o} to 90^{o}, and a mixture of both modes between 30^{o} and 45^{o}.

ACOUSTIC EMISSION STUDIES

CHAPTER SEVEN

ACOUSTIC EMISSION STUDIES

7.1 PREAMBLE

This chapter needs to be read in conjunction with chapters four, five and six, which contain descriptions of materials and fabrication techniques for Continuous aligned, Discontinuous aligned and Inclined and Random Fibre composites respectively.

The purpose of the investigation was to acertain whether acoustic emission data could provide information on internal deformation mechanisms. In particular whether fibre played any role before the onset of cracking, the mechanisms by which the fibre influenced the multiple cracking process and the emission characteristics of the matrix itself.

A brief review of the acoustic emission literature is included to provide background information.

7.2 PRINCIPLES OF ACOUSTIC EMISSION

7.2.1 Generation of Acoustic Emission

Acoustic emission is a transient elastic wave generated by the rapid release of energy within a material[67]. Standard definitions[68] of terms relating to acoustic emission are given in appendix A. This phenomenon has been seriously studied in materials for the last thirty years. Acoustic emission has been used to non-destructively test

many materials, ranging from metals to composites. It has been applied both as an early warning system to catastrophic failure and as a laboratory tool to study basic material fracture mechanisms.

There is a great variety in acoustic emissions produced by materials. Some materials produce acoustic emissions copiously when stressed, whilst others are quiet by comparison. When a material is loaded, strain energy is stored in the specimen, where most of it remains until the specimen is unloaded, if the load is confined to the elastic range. If the specimen is taken to the plastic range, part of the energy is stored as plastic strain energy and part is converted to heat. Energy partition into plastic strain, heat, sound and energy to create a new surface occurs if the specimen fractures. In both the so-called elastic range and in the plastic range, however, a small fraction of the energy is lost in the form of high frequency bursts of sound; these bursts are the acoustic emission. In the elastic range, it is assumed that these sounds are emitted from local volumes where plastic processes are occurring. The fact that the acoustic emission process is an irreversible process supports the contention that plastic processes are involved[69].

7.2.2 Detection of Acoustic Emission

It is fundamental that a stress wave which is created inside a material must travel through the specimen in order to reach a sensor, the preferred route being along the surface layer. Changes occur in the waveform and frequency spectrum of the stress wave on its journey because of phenomena[70] such as absorption, scattering, dispersion and material inhomogeneities. However, it is still essential that a

transducer must be used which is capable of efficiently and faithfully converting the mechanical waves reaching the specimen surface into electrical signals. The most frequently used transducer for this purpose is of the resonant piezoelectric type.

Piezoelectric transducers are made from materials which will generate a surface charge density under an applied stress. Several naturally occurring substances, notably quartz, produce the effect, but the most popular piezoelectric material for acoustic emission work is polarised lead-zirconate-titanate, because of its low electrical impedance and high electromechanical coupling coefficient. These two properties are very important, since they influence the noise level of the transducer and its efficiency in converting mechanical energy into electrical energy. Most applications of acoustic emission have used piezoelectric detectors principally because of their sensitivity at high frequencies, their low sensitivity to mechanical noise and their robustness. Apart from using efficient transducers it is essential that location, mounting and coupling of the transducer is carried out properly, as this will also determine the quality and quantity of the raw data[71].

7.2.3 Signal Processing and Analysis

The signal from the transducer at this stage can be considered as a wave train corresponding to a distinct acoustic event in the specimen. Figure 7.1 shows a representation of an acoustic emission event and different parameters. This signal is first fed into a pre-amplifier (see Figure 7.2, which shows a block diagram of acoustic emission detection equipment) which amplifies the signal. It is then filtered

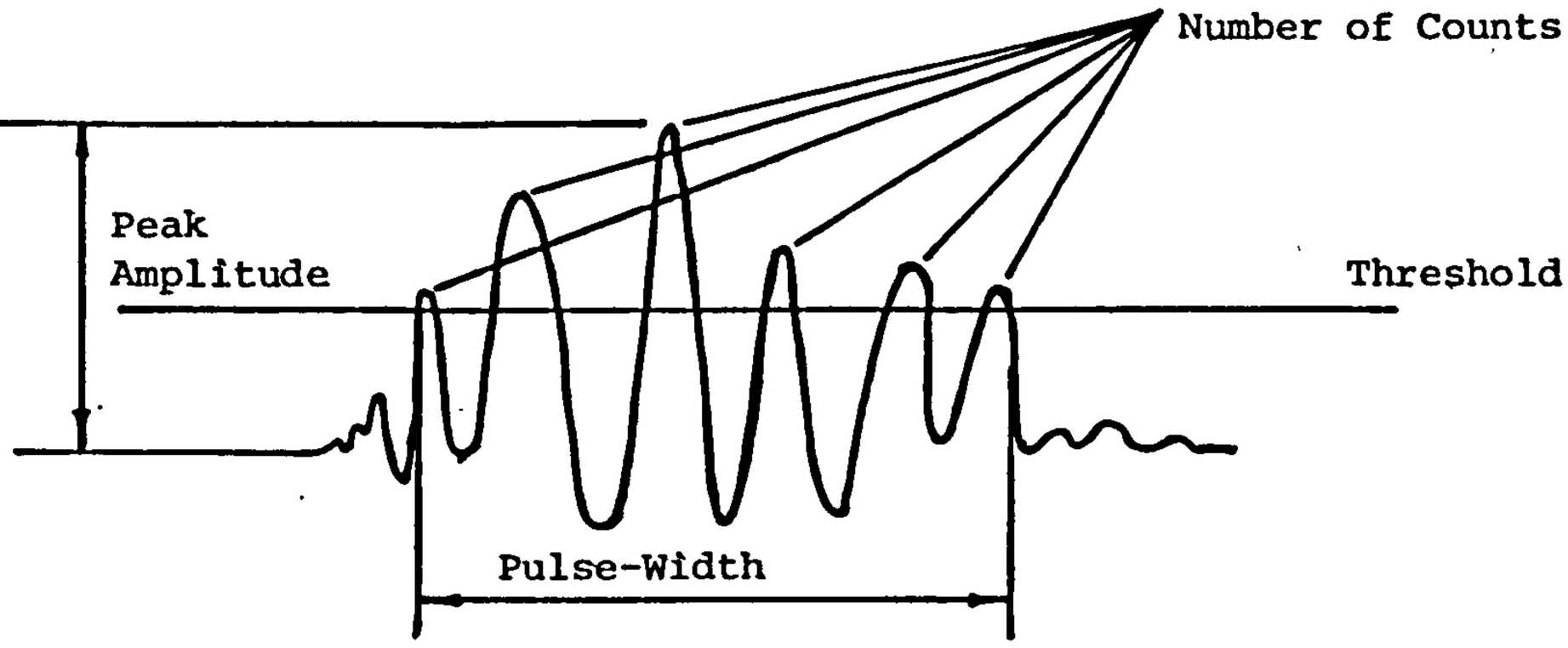

FIGURE 7.1 - REPRESENTATION OF AN ACOUSTIC EMISSION EVENT AND DIFFERENT PARAMETERS

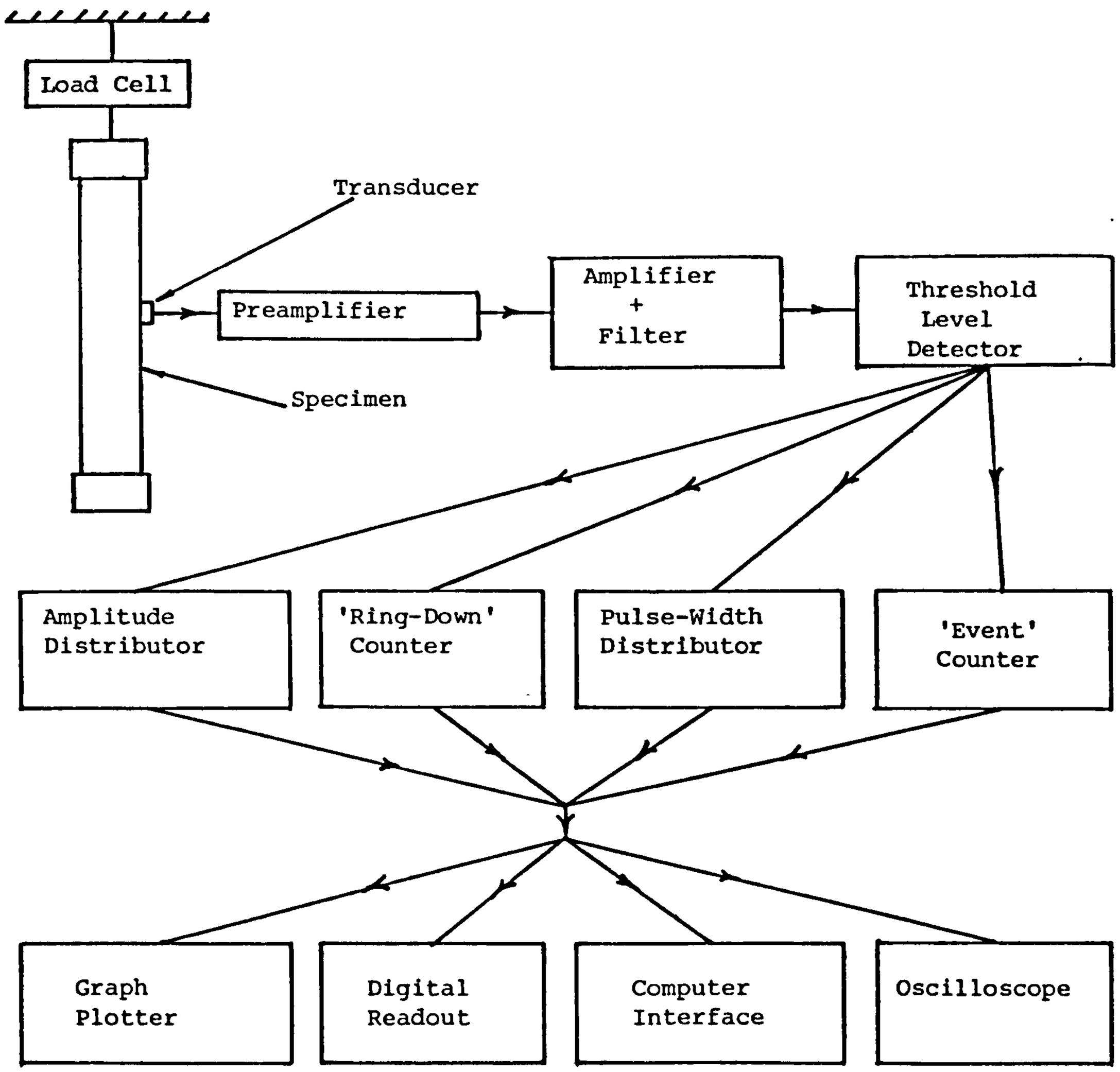

FIGURE 7.2 - BLOCK DIAGRAM OF ACOUSTIC EMISSION DETECTION EQUIPMENT

to remove unwanted frequencies such as low frequency vibrations from mechanical equipment below 100 kHz and further amplified to produce gains of up to 100 dB. The signal is then fed into a threshold-level detector, which will only pass those peaks above the threshold level, and which is usually fixed arbitrarily at one volt. If the signal is then fed into a counter, the number of peaks in the signal which are above one volt threshold will be recorded; each peak is known as a count. This number of counts is known as the ringdown count of the signal (see Figure 7.3). This method of counting is most widely used in acoustic emission detection systems. Acoustic emission equipment can also record amplitude and pulse-width distributions and these may be used to characterise emission from a material. Amplitude and pulse-width relate to energy, so it is relatively easy to discern the physical meaning of this kind of signal processing. Both types of distributions depend quite strongly on the material and on the deformation mechanisms, so there are good prospects for making a diagnosis of internal mechanisms[72]. If required, direct energy measurement can be implemented by acoustic emission systems. The detected acoustic emission signal voltage is first squared and then the area under the voltage squared versus time curve is measured. However, it must be pointed out that it is the energy of the electrical signals generated by the transducer that is being measured which is not necessarily proportional to the energy of the acoustic wave or the acoustic emission source. The actual measurement of the acoustic energy would have to consider the acoustic impedance of the transducer and specimen, the transducer efficiency as a function of frequency and stress wave mode, the geometry, attenuation and elastic properties of the sample, the amplifier gain and frequency response[73].

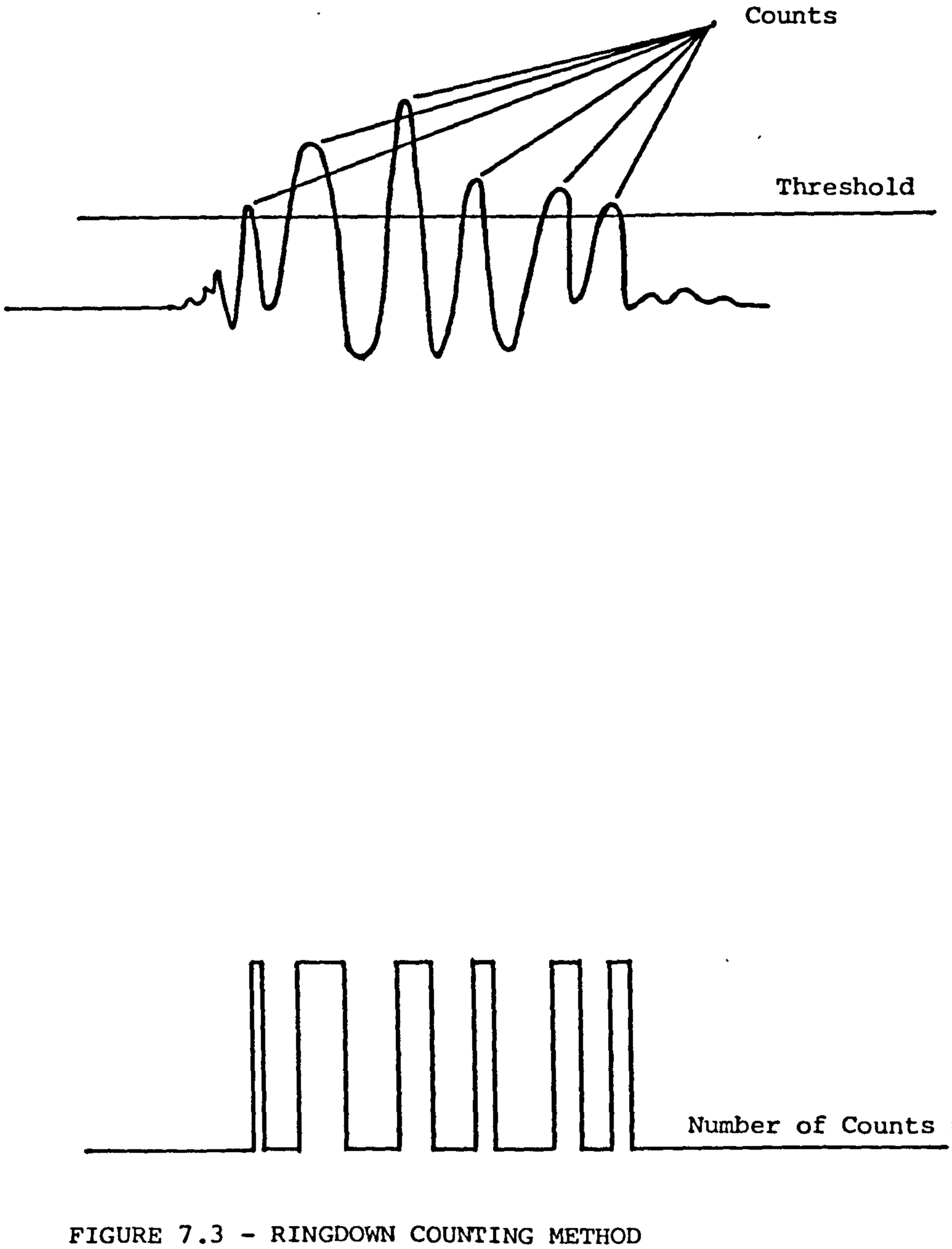

FIGURE 7.3 - RINGDOWN COUNTING METHOD

In some systems acoustic emission data can be processed by spectral analysis, which is the study of the distribution of acoustic emission energy in terms of frequency[74].

Several methods of recording and displaying the data are available. An almost indispensable tool for acoustic emission work is the cathode ray oscilloscope. It serves as a monitor and displays the information that is to be presented to the more permanent recording system. A few minutes of observation of acoustic emission signals on an oscilloscope screen are of more value than any amount of verbal description of those signals. The recording of the data in the form of a hard copy can be accomplished by graph plotters or on-line computer systems[75].

7.3 HISTORICAL BACKGROUND

Historically, the earliest use of acoustic emission analysis occurred in the study of seismology[76]. Analysis of the elastic waves produced by an earthquake was used to characterise fault movement in terms of energy released, location and depth. Mine-workers know well the ominous cracking sounds heard immediately prior to a cave-in, while construction workers are familiar with the creaking sound associated with impending failure of overloaded wooden structures.

Early observation of acoustic emissions in metals were made by tinsmiths who noted "tin cry" or twinning during deformation of tin. Audible sounds noted during heat treatment of steels were later related to the martensitic transformation.

The first serious investigation of acoustic emission was made by

Kaiser[77] in 1950; with the use of amplifiers he detected emission in copper, aluminium, tin, brass, zinc, and lead samples undergoing tensile tests, as well as in steel, to which he devoted most of his attention. He measured the frequency and amplitude of the emissions and reported regular characteristic variations of these parameters with stress. He tentatively interpreted these variations in terms of the deformation processes believed to be active during the various stages of the test. Kaiser also studied the acoustic emissions during solidification, liquefaction and phase transitions in alloy systems. Working with polycrystalline specimens, Kaiser concluded that acoustic vibrations originate in grain boundary interfaces. However, Kaiser's greatest contribution was the observation that acoustic emission activity was irreversible. He found that when a previously loaded sample was reloaded, no emissions were generated until the stress level exceeded its previous high; this behaviour has been named the "Kaiser effect", and the effect tends to hold only for real emissions, whilst frictional sources are active for all loadings.

In 1955, Schofield[78] initiated an extensive investigation of acoustic emission phenomena. He found that emissions did not originate entirely from grain boundaries, as Kaiser concluded, but that single crystals also emitted.

In most of the early studies the frequency range used was below 60 kHz. A significant advance in experimental technique was the extension of experiments into the 100 kHz and 1 MHz range, first reported by Dunegan, Tatro and Harris[79]. This eliminated the need for elaborate soundproof facilities by eliminating the effects of extraneous laboratory noise by working with instrumentation whose frequency range was well above the audio range.

Acoustic emission technology developed rapidly from this point onwards, largely because of advances in instrumentation. This is reflected in the number of technical papers published; a bibliography given in appendix B lists those references which were consulted but not directly referred to here. Metallurgists have used the phenomenon to study martensitic transformations and plastic zone growth[80] and also considerable success has been achieved relating acoustic emission to fracture mechanics parameters[81].

7.4 ACOUSTIC EMISSION IN FIBRE REINFORCED COMPOSITES

Like many other materials, fibre reinforced composites generally emit sonic and ultrasonic vibrations as they incrementally deteriorate when subjected to stress. Fibre materials such as whiskers, metals, glass, ceramic, mineral and polymer materials are used to reinforce varieties of matrices, including ceramics, polymers and metals.

The purpose of using acoustic emission techniques to study composite materials is to obtain information about the stress-strain curve and, if possible, to determine whether there are acoustic emission signatures corresponding to basic fracture mechanisms, which can be used to predict the failure or residual life of a component[82]. Acoustic emissions can be generated in a number of ways during the deformation of a fibre reinforced composite material. They may result from:

(A) plastic deformation or fracture of the fibres,

(B) plastic deformation or fracture of the matrix material,

(C) debonding and/or pull-out of the fibre from matrix.

Each mechanism can be expected to release a different amount of energy and hence to generate different amounts of acoustic emission[83], e.g. the energy liberated by fibre failure is much greater than that

associated with debonding or matrix cracking in carbon fibre composites. However, whereas most deformation or failure processes within a material may yield acoustic emissions, they will only account for a fraction of the total energy involved. Plastic strain, heating, the creation of new surfaces and frictional forces will all share in the overall dissipation of energy, and reflections at interfaces and boundaries of the specimen will complicate the interpretation of emissions recorded at the surface[82]. It is obviously necessary to show that the acoustic activity is emanating from the specimen rather than the loading device[84] before considering the acoustic emission result in detail.

Only a limited amount of work has been reported on acoustic emission in fibre composites. Rotem and Baruch[85] also Rotem[86] monitored acoustic emission during axial loading of unidirectional E glass epoxy composite tensile specimens. They were able to identify fibre fracture associated with a particular type of acoustic emission.

Rotem and Altus[83] were able to relate the energy released by the fracture process to the energy detected by the acoustic emission sensor. Their results indicated that within the same material there was a linear relationship between the acoustic energy and the energy released by fracture.

Bunsell[87] observed that carbon fibre reinforced plastic was acoustically quiet on reloading until about 93% of the previous maximum load, rather than 100%, as predicted by Kaiser effect. This behaviour was explained by considering that the deformation on the fibres was purely elastic, whereas that of the matrix was inelastic.

7.5 TEST PROCEDURE

7.5.1 Tensile Strength

Load was applied by means of a Losenhausen Servo hydraulic UHS6 testing machine, as described in section 3.8.1.

7.5.2 Acoustic Emission Instrumentation and Setting-up Procedure

Dunegan/Endevco 3000 series acoustic emission equipment was used during the investigation (see Plate 7.1, which shows the front view). The instrumentation consisted of a S1000BM transducer, 1801 preamplifier, 602 energy processor, 302A dual signal conditioner, 303 dual counter, 921 amplitude detector, 920 distribution analyser, 922 external memory, Tektronix 604 oscilloscope and X-Y recorders. Since the equipment is available off the shelf as a standard package with instructions, only the pertinent points are given below.

(A) Transducer:

Miniature piezoelectric ceramic acoustic emission transducers (as shown in Plate 7.2) having frequency sensitivity between 20 kHz and 1.8 MHz, with maximum sensitivity at 0.9 MHz, were used. The procedure for attaching the transducer to the specimen was simply to apply couplant (AC-V9) to the transducer face and wring on to test specimen by hand, rotating to and fro to produce a thin layer of couplant at the interface, free of air bubbles. The transducer is then secured to the test specimen with electric insulating tape, hence providing positive contact force between transducer and specimen.

PLATE 7.1 - DUNEGAN/ENDEVCO 3000 SERIES ACOUSTIC EMISSION INSTRUMENTATION

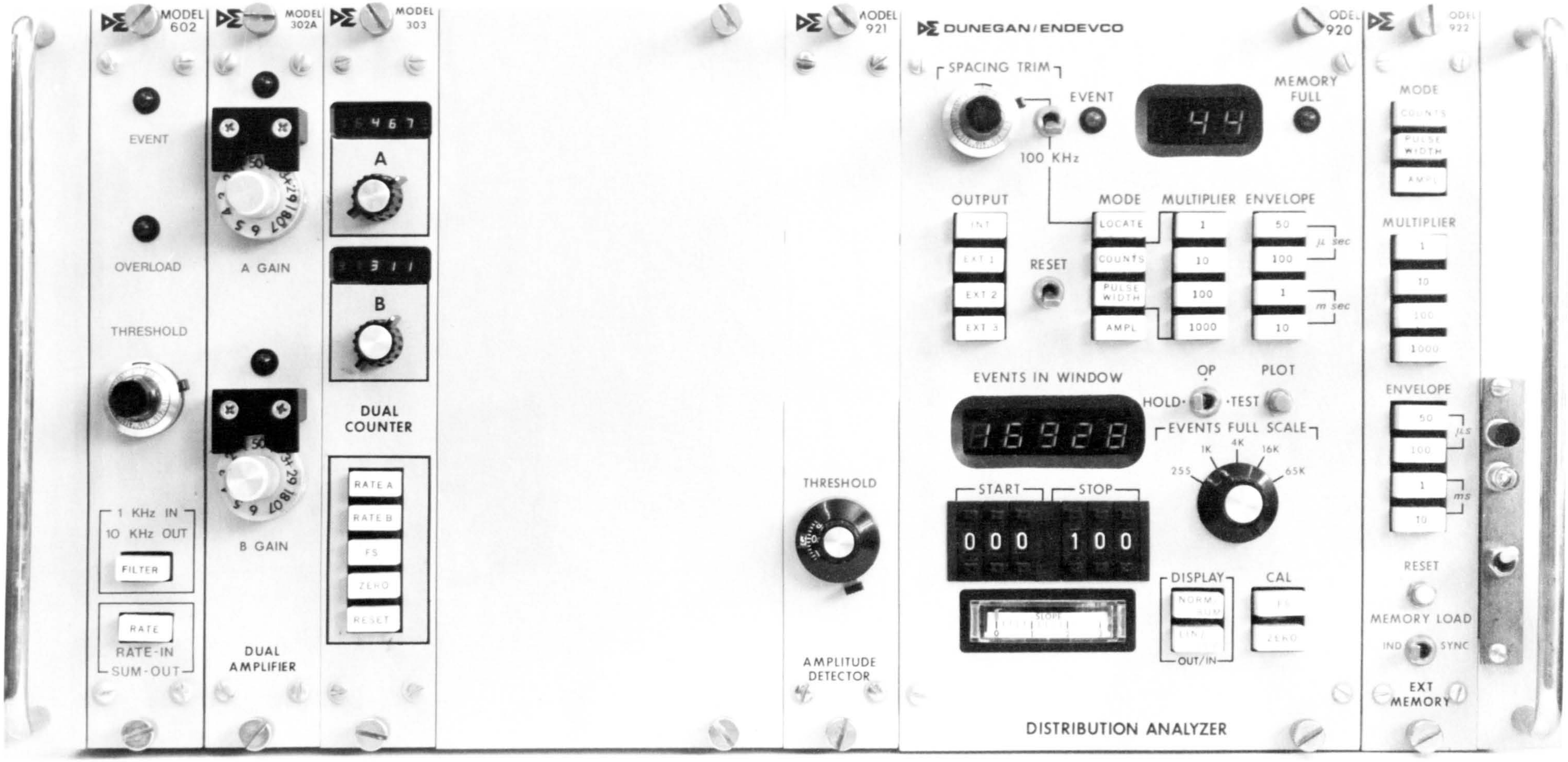
MODEL 602
EVENT
OVERLOAD
THRESHOLD
1 KHz IN
10 KHz OUT
FILTER
RATE
RATE-IN
SUM-OUT
MODEL 302A
A GAIN
B GAIN
DUAL AMPLIFIER
MODEL 303
A
B
DUAL COUNTER
RATE A
RATE B
FS
ZERO
RESET
MODEL 921
THRESHOLD
AMPLITUDE DETECTOR
DUNEGAN/ENDEVCO
MODEL 920
SPACING TRIM
EVENT
100 KHz
MEMORY FULL
OUTPUT
INT
EXT 1
EXT 2
EXT 3
RESET
MODE
LOCATE
COUNTS
PULSE WIDTH
AMPL
MULTIPLIER
1
10
100
1000
ENVELOPE
50
100
1
10
μ sec
m sec
EVENTS IN WINDOW
OP
HOLD
TEST
PLOT
EVENTS FULL SCALE
1K
4K
16K
255
65K
START
STOP
000 100
DISPLAY
NORM
CUM
LIN
OUT/IN
CAL
FS
ZERO
DISTRIBUTION ANALYZER
MODEL 922
MODE
COUNTS
PULSE WIDTH
AMPL
MULTIPLIER
1
10
100
1000
ENVELOPE
50
100
1
10
μs
ms
RESET
MEMORY LOAD
IND
SYNC
EXT MEMORY

PLATE 7.2 - ACOUSTIC EMISSION TRANSDUCERS

PLATE 7.3 - ACOUSTIC EMISSION PREAMPLIFIERS

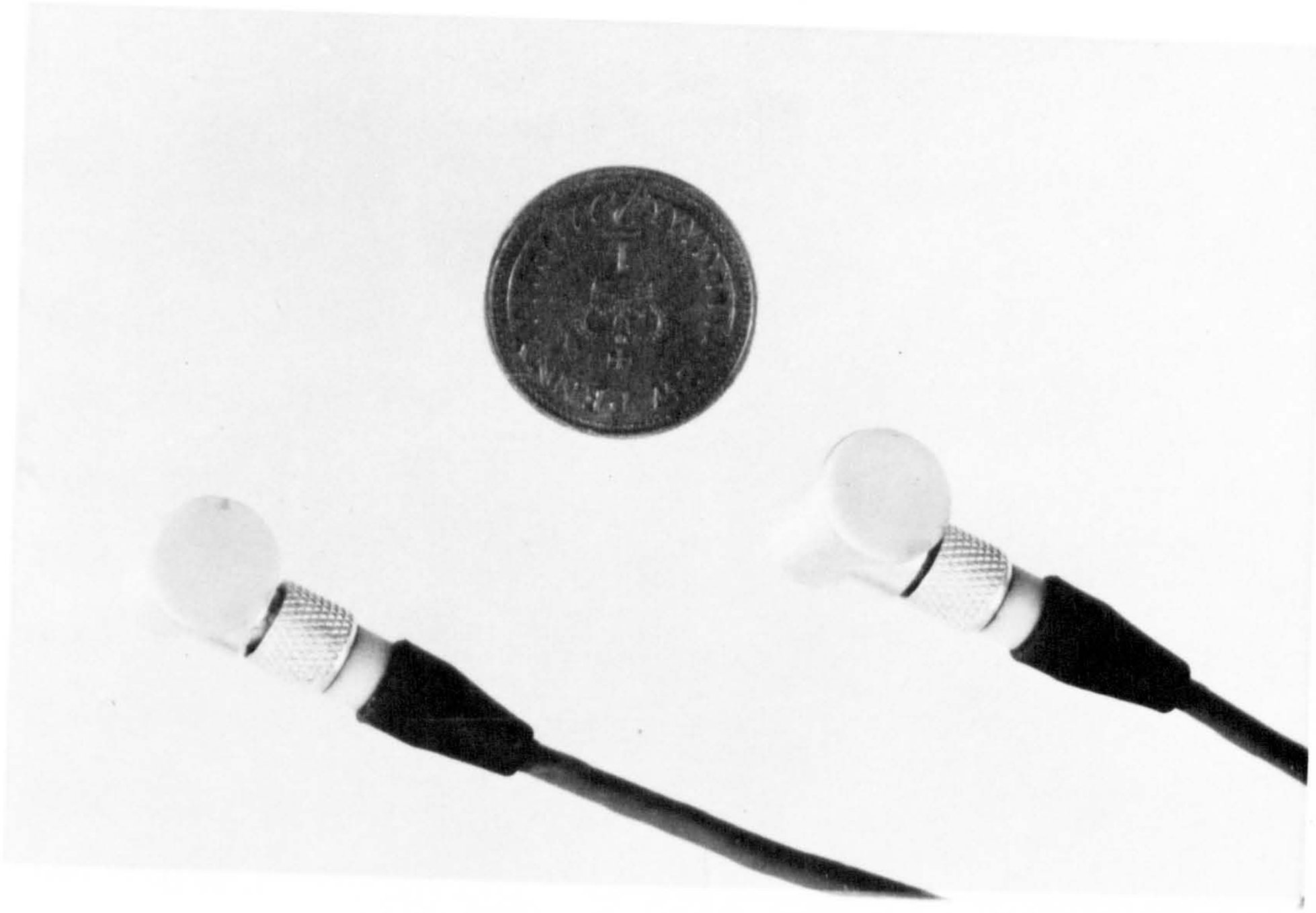

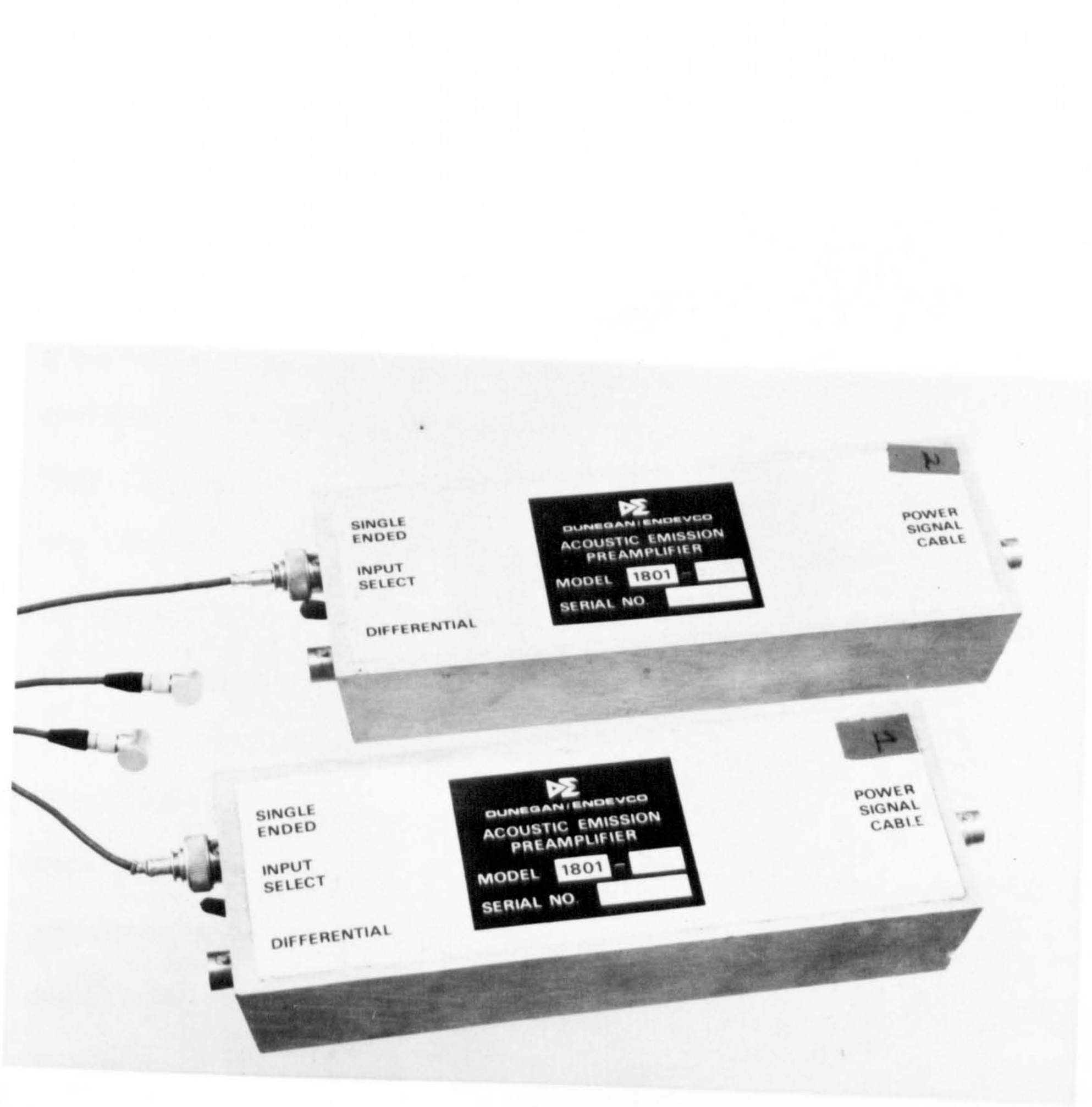
SINGLE ENDED
INPUT SELECT
DIFFERENTIAL
DUNEGAN/ENDEVCO
ACOUSTIC EMISSION PREAMPLIFIER
MODEL 1801 -
SERIAL NO.
POWER SIGNAL CABLE
SINGLE ENDED
INPUT SELECT
DIFFERENTIAL
DUNEGAN/ENDEVCO
ACOUSTIC EMISSION PREAMPLIFIER
MODEL 1801 -
SERIAL NO.
POWER SIGNAL CABLE

(B) Preamplifier:

This provides a fixed gain of 40 dB* (see Plate 7.3) and is located near the transducer. Its function is to amplify the signal sufficiently to allow transmission over long distances.

(C) Energy Processor:

This unit monitors the whole acoustic signal detected by the transducer and represents in terms of its associated energy in arbitrary unit; thus the data is displayed from 0 to 999,999 units in real time.

(D) Dual Signal Conditioner:

This unit provides further signal amplification and in addition applies a 1 volt threshold to the signal before outputting to the other units for the analysis of counts and pulse width. A voltage gain between 0 to 60 dB can be obtained in 1 dB increments, which when combined with the fixed preamplifier gain of 40 dB, provides a total potential gain of 100 dB. A value of 50 dB on the model 302A was used, providing a total gain of 90 dB.

(E) Dual Counter:

The counter A, displayed cumulative counts of all the events detected by the transducer during the test and counter B displayed energy units as described in (C) above. Both the variables were plotted on X-Y recorders as the test progressed.

(F) Distribution Analyser:

This first of all quantifies each acoustic emission event in terms of a pre-selected parameter such as counts, pulse width and maximum amplitude per event. The numerical value of the parameter is then measured on a scale 0 to 100. The number of events occurring at

---

* For example 1 μV is amplified to 10 μV by 20 dB gain, to 100 μV by 40 dB gain, etc.

each of the hundred scale positions is recorded and continually updated as the test progresses. This distribution of the number of events occurring at a particular parameter value is displayed on an oscilloscope screen. With the horizontal axis indicating the parameter values and the vertical axis the number of events.

(G) External Memory:

This operates in conjunction with the distribution analyser, to allow a simultaneous distribution analysis of more than one parameter of acoustic emission signal. During the investigation, any two parameters could be studied at a given time, i.e. one parameter on model 920 and the other on external memory (model 922).

(H) Instrument Setting:

The following values were used for the various variable controls:

Energy Processor Threshold	0.96
Dual Signal Conditioner	50 dB gain
Amplitude Detector	30 dB
Distribution Analyser	
(i) Multiplier	1
(ii) Envelope	100 µS

7.5.3 Data Recording and Processing

7.5.3.1 Position control

During the initial stage of the acoustic emission investigation, the constant position control as described in section 3.8.1 was adopted and the test specimen prepared and mounted as described in section 7.5.2(A) and as shown in Plate 7.4. The entire test set-up is shown in Plate 7.5. During the test, energy and

PLATE 7.4 - TRANSDUCERS SECURED ON TO THE TEST SPECIMEN WITH INSULATING TAPE AND PREAMPLIFIERS ARE LOCATED NEAR THE TRANSDUCERS

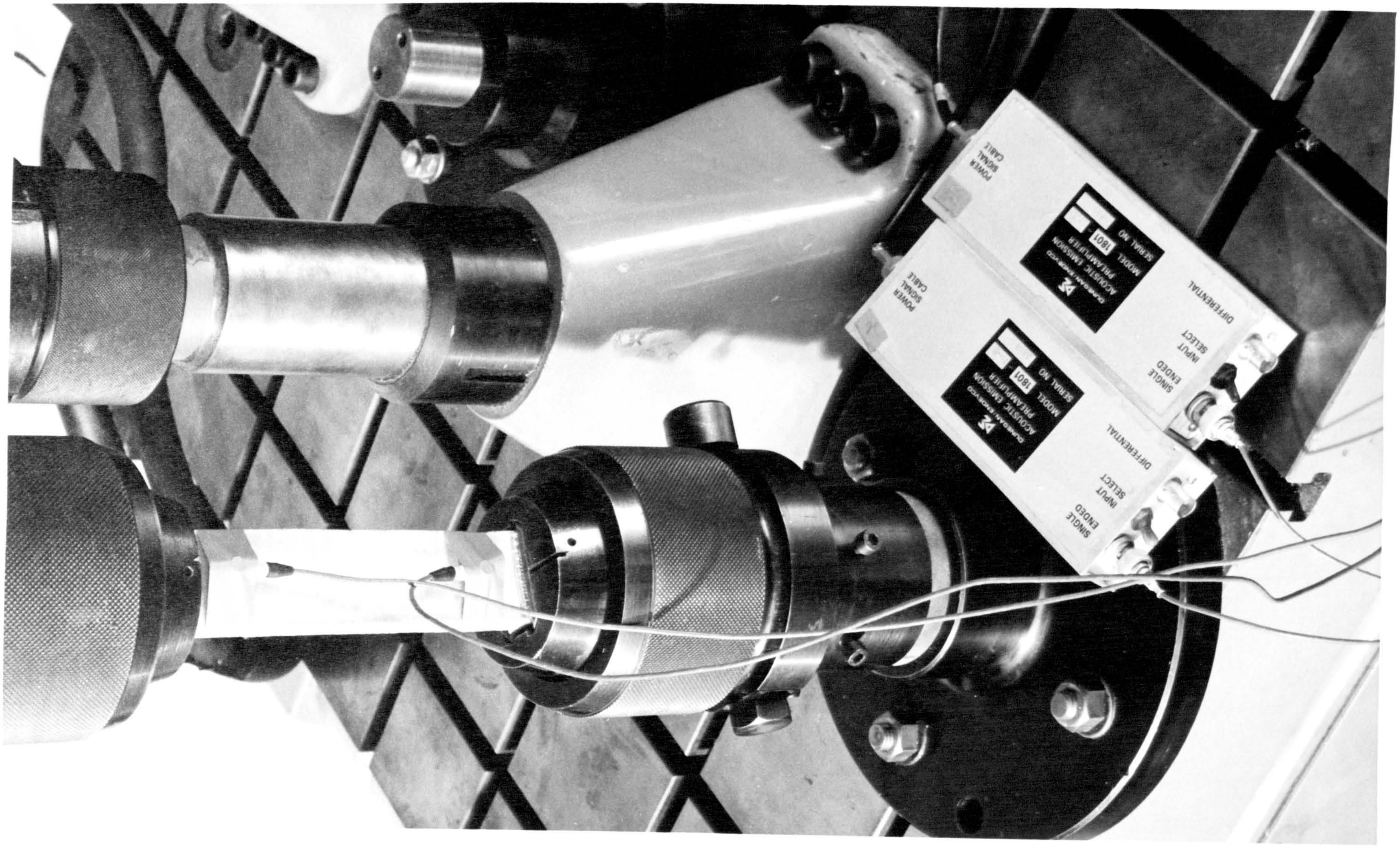
MODEL 1801
SERIAL NO
SINGLE ENDED
INPUT SELECT
DIFFERENTIAL
POWER SIGNAL CABLE

PLATE 7.5 - SHOWS ENTIRE TEST SET UP, WHICH INCLUDES LOSENHAUSEN TESTING MACHINE, DUNEGAN/ENDEVCO 3000 SERIES ACOUSTIC EMISSION EQUIPMENT WITH OSCILLOSCOPE AND VARIOUS X-Y RECORDERS


LOS
SYSTEM

cumulative counts were recorded by means of X-Y recorders, as shown in Plate 7.6. After completion of the test, depending on the mode being investigated, the final distributions of two of the following parameters were recorded per test, events in the count (C), pulse width (P) and amplitude (A) mode. In addition, a record was made of the summation of the respective parameters. The method employed for recording these various distributions was to photograph the corresponding oscilloscope display. This resulted in at least four photographs, i.e. two photographs for the two modes being investigated, and the other two photographs for the summation of the respective modes. Having carried out several tests in this manner, films were developed and printed. It was apparent by studying the photographs that a single photograph taken at the end of a test did not reveal much information. This led to the next stage when it was decided to take sufficient photographs during the test to allow a progressive account of the test to be recorded and studied subequently. This was carried out by stopping the test at a particular increment of load and photographing the oscilloscope screen, the procedure taking approximately five minutes. The procedure was repeated until the specimen reached its maximum load.

However, when the test specimen was stopped at a particular load, it was observed that the normal "hunting effect" of the servo-hydraulic machine control system caused small fluctuations in the load. This was because in the position control the long stroke control transducer was working at its limit of sensitivity.

To avoid this, tests were carried out under constant load control,

PLATE 7.6 - HEWLETT-PACKARD X-Y RECORDER PLOTTING LOAD v ACOUSTIC ENERGY

7035B X-Y RECORDER
HEWLETT · PACKARD

~ LINE ON OFF
SERVO ON OFF
CHART HOLD RELEASE
PEN DOWN UP

Photo | Load (lbs) | Stress N/mm²
1 | 102
2 | 300
3 | 500
4 | 706
5 | 1000 | 1st Crack
6 | 1500
7 | 2000
8 | 2500
9 | 3000 | Failure of Spe

Load (lbs)

1st Crack | Cracks | 81236 failure

TEST DG – Acoustic Emission

X-sectional area 544.05 mm²

8·7% of weighted & continuous

W/c = 0·4

cast from 6/10/80

Test from 13/10/80

7 days cured in water.

Spec Dims = 13·5 × 40·3 × 250

No of cracks during = 5

Constant Load control 5 on 0·1 scale.

RANGE
100
10
1
mV/IN
V/IN
CAL
VERNIER
LOCK
GAIN
INPUT
ZERO
LOCK
30V≂ MAX
GUARD
30V≂ MAX
+
−

which gave greater accuracy because of the larger load cell output signal for the corresponding load.

7.5.3.2 Load control

Tests were carried out at a constant rate of loading of 112 N/min. The procedure finally adopted for recording and processing the acoustic emission data in this mode of testing, which constituted the majority of the investigation, was as follows.

The basic approach was to hold the load at the various intervals during the test to allow photographic recording of the oscilloscope display of the parameters under investigation. This took the same period of time (approximately five minutes) as with the position control mode. During this procedure the load was steady and no creep deformation was observed. Illustrations of the types of displays obtained are shown in Plates 7.7 to 7.12, which show the oscilloscope displays of amplitude, sum amplitude, counts, sum counts, pulse width and sum pulse width modes respectively, for a continuous aligned fibre reinforced cement paste containing 5.5% by volume of fibres. Having obtained a set of photographs for a particular parameter under investigation during the test, the next procedure was to represent numerically the photographic information. This was achieved by considering the peak number of events (maximum) counted at the most frequently occurring parameter value; for example, in Plate 7.7, a total of 358 events occurred at an amplitude of 32 dB. It was considered that this method was more appropriate than considering the number of events at a fixed parameter value.

PLATE 7.7 - TYPICAL EXAMPLE OF EVENTS IN AMPLITUDE MODE OF CONTINUOUS ALIGNED FIBRE REINFORCED CEMENT PASTE CONTAINING 5.5% V_f

PLATE 7.8 - TYPICAL EXAMPLE OF EVENTS IN SUM AMPLITUDE MODE OF CONTINUOUS ALIGNED FIBRE REINFORCED CEMENT PASTE (CONTAINING 5.5% V_f (SUMMATION OF PLATE 7.7 DATA FROM RIGHT TO LEFT)

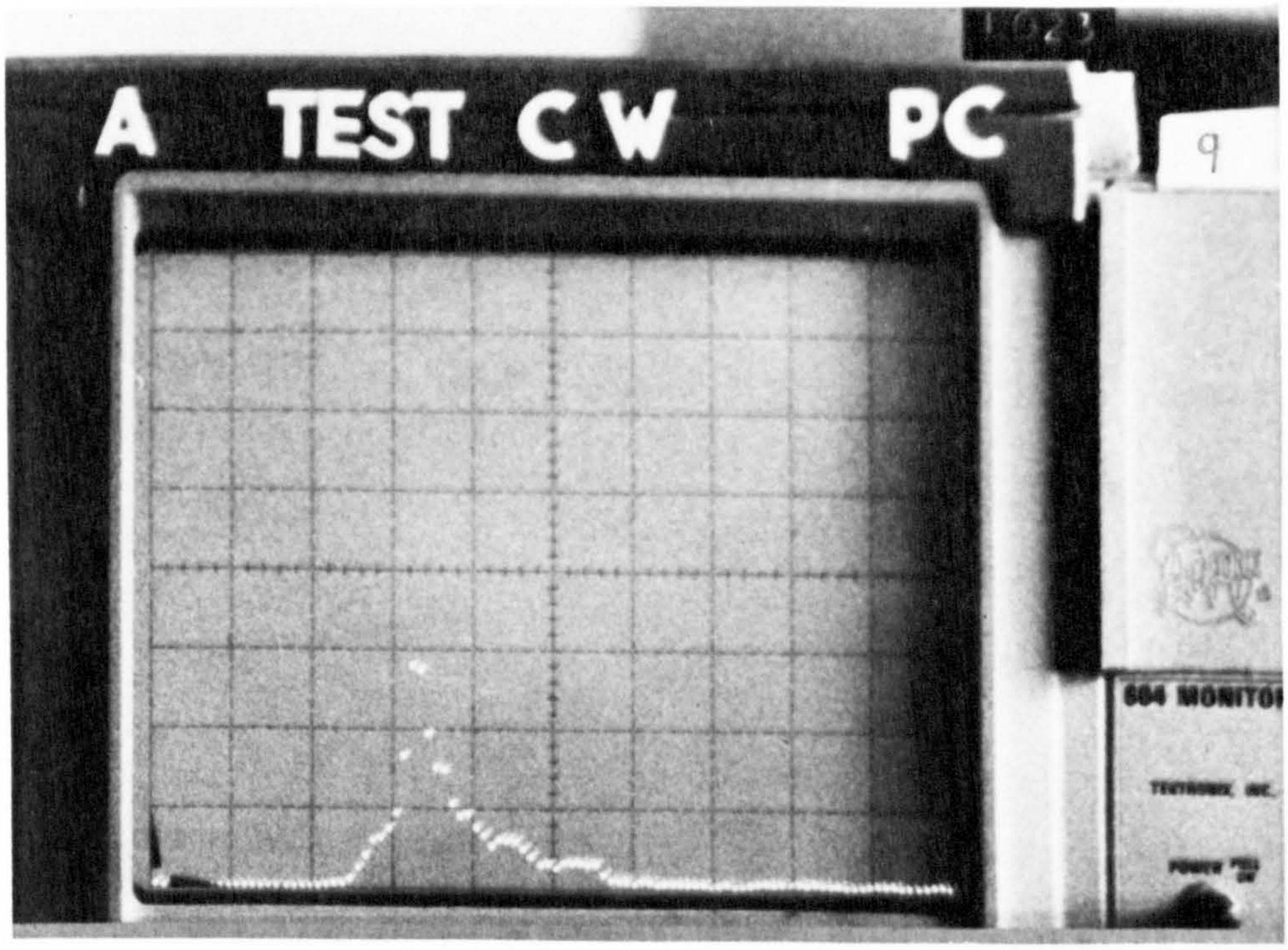
A TEST C W PC
1023
9
604 MONITOR
TEKTRONIX, INC.

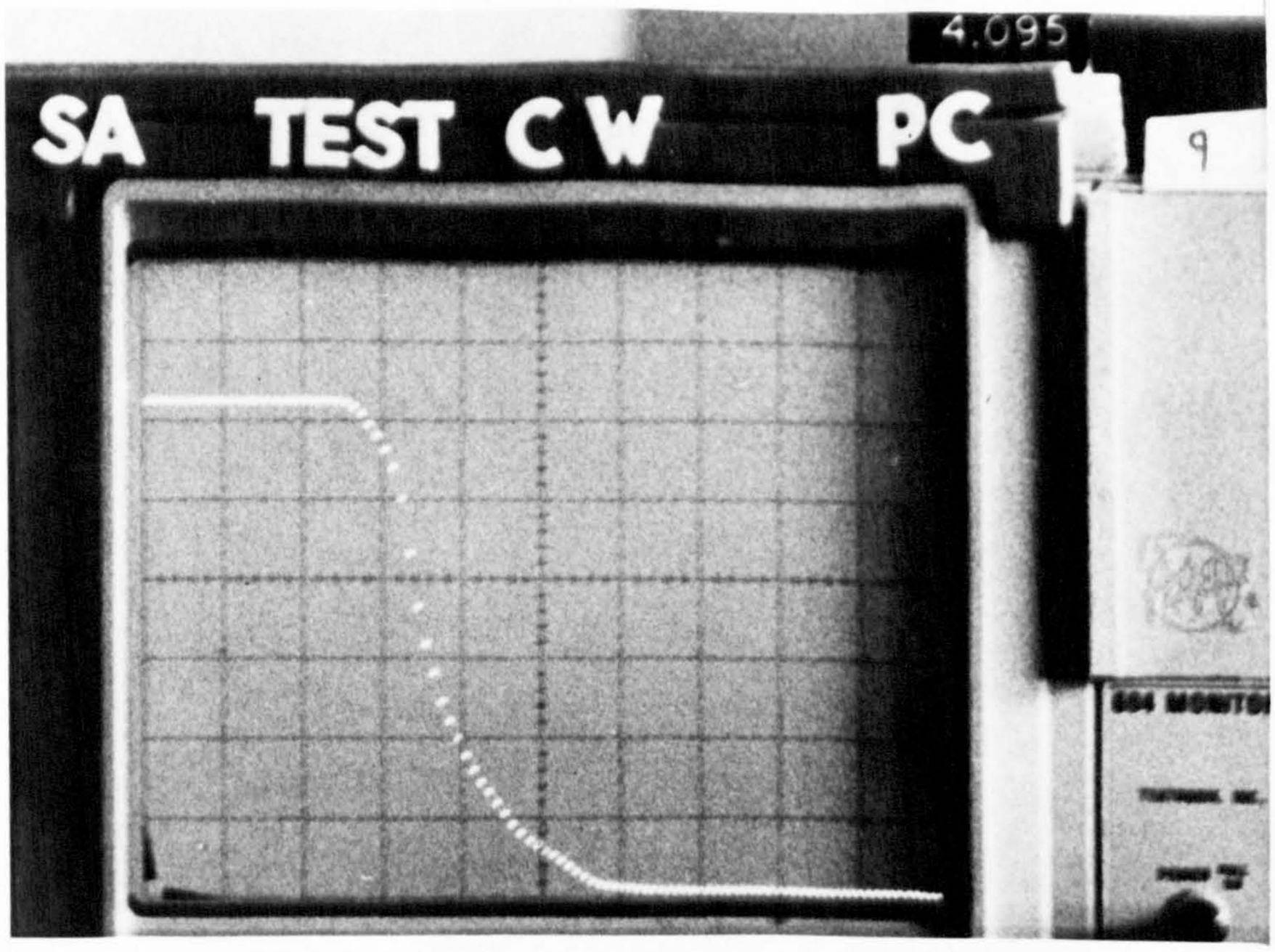
SA TEST C W PC
4.095
9
604 MONITOR
TEKTRONIX, INC.

PLATE 7.9 - TYPICAL EXAMPLE OF EVENTS IN COUNTS MODE OF CONTINUOUS ALIGNED FIBRE REINFORCED CEMENT PASTE CONTAINING 5.5% V_f

PLATE 7.10 - TYPICAL EXAMPLE OF EVENTS IN SUM COUNTS MODE OF CONTINUOUS ALIGNED FIBRE REINFORCED CEMENT PASTE CONTAINING 5.5% V_f (SUMMATION OF PLATE 7.9 DATA FROM RIGHT TO LEFT)

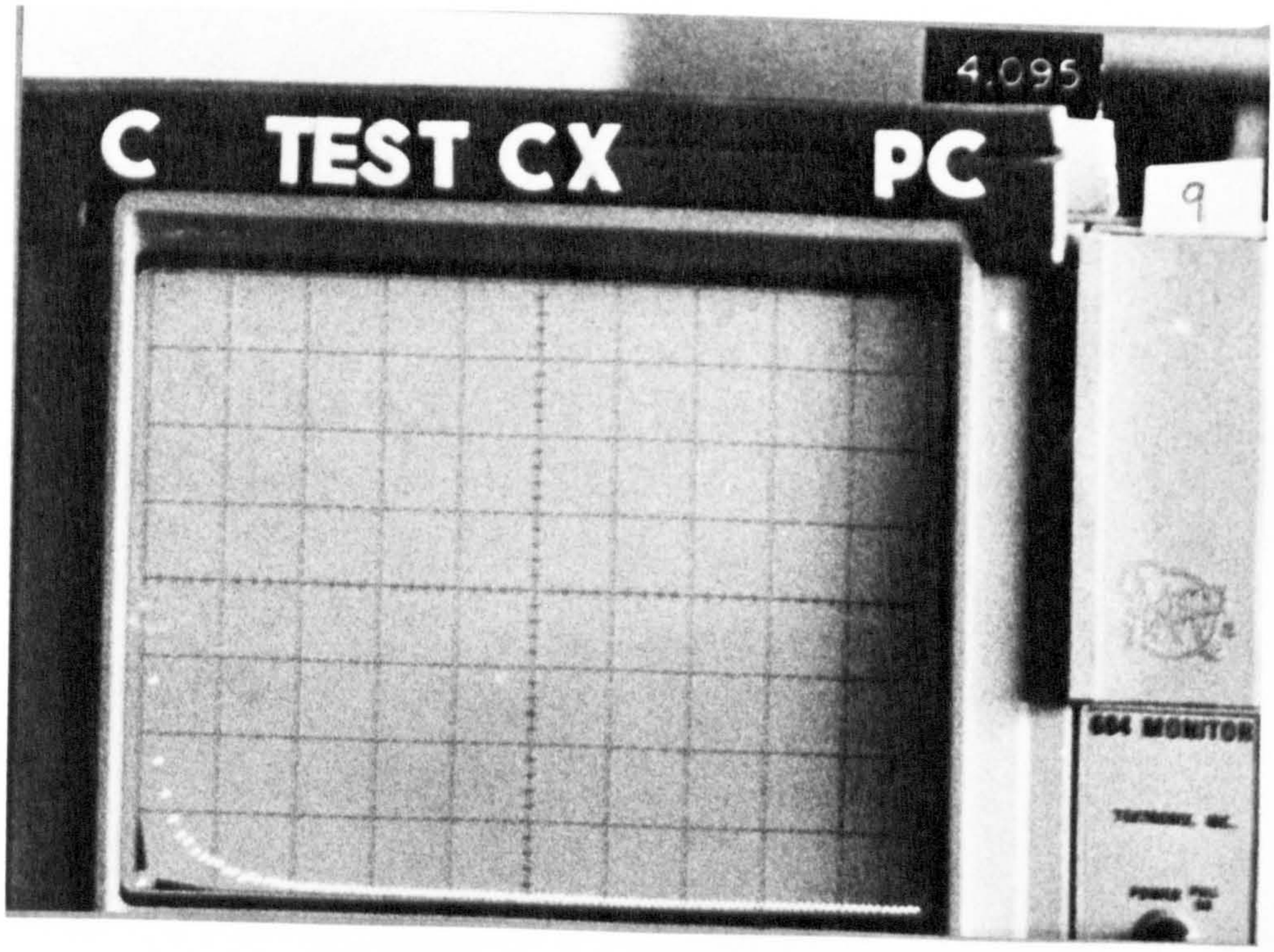
4.095
C TEST CX PC
9
604 MONITOR

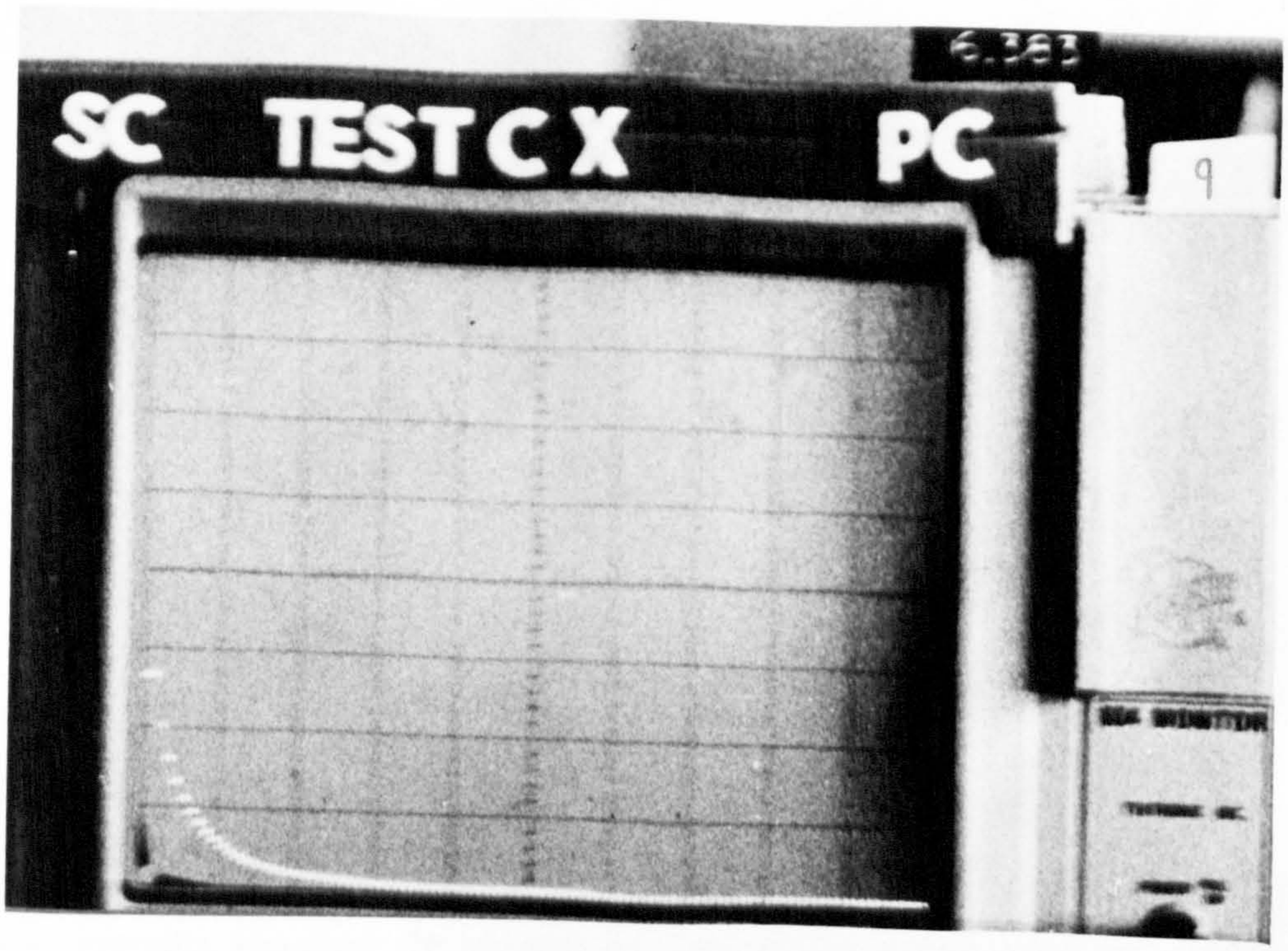
SC TEST C X PC
9

PLATE 7.11 - TYPICAL EXAMPLE OF EVENTS IN PULSE WIDTH MODE OF CONTINUOUS ALIGNED FIBRE REINFORCED CEMENT PASTE CONTAINING 5.5% V_f

PLATE 7.12 - TYPICAL EXAMPLE OF EVENTS IN SUM PULSE WIDTH MODE OF CONTINUOUS ALIGNED FIBRE REINFORCED CEMENT PASTE CONTAINING 5.5% V_f (SUMMATION OF PLATE 7.11 DATA FROM RIGHT TO LEFT)

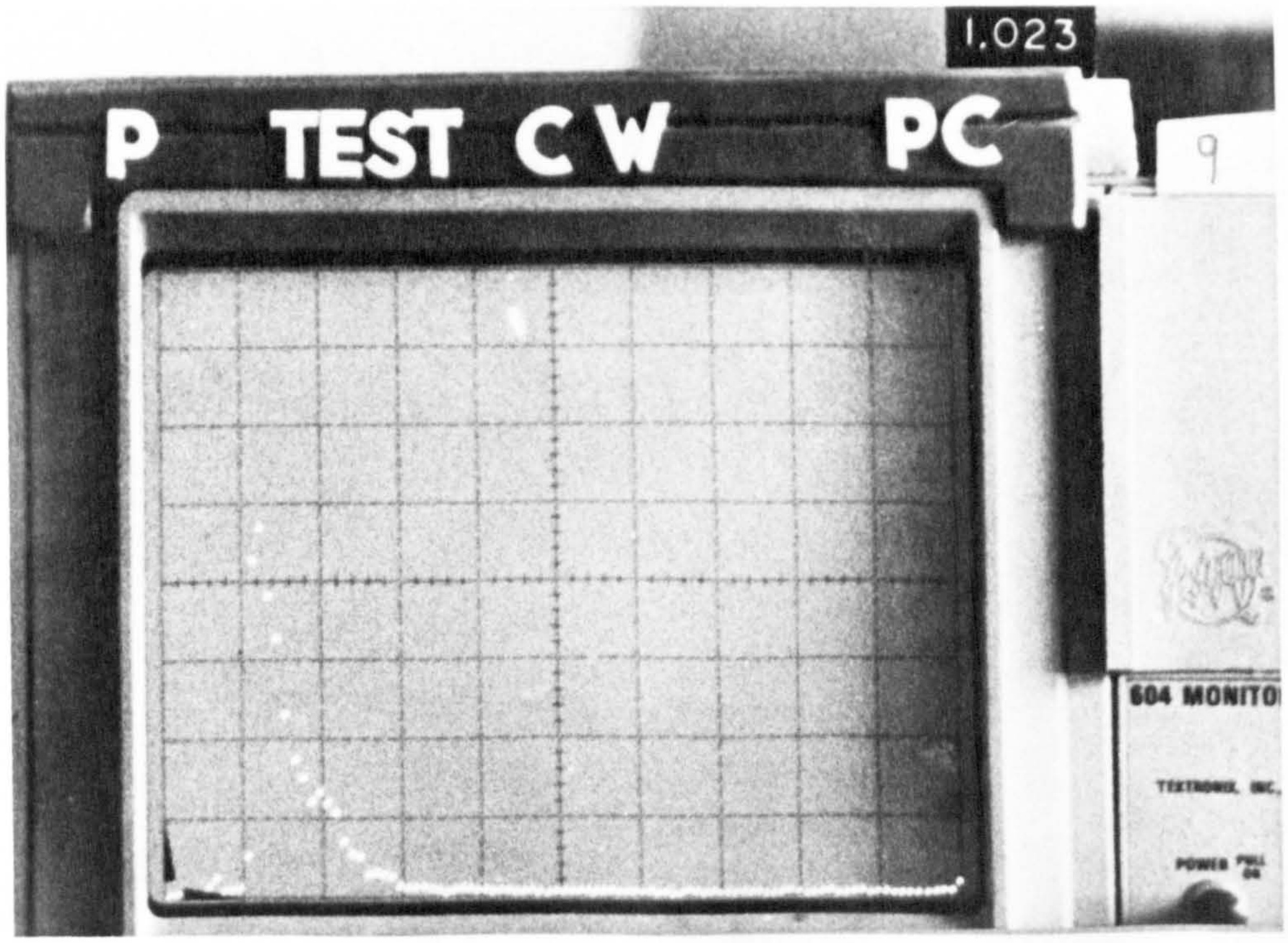
1.023
P TEST C W PC
9
604 MONITO
TEKTRONIX, INC.

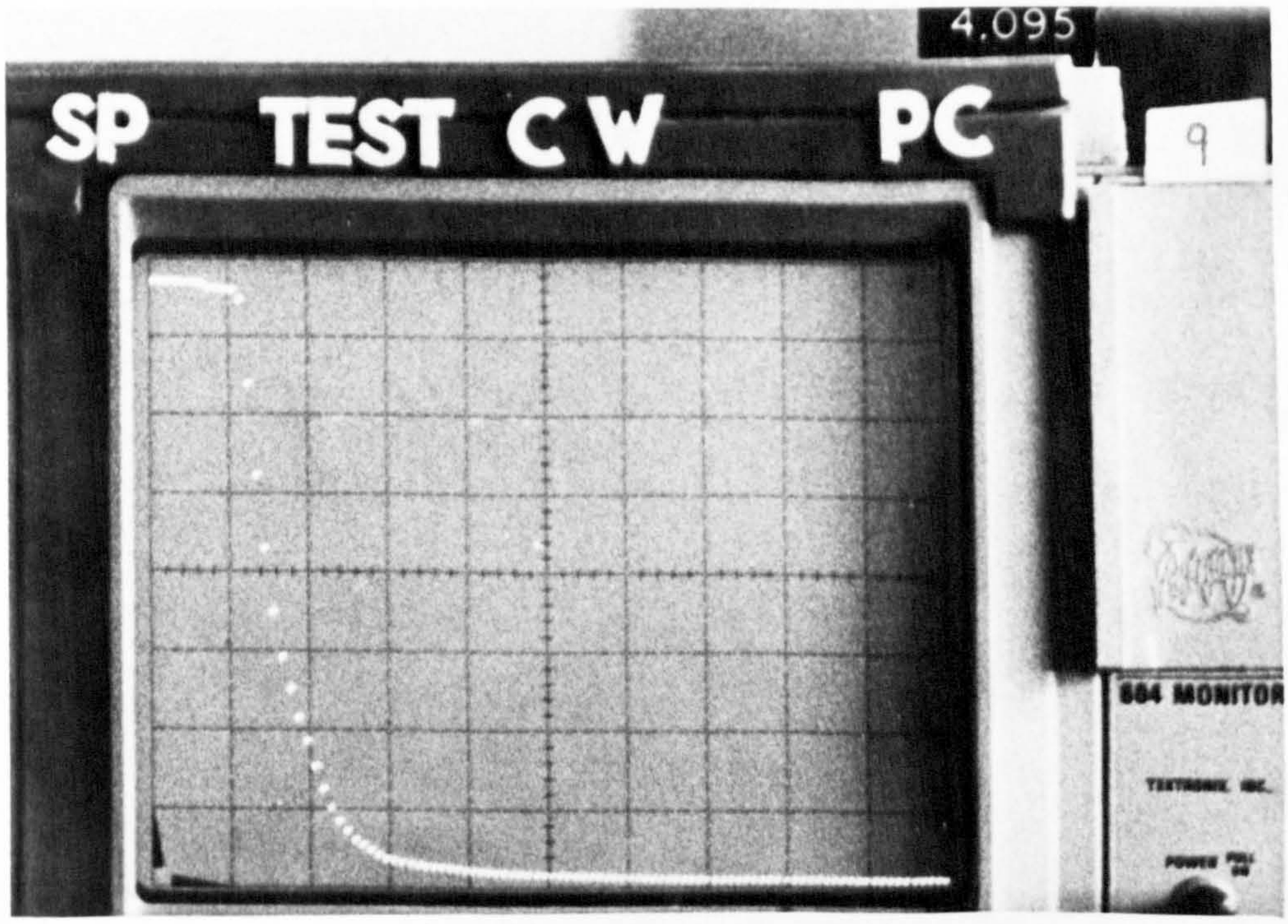
4.095
SP TEST C W PC
9
604 MONITOR
TEKTRONIX, INC.

These readings were represented both in a tabular (Tables 7.1 to 7.6) as well as in a graphical form (Figures 7.4 to 7.9), which shows the relation between stress and either maximum value of events or total number of events in the amplitude, counts and pulse width modes respectively. Also during the test, load versus energy and load versus cumulative counts were plotted (see Figures7.10 and 7.11 respectively).

On average, forty to fifty photographs of the oscilloscope display were taken for each specimen tested, thus allowing approximately ten stages of specimen deformation to be examined. Normally four replicate tensile specimens had their acoustic emission characteristics monitored. The monitoring arrangements for the testing of the four specimens would be as follows. Specimen one would be tested to ascertain the effects in the amplitude and counts modes; specimen two in the amplitude and pulse width modes; specimen three in the counts and pulse width; and finally, specimen four was tested in the amplitude and counts mode again.

Although the total number of photographs taken during the investigation (approximately five thousand) was rather large, the time and cost effectiveness of the method compared favourably with acquiring a computer interface facilities and expertise.

TABLE 7.1 - TYPICAL EXAMPLE OF MAXIMUM NUMBER OF EVENTS IN AMPLITUDE MODE FOR CONTINUOUS ALIGNED FIBRE REINFORCED CEMENT PASTE CONTAINING 5.5% V_f

TEST CW			
Photograph Number	Load (N)	Stress (N/mm^2)	Maximum Number of Events in Amplitude Mode A
1	101	0.18	2
2	400	0.71	64
3	800	1.43	194
4	1200	2.14	243
5	1500	2.68	249
6	2000	3.57	253
7	2503	4.47	258
8	4000	7.14	278
9	4475	7.99	358

TABLE 7.2 - TYPICAL EXAMPLE OF MAXIMUM NUMBER OF EVENTS IN SUM AMPLITUDE MODE FOR CONTINUOUS ALIGNED FIBRE REINFORCED CEMENT PASTE CONTAINING 5.5% V_f

TEST CW			
Photograph Number	Load (N)	Stress (N/mm^2)	Maximum Number of Events in Sum Amplitude Mode SA
1	101	0.18	4
2	400	0.71	330
3	800	1.43	1254
4	1200	2.14	1543
5	1500	2.68	1625
6	2000	3.57	1669
7	2503	4.47	1702
8	4000	7.14	1856
9	4475	7.99	3181

TABLE 7.3 - TYPICAL EXAMPLE OF MAXIMUM NUMBER OF EVENTS IN COUNTS MODE FOR CONTINUOUS ALIGNED FIBRE REINFORCED CEMENT PASTE CONTAINING 5.5% V_f

TEST CX			
Photograph Number	Load (N)	Stress (N/mm^2)	Maximum Number of Events in Counts Mode C
1	150	0.28	45
2	400	0.74	201
3	800	1.48	732
4	1100	2.04	959
5	1501	2.78	1165
6	2003	3.71	1280
7	2500	4.63	1280
8	3200	5.93	1280
9	4620	8.56	1881

TABLE 7.4 - TYPICAL EXAMPLE OF MAXIMUM NUMBER OF EVENTS IN SUM COUNTS MODE FOR CONTINUOUS ALIGNED FIBRE REINFORCED CEMENT PASTE CONTAINING 5.5% V_f

TEST CX			
Photograph Number	Load (N)	Stress (N/mm^2)	Maximum Number of Events in Sum Counts Mode SC
1	150	0.28	120
2	400	0.74	1152
3	800	1.48	2739
4	1100	2.04	3724
5	1501	2.78	4761
6	2003	3.71	5120
7	2500	4.63	5120
8	3200	5.93	5170
9	4620	8.56	5376

TABLE 7.5 - TYPICAL EXAMPLE OF MAXIMUM NUMBER OF EVENTS IN PULSE WIDTH MODE FOR CONTINUOUS ALIGNED FIBRE REINFORCED CEMENT PASTE CONTAINING 5.5% V_f

TEST CW			
Photograph Number	Load (N)	Stress (N/mm^2)	Maximum Number of Events in Pulse Width Mode P
1	101	0.18	3
2	400	0.71	69
3	800	1.43	269
4	1200	2.14	309
5	1500	2.68	323
6	2000	2.57	332
7	2503	4.47	345
8	4000	7.14	380
9	4475	7.99	596

TABLE 7.6 - TYPICAL EXAMPLE OF MAXIMUM NUMBER OF EVENTS IN SUM PULSE WIDTH MODE FOR CONTINUOUS ALIGNED FIBRE REINFORCED CEMENT PASTE CONTAINING 5.5% V_f

TEST CW			
Photograph Number	Load (N)	Stress (N/mm^2)	Maximum Number of Events in Sum Pulse Width Mode SP
1	101	0.18	3
2	400	0.71	396
3	800	1.43	1543
4	1200	2.14	1920
5	1500	2.68	1996
6	2000	2.57	2048
7	2503	4.47	2099
8	4000	7.14	2180
9	4475	7.99	3929

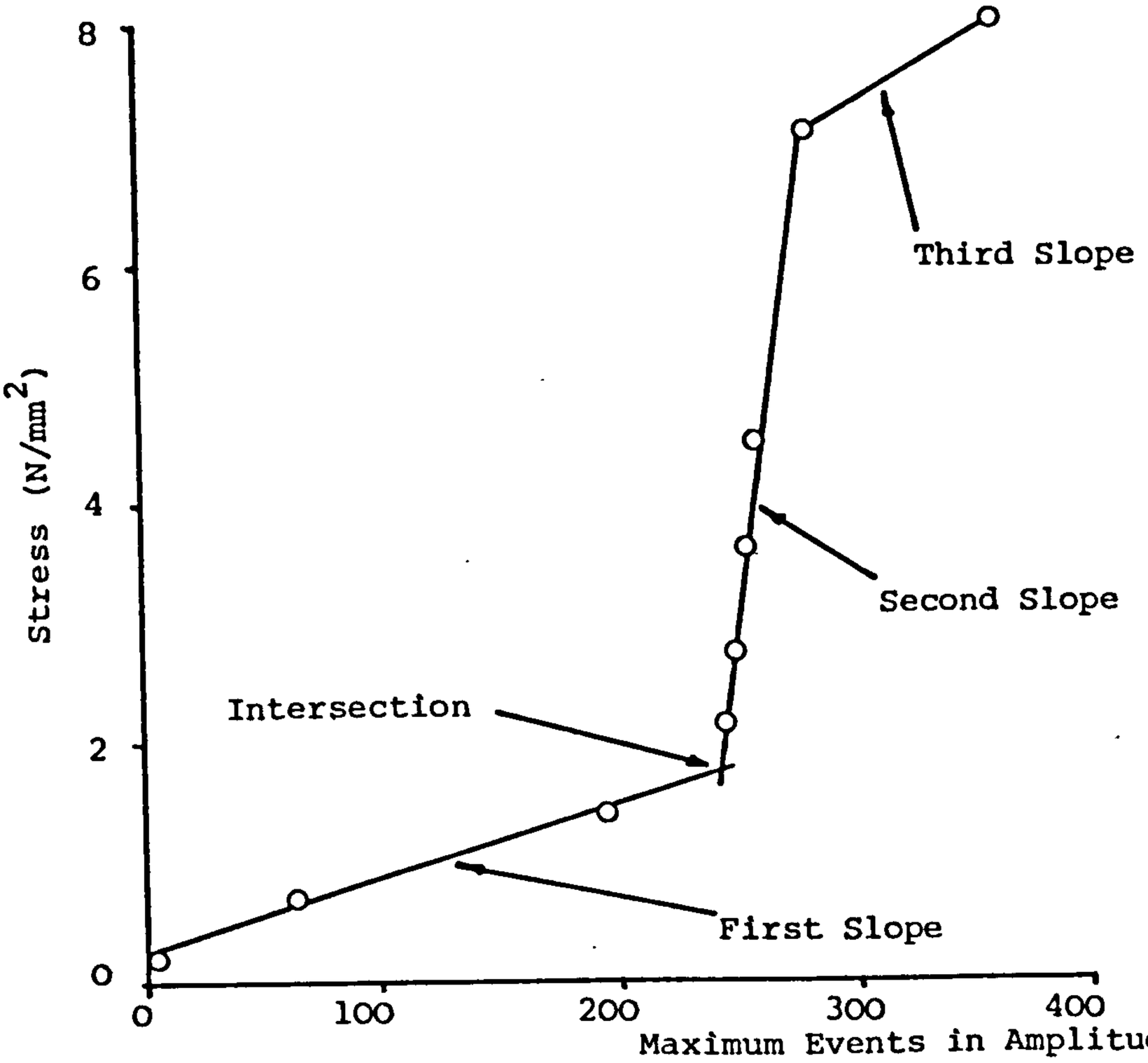

FIGURE 7.4 - TYPICAL STRESS v MAXIMUM NUMBER OF EVENTS IN AMPLITUDE MODE CURVE FOR CONTINUOUS ALIGNED FIBRE SYSTEM CONTAINING 5.5% VOLUME CONCENTRATION

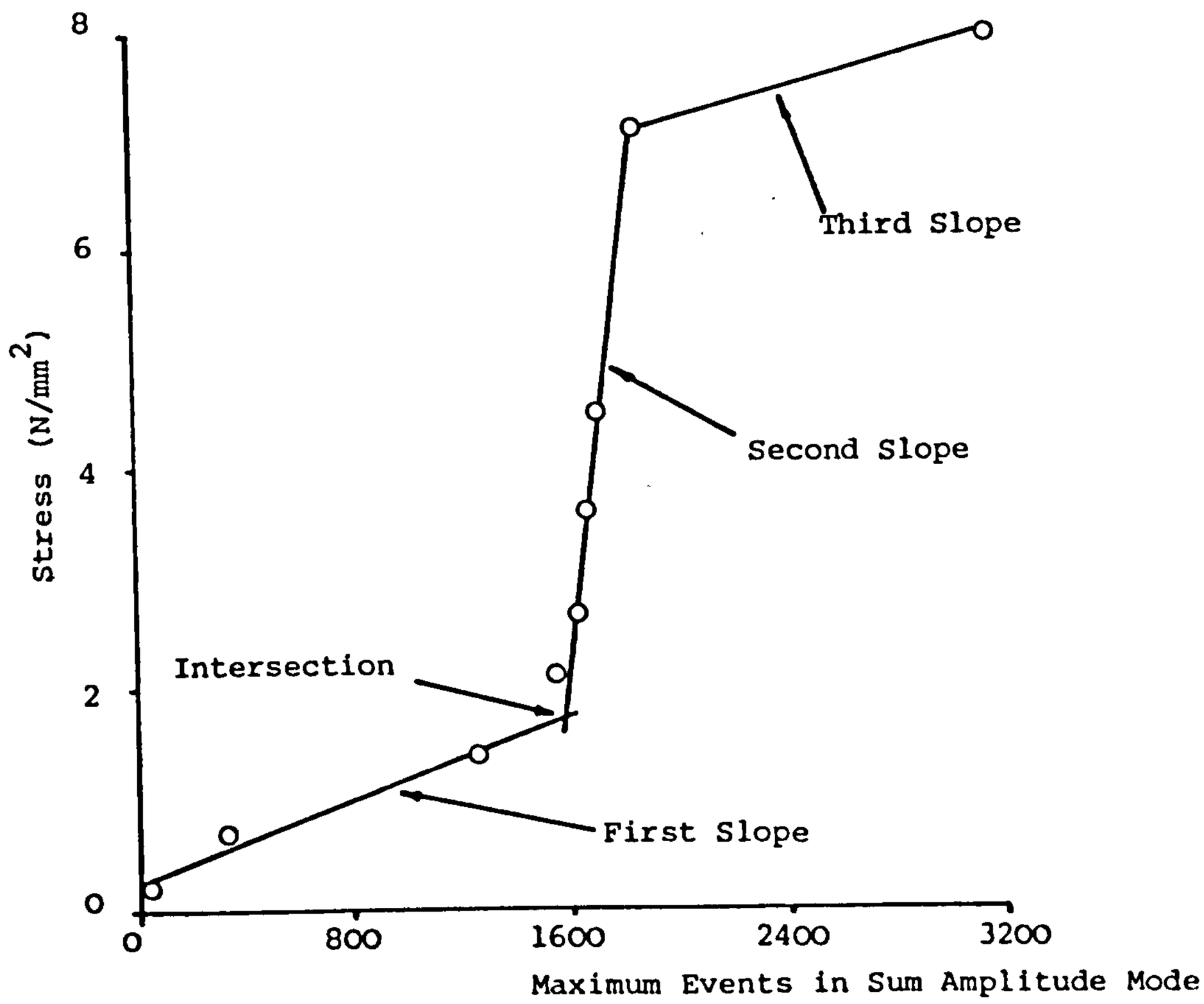

FIGURE 7.5 - TYPICAL STRESS v MAXIMUM NUMBER OF EVENTS IN SUM AMPLITUDE MODE CURVE FOR CONTINUOUS ALIGNED FIBRE SYSTEM CONTAINING 5.5% VOLUME

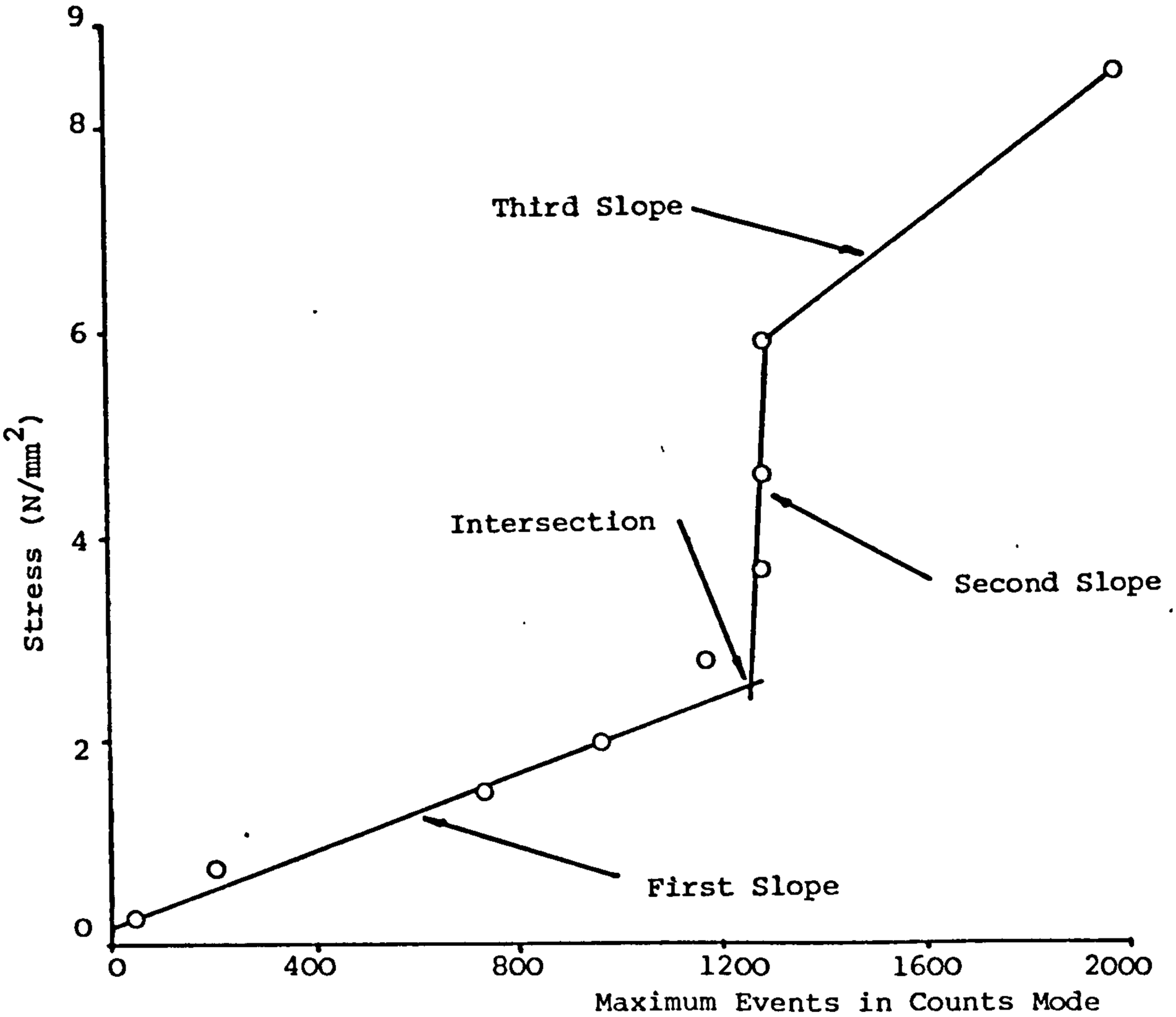

FIGURE 7.6 - TYPICAL STRESS v MAXIMUM NUMBER OF EVENTS IN COUNTS MODE CURVE FOR CONTINUOUS ALIGNED FIBRE SYSTEM CONTAINING 5.5% V_f

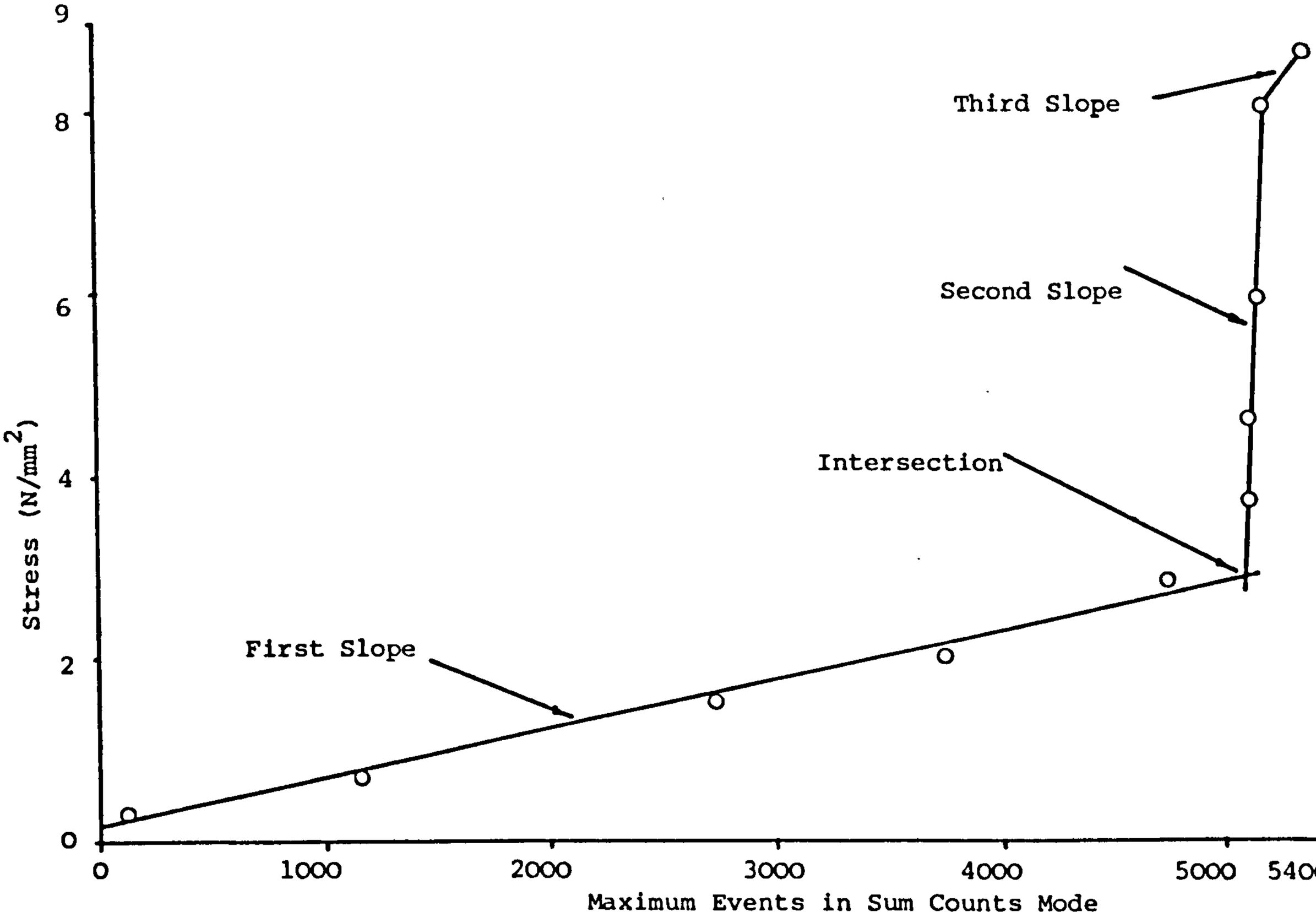

FIGURE 7.7 - TYPICAL STRESS v MAXIMUM NUMBER OF EVENTS IN SUM COUNTS MODE CURVE FOR CONTINUOUS ALIGNED FIBRE SYSTEM CONTAINING 5.5% V_f

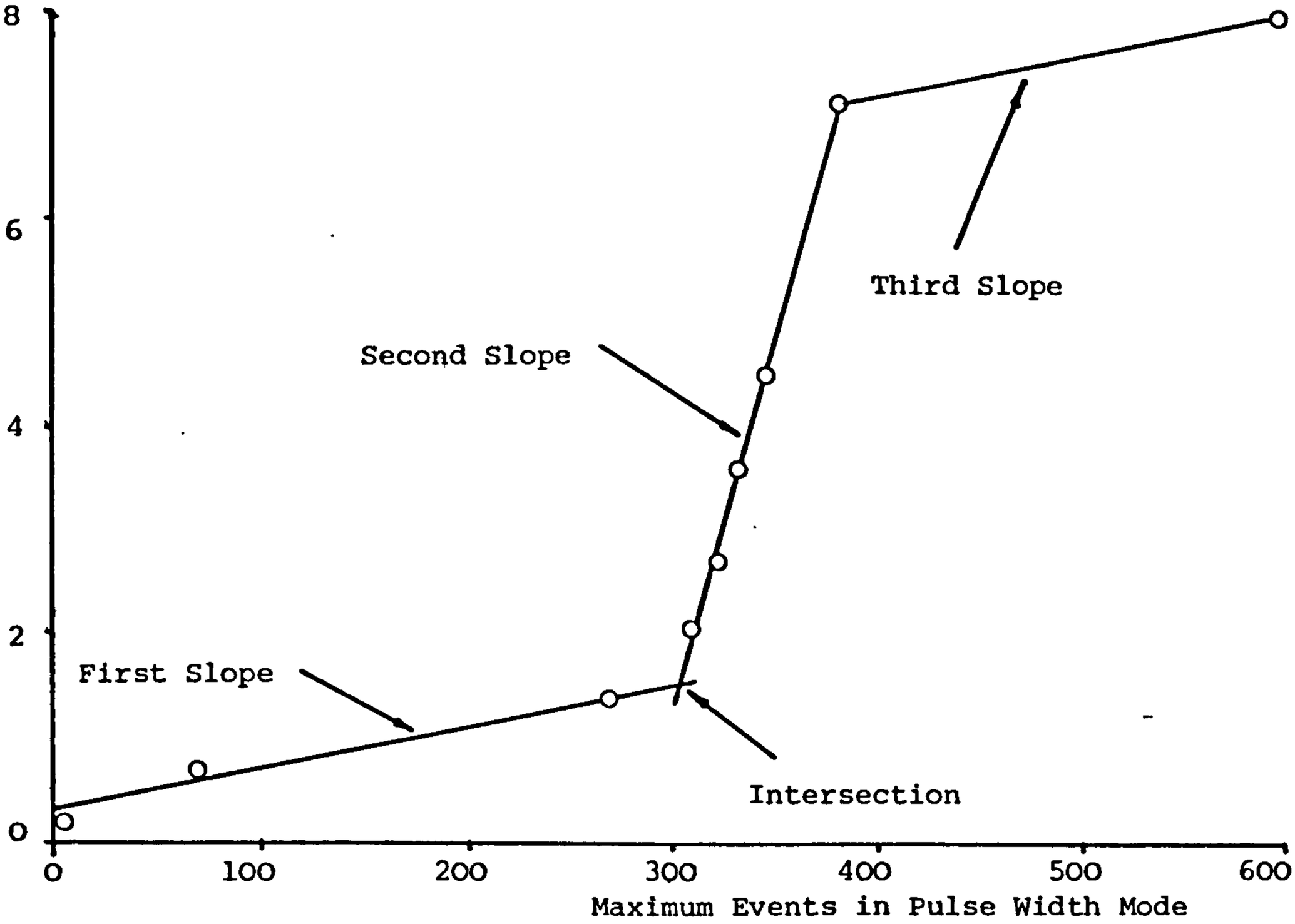

FIGURE 7.8 - TYPICAL STRESS v MAXIMUM NUMBER OF EVENTS IN PULSE WIDTH MODE CURVE FOR CONTINUOUS ALIGNED FIBRE SYSTEM CONTAINING 5.5% V_f

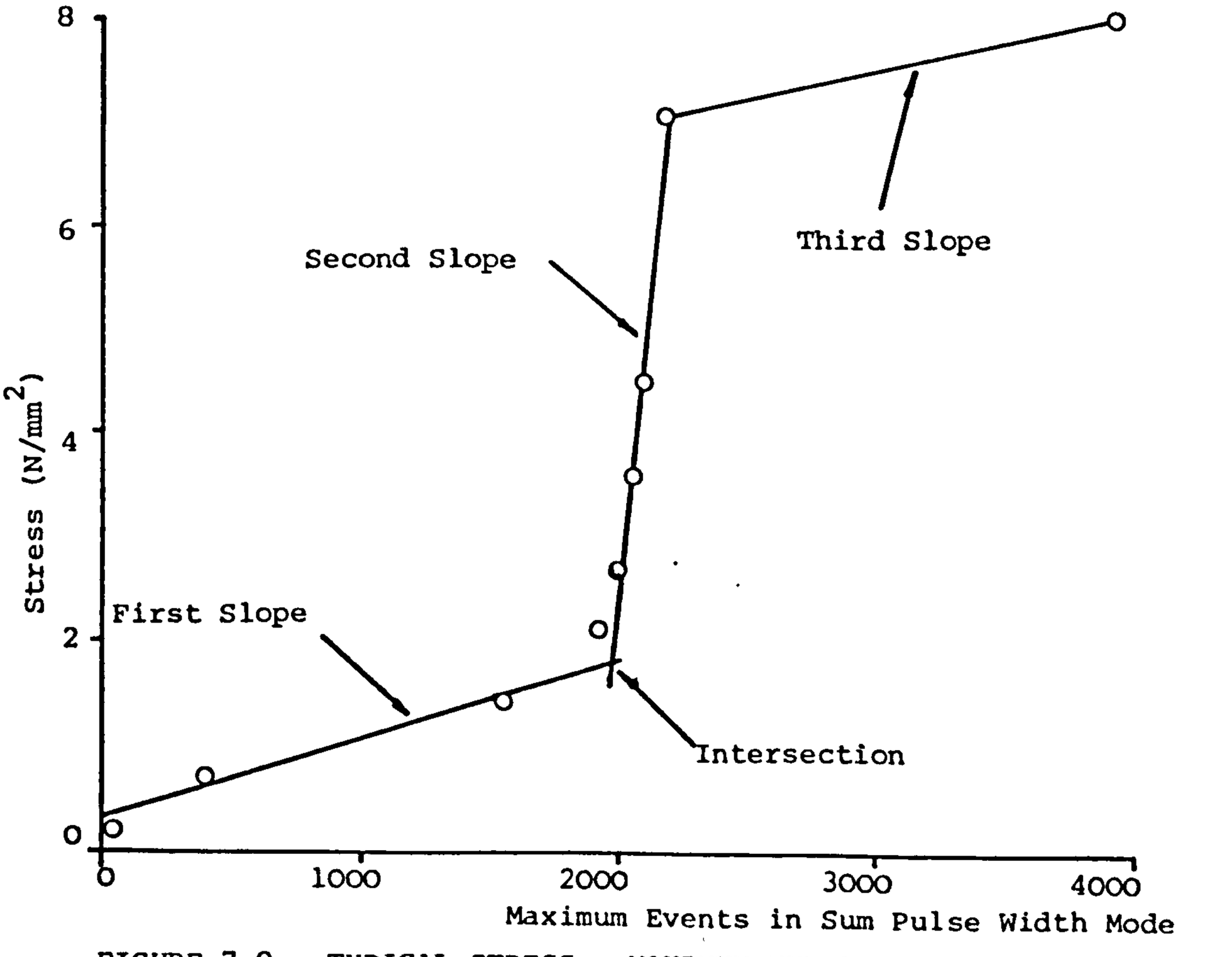

FIGURE 7.9 - TYPICAL STRESS v MAXIMUM NUMBER OF EVENTS IN SUM PULSE WIDTH MODE CURVE FOR CONTINUOUS ALIGNED FIBRE SYSTEM CONTAINING 5.5% V_f

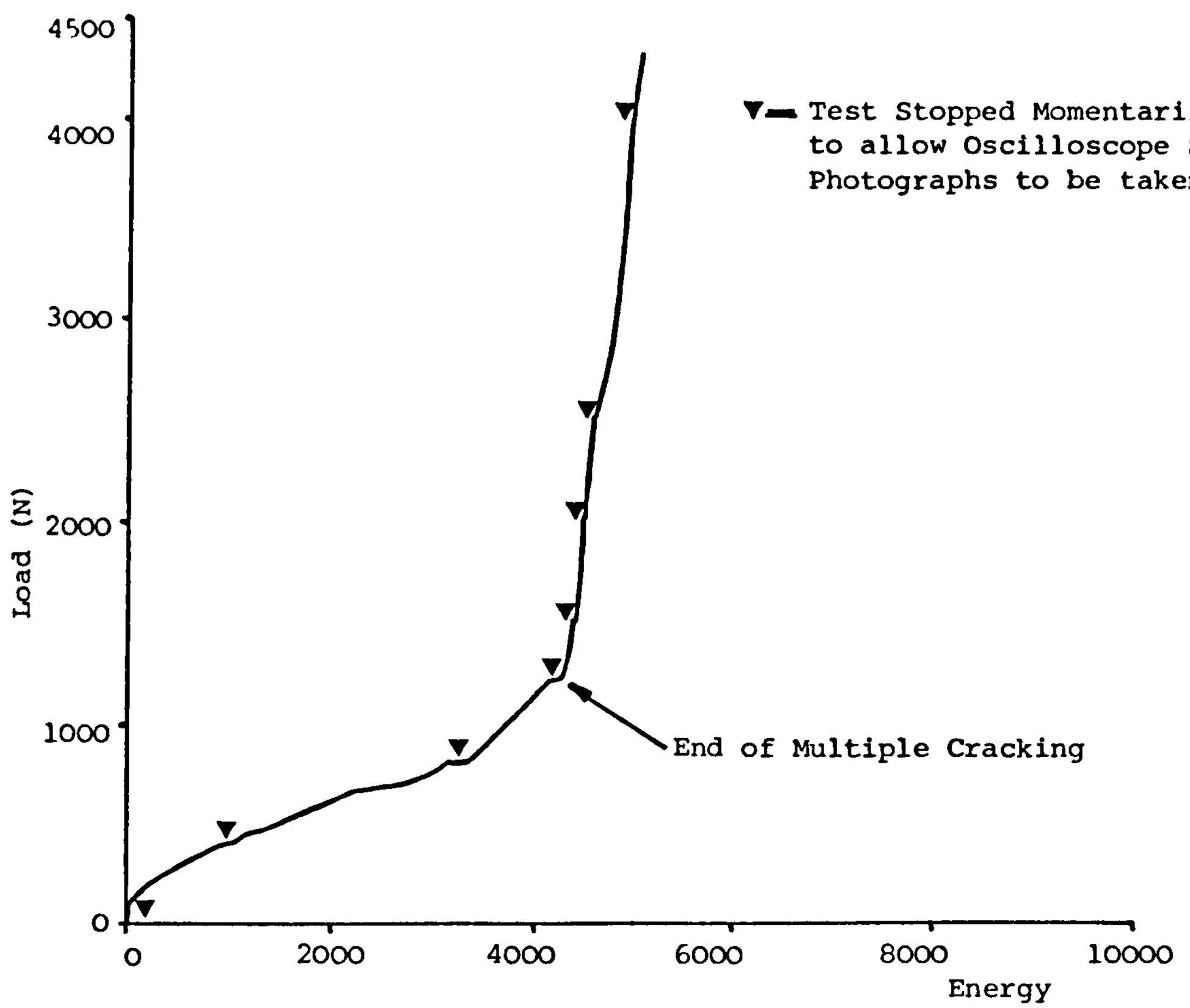

FIGURE 7.10 - TYPICAL LOAD v ENERGY CURVE FOR CONTINUOUS ALIGNED FIBRE SYSTEM CONTAINING 5.5% V_f

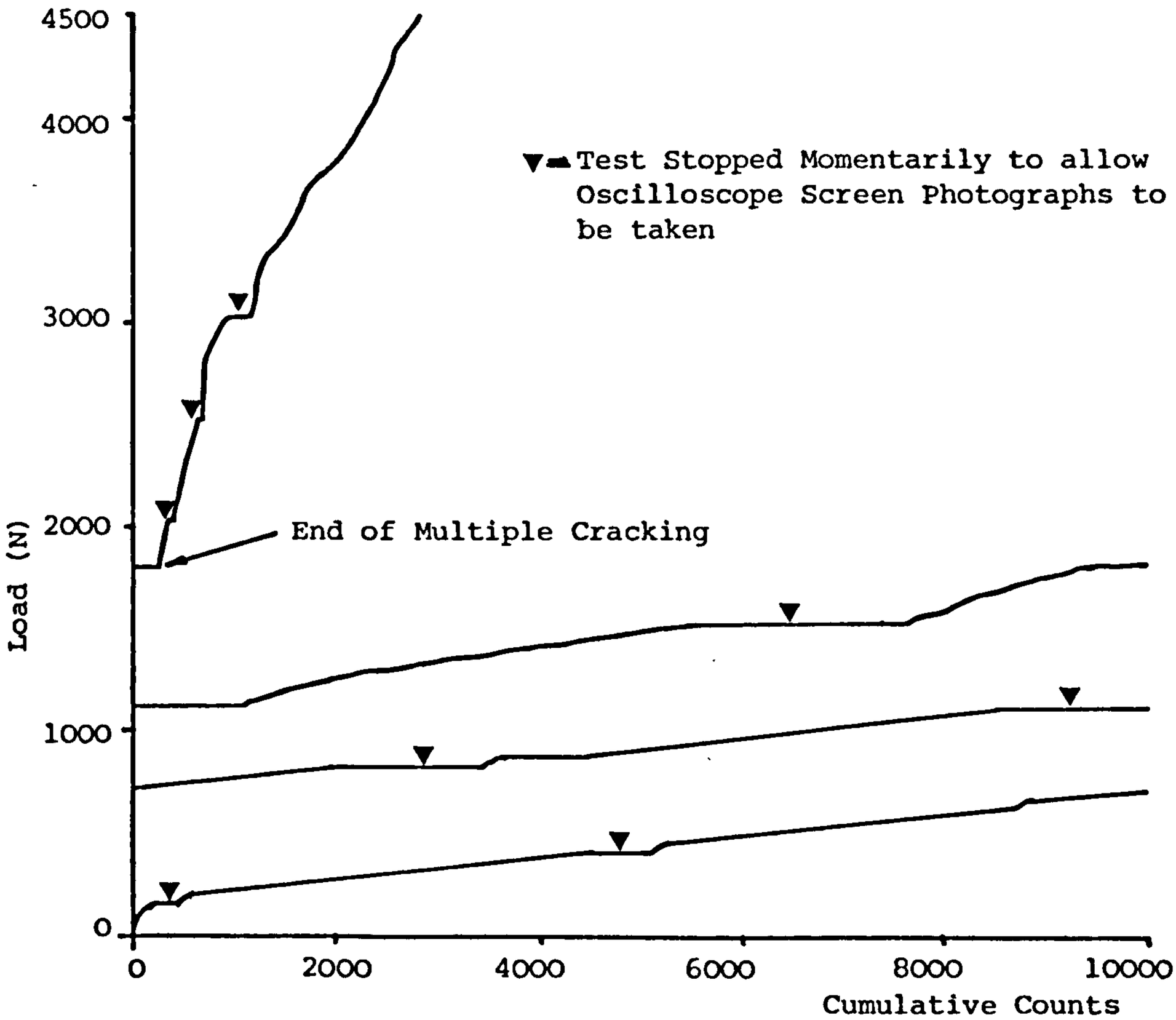

FIGURE 7.11 - TYPICAL LOAD v CUMULATIVE COUNTS CURVE FOR CONTINUOUS ALIGNED FIBRE SYSTEM CONTAINING 5.5% V_f

7.6 ANALYSIS AND DISCUSSION OF RESULTS

7.6.1 Kaiser Effect

(A) Gripping Noise

In order to establish whether any significant noise was generated by the gripping system, the Kaiser effect[77] was utilised.

A neat cement paste specimen of water/cement ratio 0.4 was loaded under constant load control from 0(N) to 202(N) and the amount of acoustic emission energy and the cumulative counts occurring were recorded against load, as shown in Figures 7.12 and 7.13 respectively. The specimen was then unloaded from 202(N) to 21(N) and again reloaded to 202(N) during which no further acoustic emissions occurred, hence indicating that the Kaiser effect[77] was obeyed and that no frictional noise was being generated from the gripping system.

The specimen was further loaded from 202(N) to 400(N) and acoustic emissions occurred. Unloading to 202(N) and reloading to 400(N) proceeded without any emissions.

The specimen load was then increased from 400(N), during which emissions again occurred and finally the specimen failed at 880(N).

This experiment clearly indicated that not only was there no frictional noise generated from the gripping system, but also that there was no noise generated due to the relative movement between the transducer and the specimen during deformation.

Since the various systems studied during the investigation were tested

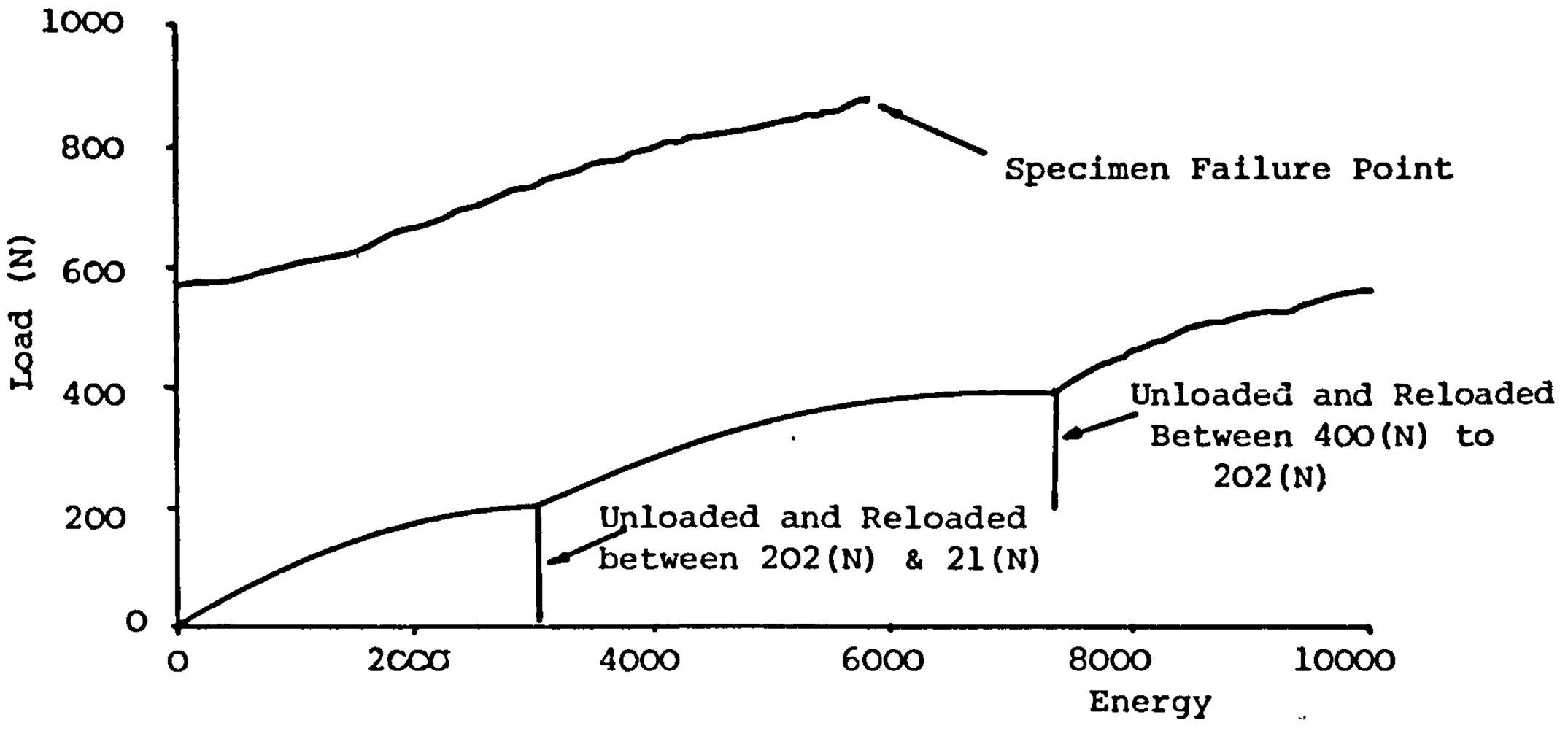

FIGURE 7.12 - NEAT CEMENT PASTE SPECIMEN LOADED, UNLOADED AND RELOADED TO ASCERTAIN GRIP NOISE. LOAD v ENERGY PLOTTED.

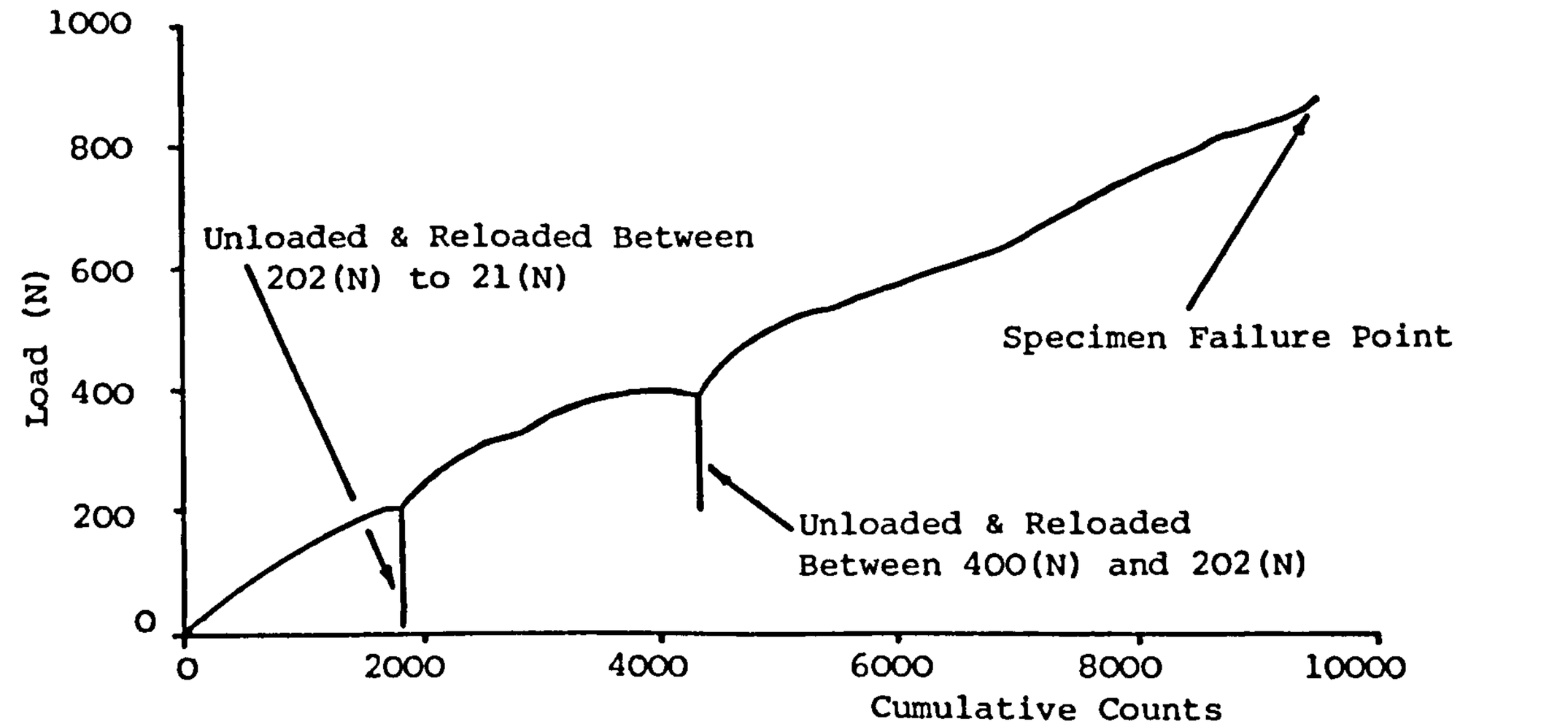

FIGURE 7.13 - NEAT CEMENT PASTE SPECIMEN LOADED, UNLOADED AND RELOADED TO ASCERTAIN GRIP NOISE. LOAD v CUMULATIVE COUNTS PLOTTED.

using the same machine, the same wedge type grips and the same type of gripping pad material attached to the specimen, it was assumed that the acoustic emissions generated during the subsequent tests were the result of deformations taking place in the specimens and not due to outside factors such as gripping noise.

(B) Fibre/Matrix Interaction

Kaiser effect[77] was also checked in the composite material. A specimen containing 1.4% by volume of fibre was loaded from 0(N) to 400(N) and Figures 7.14 and 7.15 show load versus energy and load versus cumulative counts plots respectively. Amplitude and counts events were also observed during loading.

The specimen was then unloaded from 400(N) to 50(N). During the unloading there were 15 events in the amplitude and 20 events in the counts mode observed. When the composite specimen was reloaded to 400(N), acoustic emissions were observed when the load reached 395(N), 12 events in the amplitude mode and 14 events in the counts mode. This indicates that the Kaiser effect[77] was not apparently occurring. The specimen was further loaded from 400(N) to 701(N) during which the activities continued and the specimen cracked. When the specimen was unloaded from 701(N) to 400(N), there were 3 events in the amplitude and 6 events in the counts mode. Upon reloading from 400(N) to 701(N), there were 9 and 11 events in the amplitude and counts mode respectively, occurring between 695(N) and 701(N).

Finally, the specimen was loaded from 701(N) to 1566(N), when activities were observed to occur and also the crack width was increasing. There were 27 and 33 events in the amplitude and the counts mode respectively

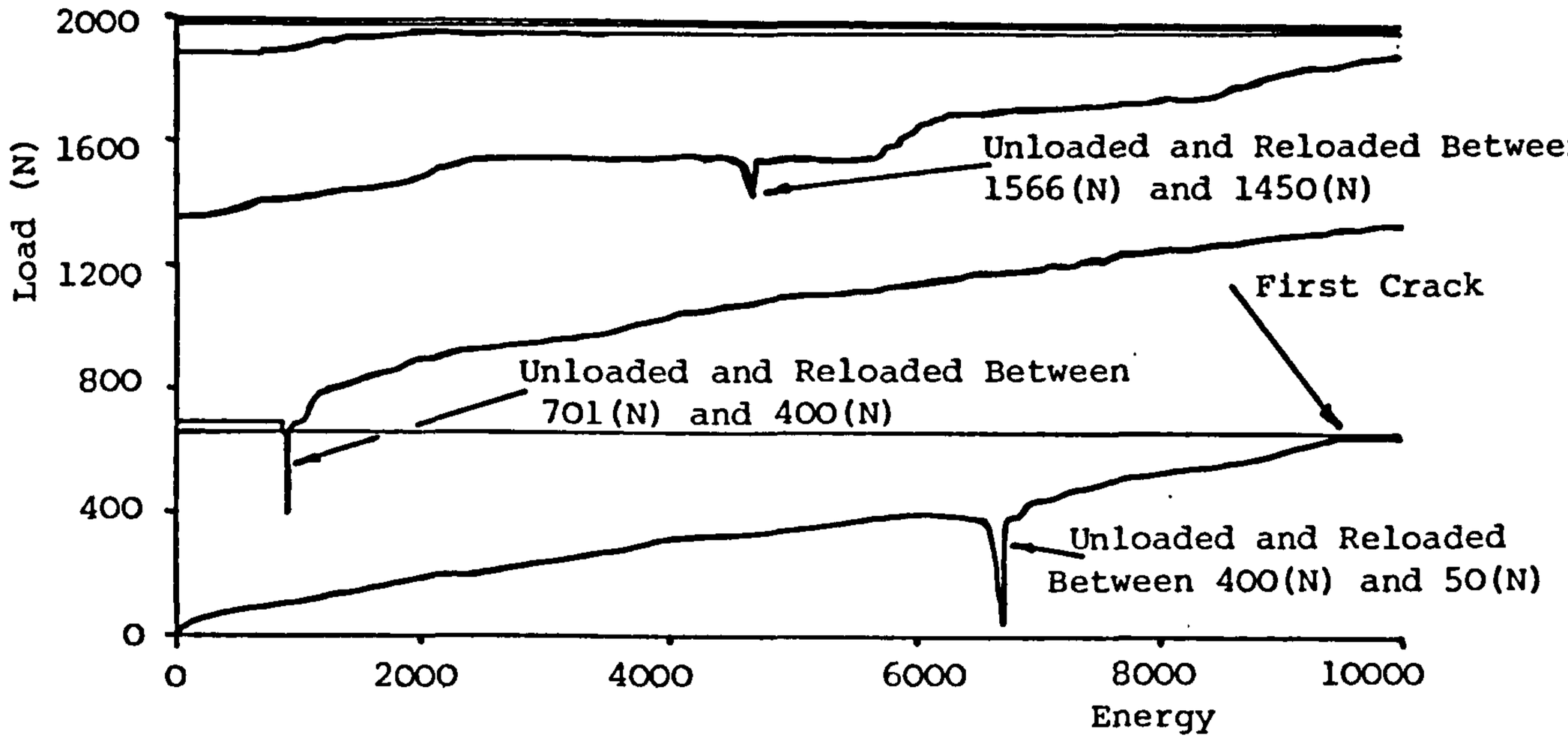

FIGURE 7.14 - CHECKING FOR KAISER EFFECT IN CONTINUOUS ALIGNED FIBRE SYSTEM CONTAINING 1.4% V_f

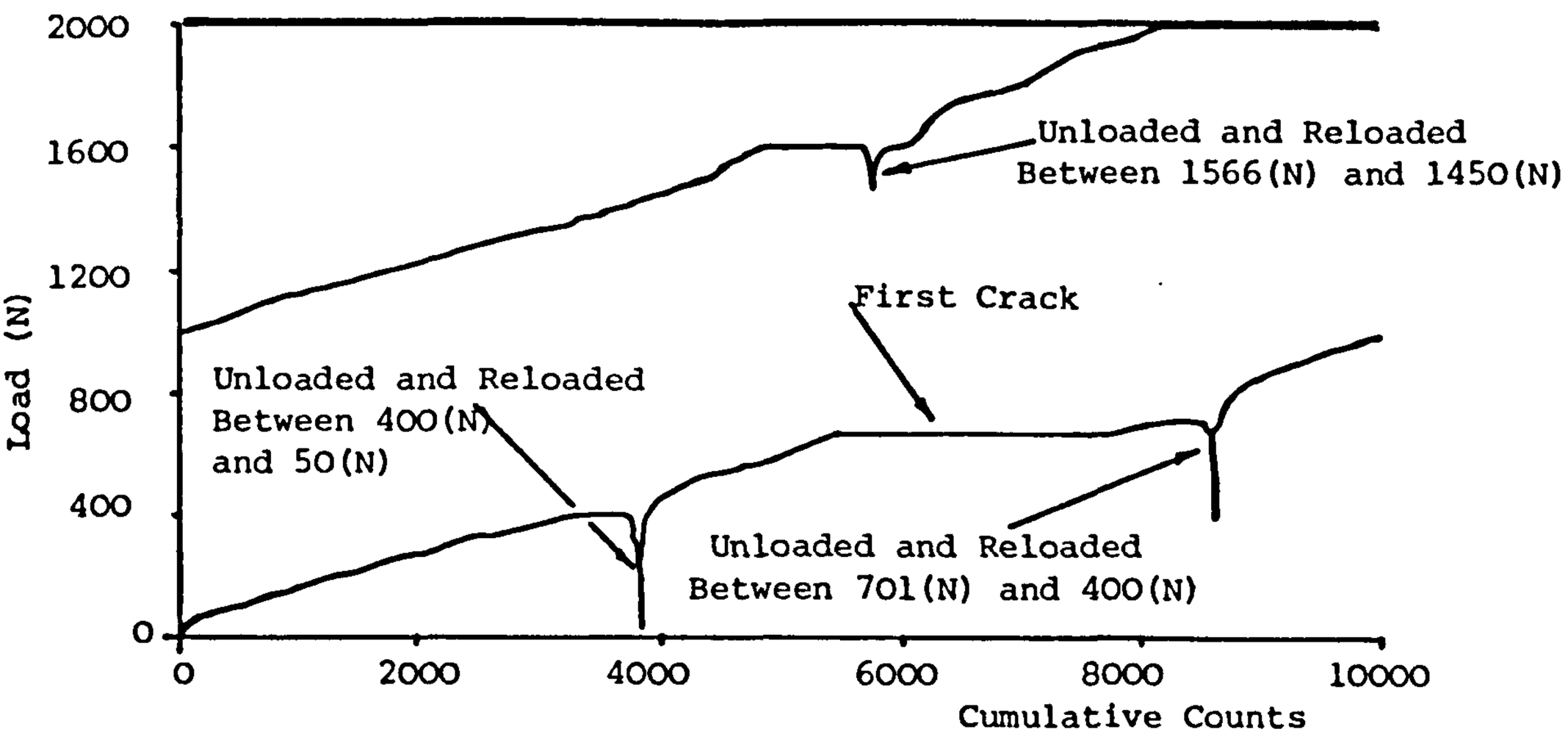

FIGURE 7.15 - CHECKING FOR KAISER EFFECT IN CONTINUOUS ALIGNED FIBRE SYSTEM CONTAINING 1.4% V_f

during unloading from 1566(N) to 1450(N). Upon reloading from 1450(N) to 1566(N) a further 26 and 28 events in the amplitude and the counts mode occurred respectively; subsequently the specimen was loaded to failure, which occurred by fibre pull-out accompanied by a large number of emissions.

The above sequence of events indicates that there are at least two sources of acoustic emission. The majority of emission is irreversible and is probably associated with the matrix deformation. The very small 'reversible' emissions, i.e. occurring during unloading and reloading must be frictional in origin and therefore produced by fibre/matrix relative movement. The observation that re-emission during loading only occurs at a load slightly below the previous maximum, indicates that the fibre is not slipping through the matrix until at least 1450(N) load; otherwise emission would have occurred throughout the loading range. It is thought that the very small relative movement during the elastic deformation arises at the fibre ends only. A further implication is that if there is a very slight relative movement of the fibre ends during loading, then it is not completely reversible, i.e. on unloading the specimen the fibre does not return to its original position, so that the subsequent reloading only causes movement as the previous maximum load is approached.

The emission associated with the final reloading sequence, which occurs throughout the load range, suggests that fibre pull-out is occurring at this stage. It appears that transition from static to dynamic friction has been detected.

7.6.2 Position Control

Neat cement paste and continuous aligned fibre reinforced cement paste containing 1.4, 2.4, 4.2, 5.5 and 8.7% by volume of fibre, all of water/cement ratio 0.4, were tested under constant position control, i.e. constant cross-head movement of 1 mm/min.

During the test, load versus energy and load versus cumulative counts were plotted and typical plots, as shown in Figures 7.16 and 7.17 respectively, were obtained for a continuous aligned fibre reinforced cement paste specimen containing 5.5% by volume of fibre. It can be seen from Figure 7.17 up to the final visible crack, there is an approximately linear relationship with the load and cumulative counts, showing momentary load drops corresponding to the occurrence of major matrix cracks.

It can be seen from Figures 7.16 and 7.17, that after the multiple cracking has finished, an increase in slope occurs, which corresponds to a lower rate of emissions.

Finally, during the last stages of the deformation when the load was decreasing, the rate of acoustic emission also decreased.

7.6.3 Continuous Aligned Fibre Reinforced Cement Paste

The acoustic emission characteristics of continuous aligned fibre composite specimens containing 1.4, 2.4, 4.2, 5.5 and 8.7% by volume of fibre, all of water/cement ratio 0.4, were tested. A typical example of continuous aligned fibre composites containing 5.5% by volume of fibre is presented in the form of load versus the following parameters, maximum number of events in the amplitude, counts and pulse

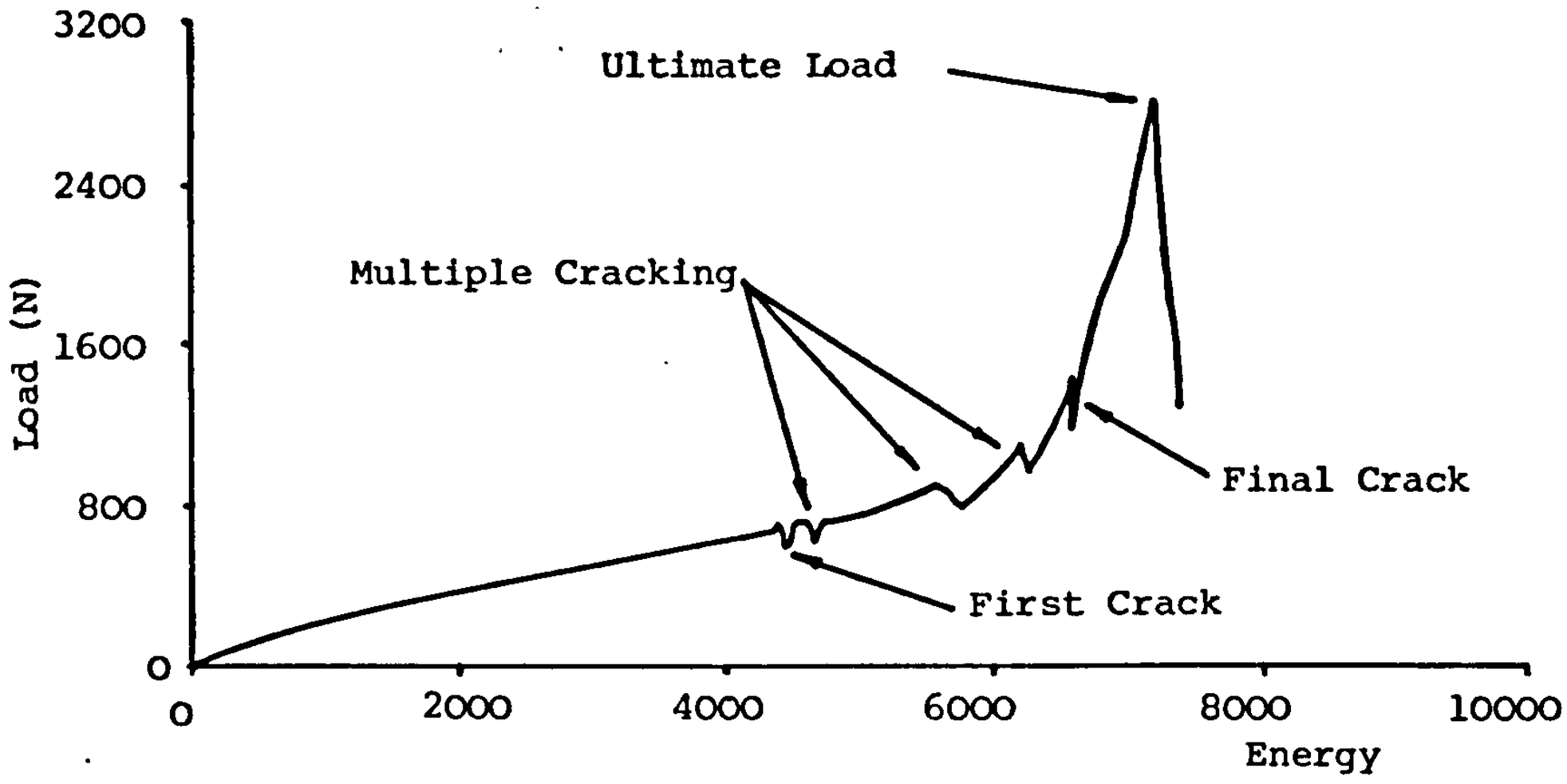

FIGURE 7.16 - TYPICAL TENSILE LOAD v ENERGY CURVE FOR CONTINUOUS ALIGNED FIBRE REINFORCED CEMENT PASTE CONTAINING 5.5% VOLUME CONCENTRATION OF FIBRE

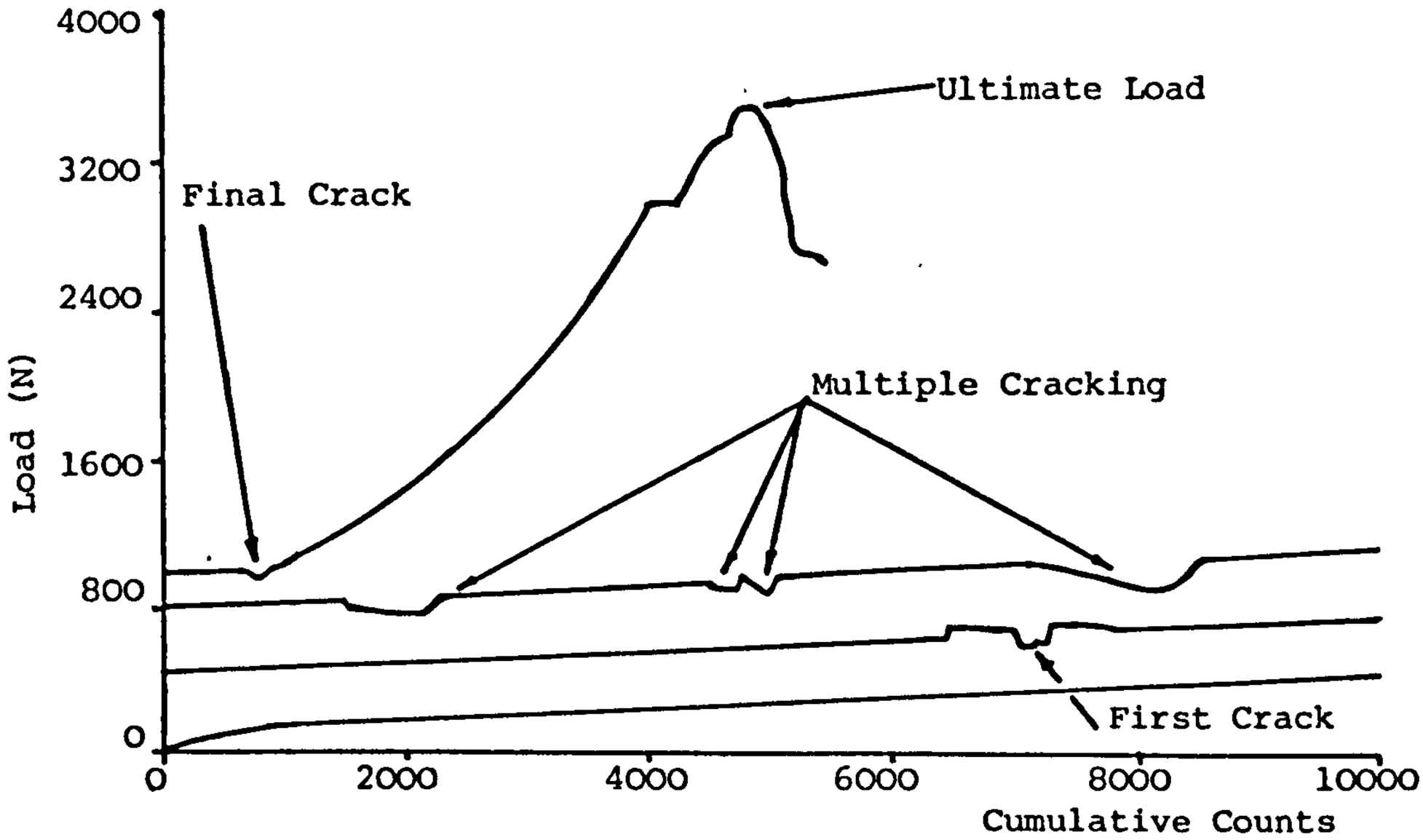

FIGURE 7.17 - TYPICAL TENSILE LOAD v CUMULATIVE CURVE FOR CONTINUOUS ALIGNED FIBRE REINFORCED CEMENT PASTE CONTAINING 5.5% VOLUME CONCENTRATION OF FIBRE

width modes and their corresponding summations, as shown in Figures 7.4 to 7.9. In addition, load versus energy and load versus cumulative counts were also plotted (see Figures 7.10 and 7.11 respectively).

It can be seen that in every case the same trend was observed, that is three different linear slopes.

The first region identifies the load/emission characteristics up to the first visible crack in the composite. The second region identifies the characteristics during the multiple cracking and is invariably of a higher slope value, indicating less acoustic emissions. The final region relates to the emissions generated during post-multiple cracking deformation and has a gradient similar to that of the first region. The change over from the first to second region can be characterised by the co-ordinates of the intersection point of the linear first and second slopes. Appendices C, D and E tabulate the first slope, second slope and intersection values respectively.

First Slope

No systematic relationship between the number of acoustic events emitted and volume fibre concentration was observed. This indicates that the major source of emission up to the first crack is from the matrix; that is, the fibres are acoustically quiet, and provides further evidence that there is no fibre/matrix relative movement in the body of the matrix. Since the latter two mechanisms would have produced a significant dependency on volume concentration of fibres in the matrix. The actual mechanisms occurring within the cement paste which give rise to acoustic emissions are thought to be a combination of microcracking and possibly particle rearrangement. It is worth noting that emission

started to occur almost as soon as the load was applied to the specimens and that the linear relationship between load and events in the various modes indicates a straight forward deformation dependent effect.

Second Slope

The most significant aspect of the increased second slope is that it indicates that crack propagation does not result in large quantities of emissions (higher slope means lower emissions). However, audible cracking noises could be heard during multiple cracking; this suggests that the acoustic energy distribution is concentrated at lower frequencies during crack propagation. In the case of the second slope, a systematic relationship was observed between the average second slope and the values of the events in the amplitude mode and the volume concentration of fibres (see Figure 7.18). This shows that the greater the fibre volume concentration the less emissions recorded. There are several possible explanations for this effect. The first point to make is that an increase in volume concentration of fibre corresponds to the increase in the number of matrix cracks. It follows that a simple explanation of the relationships could be that the discontinuities caused by the cracks could filter out part of the emission, although no direct evidence could be obtained for such an effect. An alternative explanation could be that as the number of the cracks increases, so does the amount of relaxed matrix region; hence the amount of unrelaxed matrix must correspondingly decrease and the emissions associated with the matrix deformation should also decrease. In conjunction with this effect, it is to be expected that the frictional noise should increase because of the relative movement between the fibre/matrix during relaxation. It is also possible that a small amount of fibre pull-out might be occurring, which could also contribute to the

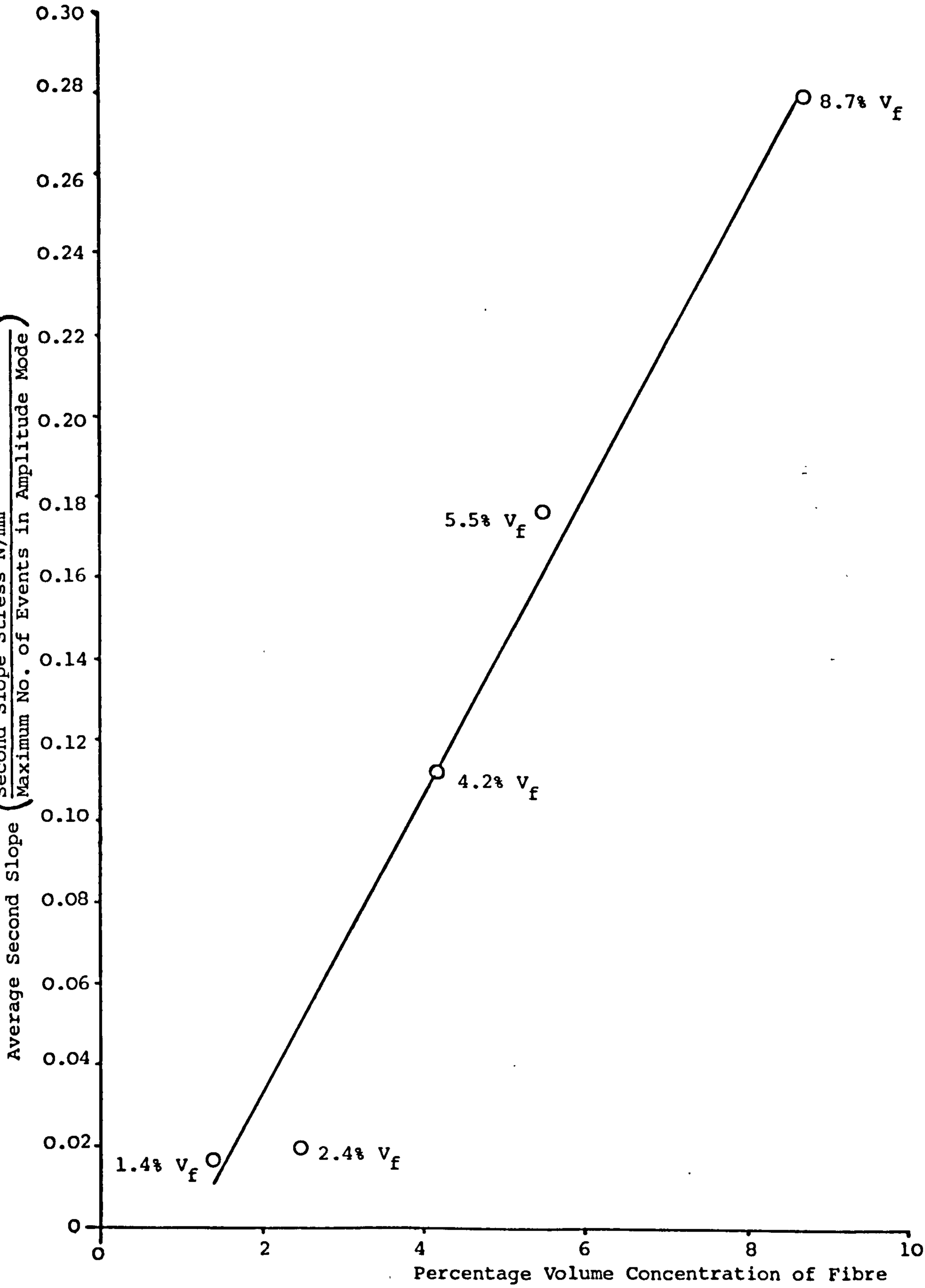

FIGURE 7.18 - RELATIONSHIP BETWEEN AVERAGE SECOND SLOPE FOR MAXIMUM NUMBER OF EVENTS IN AMPLITUDE MODE AND VOLUME CONCENTRATION OF ALIGNED FIBRES IN SPECIMENS

frictional noise. However, since the sum total of these effects is a reducing emission with increasing number of cracks, the matrix emission characteristics are still dominant in this region.

Third Slope

The third slope provides a measure of the total emissions occurring as the composite is pulled very rapidly (because of the load control method of test) to a maximum extension of approximately 50 mm.

During the third slope region, deformation is proceeding primarily by fibre pull-out through the shortest end block of matrix, although fibre stretching, chiselling and a little matrix deformation may also be occurring. The main source of acoustic emission in this region is thought to be due to fibre pull-out. Unfortunately, it was not possible to separate the effects of fibre concentration from the effects of length of the end block of matrix, from which the fibres were pulled out. However, the significantly larger number of events that occurred during the third slope deformation, as compared to the second slope region, indicates that a different major source of emission is being activated. Since neither the matrix nor fibres are being subjected to any significantly increased deformation in this latter stage, the only remaining mechanism for generating emission is at the fibre/matrix interface, i.e. relative movement.

7.6.4 Discontinuous Aligned Fibre Reinforced Cement Paste

The results of acoustic emission studies on specimens containing 1.4 and 4.2% by volume fractions of both 26 and 60 mm fibre lengths are tabulated in appendices C, D and E. Plots of load versus events in the amplitude, counts and pulse width modes identified only a single slope up to the first crack. Deformation beyond the first crack

proceeded so rapidly that only the final, i.e. the total number of events, were recorded.

No significant effect of fibre concentration or fibre length was observed, which reinforces the evidence obtained with the continuous aligned fibre composites, that the matrix deformation is the major source of emission up to the first crack. No conclusions can be drawn as to the sources of emission beyond the first crack stage.

7.6.5 Inclined and Random Fibre Reinforced Cement Paste

The results of acoustic emission studies on specimens containing 3.5 to 3.86% volume concentration of 15^{o}, 30^{o}, 45^{o}, 60^{o}, 75^{o} and 90^{o}-90^{o} inclined fibres and 4.2% V_f of lengths 26 and 60 mm, random fibre distribution, are tabulated in appendices C, D and E.

First slope values obtained from the plots of load versus number of events in the various modes, indicated that there is no effect of either fibre inclination angle or fibre length and the quantity of acoustic emission generated. Once again the evidence indicates that only the matrix is a significant contributor to acoustic events.

A second slope was in evidence for only the 15^{o} and 90^{o}-90^{o} fibre inclinations. In the case of the other angles of inclinations and the randomly distributed fibres, the same rapid deformation beyond the first crack occurred as with the discontinuous aligned fibre composite specimens.

The relationship between the first and second slope was similar to those obtained for the continuous aligned fibre composite specimens, which indicates that at 15^{o} and 90^{o}-90^{o} inclinations the reinforcement

is behaving to some degree as if it were continuously aligned.

No relationships could be identified between either the third slope region or the total number of acoustic emission events and variables of fibre inclinations and random fibre concentrations.

7.7 CONCLUSIONS

The overall conclusions that can be drawn from the brief review of acoustic emission literature show that, whilst the acoustic emission signals are believed to contain potentially useful information about the source mechanisms, to date signal processing and analysing techniques such as threshold counting and amplitude distribution, have not unambiguously extracted such information from fibre composites. The difficulties lie in the inherent complexity of the microstructural mechanical behaviour of the material, the wave propagation details and the precise physical meaning of the sensor mechanical-electrical conversion process.

Specific conclusions resulting from the investigation can be listed as follows:

(1) There was no evidence of noise being generated by the gripping system and therefore the acoustic events detected must have originated from the body of the specimen during deformation.

(2) The Kaiser effect investigation on continuous aligned fibre composites containing 1.4% V_f showed that there were at least two sources of acoustic emission. The majority of the emission was irreversible and probably associated with the matrix deformation. The very small reversible emissions were thought

to be frictional in origin and produced by fibre/matrix relative movement at the fibre ends.

(3) Three different linear slopes were obtained for the continuous aligned fibre composite system when stress versus peak number of events plotted for various acoustic emission parameters. The first slope related load/emission characteristics up to the first visible crack; the second slope identified this relation for the multiple cracking region, and the third slope was associated with post-multiple cracking deformation of the specimen.

The major source of emission up to the first crack was from within the matrix, probably due to microcracking and particle rearrangement. The sources of emission during multiple cracking were thought to be fibre/matrix relative movement, fibre pull-out and matrix deformation. With the first two mechanisms giving increasing acoustic emissions with increasing specimen deformation and the latter decreasing emissions with increasing deformation. Acoustic emissions during post-cracking deformation were attributed primarily to frictional noise developed by fibre pull-out.

(4) Discontinuous aligned, Inclined and Random fibre composite specimens all exhibited linear slope up to the first crack. No significant effect of fibre concentration, fibre length, fibre inclination angle were observed. Probably matrix deformation was the major source of emission as in the continuous aligned fibre composites.

Beyond the first crack, deformation proceeded very rapidly, except in the case of 15^{o} and 90^{o}-90^{o} fibre inclination, for which second and third slopes were obtained, which indicated that for these two

fibre inclinations the reinforcement was behaving as if it were continuously aligned.

CONCLUSIONS AND RECOMMENDATIONS FOR FURTHER INVESTIGATIONS

CHAPTER EIGHT

CONCLUSIONS AND RECOMMENDATIONS FOR FURTHER INVESTIGATIONS

8.1 CONCLUSIONS

The general conclusions deduced from the present investigation may be summarised as follows.

Fibre

(1) The evidence indicates that the modulus of polypropylene fibre can be influenced by optimising production parameters such as extrusion temperature, hot roller temperature and haul off speed ratio; the latter parameter has the greatest influence.

(2) Increasing the rate at which the fibre is tested from 10 to 500 mm/min does not significantly influence the modulus value.

Matrix

(1) A satisfactory method of gripping cement paste specimens was developed, which minimised specimen failure in the grips.

(2) The average tensile strength and elastic modulus values of the neat cement paste specimens of water/cement ratio 0.4 were found to be 1.74 N/mm^2 and 14.76 kN/mm^2 respectively.

Continuous Aligned Fibre Composite

(1) Multiple cracking occurred in uniaxially aligned polypropylene fibre reinforced cement composites, despite the unfavourable fibre modulus and Poisson's ratio. The fibre/matrix contact

necessary to induce this multiple cracking was thought to result from

(a) Matrix relaxation near the crack surfaces

(b) The presence of asperities on the fibre surface

(c) The surfaces of a matrix crack displacing laterally as well as longitudinally relative to each other and to the fibre array

(d) Slight departure from parallelism of reinforcing fibres.

(2) A simple theoretical model for the influence of Poisson's ratio on multiple cracking predicted that multiple cracking should occur in any continuously aligned fibrous composite providing that a critical specimen diameter and a critical volume fraction of fibres are exceeded.

(3) The average interfacial shear stress (τ) was found to be 0.104 N/mm^2, when determined by the crack spacing method and 0.274 N/mm^2 ($\tau_{dynamic}$) when determined by multiple fibre pull-out.

(4) Multiple cracking takes place at successively higher stress levels rather than at a constant limiting value.

(5) The number of cracks and the ultimate tensile stress increased as the fibre volume increased.

(6) Final failure of the specimens invariably occurred by fibre pull-out and not by fibre failure.

Discontinuous Aligned Fibre Composite

(1) Multiple cracking occurred in discontinuous aligned polypropylene fibre reinforced cement paste specimens.

(2) The interfacial shear stress increased with decreasing fibre length.

(3) The ultimate stress values were very much lower than those for specimens containing a similar volume fraction of fibres but continuously aligned.

Inclined and Random Fibre Composite

(1) These systems were not as effective as the continuous aligned fibre reinforcement in increasing the ultimate strength of the composite.

(2) The number of cracks induced along the length of the specimen increased with a decreasing fibre inclination angle.

(3) The presence of fibres inclined at an angle greater than 45^{o} reduces the first crack strength.

Acoustic Emission

(1) The transducer detected only those acoustic events emitted from within the body of the specimen.

(2) Three different linear slopes were obtained for the continuous aligned fibre composite system when stress versus peak number of events plotted for various acoustic emission parameters. The first slope related the load/emission characteristics up to the first visible crack; the second slope identified the multiple cracking region, and the third slope identified the post-multiple cracking region. The major source of emission in the first slope region was probably from the matrix in the form of microcracking and particle rearrangement. In the second slope region fibre/matrix relative movement, fibre pull-out and matrix deformation were all thought to contribute to the emission, whereas in the third slope region the emissions were primarily associated with fibre pull-out.

8.2 RECOMMENDATIONS FOR FURTHER INVESTIGATIONS

(1) Further work is necessary to complete the study of the basic continuous aligned polypropylene fibre composites, namely the effect of

(A) Fibre/matrix bond

(B) Fibre modulus

(C) Fibre diameter

(2) In order to carry out the fibre diameter study, a practical continuous aligned fibre fabrication technique would have to be devised.

(3) In view of the increased opportunity for fibre/matrix contact in flexural deformation as compared to tensile deformation, it is necessary to establish the relationship between the two methods of testing.

(4) Further studies of acoustic emission behaviour should concentrate on distinguishing between reversible and irreversible acoustic emissions by utilising the Kaiser effect during repeated load cycles.

(5) An assessment is required of the other relevant properties of polypropylene fibre reinforced composite material such as durability and fire resistance.

REFERENCES

REFERENCES

1. KRENCHEL, H. and HEJGAARD, O. — Can Asbestos be Completely Replaced One Day? RILEM Symposium, Fibre Reinforced Cement and Concrete, held in London, 1975, pp.335-346.

2. KLOS, H.G. — Properties and Testing of Asbestos Fibre Cement. RILEM Symposium, Fibre Reinforced Cement and Concrete, held in London, 1975, pp.259-267.

3. ELLIS, D.G. — Use of Polypropylene as a Reinforcing Medium in Various Substrates. Plastics and Rubber: Materials and Applications, August 1980, pp.133-138.

4. RAHMAN, T.A. — The Effect of Fibre Reinforcements on the Theoretical and Structural Properties of Concrete Mixes. M.Sc. Thesis, Department of Civil Engineering, University of Strathclyde, 1972.

5. BROUTMAN, L.J. and KROCK, R.H. — Modern Composite Materials. Addison-Wesley Publishing Company, 1967, p.581.

6. SWAMY, R.N. — Fibre Reinforcement of Cement and Concrete. Materials and Structures, Vol.8, No.45, 1975, pp.235-254.

7. PORTER, H.F. — The Preparation of Concrete from Selection of Materials to Final Deposition. Journal of the American Concrete Institute, Vol.6, 1910, pp.237-303.

8. BIRYUKOVICH, K.L., BIRYUKOVICH, Y.U.L. and BIRYUKOVICH, D.L. — Glass Fibre Reinforced Cement. Translation No.12, Civil Engineering Research Association, London, 1965, pp.1-40.

9. KRENCHEL, H. — Fibre Reinforcement, Akademisk Forlag, Copenhagen, 1964, p.159.

10. ROMUALDI, J.P. and BATSON, G.B. — Behaviour of Reinforced Concrete Beams with Closely Spaced Reinforcement. Journal of the American Concrete Institute, Vol.60, No.6, June 1963, pp.775-789.

11. ROMUALDI, J.P. and BATSON, G.B. — Mechanics of Crack Arrest in Concrete. Proceedings of the American Society of Civil Engineers, Journal of the Engineering Mechanics Division, Vol.89, No.EM3, June 1963, pp.147-168.

12. AVESTON, J., COOPER, G.A. and KELLY, A. — Single and Multiple Fracture. Proceedings of the Conference, The Properties of Fibre Composites, National Physical Laboratory, London, November 1971 (IPC Science and Technology Press Ltd., 1971) Paper 2, pp.15-26.

13. ROMUALDI, J.P. and MANDEL, J.A. — Tensile Strength of Concrete Affected by Uniformly Distributed and Closely Spaced Short Lengths of Wire Reinforcement. Journal of the American Concrete Institute, Vol.61, No.6, 1964, pp.657-671.

14. BROMS, B.B. and SHAH, S.P. — Discussion of Reference (6). Proceedings of the American Society of Civil Engineers, Journal of the Engineering Mechanics Division, Vol.90, 1964, pp.167-171.

15. SHAH, S.P. and RANGAN, V. — Fibre Reinforced Concrete Properties. Journal of the American Concrete Institute, Vol.68, 1971, pp.126-135.

16. HANNANT, D.J. — The Tensile Strength of Concrete: a Review Paper. The Structural Engineer, Vol.50, No.7, July 1972, pp.253-258.

17. WRIGHT, P.J.F. — The Effect of the Method of Test on the Flexural Strength of Concrete. Magazine of Concrete Research, No.11, October 1952, pp.67-76.

18. AVESTON, J. — Fibre Reinforced Materials. Proceedings of the Conference, Practical Metallic Composites, Institution of Metallurgists, March 1974, pp.B1-B10.

19. MAJUMDAR, A.J. — Properties of Fibre Cement Composites. RILEM Symposium, Fibre Reinforced Cement and Concrete, held in London, 1975, pp.279-313.

20. BRIGGS, A., BOWDEN, D.H. and KOLLEK, J. — Mechanical Properties and Durability of Carbon Fibre Reinforced Cement Composites. Proceedings of International Conference on Carbon Fibres - their Place in Modern Technology, Second International Carbon Fibre Conference, The Plastic Institute, London, February 1974, pp.114-121.

21. CONCRETE SOCIETY — Fibre Reinforced Cement Composites. Report Produced by the Materials Technology Division of the Concrete Society, Technical Report 51.067, July 1973, p.77.

22. RILEY, V.R. and REDDAWAY, J.L. — Tensile Strength and Failure Mechanics of Fibre Composites. Journal of Materials Science, 3, 1968, pp.41-46.

23. HIGGINS, D.D. and BAILEY, J.E. — Fracture Measurements on Cement Paste. Journal of Materials Science, 11, 1976, pp.1995-2003.

24. BRIGGS, A. — Review, Carbon Fibre Reinforced Cement. Journal of Materials Science, 12, 1977, pp.384-404.

25. SARKAR, S. and BAILEY, M.B. — Structural Properties of Carbon Fibre Reinforced Cement. RILEM Symposium, Fibre Reinforced Cement and Concrete, held in London, 1975, pp.361-371.

26. ALLEN, H.G. — Stiffness and Strength of Two Glass Fibre Reinforced Cement Laminates. Journal of Composite Materials, Vol.5, April 1971, pp.194-207.

27. MAJUMDAR, A.J. and RYDER, J.F. — Glass Fibre Reinforcement of Cement Products. Building Research Station, Current Paper 67/68, September 1968, pp.78-84.

28. ALI, M.A., MAJUMDAR, A.J. and SINGH, B. — Properties of Glass Fibre Cement - the Effect of Fibre Length and Content. Journal of Materials Science, 10, 1975, pp.1732-1740.

29. EDGINGTON, J., HANNANT, D.J. and WILLIAMS, R.I.T. — Steel Fibre Reinforced Concrete. Building Research Establishment, Current Paper 69/74, July 1974, p.17.

30. AVESTON, J., MERCER, R.A. and SILLWOOD, J.M. — Fibre Reinforced Cements - Scientific Foundations for Specifications. National Physical Laboratory Conference Proceedings, Composites-Standards Testing and Design, April 1974, pp.93-103.

31. HANNANT, D.J. and SPRING, N. — Steel Fibre Reinforced Mortar: a Technique for Producing Composites with Uniaxial Fibre Alignment. Magazine of Concrete Research, Vol.26, No.86, March 1974, pp.47-48.

32. ALLEN, H.G. — Tensile Properties of Seven Asbestos Cements. Composites, June 1971, pp.98-103.

33. EWINS, P.D. — Techniques for Measuring the Mechanical Properties of Composite Materials. National Physical Laboratory Conference Proceedings, Composites-Standard Testing and Design, April 1974, pp.144-153.

34. HANNANT, D.J. — The Effect of Post Cracking Ductility on the Flexural Strength of Fibre Cement and Fibre Concrete. RILEM Symposium, Fibre Reinforced Cement and Concrete, held in London, Volume 2, 1975, pp.499-508.

35. SWAMY, R.N. and MANGAT, P.S. — A Theory for the Flexural Strength of Steel Fibre Reinforced Concrete. Cement and Concrete Research, Vol.4, 1974, pp.313-325.

36. LANKARD, D.R. — Application of Wire Reinforced Concrete. Fibrous Concretes U.S.A. and U.K., Symposium held at University of Birmingham, September 1972, by the Concrete Society, p.7.

37. MARSH, H.N. and CLARKE, LL. — Glass Fibres in Concrete. An International Symposium, Fibre Reinforced Concrete, American Concrete Institute, Special Publication 44, 1974, pp.247-257.

38. ALI, M.A., MAJUMDAR, A.J. and RAYMENT, D.L. — The Strength and Durability of Carbon Fibre Reinforced Cement Composites. Proceedings of the Conference, The Properties of Fibre Composite, National Physical Laboratory, London, November 1971 (IPC Science and Technology Press Ltd., 1971) pp.27-28.

39. SWIFT, D.G. and SMITH, R.B.L. — The Flexural Strength of Cement Based Composites Using Low Modulus (Sisal) Fibres. Composites, July 1979, pp.145-148.

40. HANNANT, D.J. — Fibre Cements and Fibre Concretes. A Wiley-Interscience Publication, 1978, p.219.

41. BADER, M.G. — Charpy Impact Strength of Uniaxial Carbon Fibre Reinforced Plastic. National Physical Laboratory Conference Proceedings, Composites-Standards, Testing and Design, April 1974, pp.160-163.

42. NAK-HOSUNG, TERENCE, J.J. and SUH, N.P. — Strain Rate Sensitive Tough Fibre Reinforced Composites. Journal of Materials Science, 12, 1977, pp.239-250.

43. ALI, M.A. and SINGH, B. — The Effect of Porosity on the Properties of Glass Fibre Reinforced Gypsum Plaster. Journal of Materials Science, 10, 1975, pp.1920-1928.

44. RYDER, J.F. — Applications of Fibre Cement. RILEM Symposium, Fibre Reinforced Cement and Concrete, held in London, 1975, pp.23-35.

45. HALE, D.K. — Fibre Pull-Out in Multiply Cracked Discontinuous Fibre Composites. RILEM Symposium, Fibre Reinforced Cement and Concrete, held in London, 1975, pp.55-68.

46. DEVEKEY, R.C. and MAJUMDAR, A.J. — Determining Bond Strength in Fibre Reinforced Composites. Magazine of Concrete Research, Vol.20, No.65, December 1968, pp.229-234.

47. PINCHIN, D.J. and TABOR, D. — Mechanical Properties of the Steel/Cement Interface - Some Experimental Results. RILEM Symposium, Fibre Reinforced Cement and Concrete, held in London, Vol.2, 1975, pp.521-526.

48. NAAMAN, A.E. and SHAH, S.P. — Bond Studies on Oriented and Aligned Steel Fibres. RILEM Symposium, Fibre Reinforced Cement and Concrete, held in London, 1975, pp.171-178.

49. OPOCZKY, L. and PENTEK, L. — Investigation of the 'Corrosion' of Asbestos Fibre in Asbestos Cement Sheet Weathered for Long Times. RILEM Symposium, Fibre Reinforced Cement and Concrete, held in London, 1975, pp.269-276.

50. HANNANT, D.J., ZONSVELD, J.J. and HUGHES, D.C. — Polypropylene Film in Cement Based Materials. Composites, April 1978, pp.83-88.

51. KRENCHEL, H. — Fibre Reinforced Brittle Matrix Materials. Fibre Reinforced Concrete, American Concrete Institute Special Publication 44, 1974, pp.45-78.

52. MACKINTOSH, D.M. — Certain Aspects of Polypropylene Fibre Reinforcement of Concrete. M.Sc. Thesis, University of Strathclyde, 1970.

53. HUGHES, B.P. and FATTUHI, N.I. — Load Deflection Curves for Fibre Reinforced Concrete Beams in Flexure. Magazine of Concrete Research, Vol.29, No.101, December 1977, pp.199-206.

54. NANDA, V.K. — A Laboratory Investigation of Fibre Reinforced Concretes. M.Sc. Thesis, University of Surrey, 1968.

55. GOLDFEIN, S. — Plastic Fibrous Reinforcement for Portland Cements. United States Army Engineer Research and Development Laboratories, Fort Belvoir, Virginia, Technical Report 1757-TR, October 1963, p.13.

56. RAOUF, Z.A. AL-HASSANI, S.T.S. and SIMPSON, J.W. — Explosive Testing of Fibre Reinforced Cement Composites. Concrete, April 1976, pp.28-30.

57. FAIRWEATHER, A.D. — The Use of Polypropylene Film Fibre to Increase Impact Resistance of Concrete. Conference Proceedings of the International Building Exhibition Conference, Building Research Station, London, November 1971, pp.41-44.

58. WALTON, P.L. and MAJUMDAR, A.J. — Cement Based Composites with Mixtures of Different Types of Fibres. Composites, September 1975, pp.209-216.

59. RITCHIE, A.G.B. and MACKINTOSH, D.M. — Selection and Rheological Characteristics of Polypropylene Fibres. Concrete, August 1972, pp.36-39.

60. GRIFFITH, A.A. — The Phenomena of Rupture and Flow in Solids. Philosophical Transactions of the Royal Society of London, A221, 1920, pp.163-198.

61. KELLY, A. and ZWEBEN, C. — Poisson Contraction in Aligned Fibre Composites Showing Pull-Out. Journal of Materials Science, 11, 1976, pp.582-587.

62. PINCHIN, D.J. — Poisson Contraction Effects in Aligned Fibre Composites. Journal of Materials Science, 11, 1976, pp.1578-1581.

63. BOWDEN, P.B. — The Effect of Hydrostatic Pressure on the Fibre Matrix Bond in a Steel-Resin Model Composite. Journal of Materials Science, 5, 1970, pp.517-520.

64. LAWS, V., LAWRENCE, P. and NURSE, R.W. — Reinforcement of Brittle Matrices by Glass Fibres. Journal of Physics D: Applied Physics, Vol.6, 1973, pp.523-537.

65. PINCHIN, D.J. — A Cement-Steel Interface: Friction and Adhesion. Ph.D. Thesis, University of Cambridge, 1977.

66. AVESTON, J., MERCER, R.A. and SILLWOOD, J.M. — The Mechanism of Fibre Reinforcement of Cement and Concrete. National Physical Laboratory Report No.SI, No.90/11/98, Part 1, January 1975, p.63; Part 2, DMA228, February 1976, p.13.

67. LIPTAI, R.G.(Chairman) — Terminology. A Symposium on Acoustic Emission, American Society for Testing and Materials Special Technical Publication 505, December 1971, pp.335-336.

68. FREDERICK, J.L. — Standard Definitions of Terms Relating to Acoustic Emission. American Society for Testing and Materials Sub-Committee 07.04.01, July 1977.

69. TATRO, C.A. — Design Criteria for Acoustic Emission Experimentation. A Symposium on Acoustic Emission, American Society for Testing and Materials Special Technical Publication 505, December 1971, pp.84-99.

70. CARLYLE, J.M. — Acoustic Emission in Fibre Reinforced Composites. M.Tech. Dissertation, Brunel University, 1974.

71. SWINDLEHURST, W. — Acoustic Emission - 1. Index Publishing Company Science and Technology Press, reprinted from Non-Destructive Testing, 1975, p.11.

72. POLLOCK, A.A. — Acoustic Emission Amplitudes. Non-Destructive Testing, October 1973, pp.264-269.

73. HSU, N.N. and HARDY, S.C. — Experiments in Acoustic Emission Waveform Analysis for Characterisation of Acoustic Emission. Elastic Waves and Non-Destructive Testing of Materials - The Winter Annual Meeting of the American Society of Mechanical Engineers, California, December 1978, pp.85-106.

74. EGAN, D.M. — Acoustic Emission Analysis of Fibre Composite Failure Mechanisms. M.Sc. Thesis, Massachusetts Institute of Technology, U.S.A., 1977.

75. HSU, N.N., SIMMONS, J.A. and HARDY, S.C. — An Approach to Acoustic Emission Signal Analysis Theory and Experiment. Materials Evaluation, Vol.35, Part 11, October 1977, pp.100-106.

76. LIPTAI, R.G., HARRIS, D.O., ENGLE, R.B. and TATRO, C.A. — Acoustic Emission Techniques in Materials Research. International Journal of Non-Destructive Testing, Vol.3, No.3, December 1971, pp.215-275.

77. KAISER, J. — Erkenntnise und Folgerunger aus der Messung von Gerauschen bei zug Beanspruchung von Metallischen Werkstoffen. Archiv. Für das Elesenhüttenwesen, Vol.24, no.1/2, January/February 1953, pp.43-45.

78. SCHOFIELD, B.H. — Acoustic Emission Under Applied Stress. Final Report, Contract AF33(616)-5640, Project 7021, Task 70663, Aeronautical Research Laboratory, Wright-Patterson Air Force Base, Ohio, 1964, p.36.

79. DUNEGAN, H.L., TATRO, C.A. and HARRIS, D.O. — Acoustic Emission Research. Report UCID-4868, Revision 1, Lawrence Radiation Laboratory, Livermore, California, 1964, p.27.

80. POLLOCK, A.A. — Quantitative Evaluation of Acoustic Emission from Plastic Zone Growth. Technical Report DE76-8, Dunegan/Endevco, California, 1976, p.17.

81. HILL, R. and EL-DARDIARY, S.M.A. — The Effect of Geometry on Acoustic Emission. Proceedings of the Institute of Acoustics, Conference held at Chelsea College, London, December 1976, p.12.

82. FUWA, M., BUNSELL, A.R. and HARRIS, B. — An Evaluation of Acoustic Emission Techniques Applied to Carbon Fibre Composites. Journal of Physics D: Applied Physics, Vol.9, 1976, pp.353-364.

83. ROTEM, A. and ALTUS, E. Fracture Modes and Acoustic Emission of Composite Materials. Journal of Testing and Evaluation, Vol.7, No.1, January 1979, pp.33-40.

84. LLOYD, D.J. and TANGRI, K. Acoustic Emission from Al_2O_3-Mo Fibre Composites. Journal of Materials Science, 9, 1974, pp.482-486.

85. ROTEM, A. and BARUCH, J. Determining the Load Time History of Fibre Composite Materials by Acoustic Emission. Journal of Materials Science, 9, 1974, pp.1789-1798.

86. ROTEM, A. The Discrimination of Micro-Fracture Mode of Fibrous Composite Materials by Acoustic Emission Technique. Fibre Science and Technology, Vol.10, 1977, pp.101-121.

87. BUNSELL, A.R. Acoustic Emission for Proof Testing of Carbon Fibre Reinforced Plastics, Non-Destructive Testing International, February 1977, pp.21-25.

APPENDICES

APPENDIX A - STANDARD DEFINITIONS OF TERMS RELATING TO ACOUSTIC EMISSION, AFTER REFERENCE (68)

Acoustic Emission: The class of phenomena whereby transient elastic waves are generated by the rapid release of energy from a localised source or sources within a material, or the transient elastic wave(s) so generated.

Acoustic Emission Count: The number of times the acoustic emission signal amplitude exceeds a preset threshold during any selected portion of a test.

Acoustic Emission Count Rate: The rate at which emission counts occur.

Acoustic Emission Energy: The total elastic energy released as acoustic emission.

Acoustic Emission Event: A local material change giving rise to acoustic emission.

Acoustic Emission Signal: A signal obtained by detection of one or more acoustic emission events.

Acoustic Emission Signature: A set of identifiable characteristics of acoustic emission signals associated with a specific test article as observed with a particular instrumentation system under specified test conditions.

Burst Emission: A qualitative description of the discrete signal(s) related to individual emission event(s) occurring within the material. Use of the term 'burst emission' is recommended only for describing the qualitative appearance of emission signals.

Continuous Emission: A qualitative description of the sustained signal level produced by rapidly occurring acoustic emission events. Use of the term 'continuous emission' is recommended only for describing the qualitative appearance of emission signals.

Kaiser Effect: The absence of detectable acoustic emission until previously applied stress levels are exceeded.

APPENDIX B - BIBLIOGRAPHY

During the preparation of this thesis, the following references were also consulted but not directly referred to.

ARRINGTON, M. and EVANS, B.M. — Acoustic Emission Testing of High Alumina Cement Concrete. Non-Destructive Testing International, April 1977, pp.81-87.

ARRINGTON, M. — Some Industrial Applications of Acoustic Emission Monitoring. Non-Destructive Testing International, June 1978, pp.117-120.

BARTLE, P.M. — Stress Wave Emission: An Introduction. The Welding Institute Research Bulletin, Vol.13, July 1972, pp.203-208.

BEATTIE, A.G. and JARAMILLO, R.A. — The Measurement of Energy in Acoustic Emission. Review of Scientific Instruments, Vol.45, No.3, March 1974, pp.352-357.

BECHT, J., SCHWALBE, H.J. and EISENBLAETTER, J. — Acoustic Emission as an Aid for Investigating the Deformation and Fracture of Composite Materials. Composites, October 1976, pp.245-248.

BIANCHETTI, R., HAMPSTAD, M.A. and MUKHERJEE, A.K. — Origin of Burst Type Acoustic Emission in Unflawed 7075-T6 Aluminium. Journal of Testing and Evaluation, Vol.4, No.5, September 1976, pp.313-318.

BROWN, A.E. and LIPTAI, R.G. — Round Robin Testing of Acoustic Emission Source. American Society for Testing and Materials, Special Technical Publication 505, December 1971, pp.318-331.

BUNSELL, A.R. and HARRIS, B. — Hybrid Carbon and Glass Fibre Composites. Composites, July 1974, pp.157-164.

CURTIS, G.J. — Acoustic Emission in Stressed Epoxy Bonded Structures. Materials Physics Division, Atomic Energy Research Establishment, Harwell, Oxfordshire, Final Report, March 1974, p.27.

DEAN, D.S. and KERRIDGE, L.A. — An Immersion Technique for the Detection of Acoustic Emission in Carbon Fibre Reinforced Plastics Pressure Vessels. Non-Destructive Testing International, October 1976, pp.233-238.

DUNEGAN, H.L., HARRIS, D.O. and TATRO, C.A. — Fracture Analysis by Use of Acoustic Emission. Engineering Fracture Mechanics, Vol.1, 1968, pp.105-122.

DUNEGAN, H.L. and HARRIS, D. — Acoustic Emission a New Non-Destructive Testing Tool. Ultrasonics, July 1969, pp.160-166.

DUNEGAN, H.L. and TETELMAN, A.S. — Acoustic Emission. Research/Development, May, 1971, pp.20-24.

DUNEGAN, H.L. and GREEN, A.T. — Factors Affecting Acoustic Emission Response From Materials. American Society for Testing and Materials, Special Technical Publication 505, 1971, pp.100-113.

EGAN, D.M. and WILLIAMS, J.H. — Acoustic Emission Spectral Analysis of Fibre Composite Failure Mechanisms. National Aeronautics and Space Administration Contractor Report 2938, 1978, p.33.

FITZ-RANDOLPH, J., PHILIPS, D.C., BEAUMONT, P.W.R. and TETELMAN, A.S. — Acoustic Emission Studies of a Boron Epoxy Composite. Journal of Composite Materials, Vol.5, October 1971, pp.542-548.

FITZ-RANDOLPH, J., PHILIPS, D.C., BEAUMONT, P.W.R. and TETELMAN, A.S. — The Fracture Energy and Acoustic Emission of Boron Epoxy Composite. Journal of Materials Science, 7, 1972, pp.289-294.

FOWLER, K.A. — Acoustic Emission Simulation Test Set. Materials Research and Standards American Society for Testing and Materials, Vol.11, No.3, 1971, pp.35-36.

FOWLER, T.J. — Acoustic Emission Testing of Fibre Reinforced Plastics. American Society of Civil Engineers, Annual National Convention and Exhibit, October 1977, p.16.

FUWA, M., BUNSELL, A.R. and HARRIS, B. — Tensile Failure Mechanism in Carbon Fibre Reinforced Plastics. Journal of Materials Science, 10, 1975, pp.2062-2070.

FUWA, M., HARRIS, B. and BUNSELL, A.R. — Acoustic Emission Cyclic Loading of Carbon Fibre Reinforced Plastics. Journal Physics D: Applied Physics, Vol.8, 1975, pp.1460-1471.

GERBERICH, W.W. and HARTBOWER, C.E. — Some Observations on Stress Wave Emission as a Measure of Crack Growth. International Journal of Fracture, Vol.3, 1967, pp.185-191.

GILLIS, P.P. — Dislocation Mechanisms as Possible Sources of Acoustic Emission. Materials Research and Standards, American Society for Testing and Materials, Vol.11, No.3, 1971, pp.11-13.

GLOVER, A.G., HOLT, J. and WILLIAMS, J.A. — The Examination of a Mild Steel Pressure Vessel Under Creep Loading Using Acoustic Emission. Proceedings of the German Metallurgical Society - Acoustic Emission, Munich, April 1974, pp.118-132.

GRABEC, I. — Relation Between Development of Defects in Materials and Acoustic Emission. Utrasonics, January 1980, pp.9-12.

GREEN, G. and CLARK,G. — An Investigation of the Reproducibility of Acoustic Emission Measurements. British Journal of Non-Destructive Testing, Vol.22, Part 2,March 1980, pp.62-68.

GUILD, F.J., WALTON, D., ADAMS, R.D. and SHORT, D. — The Application of Acoustic Emission to Fibre Reinforced Composites Materials. Composites, July 1976, pp.173-179.

HAGEMAIER, D.J., McFAUL, H.J. and MOON, D. — Non-Destructive Testing of Graphite Fibre Composite Structures. Materials Evaluation, June 1971, pp.133-140.

HAMEL, F., BAILON, J.P. and BASSIM, M.N. — Constructive and Destructive Interference in Acoustic Emission During Fatigue Crack Propagation. Ultrasonics, May 1979, pp.125-127.

HAMPSTAD, M.A. and CHIAO, T.T. — Acoustic Emission During Burst Tests of Filament Wound Bottles. Journal of Composite Materials, Vol.7, July 1973, pp.320-332.

HAMPSTAD, M.A. and MUKHERJEE, A.K. — The Dependence of Acoustic Emission on Strain Rate in 7075-T6 Aluminium. Experimental Mechanics, January 1974, pp.33-41.

HARRIS, B., ANKARA, A.O., CAWTHORNE, D. and BYE, S.M.T. — Cyclic Loading and the Strength of Dough Moulding Compounds. Composites, July 1977, pp.185-189.

HARRIS, D.O., TETELMAN, A.S. and DARWISH, F.A. — Detection of Fibre Cracking by Acoustic Emission. American Society for Testing and Materials Special Technical Publication 505, October 1971, pp.238-249.

HENNEKE, E.G. II, HERAKOVICH, C.T., JONES, G.L. and RENIERI, M.P. — Acoustic Emission From Composite Reinforced Metals. Experimental Mechanics, January 1975, pp.10-16.

HILL, R. and STEPHENS, R.W.B. — Simple Theory of Acoustic Emission - A Consideration of Measurement Parameters. Acustica, Vol.31, 1974, pp.224-230.

HUTTON, P.H. and PARRY, D.L. — Assessment of Structural Integrity by Acoustic Emission. Materials Research and Standards, American Society for Testing and Materials, Vol.11, No.3, 1971, pp.25-32.

ISHIKAWA, K. and KIM, H.C. — Stress Wave Emission and Plastic Work of Notched Specimens. Journal of Materials Science, 9, 1974, pp.737-741.

JONES, M.H. and BROWN, W.F. Jr. — Acoustic Detection of Crack Initiation in Sharply Notched Specimens. Materials Research and Standards, March 1964, pp.120-129.

KIM, H.C., RIPPER-NETO, A.P. and STEPHENS, R.W.B. — Some Observations on Acoustic Emission During Continuous Tensile Cycling of a Carbon Fibre Epoxy Composite. Nature Physical Science, Vol.237, May 1972, pp.78-80.

LIPTAI, R.G. — Acoustic Emission From Composite Materials. Composite Materials: Testing and Design, American Society for Testing and Materials Special Technical Publication 497, April 1971, pp.285-298.

LIPTAI, R.G., HARRIS, D.O. and TATRO, C.A. — An Introduction to Acoustic Emission. American Society for Testing and Materials Special Technical Publication 505, December 1971, pp.3-10.

LIPTAI, R.G. and HARRIS, D.O. — Acoustic Emission - An Introductory Review. Materials Research and Standards, American Society for Testing and Materials, Vol.11, No.3, 1971, pp.8-10.

MEHAN, R.L. and MULLIN, J.V. — Analysis of Composite Failure Mechanisms Using Acoustic Emission. Journal of Composite Materials, Vol.5, April 1971, pp.266-269.

MULLIN, J.V. and MEHAN, R.L. — Evaluation of Composite Failures Through Fracture Signal Analysis. Journal of Testing and Evaluation, Vol.1, No.3, 1973, pp.215-219.

NICHOLS, R.W. — Acoustic Emission. Applied Science Publishers Limited, 1976, p.117.

ONO, K. and UCISIK, J. — Acoustic Emission Behaviour of Aluminium Alloys. Materials Evaluation, Vol.34, Part 2,February 1976, pp.32-44.

PALMER, I.G. and HEALD, P.T. — The Application of Acoustic Emission Measurements to Fracture Mechanics. Materials Science and Engineering, 11, 1973, pp.181-184.

PAO, Y.H. — Theory of Acoustic Emission. Elastic Waves and Non-Destructive Testing of Materials - The Winter Annual Meeting of the American Society of Mechanical Engineers, California, December 1978, pp.107-128.

POLLOCK, A.A. — Acoustic Emission From Materials. Non-Destructive Testing, Views, Reviews, Previews; United Kingdom Atomic Energy Authority Research Group, 1969, pp.63-70.

PRAKASH, R. — Non-Destructive Testing of Composites. Composites, October 1980, pp.217-224.

RADON, J.C. and POLLOCK, A.A. — Acoustic Emission and Energy Transfer During Crack Propagation. Report FRR-31, Mechanical Engineering Department, Imperial College, London, July 1970, p.25.

ROTEM, A. and HASHIN, Z. — Failure Modes of Angle Ply Laminates. Journal of Composite Materials, Vol.9, April 1975, pp.191-206.

ROTEM, A. — Effect of Strain on Acoustic Emission from Fibre Composites. Composites, January 1978, pp.33-36.

ROTHWELL, R. and ARRINGTON, M. — Acoustic Emission Micromechanical Debond Testing. Nature Physical Science, Vol.233, October 1971, pp.163-164.

SCHWALBE, H.J. — Acoustic Emission as an Aid for Inspecting Glass Fibre Reinforced Plastic Pressure Tubes. Proceedings of the 2nd International Conference on Composite Materials, Toronto, 1978, pp.1093-1104.

STONE, D.E.W. and DINGWALL, P.F. — The Kaiser Effect in Stress Wave Emission Testing of Carbon Fibre Composites. Nature Physical Science, Vol.241, January 1973, pp.68-70.

STONE, D.E.W. and DINGWALL, P.F. — Acoustic Emission Parameters and Their Interpretation. Non-Destructive Testing International, April 1977, pp.51-62.

SWINDLEHURST, W.E. and WILSHAW, T.R. — Acoustic Emission in Brittle Solids. Journal of Materials Science, 11, 1976, pp.1653-1660.

SWINDLEHURST, W.E. and ENGEL, C. — A Model for Acoustic Emission Generation in Composite Materials. Fibre Science and Technology, Vol.11, Part 6, November 1978, pp.463-479.

TATRO, C.A. — Experimental Considerations for Acoustic Emission Testing. Materials Research and Standards, American Society for Testing and Materials, Vol.11, No.3, 1971, pp.17-20.

TATRO, C.A. — Design Criterion for Acoustic Emission Experimentation. American Society for Testing and Materials, Special Technical Publication 505, December 1971, pp.84-99.

TETELMAN, A.S. — Acoustic Emission Testing and Microfracture Processes. Materials Research and Standards American Society for Testing and Materials, Vol.11, No.3, 1971, pp.13-16.

WHITE, R.G. and TRETOUT, H. — Acoustic Emission Detection Using a Piezoelectric Strain Gauge for Failure Mechanism Identification in Carbon Fibre Reinforced Plastics, Composites, April 1979, pp.101-109.

WILLIAMS, J.H. Jr. and LEE, S.S. — Acoustic Emission Monitoring of Fibre Composite Materials and Structures. Journal of Composite Materials, Vol.12, October 1978, pp.348-371.

WILLIAMS, R.S. and REIFSNIDER, K.L. — Investigation of Acoustic Emission During Fatigue Loading of Composite Specimens. Journal of Composite Materials, Vol.8, October 1974, pp.340-355.

APPENDIX C - AVERAGE FIRST SLOPE VALUES FOR DIFFERENT MODES OF ACOUSTIC EMISSION TESTS CARRIED OUT UNDER CONSTANT LOAD CONTROL

Test Code	Vol.% Fibre	Fibre Systems	A*	SA*	C*	SC*	PW*	SPW*
BZ, CA, CB, CC	Cement Paste	-	0.0092	0.00134	0.0028	0.00093	0.0049	0.000955
CK, CL, CM	1.4	CA*	0.0084	0.00607	0.0031	0.000978	0.0052	0.000605
CN, CO, CP, CQ	2.4	CA	0.0072	0.00117	0.0036	0.000973	0.0055	0.00079
CR, CS, CT, CU	4.2	CA	0.0033	0.00062	0.0023	0.00063	0.0043	0.00181
CV, CW, CX, CY	5.5	CA	0.0049	0.000757	0.0073	0.000583	0.0029	0.000625
CZ, DA, DB, DC	8.7	CA	0.028	0.00358	0.0078	0.00269	0.0097	0.00173
FL, FM, FN, FO	1.4	DA*/26 mm	0.00463	0.000645	0.00170	0.000727	0.006	0.00125
ET, EU, EV	1.4	DA/60 mm	0.0147	0.00247	0.00964	0.00316	0.0155	0.00297
FS, FT, FU, FV	4.2	DA/26 mm	0.0094	0.00147	0.00275	0.00769	0.011	0.00217
FD, FE, FF, FG	4.2	DA/60 mm	0.00755	0.00111	0.0028	0.000947	0.00539	0.00091
EH, EI, EJ, EK	3.5	15° I*	0.0101	0.00139	0.00459	0.00144	0.0171	0.00118
BV, BW, BX, BY	3.65	30° I	0.0189	0.00292	0.0059	0.00197	0.092	0.00237
BS, BT, BU	3.61	45° I	0.013	0.00495	0.012	0.00165	0.008	0.00182
DR, DS, DT, DU	3.65	60° I	0.0196	0.00319	0.0227	0.00303	0.0166	0.00311
EP, EQ, ER, ES	3.5	75° I	0.0178	0.00319	0.00585	0.00195	0.0088	0.00257
EL, EM, EN, EO	3.86	90°-90° Mesh	0.0144	0.00186	0.00520	0.00165	0.0117	0.00127
FW, FX, FY, FZ	4.2	R*/26 mm	0.0157	0.00234	0.0056	0.0024	0.02	0.00333
FH, FI, FJ, FK	4.2	R/60 mm	0.010	0.00152	0.00382	0.00127	0.00753	0.00127

*

CA = Continuous Aligned
DA = Discontinuous Aligned
A = Amplitude Mode
SA = Sum Amplitude Mode
I = Inclined
R = Random
C = Counts Mode
SC = Sum Counts Mode
PW = Pulse Width Mode
SPW = Sum Pulse Width Mode

APPENDIX D - AVERAGE SECOND SLOPE VALUES FOR DIFFERENT MODES OF ACOUSTIC EMISSION TESTS CARRIED OUT UNDER CONSTANT LOAD CONTROL

Test Code	Vol.% Fibre	Fibre Systems	A*	SA*	C*	SC*	PW*	SPW*
BZ, CA, CB, CC	Cement Paste	-	-	-	-	-	-	-
CK, CL, CM	1.4	CA*	0.017	0.00234	0.006	0.00196	0.0115	0.00159
CN, CO, CP, CQ	2.4	CA	0.02	0.00253	0.0084	0.00205	0.0115	0.00159
CR, CS, CT, CU	4.2	CA	0.113	0.018	0.046	0.00803	0.077	0.0072
CV, CW, CX, CY	5.5	CA	0.177	0.0253	0.0915	0.0232	0.058	0.015
CZ, DA, DB, DC	8.7	CA	0.288	0.0384	0.085	0.022	0.135	0.0238
FL, FM, FN, FO	1.4	DA*/26 mm	-	-	-	-	-	-
ET, EU, EV	1.4	DA/60 mm	-	-	-	-	-	-
FS, FT, FU, FV	4.2	DA/26 mm	-	-	-	-	-	-
FD, FE, FF, FG	4.2	DA/60 mm	-	-	-	-	-	-
EH, EI, EJ, EK	3.5	15° I*	0.0945	0.00722	0.0793	0.00467	0.0238	0.00384
BV, BW, BX, BY	3.65	30° I	-	-	-	-	-	-
BS, BT, BU	3.61	45° I	-	-	-	-	-	-
DR, DS, DT, DU	3.65	60° I	-	-	-	-	-	-
EP, EQ, ER, ES	3.5	75° I	-	-	-	-	-	-
EL, EM, EN, EO	3.86	90°-90° Mesh	0.169	0.0091	0.0144	0.00328	0.225	0.009
FW, FX, FY, FZ	4.2	R*/26 mm	-	-	-	-	-	-
FH, FI, FJ, FK	4.2	R/60 mm	-	-	-	-	-	-

*

CA = Continuous Aligned
DA = Discontinuous Aligned
A = Amplitude Mode
SA = Sum Amplitude Mode
PW = Pulse Width Mode

I = Inclined
R = Random
C = Counts Mode
SP = Sum Counts Mode
SPW = Sum Pulse Width Mode

APPENDIX E - INTERSECTION VALUES OF AVERAGE FIRST AND SECOND SLOPES UNDER DIFFERENT MODES OF ACOUSTIC EMISSION TESTS CARRIED OUT UNDER CONSTANT LOAD CONTROL

Test Code	Vol.% Fibre	Fibre Systems	A* Stress/ Events	SA* Stress/ Events	C* Stress/ Events	SC* Stress/ Events	PW* Stress/ Events	SPW* Stress/ Events
BZ, CA, CB, CC	Cement Paste	-	-	-	-	-	-	-
CK, CL, CM	1.4	CA*	1.93/136	1.54/1553	1.38/435	1.88/1900	1.53/322	1.15/1590
CN, CO, CP, CQ	2.4	CA	1.92/212	2.14/1947	2.27/612	2.58/2646	2.04/358	2.13/2485
CR, CS, CT, CU	4.2	CA	1.52/471	1.87/3337	1.85/782	1.68/2713	1.87/556	1.63/3323
CV, CW, CX, CY	5.5	CA	1.83/408	1.92/2922	2.07/1135	2.5/4593	1.93/886	2.2/3400
CZ, DA, DB, DC	8.7	CA	2.73/112	2.63/1018	2.23/437	2.38/1443	2.45/258	2.63/1488
FL, FM, FN, FO	1.4	DA*/26 mm	-	-	-	-	-	-
ET, EU, EV	1.4	DA/60 mm	-	-	-	-	-	-
FS, FT, FU, FV	4.2	DA/26 mm	-	-	-	-	-	-
FD, FE, FF, FG	4.2	DA/60 mm	-	-	-	-	-	-
EH, EI, EJ, EK	3.5	15° I*	1.64/147	1.85/1282	1.78/415	1.8/1413	1.7/229	1.83/1390
BV, BW, BX, BY	3.65	30° I	-	-	-	-	-	-
BS, BT, BU	3.61	45° I	-	-	-	-	-	-
DR, DS, DT, DU	3.65	60° I	-	-	-	-	-	-
EP, EQ, ER, ES	3.5	75° I	-	-	-	-	-	-
EL, EM, EN, EO	3.86	90°-90° Mesh	1.25/101	1.10/948	0.80/132	0.60/400	1.25/210	1.2/1660
FW, FX, FY, FZ	4.2	R*/26 mm	-	-	-	-	-	-
FH, FI, FJ, FK	4.2	R/60 mm	-	-	-	-	-	-

*

CA = Continuous Aligned
DA = Discontinuous Aligned
A = Amplitude Mode
SA = Sum Amplitude Mode
PW = Pulse Width Mode
I = Inclined
R = Random
C = Counts Mode
SC = Sum Counts Mode
SPW = Sum Pulse Width Mode